IDENTIFICATION OF NOVEL TARGETS FOR THE TREATMENT OF TYPE 2 DIABETES

Michael J. Cripps

Director of Studies: Dr. Mark D. Turner

Secondary Supervisor: Professor John Wallis

Tertiary Supervisor: Dr. Elisabetta Verderio Edwards

Thesis submitted for the degree of Doctor of Philosophy (PhD)

Interdisciplinary Biomedical Research Building

Nottingham Trent University

January 2019

Work from this thesis contributed towards the following publication:

Cripps, M.J., Hanna, K., Lavilla, C., Sayers, S.R., Caton, P.W., Sims, C., Girolamo, L., Sale, C. and Turner, M.D., 2017. Carnosine scavenging of glucolipotoxic free radicals enhances insulin secretion and glucose uptake. *Scientific Reports,* 7 (1), 13313

Abstract

Introduction

With the worldwide prevalence of diabetes continuing to increase, and current treatments aimed at increasing insulin secretion often losing effectiveness over time, it is imperative to develop new therapeutic strategies that function through independent mechanisms to those already developed.

Methods and aims

Isolated CD1 mouse islets, INS-1 β-cells and C2C12 skeletal muscle cells were cultured in control or glucolipotoxic environments as a model of type 2 diabetes. Using a combined approach of transcriptomics, PCR analysis, protein expression, fluorescent probes, *in silico* modelling, and cellular function assays, new therapeutic targets and treatments to augment insulin secretion in type 2 diabetes have been identified.

Results

Carnosine and β-alanine supplementation was shown to inhibit reactive species generation and to increase stimulated insulin secretion. Importantly it was also able to reverse glucolipotoxicity-associated inhibition of insulin secretion typically seen in type 2 diabetes. However, due to rapid hydrolysis of carnosine by carnosinase enzymes in the body, these treatment strategies are likely to be of only modest benefit to patients. *In silico* derived compounds designed to inhibit carnosinase-2 activity had surprisingly little effect on reactive species scavenging or cellular function in β-cells however. Nevertheless, carnosinase inhibitors may still offer a

realistic treatment strategy in patients, as β-cells are limited by carnosine concentrations ~1,000 fold lower than those observed in tissues linked to insulin resistance, such as skeletal muscle.

Illumina HiSeq gene expression analysis identified trace amine associated receptor (TAAR) expression as being significantly downregulated by glucolipotoxicity. Furthermore, TAARs were shown to regulate insulin secretion through adenylyl cyclase activation and cAMP mediated enhanced insulin secretion. Addition of physiological TAAR ligands was also shown to be able to amplify secretagogue-stimulated insulin release.

Conclusion

This body of work will pave the way for future studies seeking to develop and further characterise carnosine and novel carnosine derived analogs as potential therapeutic agents to reverse glucolipotoxic cellular dysfunction. Modulation of heterotrimeric G-protein coupled receptor signalling through TAAR agonists may also represent a new therapeutic strategy to combat type 2 diabetes.

Table of Contents

Figure List

Table List

Abbreviations

3-NT – 3-nitrotyrosine

4-HNE – 4-hydoxynonenal

ADCY – Adenylyl cyclase

ADP – Adenosine diphosphate

AGE – Advanced glycation end product

ALE – Advanced lipidation end product

AMP – Adenosine monophosphate

AMPK - AMP-activated protein Kinase

APS – Ammonium Persulfate

ATF6 - transcription factor activating transcription factor 6

ATP – Adenosine triose phosphate

ATPGD1 – Carnosine Synthase

BCA – Bicinchoninic acid

BSA – Bovine Serum Albumin

cAMP – cyclic adenosine monophosphate

CHOP - CCAAt/-enhancer-binding protein homologous protein

CML - N-carboxymethyl-lysine

CN1 – Carnosinase 1

CN2 – Carnosinase 2

CPT-1 carnitine-palmitoyl transferase-1

CRE – cAMP response element

Ct value – Threshold cycle value

DCFDA - 2',7'-Dichlorofluorescin diacetate

eIF2a - eukaryotic initiation factory 2a

elF2 - translational initiation factor-2

ER – Endoplasmic reticulum

FFA – free fatty acid

GD – Gestational Diabetes

GDP – Gross domestic product

GLT - Glucolipotoxicity

GLUT2 - Glucose transporter 2

GPCR – G-protein coupled receptor

GSIS – Glucose stimulated insulin secretion

HbA1c - glycated haemoglobin

HPLC – High performance liquid chromatography

IBMX - 3-isobutyl-1-methylxanthine

IDE – insulin degrading enzyme

iNOS – Inducible nitric oxide synthase

IRE1 - serine/threonine protein kinase/endoribonuclease

K_{ATP} - ATP sensitive Potassium channels

MDA – Malondialdehyde

MMP - matrix metalloproteins

mRNA – messenger RNA

NADPH - Nicotinamide adenine dinucleotide phosphate

NF-κB - nuclear factor kappa B

NHS – National Health Service

NO – Nitrous oxide

$O_2^{\cdot -}$ – superoxide

OCT1 - Organic cation transporter 1

OGTT – Oral glucose tolerance test

ONO_2^- - peroxynitrite

PCR – Polymerase chain reaction

PERK - RNA-like endoplasmic reticulum kinase

PKC – Protein kinase C

PMA - phorbol 12-myristate 13-acetate

PP1 – protein phosphatase 1

PPARγ - peroxisome-proliferator activated receptor gamma

PPRE - PPARγ response element

qPCR – quantitative polymerase chain reaction

RCS – Reactive Carbonyl species

RIN – RNA Integrity number

RIPE3b 1/2 - Rat insulin promoter element 3b 1/2

RNAseq – Next generation sequencing

RONS – Reactive Oxygen and Nitrogen Species

ROS – Reactive oxygen species

RPMI – Roswell Park Memorial Institute

rRNA – ribosomal RNA

SDS – Sodium dodecyl sulphate

SDS PAGE – Sodium dodecyl sulphate polyacrylamide gel electrophoresis

SEM – Standard error of mean

SNARE - soluble N-ethylmaleimide sensitive factor attachment protein receptor

SRP - Signal recognition particles

SSIS – secretagogue stimulated insulin secretion

SUR – sulphonylurea receptor

T1D – Type 1 Diabetes

T2D – Type 2 Diabetes

TBS – Tris-buffered saline

TBST – TBS + 0.1% TWEEN20

TCA - Tricarboxylic acid

Temed – Tetramethylethylenediamine

TZD - Thiazolidinediones

VAMP – v-SNARE

VAMP2 – synaptobrevin

WHO - World Health Organisation

Acknowledgments

I would firstly like to thank my director of studies Dr. Mark D. Turner, for his continuous and persistent support and guidance both in and outside of working matters. Thank-you to my supervisory team of Professor John Wallis, Dr. Elisabetta Verderio Edwards, and Independent Assessor Dr. Sergio Colombo. Thank you also to other members of NTU staff who have aided in the direction and publishing of elements of my doctoral research, and in particular Dr. Luigi De Girolamo, Professor Craig Sale and Dr. Carl Nelson.

Secondly, thank you to Dr. Paul W. Caton and Dr. Sophie Sayers from King's College London for collaborative *ex-vivo* mouse islet data that supports and increases the validity and impact of this work.

Thirdly, I would like to thank Dr. Marta Bagnati, Dr. Tania Jones, Dr. Babatundi Ogunkolade, Dr. Robert Lowe, and Professor Graham A. Hitman from Bart's and The Royal London School of Medicine for their contribution to transcriptomic analysis and MetaCore pathway analysis. Similarly thank you to Professor Mark D. Berry of the Memorial University of Newfoundland for help and guidance in regard to the heterotrimeric G protein coupled receptor research.

Fourthly, to the Nottingham Trent Chemistry department, in particular Dr. Christopher Garner, Suniya Khatun, Daniel Cotton and team for the *in-silico* screening and modelling of chemical library's for potential carnosinase inhibitors.

I would also like to thank Craig Sims for preliminary insulin secretion data, Dr. Katie Hanna for help with qPCR analysis, generation of the 4-HNE figure and HPLC samples, Dr. Ruth James for HPLC sample analysis, and Charlie Lavilla for the culturing and differentiation of C2C12 skeletal muscle cells.

Thank you to everyone in the Interdisciplinary Biomedical Research Centre for making my time very enjoyable, particularly those based in IBRC laboratory 009 such as Laura Lopez-Gonzales, Merell Billacura, Akashdeep Singh and honorary members Henry Pegram and Joseph Chemmarappally. Also, to the MSc students that have helped cross-validate my research such as Kathryn Fair and Lamis Osman.

Thank you finally and most importantly to all those people that have supported me throughout my PhD research, in particular, thank you to Faye McDaniel for all the love and support I could ever ask for, I couldn't have done it without you.

I am where I am because of all of you, thank you all.

1. INTRODUCTION

1.1. β-cell characterisation

1.1.1. Islet of Langerhans Composition

The pancreas is an endocrine organ that develops from the foregut endoderm as ventral and dorsal buds in gestation and in maturation sits behind the stomach on top of the large intestine (Ackermann and Gannon 2007). The pancreas constitutes primarily of cell aggregates named after their discoverer and shape. These so-called Islets of Langerhans contain five major cell types; Alpha (α) cells that secrete glucagon, Beta (β) cells that secrete insulin, Delta (δ) cells that secrete somatostatin, Ghrelin positive cells that secrete ghrelin and F cells that secrete pancreatic polypeptides that account for 15-20%, 65-90%, 3-10%, 1% and 1% of the total islet populations respectively. Two further islet cell types have been identified; enterochromaffin cells that secrete serotonin, and G-cells that secrete gastrin (Elayat, el-Naggar and Tahir 1995; Da Silva Xavier 2018). Islets are typically oval and share a common arrangement of cells amongst mammals typically exhibited as a core of β-cells enclosed within non β-cell types (Kulkarni 2004). In humans, β-cells have been shown to be sandwiched between two α-cell enriched layers and folded, to allow increased blood vessel contact (Bosco, et al. 2010). The concentration of pancreatic islets is also reportedly more than two fold higher in the tail of the organ compared to the head and body region that share a similar concentration (Wittingen and Frey 1974; Wang, et al. 2013).

1.1.2. Insulin Biosynthesis, Maturation, Structure and Storage

Insulin is a key hormone in controlling glucose homeostasis through its action at target tissues. β-cells monitor and respond to dietary nutrients in the blood such as

glucose, amino acids, fatty acids and monosaccharides and maintain a healthy blood glucose concentration by secreting insulin. The insulin gene encodes a 110 amino acid, pre-proinsulin, that after translocation through the rough endoplasmic reticulum (ER) through the interaction of its hydrophobic N-terminal with cytosolic ribonucleoprotein signal recognition particles (SRP) (Egea, Stroud and Walter 2005) is cleaved to proinsulin by a peptidase removing the N-terminal (Patzelt, et al. 1978). The proinsulin is then folded into a three-dimensional structure by the formation of three disulphide bonds (Huang and Arvan 1995) and packed into immature secretory granules at the *trans*-Golgi network. During granule maturation, proinsulin is cleaved to mature 51 amino acid insulin by removal of the C-peptide through proteolysis by the endoproteases PC1/3 and PC2, and trimming of the C-terminal by carboxypeptidase E (Hou, Min and Pessin 2009). Conversion of immature insulin to mature insulin is optimal at acidic pH concentrations due to the pH optimum of the endoproteases enzymes. Granules become acidic as they mature due to an ATP-dependent proton pump that ensures the acidic environment optimally facilitating insulin conversion from proinsulin (Orci, et al. 1986; Davidson, Rhodes and Hutton 1988).

Mature monomeric insulin consists of a 21-amino acid A chain and a 30 amino acid B chain linked by the aforementioned disulphide bonds; two between chain A and B and one within chain A itself. Chain A is formed of two antiparallel α-helices between amino acid residues A2-A8 and A13-A19. The confirmation of these bring the two ends of the A chain into close proximity of one another and bind the helices at amino acids A9-A12. Chain B is comprised of both α-helices and β-sheets allowing the chain

to fold into a V shape. The two chains are linked by disulphide bonds derived from cysteine residues at amino acid A7-B7 and A20-B19 with an internal sulphide bond between chain A at residue A6 to A11 as shown in figure 1.1. These bonds facilitate the high stability of the three dimensional structure (Murray, et al. 2003; Weiss, Steiner and Philipson 2000; Pittman, Philipson and Steiner 2010).

Figure 1.1; Structure of human insulin and proinsulin.
The A chain consists of 21 amino acids and the B chain 30 amino acids. Two disulphide bridges at Cys7A-Cys7B and Cys20A-Cys19B bind chains A and B. C-peptide is cleaved in maturation (Murray, et al. 2003).

At micromolar concentrations, mature insulin dimerises, maintained by the antiparallel β-sheets of the B chain. However due to the hydrophobic nature of the amino acid residues, insulin aggregates to form a higher ordered structure, with 6

molecules of insulin arranged as 3 dimers around a central Zn^{2+} ion at a concentration of ~40mM (De Meyts 2004). The total amount of granules per β-cell is disputed with some reports suggesting a typical mouse β-cell contains ~13,000 insulin granules containing ~200,000 insulin molecules each, accounting for ~11.5% of the total cells volume (Howell 1984; Dean 1973). Studies that are more recent suggest that this is actually much lower due to a reduced estimation in β-cell volume and only 5000-6000 granules that contain two-fold more insulin than previously thought (Fava, et al. 2012).

1.1.3. Regulation of Insulin Transcription and Translation

Insulin biosynthesis is regulated at both a transcription and a translation level. The former is generally responsible for β-cells ability to respond to intracellular signals allowing insulin concentrations to fluctuate in response to high and low levels of nutrients. Five sequence elements named A, C, E, Z and CRE (cAMP response element), found within the promoter region of the insulin gene, act as binding sites for transcription factors enabling the regulation of gene expression (Hay and Docherty 2006).

The A elements, found in the control region of the insulin gene are rich in A/T base pairs, with a conserved TAAT core that acts as a DNA binding recognition motif for the transcription factor proteins PDX-1, Isl-1 and Cdx-2 which all play various roles in islet function (German, et al. 1995; Gehring, Affolter and Burglin 1994; Ohlsson, Karlsson and Edlund 1993; German, et al. 1992; Karlsson, et al. 1990). There are two C-elements within the insulin gene. In rats, one of the C-elements (C1) forms a protein-DNA complex with the two factors; rat insulin promoter element 3b 1 and 2

(RIPE3b 1/2) (Shieh and Tsai 1991; Zhao, et al. 2000). Ribe3b1 also named MafA, is responsible for the enhancement of insulin gene-expression (Olbrot, et al. 2002), which is downregulated in response to prolonged fatty acid exposure (Hagman, et al. 2005). The second C-element termed PISCES (pancreatic islet cell enhancer sequence) which was found to contribute to the transcription of insulin, glucagon and somatostatin (Knepel, et al. 1991). This element also binds the transcriptional factor PAX6 which is essential for islet development and normal insulin gene transcription (Sander, et al. 1997). Rodents have two E-elements whilst most other mammals only have one (Steiner, et al. 1985). Transcription factors that bind to this element contain a helix-loop-helix motif that facilitates protein-protein interactions, whilst their amino base terminal facilitates the DNA-protein binding that enhances transcription. The Z sequence element is upstream of the A element and is specific to the human insulin gene (Sander, et al. 1998). It is believed that PDX-1 and MafA regulate insulin transcription via this element as well as others (Pino, et al. 2005). The CRE promotor region consists of four sites which are activated by CRE binding proteins all of which share a common cluster of amino acids at their N-terminus that bind to the CRE sites to initiate the gene transcription (Inagaki, et al. 1992; Metallo, Paolella and Schepartz 1997).

Pancreatic β-cells can also control the speed of proinsulin protein translation in response to nutrients such as sugar and fat. This is primarily controlled by a decrease in serine-51 phosphorylation of the eukaryotic initiation factory 2a (eIF2a) by protein phosphatase 1 activated proportionately to increasing glucose concentrations (Mierde, et al. 2007). Pancreatic ER kinases do the opposite and phosphorylate eIF2a

thereby also acting as an inhibitory regulator of insulin translation (Shi, et al. 1998). Polypyrimidine tract binding proteins also regulate the insulin genes mRNA translation as they extend mRNA viability via exon repression whilst the mRNA is undergoing splicing in the nuclei, whilst also stimulating translation initiation by recruiting ribosomes in the cytosol (Izquierdo, et al. 2005; Spellman and Smith 2006; Wollerton, et al. 2004).

1.1.4. Insulin Exocytosis

1.1.4.1. Metabolic Signalling for Insulin Exocytosis

Insulin secretion is instigated via various pathways, ultimately culminating in influx of extracellular Ca^{2+} ions via L_c-type Ca^{2+} channels, as well as cAMP-dependent signalling cascade activation. Whilst insulin secretion is sensitive to amino acids, fatty acids and others, glucose is the most studied metabolite triggering insulin exocytosis. Insulin exocytosis is important to maintain blood glucose levels within the recommended healthy limit (fasting blood glucose level <5.5mM/L, up to 7.6mM/L 2 hours after eating).

Glucose stimulated insulin secretion (GSIS) occurs as outlined in Figure 1.2. Upon glucose intake into the blood, following food consumption, it enters pancreatic β-cells through glucose transporter 2 (GLUT2) uptake. GLUT2 is the only glucose transporter expressed in β-cells and they have a low affinity for glucose (Km ~17mM) ensuring that glucose is transported proportionally into β-cells up to 10mM corresponding glucose concentrations in the blood (Suckale and Solimena 2008). Upon entry, glucose is phosphorylated by glucokinase and enters the glycolysis reaction. Glycolysis results in ATP and pyruvate production, where pyruvate is further

metabolised by pyruvate dehydrogenase and pyruvate carboxylase resulting in tricarboxylic intermediates that are passed into the mitochondria. These enter the tricarboxylic acid (TCA) chain reaction, where aerobic respiration produces further ATP molecules. The change in ATP to ADP ratio within β-cells causes ATP-sensitive K^+ channels (K_{ATP} channels) to close, which in turn depolarises the cell membrane. This localised membrane depolarisation induces the opening of L_C-type voltage-dependent Ca^{2+} channels resulting in a mass influx of extracellular Ca^{2+}. This increase in localised free calcium instigates insulin granule fusion and exocytosis through mechanisms discussed in section 1.1.4.2. (Komatsu, et al. 2013).

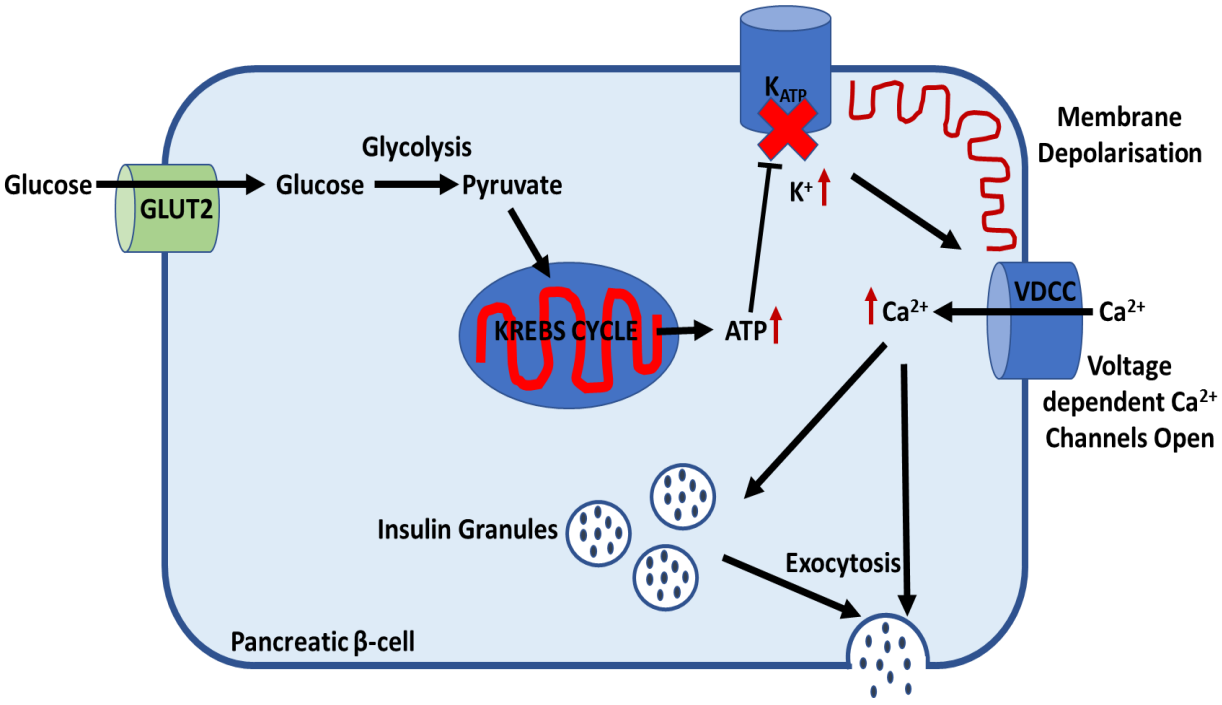

Figure 1. 2; Mechanism of glucose stimulated insulin secretion.

Glucose enters β-cells via GLUT 2 receptors before being metabolised. Resultant increase in ATP:ADP ratio causes ATP sensitive potassium channels to close causing the cell membrane to depolarise. Depolarisation causes voltage dependent calcium channels to open causing localised influx of calcium which triggers insulin exocytosis. Figure adapted from (Komatsu, et al. 2013)

Fatty acids and amino acids also augment glucose stimulated insulin secretion (GSIS). In the total absence of free fatty acids, β-cells lose the ability to secrete insulin in response to glucose, however if normal physiological concentration of fatty acids are replaced normal secretion will resume (Stein, et al. 1996). Free fatty acid (FFA) concentration regulates insulin secretion via three proposed mechanisms (Figure 1.3).

FFAs can freely diffuse across the plasma membranes into the β-cell cytosol where they are metabolised to long-chain acyl-CoA by the enzyme acyl-CoA synthase. The long-chain acyl-CoA is subsequently transported to the mitochondria by carnitine palmitoyl transferase -1 where it enters the β-oxidation pathway. Oxidisation of the long-chain acyl-CoA increases ATP production and sustains the basal level of insulin secretion via the K_{ATP} channel manner described in GSIS (Berne 1975; Hamilton and Kamp 1999).

Upon ingestion of a carbohydrate-containing meal, glucose and amino acids are synthesised into malonyl-CoA by acyl-CoA carboxylase. Malonyl-CoA is a regulatory compound that inhibits carnitine palmitoyl transferase-1 transport of long chain acyl-CoA into the mitochondria thereby inhibiting fatty acid metabolism. The resultant accumulation of long-chain acyl-CoA in the cytosol increases intracellular Ca^{2+} concentrations, enhances insulin granular fusion at the membrane and changes the acylation state of ion channel activity and exocytosis, all of which augment insulin secretion (Newsholme and Krause 2012).

The heterotrimeric enzyme AMP-kinase regulates the level of ATP production from FFA oxidation as it inhibits the activation of acyl-CoA carboxylase, decreasing

malonyl-CoA inhibition of carnitine palmitoyl transferase-1, increasing FFA entry into the mitochondria for metabolism (McGarry, et al. 1991). Increasing glucose concentrations dephosphorylate and inactivate β-cell AMP-kinase increasing malonyl-CoA inhibition of carnitine palmitoyl transferase-1, increasing insulin secretion (Salt, et al. 1998).

FFAs can also stimulate G-protein coupled receptors such as GPR40 (also known as free fatty acid receptor 1) and GPR119. Activation of GPR40 increases intracellular Ca^{2+} concentrations by stimulating Ca^{2+} release from the endoplasmic reticulum via Gαq-phospholipase C pathway activation, resulting in an increase in insulin exocytosis (Shapiro, et al. 2005; Kebede, et al. 2008). Similarly stimulation of GPR119 with the lipid oleoylethanolamide (a product of membrane phospholipid metabolism), increases insulin secretion through adenylyl cyclase mediated production of cAMP (Winzell and Ahrén 2007; Moran, et al. 2014)

However, chronic levels of free fatty acids, particularly in conjunction with increased glucose concentrations will reduce β-cell insulin biosynthesis and secretion capabilities over time until complete β-cell failure (Prentki, et al. 2002; Poitoit, et al. 2006).

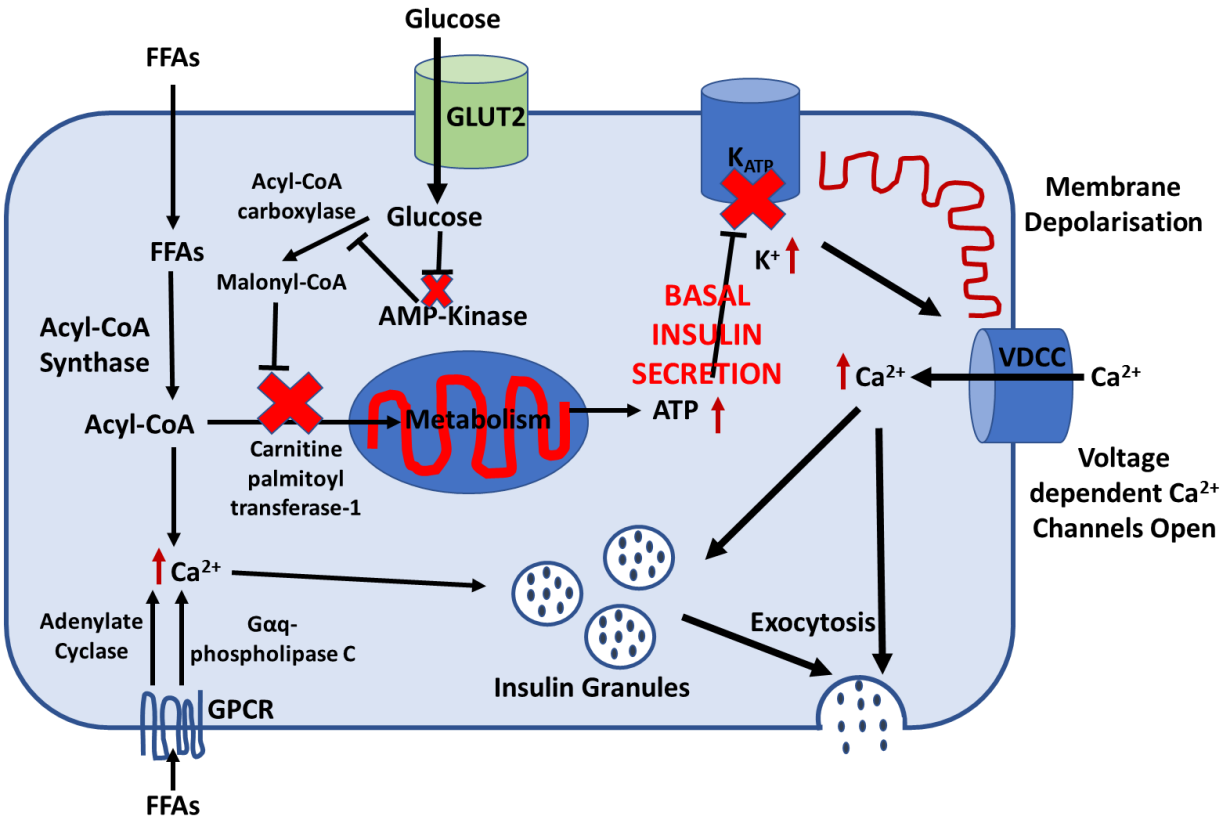

Figure 1. 3; Fatty acid regulated insulin secretion.

FFAs are converted to acyl-coA and either enter the mitochondria for metabolism which increases the ATP:ADP ratio maintaining basal insulin secretion via K_{ATP} channel pathway, or it is blocked by malonyl-CoA production and accumulates in the cytosol. This accumulation of acyl-CoA increases Ca^{2+} causing insulin exocytosis. AMP-kinase activity is inhibited with increasing glucose concentration thereby blocking fatty acid metabolism further increasing insulin secretion. FFA can also stimulate GPCRs which increase intracellular Ca^{2+} via adenylyl cyclase production of cAMP, or activation of the Gαq-phospholipase C pathway activation, resulting in an increase in insulin exocytosis. Figure inspired by (Nolan, et al. 2006)

Typical physiological concentrations of individual amino acids are poor secretagogues of insulin, however, the combination of leucine and glutamine at these same concentrations can augment GSIS. Glutamine is firstly converted into glutamate by intracellular glutaminase. Secondly, leucine activates glutamate

dehydrogenase which in turn converts the recently produced glutamate to α-ketoglutarate where it can enter the TCA cycle to increase the production of ATP. The increase in ATP increases insulin secretion via the GSIS method described previously (Sener and Malaisse 1980; Dixon, et al. 2003).

Similarly, hormones also have the potential to augment GSIS. Glucagon-like peptide 1 (GLP-1) and gastric inhibitory peptide (GIP) account for roughly 50% of the insulin released after ingesting dietary glucose (Nauck, et al. 1993). The incretin hormones secreted from L-cells in the small intestine in response to nutrient consumption bind to their receptors, (both members of the GIP receptor family (Mayo, et al. 2003)) found on β-cell membranes to activate adenylyl cyclases via stimulatory G proteins. The subsequent rise in cAMP production from adenylyl cyclase enabled ATP conversion can increase insulin secretion via PKA-dependent and PKA-independent pathways. cAMP dependent PKA activation results in phosphorylation of voltage gated and ATP dependent channels increasing the intracellular concentration of Ca^{2+}. PKA also sensitises secretory machinery to Ca^{2+}, whilst increasing secretory vesicle mobility for granule replenishment, all promoting enhanced insulin granule exocytosis.

PKA-independent cAMP insulin secretion which is mediated by Epac is much faster than PKA-dependent mechanisms (Henquin and Nenquin 2014). Epac has two isoforms Epac1 and Epac2, of which the latter is culpable for increases in insulin exocytosis. The true mechanism of Epac mediated insulin secretion is still not fully understood. Epac2 is thought to stimulate the recruitment of granules to the membrane and cause exocytosis via Rap1 interaction and activation of small GTPases

which modulate the actin cytoskeleton. Alternatively, Rap1 mobilises intracellular calcium via phospholipase C-ε causing exocytosis. In addition, Epac interaction with the SUR1 subunit of the K_{ATP} channels are a pre-requisite for granule priming whilst it also interacts with the t-SNARE and SNAP25 components of the secretory machinery crucial for exocytosis. Epac's interaction with Rim2 at the Rab3 subunit has also been implicated as the effector of incretin augmented insulin secretion (Holz 2004; Lim and Brubaker 2006; Tengholm 2012).

1.1.4.2. Granule Fusion and Exocytosis

Once the insulin containing granules have been transported to the membrane, the 35kDa vesicular v-SNARE (soluble NH_2-ethylmaleimide-sensitive fusion protein attachments protein receptor protein) VAMP2 (synaptobrevin), forms a complex with the target membrane associated receptors syntaxin 1A and SNAP25 (35kDa and 25kDa respectively) in a ratio of 1:1:2 in specific areas on the membrane called excitosomes (Figure 1.4). There are more than 30 SNARE protein family members, all of which are 60-70 amino acids in length that form a seven coiled-coil structure (Sudhof and Rothman 2009).

Upon insulin containing granules reaching the membrane, the receptor interaction and binding of exocytosis machinery results in a conformational change, forming a four-helix coiled-coil complex known as the SNAREpin that is incredibly stable with melting temperatures above 95°C (Thurmond 2007). Whilst this complex forms the catalytic exocytotic machinery required for granular docking at the membrane, the complex alone is not sufficient to induce rapid Ca^{2+} dependent exocytosis; other accessory proteins are required.

The insulin granule membrane proteins synaptotagmins are considered one of the most likely contenders to effect Ca^{2+} dependent insulin exocytosis as they are large proteins with two Ca^{2+} binding domains (Sugita, et al. 2002). Synaptotagmins of which there are 15 known mammalian isoforms (Rickman, et al. 2004) have been demonstrated to instigate rapid neurotransmitter synaptic vesicle exocytosis through complexin displacement. Complexin is a regulatory protein that inhibits spontaneous release by blocking the full assembly of the so called SNAREpin by clamping to VAMP2. This arresting of complete granular fusion essentially primes the vesicles for rapid synchronised exocytosis in response to calcium (Melia Jr 2007; Lai, et al. 2014). Calcium binding to synaptotagmins is thought to uncouple complexin from VAMP2 enabling full SNARE complex formation allowing granular fusion and exocytosis (Tang, et al. 2006).

The core exocytotic machinery for insulin secretion and neurotransmitter exocytosis is the same and whilst they share a similar requirement for increased Ca^{2+} to instigate secretion, the kinetics of exocytosis is very different, indicative of distinct regulatory machinery changes between cell types. Because of this, synaptotagmins III, V, and VII have all been implicated as mediators for Ca^{2+} induced insulin secretion in pancreatic β-cells (Gao, et al. 2000; Gustavsson, et al. 2008). Conflicting data about synaptotagmin IX has also been reported. Iezzi et al (2005) reported that adenovirus-mediated silencing of synaptotagmin 9 reduced Ca^{2+} dependent islet insulin secretion, whilst more recently, Gustavsson et al (Gustavsson, et al. 2010) reported that whilst synaptotagmin IX is important for rapid neurotransmission, it plays no role in glucose-stimulated insulin secretion regulation in β-cells. All these studies however,

only demonstrated a partial inhibition of insulin secretion upon inhibition of synaptotagmins. This, alongside the differences in kinetics between rapid synaptotagmin dependent neurotransmission and the more multiphasic insulin exocytosis, would suggest that synaptotagmins may not be the sole Ca^{2+} sensor culpable in insulin secretion and may in fact work in combination with multiple isoforms, or with different Ca^{2+} sensors altogether.

One such sensor could be the 54KDa isoform of Calpain-10. Calpain-10 has been demonstrated to interact directly with SNAP25 during Ca^{2+} dependent insulin secretion (Marshall, et al. 2005). This was successfully inhibited with a calpain protease inhibitor suppressing both SNAP25 proteolysis (postulated to be required for secretion) and insulin secretion. Calpain-10 expression is also contrastingly high in β-cells compared to synaptotagmins (Aganna, et al. 2006) which further suggests calpain-10 may perform a central role in Ca^{2+} secretion coupling in pancreatic β-cells.

MUNC18 also plays a regulatory role in insulin granule priming and fusing at the cellular membrane. MUNC18a is a competitive inhibitor for SNAP25 and VAMP2 binding to syntaxin and is thought to change the syntaxin conformational shape further inhibiting exocytosis (Dong, et al. 2007). However, conflicting research suggests that MUNC18 is required for first-phase insulin secretion and encourages granule docking (Oh, et al. 2012). One theory is that MUNC18 increases vesicle docking but inhibits vesicle priming and it is therefore critical to maintain the correct expression to promote adequate granule docking without impeding overall exocytosis (Hou, et al. 2009).

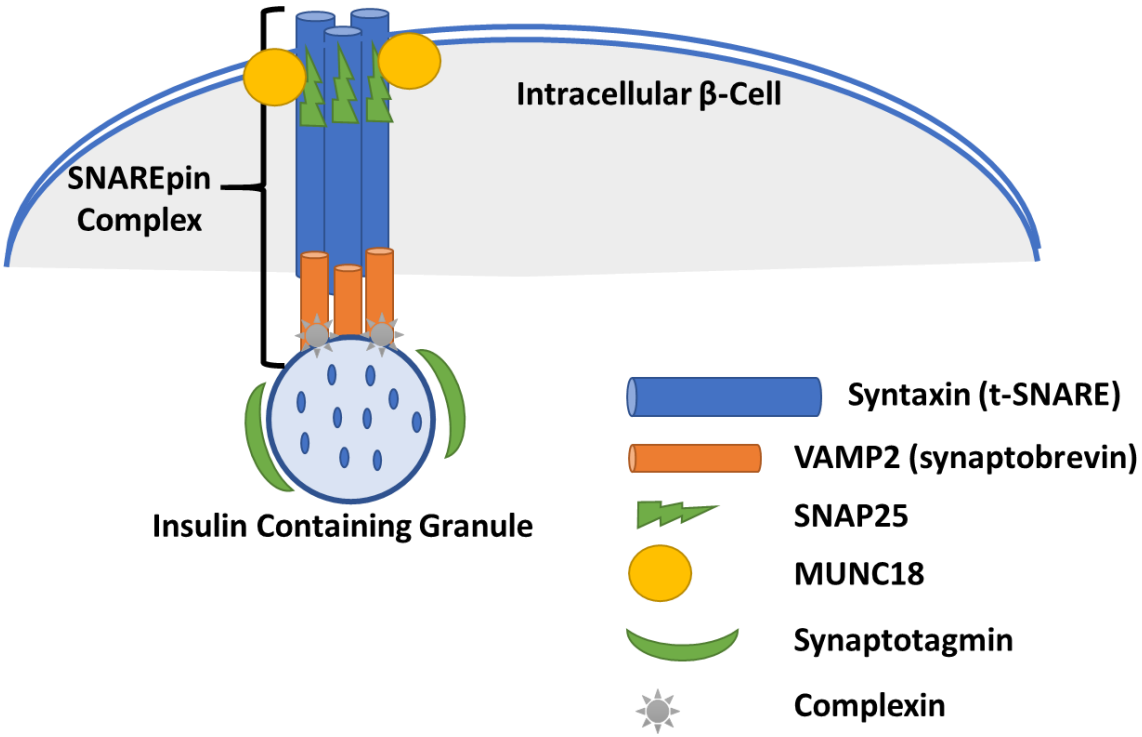

Figure 1. 4; SNARE complex of insulin exocytosis.

VAMP2 on the granule membrane form a complex with SNAP25 and syntaxin 1A on the intracellular membrane. Complexin inhibits spontaneous exocytosis, priming the granules, before Synaptotagmin activation by Ca^{2+} uncoupled complexin causing granular fusion and exocytosis. MUNC18 is also a regulator promoting granule docking but inhibiting granular fusion. Figure adapted from (Thurmond 2007).

1.1.4.3. Granule Trafficking to the Cell Membrane

It is accepted that there are at least two different insulin granule populations within pancreatic β-cells. The readily releasable pool which is pre-docked in the SNARE protein complex at the cell surface membrane (Daniel, et al. 1999) which accounts for roughly <5% (less than 50 granules of the total granule pool ~10,000 granules per cell) and is responsible for the first phase of rapid calcium-dependent insulin secretion that lasts 1-5 minutes. The second phase of insulin exocytosis is dependent

upon the reserve pools of insulin granules that are recruited to the membrane over a more prolonged period of time, ~5-60 minutes. The readily releasable pool is continually replenished which starts in the first phase of secretion. Docking and priming of previously non-releasable granules occurs at ~5-40 granules per minute per cell (Barg, et al. 2002)

F-actin and microtubule networks are thought to play a significant role in stimulated insulin secretion and granule mobilisation in particular (Figure 1.5). F-actin interacts directly with syntaxin 1A on the cellular membrane, inhibiting granule-SNARE-complex formation blocking the movement of insulin granules to the membrane. It does however also provide transportation for granules to be trafficked closer to the membrane from the cytosol. Upon glucose stimulation, F-actin blocking the syntaxin disaggregates, allowing the mobilisation of granules and fusion of VAMP2 on the vesicle membrane to SNAP25 and syntaxin at the cellular membrane resulting in insulin exocytosis. This remodelling is known to be regulated by the Rho-family of GTPases activated by glucose. In the second phase of glucose stimulated insulin secretion, microtubules traffic insulin containing granules from the central cell cytosol to the F-actin filaments near the cell membrane where they are further mobilised along the F-actin tracks to the cell surface to dock with SNARE proteins and be released (Wang and Thurmond 2009).

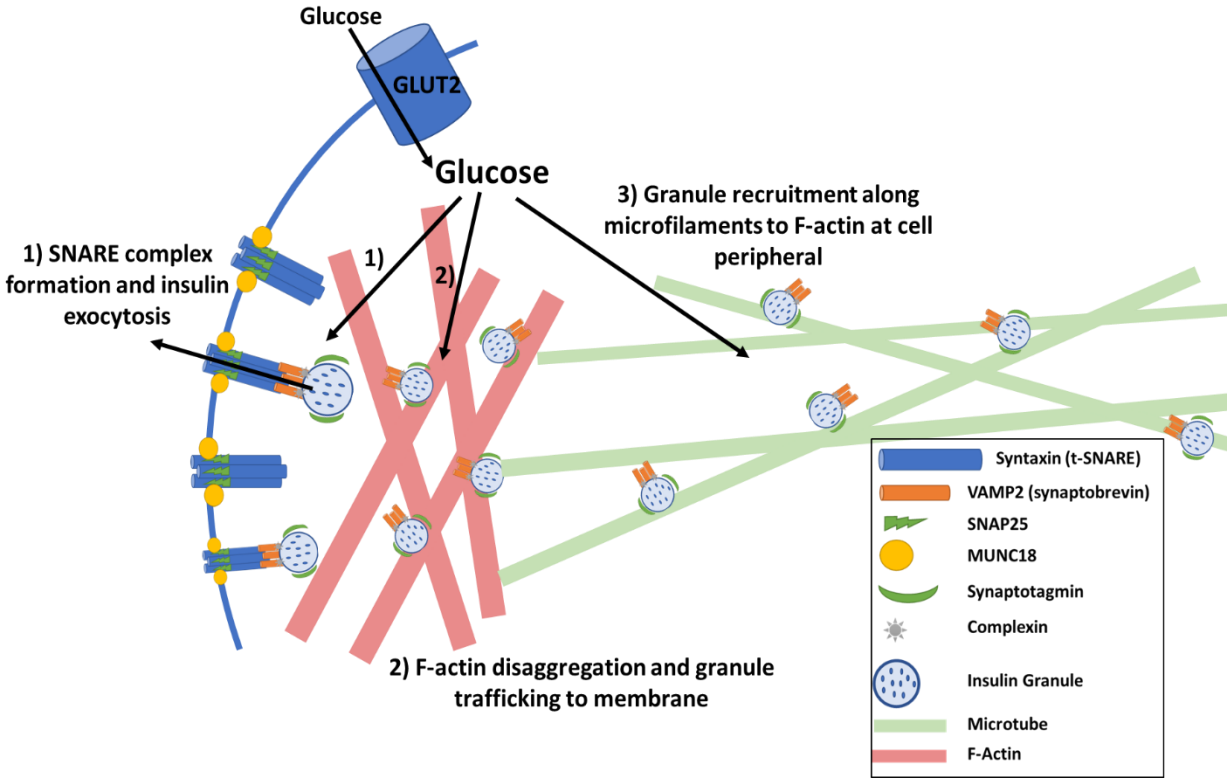

Figure 1. 5; Granule recruitment by cytoskeleton.

Insulin granules are mobilised to F-actin at the cell peripheral by microtubules in the second phase of insulin secretion. In response to glucose, F-actin which blocks the SNARE complex formation disaggregates and traffics insulin containing granules to the membrane where they fuse and are exocytosed. Figure adapted from (Wang and Thurmond 2009).

1.1.5. Insulin Signalling

Briefly, the main function of insulin signalling is to increase glucose transport into fat and muscle cells by stimulating GLUT4 translocation from intracellular sites to the cellular membrane. However, in truth it has pleiotropic actions ranging from controlling glucose, lipid and protein metabolism, cell growth, gene expression and glucose transporter expression (Figure 1.6).

Insulin binds with high affinity to the tyrosine kinase insulin receptor on the surface of skeletal muscle, liver and adipose tissues. The receptor is composed of two 135kDa α-subunits (completely extracellular) and two 95kDa β-subunits that span the membrane (Jacobs and Cuatrecasas 1981). Insulin binds at the cysteine rich domain of the α-subunit, causing the receptor to autophosphorylate six tyrosine residues in the β-subunit mediating the signal transduction by increasing the tyrosine kinase activity (Zhang and Roth 1991; Cheatham and Kahn 1995).

The autophosphorylation of the β-subunit mediates non-covalent stable bonding of substrate molecules that are rapidly phosphorylated themselves. These include, but are not limited to the insulin receptor substrate (IRS) proteins (1-6), Src-homology-collagen (SHC) proteins, growth factor receptor bound-2 (Grb-2) and the CAP/c-Cbll complex (Langlais, Mandarino and Garvey 2015).

Phosphorylation of the IRS proteins allows its SRC homology 2 (SH2) domains to associate and activate phosphoinositide 3-kinase (PI3K) by binding at its regulatory subunits. Activated PI3K phosphorylates PtdIns(3,4)P_2/PtdIns(3,4,5)P_3-dependent kinase-1 (PDK-1) at the 3’ position of the inositol ring or serine residues which in turn activates the serine kinase PKB/Akt. PKB/Akt deactivates glycogen synthase kinase 3 (GSK-3), causing glycogen synthesis to increase as well as promoting cell growth and survival. Importantly, PKB/Akt also stimulates GLUT4 translocation to the membrane allowing increased glucose uptake in response to insulin binding (Bevan 2001).

Phosphorylation of IRS, Grb2 and SHC also cause interaction with adapter proteins which activates Ras. Ras acts as a molecular switch to activate a serine kinase cascade

pathway of Raf, MEK and mitogen-activated protein kinase (MAPK) extracellular signal regulated kinase (ERK). Activated MAPK/ERK can translocate to the membrane where it can phosphorylate transcription factors regulating gene expression and cell growth and survival (Saltiel and Kahn 2001).

Stimulated GLUT4 translocation to the membrane also occurs via another separate mechanism. Insulin binding with its receptor and receptor autophosphorylation phosphorylates Cbl; a protooncogene that is in a complex with Crk and associated with the adapter protein CAP (Ribon and Saltiel 1997; Ribon, et al. 1998). Upon phosphorylation the CAP/Cbl/Crk complex, the sorbin homology domain (SOHO) of the CAP protein interacts with the lipid raft associated protein flotillin, causing the complex to migrate to the membrane (Baumann, et al. 2000; Kimura, et al. 2001). This in turn mediates guanyl nucleotide exchange factor, C3G recruitment to protein complex at the Crk element, which activates TC10. TC10 activation stimulates intracellular reserve pools of GLUT4 to translocate to the membrane enabling glucose uptake into the cell (Chiang, et al. 2001; Saltiel and Kahn 2001). GLUT4 translocation and subsequent granule fusion resulting in increased expression on the cell surface is mediated by the same SNARE complex of VAMP2 and syntaxin involved in insulin granule exocytosis (Pessin, et al. 1999).

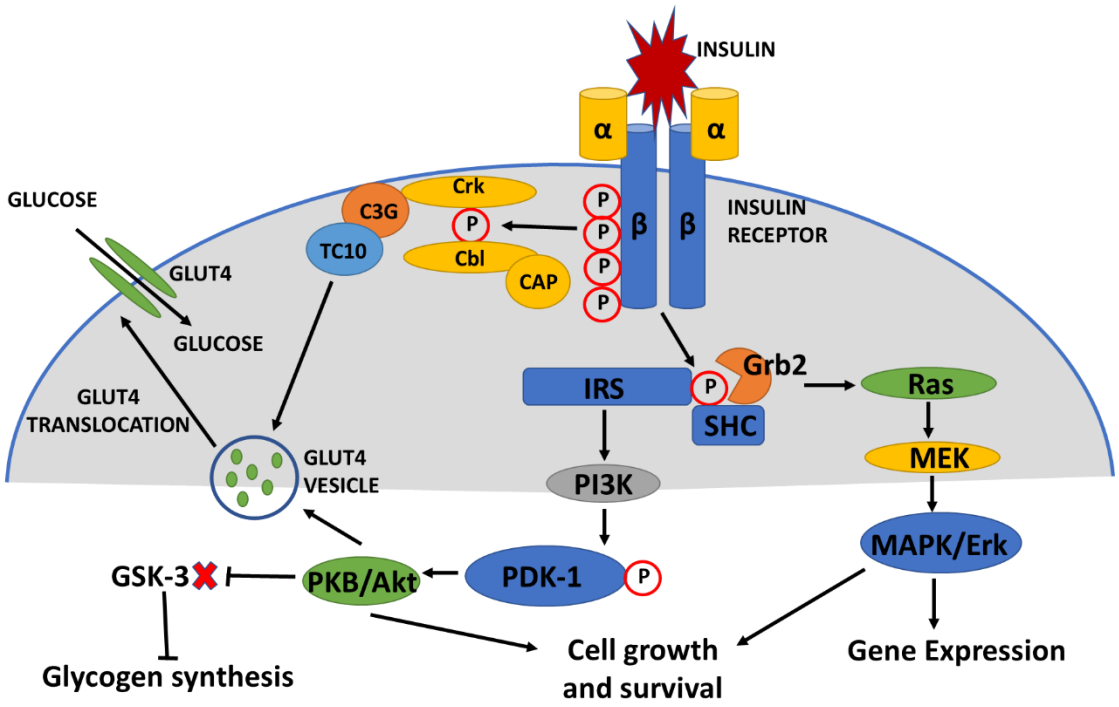

Figure 1. 6; Insulin Signalling Transduction Pathway.

Upon insulin binding to its receptor, the receptor autophosphorylates which activates the receptor as a kinase. The receptor binds and phosphorylates and activates adapter proteins IRS and CAP/Cbl/Crk complex. IRS phosphorylation activates PI3K which phosphorylates PDK-1. This activates PKB/Akt transduction pathway which stimulates GLUT4 containing vesicles to translocate to the membrane, promotes cell growth and survival and inhibits GSK-3 causing glycogen synthesis and secretion to increase. IRS phosphorylation also activates the Ras pathway resulting in MAPK driven changes in gene expression and cell growth. The insulin receptor kinase also phosphorylates the CAP/Cbl/Crk complex that associates to C3G, activating TC10 which further promotes GLUT4 vesicle translocation to the cell membrane. Figure adapted from (Saltiel and Kahn 2001).

1.1.6. Insulin Degradation

Insulin degradation is the process of removing insulin from its receptor and deactivating its signalling cascade that results in glucose uptake, as well as insulin hydrolysis by the zinc-metalloproteinase; insulin-degrading enzyme (IDE) removing the hormone from circulation. Insulin has a short half-life of 4-6 minutes in the blood

(Duckworth, Bennett and Hamel 1998) with the main insulin clearance sites being mediated in the liver and kidney in an insulin receptor dependent mechanism.

In a study by Hovorka et al (1993), 80% of total body insulin was found at the liver, where it spent ~60 minutes bound to its receptor, ~6 minutes bound to peripheral receptors and ~3 minutes in the blood (Hovorka, et al. 1993). Insulin internalisation and degradation primarily occurs in the hepatocytes of this organ tissue. In the kidney, ~50% of peripheral insulin is cleared from circulation, however, insulin degradation occurs in all insulin sensitive tissues (Rabkin and Kitaji 1983; Duckworth, et al. 1998).

Insulin receptors bound to insulin are internalised by receptor phosphorylation mediated events thought to depend on the juxtamembrane region of the receptor (Backer, et al. 1990). Internalised insulin receptors with bound insulin is packed into endocytotic vesicles called endosomes which rapidly acidify causing insulin to disassociate from its receptor. Insulin is then partially or fully degraded by IDE (Duckworth, et al. 1998). IDE is a 110kDa zinc-metalloproteinase that consists of two 55kDa domains in its monomeric form. These domains; IDE-N and IDE-C are connected by a 28 amino acid loop that forms a crypt between the two. This charged, polar and hydrophilic crypt contains the catalytic site for substrate binding, which excludes peptides bigger than 70 amino acids long (Hulse, Ralat and Wei‐Jen 2009).

IDE hydrolyses insulin initially on the B-chain, followed by hydrolysis of the disulphide bond connecting to two different chains (Seabright and Smith 1996). Unbound insulin

receptors are subsequently recycled to the plasma membrane via diacytosis where it can freely bind to other circulating insulin molecules (Duckworth, et al. 1998).

1.2. Diabetes Mellitus

Diabetes mellitus is a polygenic metabolic condition characterised by high circulating blood glucose defined as 'hyperglycaemia'. The disease is characterised by diminished insulin secretion or reduced insulin sensitivity at target tissues or a combination of both. As these deficiencies frequently coexist and work synergistically in an individual, it is often hard to determine the primary cause for the disease onset. In addition, there are numerous class types of diabetes all with different causes and risk factors (American Diabetes Association 2014). The three most common are:

- **Type 1 Diabetes (T1D)** is an autoimmune condition where the immune system attacks and destroys the pancreatic β-cells. The resultant loss of insulin secreting cells causes hyperglycaemia and further downstream complications. There are many contributing factors to the onset of this condition such as genetics, epigenetics, immunological and environmental factors. The onset occurs with increasing incidence in earlier life (under 10 years) and accounts for ~10% of all diabetics (Paschou, et al. 2018). Treatments for this will typically be insulin injections.
- **Type 2 Diabetes (T2D)** is the most common classification accounting for ~90% of all diabetics. The condition is characterised by increased hyperinsulinemia, loss of insulin sensitivity and β-cell failure and resultant hyperglycaemia. T2D has a slow onset developing over many years and has a number of

contributing elements; the main risk factor being obesity and high sugar and fat diets. A change in lifestyle, diet and oral medication is often used to treat T2D, however insulin injection may be necessary if β-cell failure is advanced.

- **Gestational Diabetes (GD)** occurs in ~5% of all pregnancies and imposes pregnancy and birth complications as well as a risk to both mother and child of developing T2D in the years following the pregnancy. GD results due to an inability for the mother to increase their insulin response by ~200-250% to maintain a euglycemic pregnancy, and is thought to be caused by pregnancy hormones as well as obesity related insulin resistance (Kampmann, et al. 2015).

1.2.1. Diabetes Mellitus Epidemiology

1.2.1.1. Worldwide Prevalence, Distribution and Cost

Diabetes is one of the fastest growing global issues of the modern world, affecting all countries regardless of economic power and social class (however a lower-socio economic status does correlate with a higher prevalence (Rabi, et al. 2006)) and continues to grow at an alarming rate. It is estimated that in 2017, 425 million people worldwide, (roughly 8.8%) aged between 20 and 79 had diabetes. This is a huge increase from the 127-182 million (4.7%) thought to have diabetes in the year 1980. This occurrence is set to increase further to a predicted 629 million people aged 20-79 by the year 2045 (International Diabetes Federation 2017; Danaei, et al. 2011; Ogurtsova, et al. 2017). Diabetes has a slightly higher estimated prevalence in males than females affecting 9.1% and 8.4% respectively, peaking between the ages 65-69 years for males and 75-79 years for females.

Age-adjusted comparative analysis indicates that North America and the Caribbean region has the highest prevalence of diabetes of 11%, followed by the middle east and North Africa (10.8%), South-East Asia (10.1%), Western Pacific (8.6%), South and Central America (7.6%), Europe (6.8%) and lastly Africa (4.4%). These varied prevalence percentages are due to many factors such as levels of obesity, nutrition, genetics and urbanisation with the concordance of the condition being higher in urban environments compared to rural locations. This trend is therefore set to continue due to sustained global urbanisation. In terms of individuals with diabetes, it's estimated China has the most (114.4 million) followed by India (72.9 million) and the United States (30.2 million) and is therefore a reflection of countries with larger populations (International Diabetes Federation 2017).

A recent study by Bommer et al, (2017) determined that the global diabetes-associated costs in the year 2015 was as high as 1.31 trillion US dollars ($) accounting for 1.8% of the world's total gross domestic product (GDP). This observably varied between countries dependent upon their GDP with the North American region having the highest total percentage spent on diabetes, whilst also having the highest absolute costs globally. Diabetes is a universally significant economic burden that is set to substantially rise in response to increasing incidences with low to middle-income countries bearing a larger portion of future expenditure burden than high-income countries (Bommer, et al. 2017; World Health Organisation 2016)

1.2.1.2. United Kingdom Prevalence, Distribution and Cost

3.2 million UK nationals have been diagnosed with diabetes as of the year 2013 with the actual occurrence rate believed to be much higher. This is estimated at more than

one in seventeen, with over half a million people living in the UK that have undiagnosed diabetes. Data from the 2012/3 quality and outcomes framework indicate that the diagnosed prevalence in England, Northern Ireland, Scotland and Wales is 6.0% (2,703,044), 5.3% (79,072), 5.2% (252,599) and 6.7% (173,299) respectively, giving an average diabetes prevalence of 6% of the total UK population. This is conservatively around 7.5% when taking into consideration diagnosed and non-diagnosed individuals. This in agreement with expected global figures is set to increase to over five million people by the year 2025 (Diabetes UK 2014). The believed cost of diabetes to the National Health Service (NHS) was £23.7 billion in 2012 with £9.8 billion accounting for direct costs. This accounts for 10% of the whole NHS budget and is projected to rise to over 17% in the next 20 years (Hex, et al. 2012).

1.2.2. Diabetes Mellitus Symptoms and Diagnosis

Detecting and diagnosing type 2 diabetes is crucial in combatting the onset of the condition. Early diagnosis of prediabetes or early stage diabetes can limit further damage to important glucose regulating insulin secreting pancreatic β-cells and insulin target tissues such as skeletal muscle and adipose tissue. This will allow the best possible outcome with multiple treatment options to permit prolonged life and avoidance of downstream complications attributed directly to diabetes. Common noticeable symptoms arise due to increased circulating blood glucose concentrations that the body can no longer manage, in response to diminished insulin secretion or diminished insulin sensitivity. The increased circulating blood glucose concentration will start to damage peripheral systems; subsequently in response, the body will try

to expel the excess glucose in the urine. The following common symptoms are a result of this:

- Urinating more frequently, particularly ay night
- Increased thirst
- Fatigue
- Unexplained weight loss
- Blurred vision
- Slow wound healing

Despite these common symptoms, as the undiagnosed patient data demonstrates it is possible to have diabetes for many years without noticing, as the condition manifests gradually over time. This can mean that it may not always present itself with any clear symptoms or symptoms that make you feel unwell (NHS 2017).

In 2011 World Health Organisation (WHO) recommended that glycated haemoglobin (HbA1c) be used as a diagnostic test for diabetes. This test indicates the level of average circulating blood glucose, and the expert advisory group recommended a level of 6.5% and above (>48mmol/mol) indicates a positive result for the condition. A reading of 6-6.4% indicates a patient with a very high risk of developing diabetes without lifestyle adjustments and warrants retesting a minimum of every three years (World Health Organization 2011; National Institute for Health and Care Excellence 2012). An oral glucose tolerance test (OGTT) is also used to classify patients that have impaired carbohydrate tolerance and has been shown to have reasonable accuracy in predicting insulin sensitivity and insulin release. After a 10 hour overnight fast,

subjects ingest a high glucose liquid with blood glucose measured at 30 minute intervals for 2 hours. A healthy individual will have a starting glucose concentration lower than 6mMol/L and less than 7.8mMol/L two hours after the test. A diabetic patient will have a starting concentration of more than 7mMol/L and more than 11mMol/L two hours after.

1.2.3. Type 2 Diabetes

Type 2 diabetes is characterised by the dysregulation of glucose homeostasis as a result of insulin resistance and impaired β-cell function. There are numerous risk factors to developing type 2 diabetes. Obesity is the largest risk factor, yet other lifestyle factors such as physical activity, smoking and alcohol as well as genetic predispositions all play a role in its development (Wu, et al. 2014).

Typically, insulin resistance in primarily muscle tissue in response to years of chronic exposure to high sugar and fat is the first sign of type 2 diabetes development (Petersen, et al. 2007). In response to the onset of insulin resistance, the pancreatic β-cells will initially adapt to combat the decrease in insulin sensitivity by increasing insulin gene expression and β-cell mass, resulting in a compensatory increase in insulin secretion to maintain normal glycaemic levels. Research suggests that β-cell mass is mainly increased in response to increased circulating nutrients. Increased circulating glucose can activate mTOR signalling directly and indirectly via AMP kinase. The mTOR pathway is known as an important regulatory process for β-cell proliferation and mass (Chang-Chen, Mullur and Bernal-Mizrachi 2008)

Stimulation of the IRS-2 with insulin-like growth factors causes PKB phosphorylation which in turn inactivates the forkhead-O transcription factor-1 increasing expression of transcription factor PDX-1, which increases insulin gene transcription and promotes proliferation and growth. Increased GLP-1 production from intestinal L-cells can also activate PKB and IRS-2 via CREB (cAMP response element-binding protein). Increased FFAs and signalling via GPCRs may also have a proliferative effect (Prentki and Nolan 2006). As a result, insulin secretion has been demonstrated to be more than double in non-diabetic morbidly obese patients compared to control patients (Camastra, et al. 2005).

The increase in cell mass and gene expression increases insulin secretion enough to overcome the initial insulin resistance, however in response to chronic exposure to high sugar and high fat for an undetermined number of years, β-cells begin to fail. The mechanism behind this are discussed in more detail in glucolipotoxicity section (section 1.3). Consequentially, prolonged exposure to hyperglycaemia and constant high demand for insulin, eventually results in decreases in insulin mRNA transcription, insulin content and insulin secretion (Olson, et al. 1993). Pancreatic β-cell mass was reported to be >40% reduced in type 2 diabetic patients with a 10-fold increase in β-cell apoptosis compared to healthy controls (Butler, et al. 2003). Diabetes is thought to clinically develop at 65% β-cell mass reduction (Meier, et al. 2012), resulting in complete dysregulation of glycaemic and fatty acid control which can be detrimental to all tissues types, including further compounded toxicity to β-cells. The action of β-cell adaptation and failure is represented in Figure 1.7.

Figure 1. 7; β-cell adaptation and failure in type 2 diabetes in response to chronic exposure to glucose and free fatty acids.

In response to insulin resistance, insulin gene expression, β-cell mass and insulin secretion increases. After an undetermined period of time, β-cells begin to fail and can no longer compensate for the higher demand and insulin. The loss of β-cell mass and function results in complete loss of glycaemic control, with levels remaining constantly within the hyperglycaemic range. Figure from (Poitout, et al. 2010)

Downstream complications of type 2 diabetes arising from poor glycaemic control in the face of β-cell failure are very serious and can be life threatening. Diabetic nephropathy is the largest cause of end stage renal failure characterised by proteinuria and diminished glomerular filtration and if untreated it can be fatal (Chaturvedi 2007). Diabetic retinopathy caused by hyperglycaemic dependent microvascular damage is the leading cause of preventative blindness in adults ages 20-74 years (Fong, et al. 2004). Diabetic neuropathy is the leading diabetic cause of

patient hospitalisation and is the most common cause of non-traumatic lower limb amputation. It kills 25-50% of patients with diabetic neuropathy within 10 years due to myocardial infarction (Bansal, Kalita and Misra 2006). Diabetes is a main risk factor for developing cardiovascular disease and is the primary cause of diabetes related mortality as a result of oxidative stress inhibited atherogenesis, myocardial damage after ischemic events and diminished low-density lipoprotein oxidation (Leon and Maddox 2015; Wu, et al. 2014).

1.3. Glucolipotoxicity in β-cells

As type 2 diabetes is characterised by both high sugar (hyperglycaemia) and high fat (hyperlipidaemia), it is important to understand the synergistic destructive mechanistic pathways of both toxic levels of sugar and fat termed 'glucolipotoxicity' and is demonstrated in Figure 1.8.

1.3.1. Glucotoxicity

Glucose is required for energy production and is stored primarily in the liver as glycogen which can be mobilised and converted back to glucose via gluconeogenesis when blood glucose concentrations are low. Glucotoxicity refers to the chronic exposure of tissues to high levels of circulating blood glucose concentrations from the diet. One central mechanism by which high glucose concentrations cause damage to pancreatic β-cells causing the onset of diabetes is through the generation of oxidative and ER stress (Hasnain, Prins and McGuckin 2016).

High levels of reactive species such as reactive oxygen and nitrogen species, ROS and RNS respectively, can be generated by hyperglycaemia in numerous key pathways.

Glyceraldehyde autoxidation occurs from enolization of the product of aerobic glycolysis; glyceraldehyde-6-phosphate, to produce α-ketoaldehydes. These can in turn be auto-oxidised to produce hydrogen peroxide (H_2O_2) and hydroxyl radicals (OH·) (Wolff and Dean 1987). Glycerol-3-phosphate can be acylated to diacylglycerol which can activate protein kinase C (PKC). PKC activation has numerous biochemical actions including nicotinamide adenine dinucleotide phosphate (NADPH) oxidase activation. NAPDH oxidase is thought to be an integral activator of receptor stimulated ROS production (Lee, et al. 2003). H_2O_2 is also produced by glucosamine production via the hexosamine pathway (Kaneto, et al. 2001). Elevated glucose also increases the mitochondrial protein gradient via electron overproduction in the TCA cycle inhibiting complexes I and III, promoting superoxide (O_2·) species production (Du, et al. 2000). Superoxide produced in the mitochondria is not able to freely move across the membrane due to its charge, so is converted to the less reactive hydrogen peroxide by superoxide dismutase. Hydrogen peroxide can freely diffuse into the cytosol where it is converted back to the more reactive hydroxyl species. Increased glucose can also induct the *NOS2* gene which encodes for iNOS resulting in elevated nitric oxide (NO) production. Numerous reactive species can then react together to form new species such as peroxynitrite formed from superoxide and NO (Hasnain, et al. 2016; Gerber and Rutter 2017).

As β-cells have very low intracellular antioxidant systems compared to other tissues they are considered more susceptible to oxidative stress. In fact, compared to the liver, β-cells express only 1% catalase, 2% glutathione peroxidase (GPX) and 29% superoxide dismutase (Lei and Vatamaniuk 2011). As a result, increases in reactive

species concentrations primarily damage the mitochondria. Reactive species can damage mitochondrial DNA and intrinsic mitochondrial proteins, which in turn affects a β-cells ability to generate ATP. As ATP is a main instigator in the insulin secretory pathway, exposure to chronically elevated glucose concentrations inhibits glucose stimulated insulin secretion (N. Li, et al. 2009).

Reactive species can also activate uncoupling protein-2 which can uncouple mitochondrial mediated oxidative phosphorylation decreasing reactive species generation, but also further diminishing ATP generation (Prentki and Nolan 2006). Furthermore, increased reactive species generation also decreases the expression of insulin gene transcription factors PDX-1 via c-Jun N-terminal kinase pathway activation and nuclear uptake of forkhead box protein O1 and MafA via p38 MAPK dysregulation further decreasing β-cell ability to synthesise and secrete insulin (Andrali, et al. 2008; Gerber and Rutter 2017).

1.3.2. Lipotoxicity

Long chain non-esterified fatty acids, also referred to as free fatty acids (FFAs) are an important energy source for most tissue types particularly in periods of intense prolonged exercise or starvation. FFAs are not only substrates for oxidative metabolism but also play a role in cell signalling, gene expression and enzymatic activity. In obesity conditions, circulating FFAs are increased and accumulate as long chain fatty acyl-CoA's which have toxic effects at a cellular level; this is termed lipotoxicity.

FFAs converted to fatty acyl-CoA's are primarily transported into the mitochondria or peroxisomes via carnitine-palmitoyl transferase-1 (CPT-1) where they undergo β-oxidation. Acyl-CoA dehydrogenases enzymatically remove two carbons from the FFA acyl-chain to produce acyl-CoA which enters as a substrate into the TCA cycle to produce ATP (Rui 2014). In obesity with increased circulating FFAs, fatty acid oxidation is increased, forcing the mitochondria electron transport chain to increase electron production, inhibiting mitochondria complex I and III driving increased production of superoxide species (Fisher-Wellman and Neufer 2012). FFA intermediate diacylglycerol can similarly induct reactive species (hydrogen peroxide and superoxide) generation through PKC activation mediated activation of NADPH oxidase (Schönfeld and Wojtczak 2008; Jaishy and Abel 2016).

Increased FFA also have the ability to uncouple mitochondrial carriers particularly via the activation of the high FFA affinity uncoupling protein-1 which in turn diminishes ATP production, inhibiting β-cell insulin secretion. This alongside FFA driven increases in pro-apoptotic gene expression (Bax and Bcl2), synthesis of ceramide and increases in reactive species production, can generate large holes in the mitochondrial membrane known as permeability transition pores. The opening of these pores releases proapoptotic factors into the cytosol initiating the lipoapoptosis cascade (Rial, et al. 2010).

It is important to note that increased circulating FFAs in the presences of high levels of glucose are blocked from fatty acid β-oxidation due to the inhibition of CPT-1 from increased malonyl-CoA production, leading to the accumulation of more harmful fat intermediates such as long chain acyl-CoA esters. Glucose resultantly exacerbates

lipotoxicity, and this combinative destructive action is what is meant by the term glucolipotoxicity (Poitout, et al. 2010).

1.3.4. Glucolipotoxic Driven ALEs and AGEs

Membrane phospholipids and triglycerides are main targets for glucolipotoxic upregulated radical hydroxyl species attack, which form lipid radicals. These radicals are subsequently oxidised allowing lipid peroxidation of their acyl chains. After bond reconfiguration, more hydroxyl radicals are captured in this process and propagate the acyl chain length. Upon nonezymatic hock cleavage, phospholipids and triglycerides with shortened acyl chains and the reactive carbonyl species (RCS) α,β-polyunsaturated lipid aldehydes are produced. The shortened acyl chain in structure, of membrane phospholipids and triglycerides disrupt membrane architecture (Hauck and Bernlohr 2016). α, β-polyunsaturated lipid aldehydes, of which 4-hydroxynonenal (4-HNE) is the most well-researched can have serious damaging effects acting as advanced lipid end product (ALE) precursors.

4-HNE can react with amino acid residues cysteine, histidine and lysine of proteins. There are two possible reactions, either with the primary amine to form a reversible Schiff base which forms more complex compounds, or it can covalently bond with the β-carbon forming a C=C bond. These reactions are known as Michael's addition, and produce ALEs as a result. ALE production can induce protein crosslinking, protein aggregation and structural reconfirmations resulting in diminishing protein function (Esterbauer, Schaur and Zollner 1991; Negre-Salvayre, et al. 2008).

Advanced glycation end products (AGEs) are produced from reducing sugars nonenzymatically reacting with amino acids in protein and lipids. Glucose is a reducing sugar and its concentrations is directly proportionate to glycation product formation. Reactive carbonyl species such as 3-deoxyglucosone formed from increased reactive oxygen species also react with amino acid residues to form AGEs via a different polyol pathway. The formation of AGE is known as the Maillard reaction consisting of a series of reactions forming Schiff bases and Amadori products. As glycation takes several weeks, long serving proteins such as structural tissue components are primary targets.

N-carboxymethyl-lysine (CML) like 4-HNE, is the most characterised AGE, produced via the glycation oxidative pathway, and is therefore sometimes referred to as a glycoxidation product. Oxidation of polyunsaturated fats can also result in CML production suggesting a synergistic role of lipid metabolism in AGE formation (Singh, et al. 2001). AGE formation and protein cross linking can cause permanent protein function dysregulation but can also directly bind to specific AGE receptors (RAGE). Binding of the tyrosine kinase RAGE receptor can stimulate reactive oxygen species production via NADPH oxidase activation and inflammatory cytokine production via nuclear factor kappa B (NF-κB) activation (Ramasamy, et al. 2005). AGE can also cause phosphorylation and activation of p38/MAPK which can inhibit glucose stimulated insulin secretion and cause apoptosis in β-cells (You, et al. 2016).

1.3.5. Glucolipotoxic Driven Endoplasmic Reticulum Stress

As β-cells primary function is to secrete insulin, the ER have a heavy biosynthetic load to cope with in response to fluctuations in glucose. Typically, in a normal healthy β-

cell, the ER will misfold roughly 20% of proinsulin (Sun, et al. 2015). The term ER stress is used when ER protein misfolding is above the normal threshold for healthy cells, which triggers transcription and signalling events known as the UPR response. There are three outcomes for UPR activation; decreased protein translation, decreased misfolded proteins and restoration of protein folding and ER associated degradation (ERAD) with the overall aim to restore normal ER protein biosynthesis (Walter and Ron 2011).

The UPR activation is initiated by three signalling arms. RNA-like endoplasmic reticulum kinase (PERK), serine/threonine protein kinase/endoribonuclease (IRE1) and transcription factor activating transcription factor 6 (ATF6) which sit on the ER membrane and detect rises in protein misfolding. In response to increases misfolded protein, BiP which was previously bound to PERK and ATF6 dissociate activating them. PERK autophosphorylates, in turn phosphorylating the translational initiation factor-2 (eIF2) transiently blocking further protein translation by inhibiting the assembly of the 80s ribosome. ATF6 activation causes translocation to the Golgi apparatus where it is cleaved and the ATF6 p50 fragment is translocated further to the nucleus to activate transcription of protein folding chaperones (Biden, et al. 2014; K. Zhang and Kaufman 2008). IRE1 is activated directly by increase in misfolded proteins and dimerises then oligomerises to promote X-box binding protein-1 (XBP-1) translocation to the nucleus where it activates the transcription of genes associated with ER expansion, protein folding and misfolded proteins. ERAD activation labels and retrotranslocates misfolded proteins out of the ER to proteasomes where they are degraded out of circulation (Walter and Ron 2011; Hasnain, et al. 2016).

ER stress is primarily lipotoxic (Cunha, et al. 2008), however chronic glucose concentrations can induce ER stress and the UPR response due to the increased demand for proinsulin biosynthesis and insulin secretion (Lipson, et al. 2006). Elevated FFA production of oxidative stress metabolites such as superoxide, peroxynitrite and nitric oxide can induce ER stress. As can FFAs effect on saturating ER lipid content and perturbing ER calcium handling resulting in protein misfolding and UPR signalling (Cnop, et al. 2010; Borradaile, et al. 2006).

In β-cells, if glucolipotoxic driven ER stress cannot be overcome by UPR adaption signalling, induction of the transcription factor CCAAt/-enhancer-binding protein homologous protein (CHOP) triggers apoptosis as part of the UPR termination pathway. Apoptosis instigation has also been linked directly to IRE1 signalling via the caspase-12 pathway and activation of the JNK protein kinase pathway (Biden, et al. 2014). β-cell death and decrease in overall insulin secretion capabilities further diminishes the ability to overcome hyperglycaemia and hyperlipidaemia compounding the onset of type 2 diabetes.

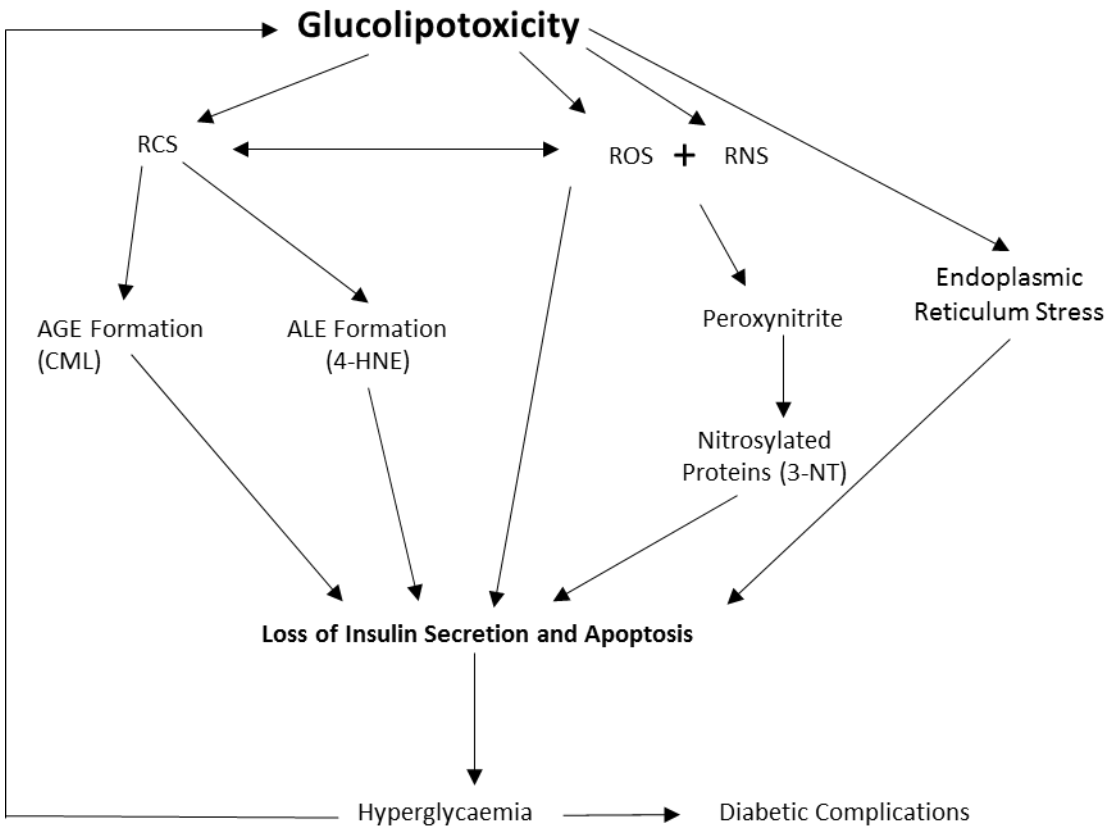

Figure 1. 8; Glucolipotoxic driven stress in pancreatic β-cells.

Increased circulation of glucose and free fatty acids increases reactive stress and ER stress causing loss of insulin secretion and apoptosis. This results in a constant state of hyperglycaemia which causes downstream diabetic complications and further glucolipotoxic driven stresses.

1.4. Current Treatments for Type 2 Diabetes

After type 2 diabetes diagnosis, achieving glycaemic control is the main target for the management of the condition. HbA1c is the main test to monitor glucose homeostasis and is used as a predictive indicator for diabetes progression and management. Anything below 5.7% HbA1c level is considered normal with anything above warranting intervention. Lifestyle changes are the initial port of call to reduce or delay the onset of diabetes. This typically includes losing weight via controlled dieting and exercising, as well as reducing alcohol and sodium intake.

If HbA1c percentages and therefore glycaemic control cannot be achieved via lifestyle changes alone, antidiabetic medication may be required. The major classes or therapeutic medications for type 2 diabetes are biguanides, sulphonylureas, meglitinides, thiazolidinediones (TZD), dipeptidyl peptidase 4 (DPP4) inhibitors, incretin mimetics and sodium-glucose cotransporter (SGLT) inhibitors. These work through three main mechanisms; to increase insulin secretion, to increase insulin sensitivity or to stop gluconeogenesis. Medications are prescribed singly, until HbA1c levels rise above 7.5% whilst medicated, then a combination of two agents or insulin may be prescribed to combat this (Chamberlain, et al. 2016). Numerous medications that operate via different mechanical pathways are required for different stages of diabetes onset and can be tailored to the individual. However, as treatments often loose effectiveness over time, it is vital to constantly develop new strategies separate to mechanisms already proposed.

1.4.1. Biguanides

Metformin (1,1-dimethylbiguanide) is a biguanide derivative that is the first-line oral agent of choice to treat type 2 diabetes across all patient groups. It was discovered in the 1940s as an antimalarial agent, before first being used to treat diabetes in 1957. After intensive scrutiny the compound was approved to treat diabetes in the US in 1995, before being adopted in the UK in 1998 as the primary agent to manage hyperglycaemia, where it is now prescribed to at least 120 million people worldwide (Viollet, et al. 2012; Bailey 2017).

The organic cation transporter 1 (OCT1) is responsible for hepatic uptake of metformin (Shu, et al. 2007) where it accumulates (more than 1000-fold higher than

anywhere else) in the mitochondria because of its positive charge. Metformin in the mitochondria inhibits Complex I of the respiratory chain, suppressing overall ATP production. The resultant change in ATP:ADP ratio and NAD^+: NADH ratio contributes to the reduction of ATP reliant gluconeogenesis. Inhibition of the respiratory chain also activates AMP-activated protein Kinase (AMPK) which increases insulin sensitivity by the phosphorylation of Acetyl-CoA carboxylase (ACC)1 and ACC2. Metformin also stimulates the up-regulation of the glucose transporters GLUT1 and GLUT4 membrane expression in skeletal muscle and adipocytes. The resultant reduction in gluconeogenesis and increase in insulin sensitivity and glucose uptake improves the control over high blood glucose levels (Klip and Leiter 1990; Rena, Hardie and Pearson 2017).

Metformin, which has a half-life of 5 hours, has minimal side effects with low risk of weight gain and hypoglycaemia, the most common side effect being nausea and vomiting, affecting ~20-30% of all patients (Diabetes Prevention Program Research Group 2012). Lactic acidosis caused by dehydration is the most dangerous adverse complication of long-term metformin medicating, affecting roughly 1-5/100,000 patients (Fitzgerald, Mathieu and Ball 2009). Metformin is highly effective during the early stages of type 2 diabetes when insulin is still being secreted by the pancreas, however, as the condition develops, and complete β-cell failure ensues, it loses its efficacy rapidly and other treatments are required.

1.4.2. Sulphonylureas and Meglitinides

Sulphonylureas increase insulin exocytosis from β-cells increasing plasma insulin concentrations, improving glucose uptake. This therefore requires some pancreatic β-cell functionality and is therefore less effective with increasing β-cell failure. Sulphonylureas function by binding to sulphonylurea receptors SUR1 and SUR2 on the cellular membrane. These receptors are members of the ATP-binding cassette superfamily, and upon sulphonylurea binding cause K_{ATP} channels to close resulting in membrane depolarisation. The consequential opening of opening of L_c-type voltage-dependent Ca^{2+} channels increases the cytosolic Ca^{2+} concentration augmenting insulin exocytosis (Sola, et al. 2015).

There are two classes of sulphonylureas. Class I included the compounds tolbutamide, nateglinide and gliclazide which bind to specifically to the A domain of SUR1. These compounds typically have a slow onset of effect and pose a higher risk of hypoglycaemia. The second class, containing compounds such as glibenclamide and glimepiride, bind non-specifically to the A and B domain of both SUR1 and SUR2 and are thought to be more potent and safer compared to the other classes of sulphonylurea compounds. Hypoglycaemia is the main risk of sulphonylurea dosing, as well as common side effect of headaches, nausea, dizziness and weight gain (Sola, et al. 2015; Chaudhury, et al. 2017).

Meglitinides such as repaglinide and nateglinide similarly bind to SUR1 and produce a rapid increase in insulin secretion via K_{ATP} channel closure. However due to their short half-life (less than one hour), they can only augment the first phase of glucose-

stimulated insulin secretion and have no bearing to affect the second phase insulin secretion response (Fuhlendorff, et al. 1998).

1.4.3. Thiazolidinediones (TZD)

Thiazolidinediones, sometimes referred to as glitazones, improve insulin sensitivity increasing metabolic control of type 2 diabetic patients. The exact function of TZDs remains unclear, however it is believed to be associated with the consequential high expression of peroxisome-proliferator activated receptor gamma (PPARγ) upon TZD administration. PPARγ upon TZD induction undergoes a conformational change from its usual heterodimer conformation with a retinoid X receptor, encouraging binding of this complex with the PPARγ response element (PPRE). This alters the transcription and translation of genes containing bound PPRE and include genes responsible for lipid metabolism (Hauner 2002). TZDs have common associated side effects such as edema, weight gain and in rare cases heart failure (Rizos, et al. 2009).

1.4.4. Incretin Mimetics; Dipeptidyl Peptidase 4 Inhibitors and GLP-1 Receptor Agonists

Incretin mimetics is the class of drugs that target the incretin system and include both DPP4 inhibitors and GLP-1 receptor agonists. The incretin effect accounts for ~50% of the insulin secretion response to oral glucose intake (Nauck, et al. 1993). They are becoming increasingly popular for type 2 diabetic prescription as they promote weight loss and decrease gastric emptying whilst increasing glucose-stimulated insulin secretion through the activation of G-proteins associated to adenylyl cyclases (Holz 2004).

The currently available GLP-1 receptor agonist medications are exenatide and liraglutide. These compounds are less susceptible to DPP4 hydrolysis allowing them to have a more sustained effect and have minimal gastrointestinal side effects of vomiting and nausea (Chaudhury, et al. 2017).

DPP4 inhibitors, sometimes referred to as gliptins, block the degradation of endogenous GLP-1 and GIP allowing increased endogenous function to increase glucose stimulated insulin secretion via the method discussed previously. Inhibitors include the compounds sitagliptin, saxagliptin, vidagliptin and others. The most common side effects are respiratory tract infections, headaches and nasopharyngitis with no apparent increased risk of hypoglycaemia (Thornberry and Gallwitz 2009; Chaudhury, et al. 2017).

1.4.5. Sodium-Glucose Cotransporter Inhibitors (SGLT)

SGLT2 inhibitors act independently of insulin, offering another strategy separate to other medications that require some β-cell functionality. SGLT2 inhibitors such as canagliflozin, dapagliflozin and empagliflozin block glucose reabsorption by sodium-glucose cotransporters in the kidneys lowering blood glucose levels, encouraging decreases in weight and blood pressure even in patients where β-cells are irreversibly damaged beyond the point of effectiveness (Riser-Taylor and Harris 2013).

1.4.6. α-Glucosidase Inhibitors

The α-glucosidase inhibitors (acarbose, voglibose and miglitol) competitively inhibit the enzymes activity in the brush border of enterocytes. The inhibition stops the hydrolysation of non-hydrolysable carbohydrates reducing blood glucose

concentrations that occur immediately after dietary consumption (Derosa and Maffioli 2012). Acarbose was also shown to reduce blood glucose concentrations by down-regulating proinflammatory cytokines associated with diabetic inflammation by activating miR-10a-5p and miR-664 in the ileum (Zhang, et al. 2013).

1.4.7. Insulin Therapy

If monotherapy of usually metformin cannot control HbA1c levels for three months, a second therapy will be administered alongside. Insulin therapy is only used when pharmacotherapy intervention strategies can no longer regulate HbA1c to within the guideline limits. Neutral protamine Hagedorn and human insulin is injected subcutaneously at alternating injection sites and has a low risk profile of hypoglycaemia and is relatively low in cost. Other insulin analogs that have a delayed onset and longer lasting effects are also available but are more expensive. Blood glucose levels are measured before meals and after insulin injections to characterise the administration profile to determine correct dosages for future reference (Chaudhury, et al. 2017).

1.5. Carnosine

1.5.1. Carnosine Physiology

Carnosine was first identified or at least mentioned in the year 1900 when acknowledged in a search for nitrogen containing non-proteins in meat extracts (Gulewitsch and Amiradžibi 1900). It is a dipeptide constituting of the two amino acids, L-histidine and β-alanine, bound by an amide bond (Figure 1.9). In mammals, only the skeletal muscle and olfactory bulb contains carnosine in the millimolar range with skeletal muscle accounting for over 99% of an organisms total carnosine content,

but has also been discovered in numerous regions of the brain, kidney, spleen, cerebrospinal fluid and plasma (Boldyrev, Aldini and Derave 2013).

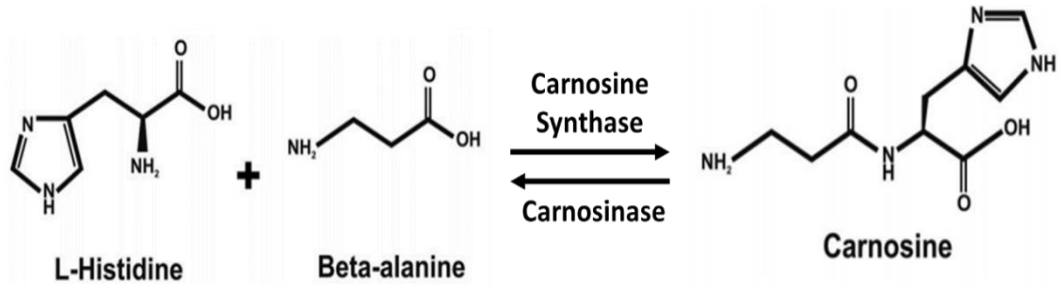

Figure 1. 9; Carnosine synthesis and degradation.
Carnosine is synthesised by carnosine synthase from l-histidine and β-alanine and degraded by carnosinases 1 and 2.

Carnosine is primarily present, and ingested, via red meat but is also endogenously synthesised from its constituent parts by the ATP and Mg^{2+} dependent reaction by carnosine synthase which produces carnosine, an inorganic pyrophosphate (currently unidentified) and either AMP or ADP (Drozak, et al. 2010). Carnosine synthase has previously been identified in the brain, olfactory bulb, heart and skeletal muscle consistent with these tissues high carnosine expression (Bulygina and Kramarenko 1995; Horinishi, Grillo and Margolis 1978; Skaper, Das and Marshall 1973a; Stenesh and Winnick 1960). The homotetramer enzyme has a molecular mass of ~430kDa whilst its 950 amino acid gene sequence is located on chromosome 11q13 in humans, spanning 9 coding exons. It is thought that carnosine synthase has a broad range of substrate specificities and is responsible for various similar peptides to carnosine, formed from subtle replacements or modifications to either β-alanine or l-histidine (Kalyankar and Meister 1959). The most common of which being

anserine, (l-histidine methylated at the nitrogen in the imidazole ring closest to the side chain) and ophidine (l-histidine methylated at the nitrogen in the imidazole ring furthest from side chain) which were identified in 1929 and 1939 respectively (Boldyrev 2012).

Carnosine is hydrolysed by an enzyme named carnosinase, which was originally identified in the kidney of a hog in 1951 (Smith 1951). However, in 1982, a human serum carnosinase was identified as separate and more highly expressed compared to the previous discovered tissue carnosinase (Lenney, et al. 1982). These two members of the M20/M28 metalloprotease family are now conventionally named: carnosinase 1 (CN1) or serum carnosinase and carnosinase 2 (CN2) a tissue cytosolic non-specific dipeptidase (Teufel, et al. 2003). A crystallography study determined that CN2 is a homodimer, where each subunit contains two domains, one for metal binding (domain A) and another for its dimer formation interface (domain B). The several residue interactions between the two domains forms the active site structure and is therefore thought to be crucial for its enzyme capabilities and substrate specificity (Unno, et al. 2008).

The human genes that encode for these enzymes are found head to tail on chromosome 18 and are named CNDP1 and CNDP2 for CN1 and CN2 respectively. CN1 has a stricter substrate specificity compared to CN2. CN1 favours binding and hydrolysis of carnosine, anserine, ophidine and homocarnosine in that order, whilst CN2 has a broader specificity and can be inhibited by a nonhydrolyzable substrate analog called bestatin (Boldyrev, et al. 2013; Unno, et al. 2008). CN1 is also reported

to have a much higher catalytic rate compared to its tissue counterpart, however both maintain the ability to degrade carnosine (Pandya, et al. 2011).

Ingested carnosine can be transported across the cell membrane through numerous proton-coupled oligopeptide transporters. PEPT1, PEPT2 (oligopeptide transporter 1 and 2) PHT1 and PHT2 (peptide/histidine transporter 1 and 2) have a broad specificity and can all transport carnosine and its various analogs (Yamashita, et al. 1997). Dietary ingested carnosine is thought to enter the intestine enterocyte cells through PEPT1, a high-capacity low-affinity transporter. Intracellularly, carnosine is in part hydrolysed by tissue carnosine-2 into β-alanine and L-histidine or transported further across the basolateral membrane by other peptide transporters into the blood, where circulation or further hydrolysis by carnosine-1 occurs (Boldyrev, et al. 2013). PHT1 is primarily expressed in skeletal muscle and the spleen suggesting that this transporter is responsible for carnosine entry into these tissues where the highest carnosine content in humans is observed (Botka, et al. 2000).

1.5.2. Carnosine Biochemistry

1.5.2.1. Metal Ion Chelating

Carnosine has been reported to form complexes with various metal ions such as copper, zinc, cobalt, nickel and cadmium. The carnosine complex formations of former two have been investigated in large detail due to their biological importance in metal toxification.

Carnosine can chelate copper using its carboxylate, amide and amino donor atoms, achieving a molar ratio of 1:1, carnosine: Cu^{2+}. This complex has been shown to form

in both a monomeric structure in solution and a dimeric structure in equilibrium, with the complex encouraged towards dimerization with increasing pHs (Baran 2000). This dimer model achieved in solution is an exact representation of binding properties and doesn't consider physiological environments. This was therefore considered improbable endogenously, due to the low concentration of intracellular copper and alterations caused from other circulating compounds. It was in fact shown via NMR spectroscopy that the copper-carnosine dimer complex was insignificant in human calf muscle samples and should therefore be carefully considered when discussing carnosine's chelating action (Schröder, Schmitz and Bachert 2008). The Zinc-carnosine complexes similarly forms most commonly in a dimer structure at neutral pH and monomerically in more acidic concentrations (Torreggiani, Bonora and Fini 2000). Little is still known about carnosine as an effective metal chelator in physiological conditions and requires further investigation to elucidate the mechanism and functional impact of its chelating capabilities.

1.5.2.2. pH Buffering

It is thought that the nitrogen atom of the imidazole ring of the L-histidine amino acid regulates the pH buffering capacity of carnosine due to its pKa value of 6.72 (Vistoli, et al. 2012). Since the overall pKa of carnosine is 6.83 (Smith 1938), the high proton sequestering capacity therefore enables the rapid reduction of pH gradients in various tissue types. Carnosine is therefore highly researched in muscle performance, to combat decreases in muscular pH caused by lactic acid production during high intensity exercise. Supplementation with β-alanine increases intracellular muscle carnosine concentrations which in turn increases high-intensity exercise capacity due

to an increase in buffering capacity (Sale, Saunders and Harris 2010). One example of this is increases in intracellular carnosine concentrations have been shown to increase sprint training performance in humans (Suzuki, et al. 2004).

1.5.2.3. Radical Species Scavenger

Carnosine is known to directly scavenge reactive species like superoxide dismutase and has a reaction rate similar to another known antioxidant ascorbic acid with carnosine measuring at 10^5 $M^{-1} \cdot s^{-1}$ (Klebanov, et al. 1997). Carnosine can sequester reactive oxygen species as it can form a charge-transfer complex at the nitrogen ion of the imidazole ring, resulting in the formation of less reactive intermediates via a base-catalysed water elimination reaction (figure 1.10) (Torreggiani 1998).

Figure 1. 10; Carnosine scavenging of hydroxyl radical.

Carnosine reacts with hydroxyl radical via a base-catalysed water elimination reaction to form a less reactive stable intermediate (Boldyrev, et al. 2013).

Carnosine has also been shown to scavenge peroxyl radicals. Decker et al (2000) demonstrated that purified carnosine within the millimolar range has the same peroxyl-scavenging capabilities as l-histidine, whilst β-alanine alone had no impact on peroxyl concentrations. This largely supports the mechanistic model suggested, attributing the functional scavenging ability of carnosine to the imidazole ring component of the l-histidine residue of carnosine. They also demonstrated that carnosine's scavenging potential largely increases when free radicals are generated via metal ion induction. This is thought to be due to its ability to chelate metal ions in a manner that doesn't interfere with its anti-oxidant activity (Decker, Livisay and Zhou 2000; Decker, Crum and Calvert 1992).

It is not just reactive oxygen species that carnosine can scavenge, but reactive nitrogen species also. Carnosine was shown to inhibit NO-dependent activation of guanylate cyclase whilst also being shown to decrease total NO concentrations, and increase formation of carnosine/NO adducts in astroglia, demonstrating the compounds ability to react directly with this radical nitrogen species (Severina, Bussygina and Pyatakova 2000; Nicoletti, et al. 2007). Carnosine is also demonstrated to protect against radical species formed from both reactive oxygen and nitrogen species. Supplementation of carnosine within the endogenous range elicited a protective effect against tyrosine nitration adduction from peroxynitrite, which is formed from the combination of superoxide and nitric oxide radicals (Fontana, et al. 2002a).

Carnosine is also reported to prevent and directly react with products of reactive carbonyl species, ALEs and AGEs which can form harmful adducts to both lipids and

proteins altering their function. The most commonly studied ALE is 4-HNE, and carnosine has been reported to directly react with it forming carnosine-HNE adducted compounds. This reaction involves the synergistic action of both amino acid constituents of carnosine and starts with the formation of a Schiff base at the aldehyde group. This is followed by a Michaels addition reaction forming a macrocyclic adduct before hydrolysing to form a stable non-reactive hemiacetal product (figure 1.11) (Aldini, et al. 2002; Boldyrev, et al. 2013). Carnosine can also inhibit AGE species adduction via transglycation, effectively reversing the Schiff base reaction in the first step of protein glycation via nucleophilic reaction on the pre-formed aldosamine. Carnosine can resultantly react directly with AGEs to form stable glucosyl proteins that are less reactive (Szwergold 2005; Seidler, Yeargans and Morgan 2004).

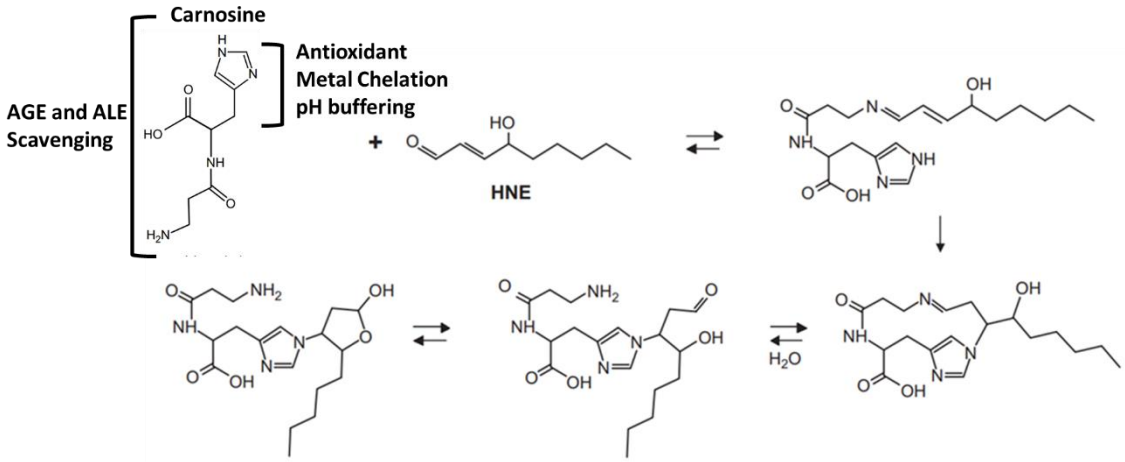

Figure 1. 11; Carnosine reaction mechanism with 4-HNE.

Carnosine forms Schiff base at aldehyde group before undergoing Michaels addition and hydrolysis to form stable derivative. Adapted from (Boldyrev, et al. 2013)

1.5.3. Carnosine in Disease

Carnosine was first investigated for its anti-neoplastic effects in 1986 when intravenous subcutaneous administration of carnosine and β-alanine in mice implanted with sarcoma-180 tumour cells saw a reduction in tumour growth (Nagai and Suda 1986). This work was further supported later when carnosine was demonstrated to reduce growth in various cancer types such as glioblastoma (Renner, et al. 2010), gut (Shen, et al. 2014), colon (Iovine, et al. 2014) and more. The somewhat contradictory anti-proliferative qualities of carnosine have been suggested to be a result of carnosine's effect on glycolytic enzyme activity, metabolic regulation, redox biology, reactive species and their products, redox biology and gene expression and apoptosis. Carnosine's effect is also thought to be specific to cancer cells due to metabolic differences between highly anaerobic cancer cells and other 'normal' cell types (Artioli, Sale and Jones 2018).

Neurodegenerative diseases such as Alzheimer's and Parkinson's present with pathophysiology's defined by neuronal mitochondrial dysfunction causing oxidative stress, loss of cellular function and eventually cell death. Alzheimer's disease is characterised by amyloid plaques and neurofibrillary triangles formed from accumulation of amyloid-β and Tau respectively (Bloom 2014). Carnosine supplementation has been reported to decrease amyloid-β accumulation in amyloid-β and Tau presenting transgenic mice and was attributed to suppressing cognitive decline (Corona, et al. 2011; Herculano, et al. 2013). Parkinson's disease is characterised by dopaminergic neuronal cell death in the substantia nigra, causing progressive disorder of movement (Moore, et al. 2005). Carnosine was recently

presented to protect against salsolinol-induced parkinsonian rat brain and endothelial cells reducing/normalising cell apoptosis, mitochondria derived reactive species and lipid peroxidation (Zhao, Shi and Zhang 2017). Oral supplementation of carnosine was also shown to increase L-dopamine therapy effectiveness at improving patient unified Parkinson disease rating scale score (Boldyrev, et al. 2008).

Acute kidney injury is a clinical syndrome defined by a sudden decrease in kidney function as a result of ATP depletion caused by ischaemic structural loss blocking blood flow. ATP depletion inhibits essential cellular processes causing oxidative stress and apoptosis or necrosis (Makris and Spanou 2016). Oral dosing of carnosine was reported to prevent renal dysfunction in rats after renal artery obstruction as a model of ischaemia (Fujii, et al. 2003), as well as reducing acute kidney injury due to septic shock (Sahin and Burukoglu Donmez 2018). Carnosine also decreased lipid peroxidation and reactive nitrogen species in a rat nephrectomised model of chronic kidney failure characterised by oxidative stress (Yapislar and Taskin 2014).

Type 2 diabetes as mentioned is characterised by chronic exposure to hyperglycaemic oxidative stress resulting in harmful protein and lipid adduction (AGE and ALE formation) and low grade chronic inflammation culminating in β-cell failure and death, and insulin resistance. Interestingly, carnosine muscle concentrations are reported to be significantly decreased by ~45% in type 2 diabetic patient muscle biopsies compared to non-diabetics. This carnosine reduction was not observed in type 1 diabetic tissue muscles supporting the theory that carnosine's lowered concentration in type 2 diabetic muscle samples is attributed to carnosine's sacrificial action to scavenge reactive metabolites and their glycation/lipidation end-products

witnessed specifically in type 2 diabetes (Gualano, et al. 2012). Similarly, a five to seven leucine repeat polymorphism to the carnosinase-1 gene is highly associated with diabetic complications such as nephropathy. Patients with lower numbers of leucine repeats had lower incidences of nephropathy and was associated with lower serum carnosinase activity. Decreased carnosinase activity would increase endogenous carnosine action, suggesting carnosine plays some protective role to offset downstream diabetic complications (Janssen, et al. 2005).

Oral carnosine supplementation has also been shown to improve glucose metabolism by decreasing plasma glucose and glycated haemoglobin concentration in an *ob/ob* diabetic mouse model (Albrecht, et al. 2017), whilst increasing serum fasting insulin concentrations in *db/db* diabetic mice (Sauerhofer, et al. 2007). Human clinical trials also suggest a potential use for carnosine as a treatment for type 2 diabetes as a four month supplementation of cinnamon, chromium and carnosine resulted in a decrease in fasting plasma glucose whilst increasing fat free mass (Liu, et al. 2015). Another trial also reported that carnosine improved diabetic patient responses to a glucose tolerance test in a subset of individuals with previously impaired glucose tolerance, however overall saw no increase in fasting insulin concentrations or witnessed any change to insulin resistance (de Courten, et al. 2016).

1.5.4. β-Alanine Supplementation

As mentioned, carnosine is endogenously synthesised from L-histidine and β-alanine. Supplementation with β-alanine for 4 weeks has shown to increase carnosine concentrations in vastus lateralis skeletal muscle by as much as 60% (Harris, et al. 2006). A similar study reported that 4 and 10 week β-alanine supplementation not

only increased muscle carnosine by ~60 and ~80% respectively, it also correlated to an increase in total work done in a cycling capacity test by 13% and 16% respectively over the two dose lengths (Hill, et al. 2007). β-alanine is an amino acid synthesised solely in the liver through the breakdown of uracil before being primarily stored in the skeletal muscle and is therefore thought to be the rate limiting step of carnosine synthesis (Bakardjiev and Bauer 1994). β-alanine supplementation is therefore currently being extensively investigated as an ergogenic tool to increase muscle carnosine concentrations and enhance skeletal muscle output particularly in an athletic performance context. Surprisingly, little to no published literature has investigated β-alanine supplementation as a means to increase carnosine content and its effects in a disease context.

1.6. Aim and Objectives of Thesis

The aim of this body of work was to identify novel treatments that can preserve or recover β-cell insulin secretory function in response to chronic exposure to high sugar and high fat; the main risk component of developing type 2 diabetes.

The initial part of this thesis details mechanistic experiments to characterise the scavenging effect of the dipeptide carnosine on glucolipotoxic driven reactive species, and to determine whether this action offers a protective effect against glucolipotoxic driven loss of insulin secretion. Secondly, this work investigated whether β-alanine or l-histidine (constituent amino acids of carnosine) supplementation, might have a similar protective action to that of carnosine through similar mechanistic studies. Subsequently, utilising *in silico* docking analysis strategies, carnosine analogs selected to fit the active site of carnosinase-2 and therefore function as carnosinase

inhibitors, were identified and investigated as a therapeutic strategy to improve endogenous carnosine function using techniques described previously.

The latter part of this thesis utilises transcriptomic gene expression analysis in order to identify individual genes, families, and pathway networks, whose expression is most perturbed when exposed to glucolipotoxicity, with the purpose of identifying new therapeutic targets that play a significant role in glucolipotoxic driven diminished insulin secretion capacity in β-cells.

Through the strategies mentioned here, the overall aim is to identify new potential targets for pharmacotherapy intervention that can augment and more importantly reverse the glucolipotoxic loss of insulin secretion in endocrine β-cells.

2. Materials and Methodology

2.1. Reagents and Solutions

2.1.1. Reagents and Materials

Unless otherwise stated, all reagents were purchased from Sigma Aldrich (Dorset, UK) and all plasticware from VWR International Ltd (Lutterworth, UK). Insulin secretion ELISA kits purchased from Mercodia (Sweden). Antibodies were purchases from Abcam (Cambridge, UK) unless otherwise stated.

2.1.2. Solutions and Buffers

SOLUTION	COMPOSITION
Krebs-Ringer Bolution (KREBS)	125 mM NaCl, 1.2 mM KH_2PO_4, 5 mM KCl, 2 mM Mg SO_4, 1.67 mM glucose, 0.1% Bovine Serum Albumin (BSA), 25 mM HEPES, pH7.4
PBS (Phosphate buffered saline) 10X	137 mM NaCl, 2.7 mM KCl, 10 mM Na_2HPO_4, 2 mM KH_2PO_4 pH7.4
RIPA Buffer	150mM NaCl, 0.5% Deoxycholate, 0.1% SDS, 50mM Tris Base, 1% Triton 100, 1x protease inhibitor tablet pH7-8
Sample Buffer	40% glycerol, 240 mM Tris HCl, 8% SDS, 0.04% Blue Bromophenol, 5% β-mercaptoethanol, pH 6.8
Lower Buffer	1.5 M Tris HCl, 0.4% SDS, pH 8.8
Upper buffer	1.5 M Tris HCl, 0.4% SDS, pH 6.8
Running Buffer	0.25 M Tris HCl, 2.5 M glycine, 1% SDS, pH 8.3
Transfer buffer	20% 5 X Trans Blot Transfer buffer (BioRad), 60% H_2O, 20% 100% Ethanol
TBS (Tris Buffered Saline)	50mM Tris-Cl, 150mM NaCl pH7.6
TBST	TBS + 0.1% TWEEN20
Glutamine Stock buffer	2.5mM L-glutamine in lithium loading buffer

Table 2. 1; Composition list of solutions and buffers used.

2.2. Cell Culture

2.2.1. Cell Line

Cell Line and Species	Characteristic
INS-1 - Rat	INS-1 cells are 2-mercaptoethanol-dependent immortal insulin secreting cells that were established from cells isolated from x-ray induced rat transplantable insulinoma. INS-1 cells secrete insulin in response to glucose within the physiological range whilst remaining stable with a high degree of differentiation. This makes them a suitable β-cell model (Asfari, et al. 1992). The passage number of these cells were unknown.
C2C12 - Mouse	C2C12 is an immortalised mouse myoblast cell line that readily proliferates and differentiates in high and low serum conditions respectively. C2C12 cells express GLUT 4 transporters that translocate and activate in response to insulin stimulation resulting in glucose uptake (Yaffe and Saxel 1977; Nedachi and Kanzaki 2006).

Table 2. 2; Table of cells lines used and their characteristics

2.2.2. Media Preparation and Cell Culture/Differentiation

INS-1 rat β-cells were cultured in Roswell Park Memorial Institute (RPMI)-1640 media where 1 litre of distilled water was supplemented with pre-prepared 10.3g of RPMI

powder (ThermoFisher, UK), 2g of Sodium Bicarbonate (26mM), 2.3g of HEPES (10mM) and 3.5µl of β-mercaptoethanol (50µM). RPMI 1640 Media was supplemented with 10% v/v foetal bovine serum (FBS) (Life Technologies, UK), 1% v/v sodium pyruvate (Life Technologies, UK), 1% v/v Penicillin/Streptomycin (Life Technologies) and 5µl β-mercaptoethanol. C2C12 mouse skeletal myoblasts were cultured in high glucose DMEM supplemented with 10% (v/v) fetal bovine serum, 10% (v/v) heat inactivated new-born calf serum and 1% (v/v) penicillin-streptomycin (Life Technologies, UK). C2C12 cells were then switched to DMEM supplemented with 2% (v/v) heat-inactivated horse serum (Life Technologies, UK) to expedite myocytic differentiation. Cells were seeded in T75 tissue culture treated flasks and incubated at 37°C in a 95% air/5% CO_2 atmosphere.

2.2.3. Cell Passage and Amplification

Cells were passaged when 80-90% confluent before loss of cell monolayer. Growth media was aspirated and then cells were incubated in 4ml Trypsin-EDTA (Life Technologies, UK) for 5 minutes at 37°C until complete cell detachment. Detached cells were collected in 4ml of complete growth media and centrifuged at 400 x G for 5 minutes at room temperature. Cell pellets were resuspended in appropriate volume of complete growth media before cell counting and seeding at specifically required densities in new tissue culture treated flasks of plates.

2.2.4. Cell Counting and Plate Seeding

Cells were seeded in 6 or 12 well plates and incubated for 3 or 5 days (72h or 120h) (refer to table 2.3). In all experiments described here out, cells growing in T75 culture

flasks had their spent media aspirated and were detached by incubating in 4ml of Trypsin EDTA (Life Technologies). Trypsin was neutralised with equal volume of complete growth media and the cell suspension collected and centrifuged at 400 x G for 5 minutes in a centrifuge tube. The supernatant was aspirated, and cell pellet was resuspended in ~8ml of complete growth media. Cells were counted manually using haemocytometer. 10µl of cell suspension was loaded into a Neubauer chamber before cell number was determined from four big squares (counting clockwise and North-West) highlighted in figure 2.1 and a cell concentration calculated using the following formula:

$$Concentration = \frac{Number\ of\ Cells \times 10000}{Number\ of\ squares \times dilution}$$

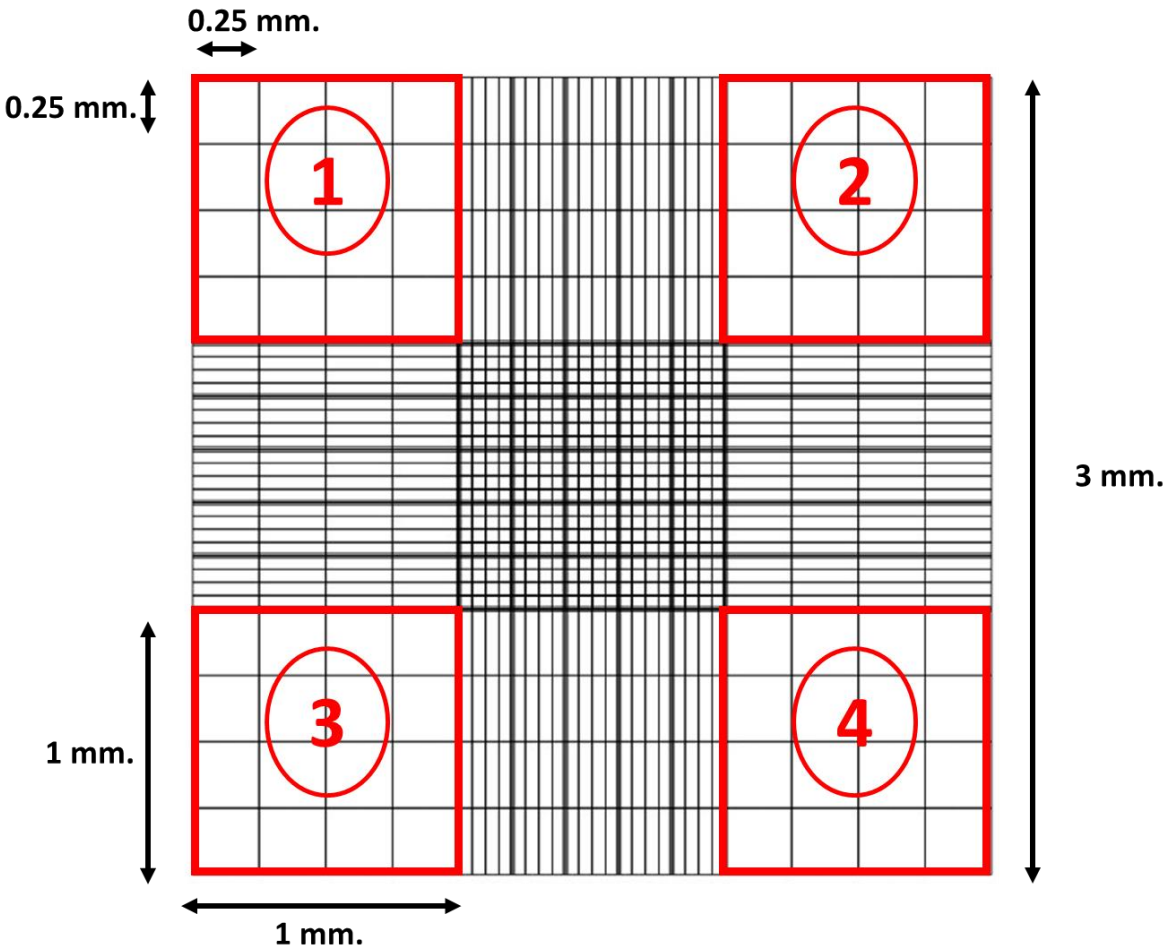

Figure 2. 1; Counting cells using haemocytometer.

Cells were seeded at the various densities specified in table 2.2.3 depending on size of plate.

Tissue Culture Plate (number of wells)	Total Volume (mls)	Experimental Incubation Period (days)	Number of Cells
6	2	3 (4 total)	~70,000
6	2 (media changed on day 2 or 3 of treatment)	5 (6 total)	~100,000
12	1	3 (4 total)	~35,000
12	1 (media changed on day 2 or 3 of treatment)	5 (4 total)	~50,000

Table 2. 3; Seeding density for various treatment lengths and plate type.

2.2.5. Cryo-conservation and Recovery of Frozen Cells

T75 flasks of cells were grown to ~80-85% confluency before aspiration of growth media and incubation in 4ml Trypsin-EDTA (LifeTechnologies, UK) for ~5minutes at 37°C to detach cells. Cells were collected in 4ml of complete growth media and centrifuged at 400 x G for 5 minutes at room temperature. Cell pellets were

resuspended in 4ml of Synth-a-freeze (liquid cryopreservation medium containing 10% dimethylsulfoxide (DMSO)) (Life Technologies, UK) and transferred into 4 cryovials (1ml each). Cells were stored in -80°C freezer in a freezing container designed to achieve a rate of cooling close to -1°C/minute for 24h - 2 months before being transferred to liquid nitrogen for long term storage.

Cells recovered from long term storage were defrosted rapidly before 4ml of complete growth media was added drop by drop. Cells were centrifuged at 400 x G for 5mins before pellet was washed in growth media, resuspended gently in 4ml of growth media and seeded in a T75 tissue culture flask and incubated at 37°C in a 95% air/5% CO_2 atmosphere.

2.2.6. Mycoplasma Screening

All cells were biannually screened for mycoplasma infection using a highly sensitive polymerase chain reaction (PCR) mycoplasma detection kit (Geneflow Ltd., Staffordshire). The primer sets used amplify a highly conserved region within the 16S rRNA gene region of mycoplasma and produces a PCR reaction product of 270bp band when run on an agarose gel.

0.5-1ml of cell culture supernatant was collected and centrifuged at 250 X g for 30 seconds to pellet any cell debris. Supernatant was transferred to a new tube before centrifugation at 20,000 X g for 10 minutes to sediment mycoplasma. The resulting supernatant was aspirated gently, and the pellet resuspended thoroughly with 50µl of buffer solution. Samples were heated at 95°C for 3 minutes.

The PCR reaction reagents were mixed as shown in table 2.4.

Reagents	Volume (µl)
H_2O	35
Pre-Prepared PCR Reaction Mix	10
Test Sample / positive control / negative control	5 / 1 / 5

Table 2. 4; Composition of PCR reaction mixture

Tubes were placed in a DNA thermal cycler with the cycling parameters for PCR shown in table 2.5.

Temperature (°C)	Time (seconds)	Cycles
94	30	1
94	30	35
60	120	
72	60	
94	30	1
60	120	
72	300	
4	∞	

Table 2. 5; PCR reaction cycling parameters

20µl of PCR product was separated by gel electrophoresis using a 2% agarose gel. A positive sample and positive control will have amplified 270bp DNA fragment. An example of a contaminated sample is shown in figure 2.2.

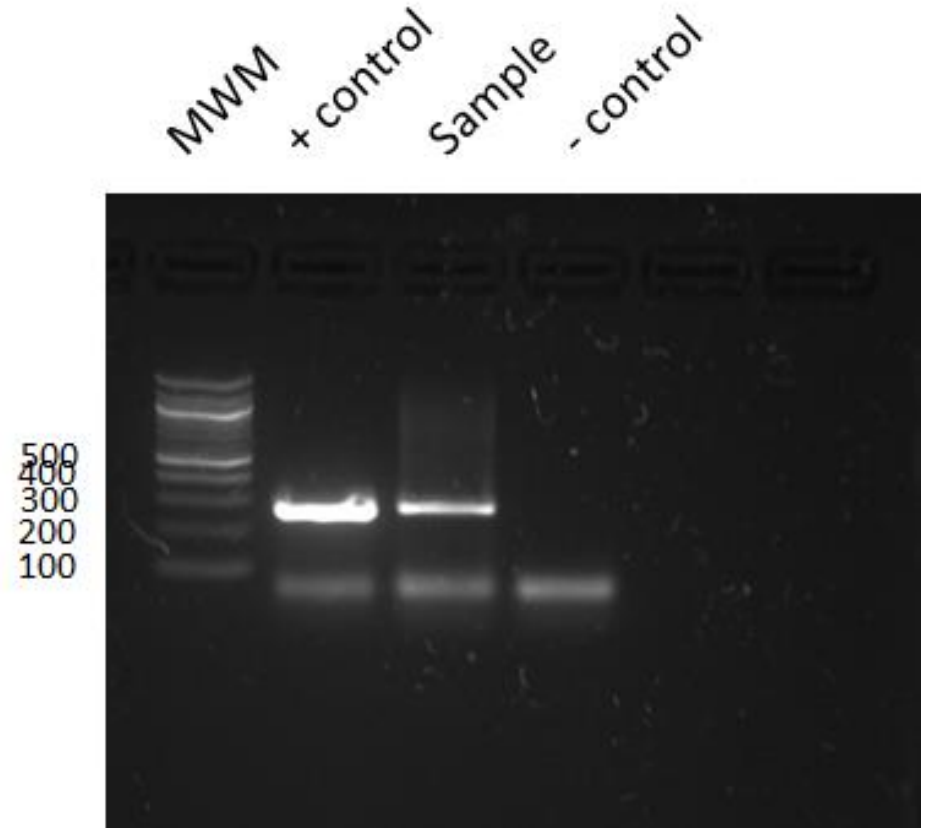

Figure 2. 2; Mycoplasma Screening.
Positive mycoplasma detection example – positive band at ~270bp

Mycoplasma PCR reaction was performed on the supernatant of cultured cells that were growing for a minimum of 24 hours.

2.2.7. Mycoplasma Decontamination and Future Prevention

To decontaminate positively infected cells, an antibiotic proven effective in the elimination of 90% of mycoplasma infections found in cell cultures was used. BIOMYC - 3 (Geneflow Ltd. Staffordshire) based upon a member of the fluoroquinolone group

was used at the recommended concentration and didn't demonstrate any cytotoxic effects to the cells. Cells were grown in media containing 1 X BIOMYC – 3 for 2 weeks and were resultantly free from mycoplasma infections. A non-toxic pharmacidal disinfectant spray (Geneflow Ltd. Staffordshire) containing n-octyl-dimethyl-benzylammonium-acetate, benzelthoniumacetate and methylbenzenethoniumacetate was sprayed in the incubator and tissue culture hoods once a week to prevent mycoplasma recontaminations.

2.3. Mice

2.3.1. Mice Strain

The mice used were CD-1 mice (Charles River, UK) maintained in a 12 hour light/ 12 hour dark cycle and fed a standard rodent diet. After 10 weeks, mice were sacrificed whilst fed (between 08:00 hours and 10:00 hours) by overdose of anaesthetic to facilitate pancreatic islet isolation.

2.3.2. Islet Isolation

CD-1 male mouse pancreata were digested by injection of ice-cold 1mg/ml collagenase P (Roche Applied Science, Switzerland) and 0.15mg/ml DNAse 1 (Roche Applied Science, Switzerland) diluted in RPMI1640 was injected directly into the pancreas duct. Upon pancreas inflation, it was excised and cut into small pieces by surgical scissors and placed in ice cold RPMI. Samples were sealed with parafilm and incubated at 37°C for 7 minutes under static conditions followed by forceful shaking every minute post incubation until suitable pancreatic tissue digestion. Digested tissue was allowed to settle before supernatant removal and transfer to black bottomed container. Islets were picked by hand using microscope and p200 pipette

and cultured in flask containing RPMI 1640 and incubated at 37°C in a 95% air/5% CO_2 atmosphere.

All animal procedures were undertaken by collaborators at King's College London (Dr. Sophie Sayers) and approved by King's College London Ethics Committee and carried out in accordance with the UK Home Office Animals (Scientific Procedures) Act 1986

2.4. BSA Conjugated Fatty Acids and Experimental Media Preparation

To imitate diabetic extracellular glucolipotoxic conditions *in vitro,* cells were incubated for the stated period in complete growth medium containing to 28mM glucose, 200µM palmitic acid and 200µM oleic acid either alone (high glucose or high fatty acid) or in combination (glucolipotoxic). Stock solution of palmitic acid and oleic acid were prepared. 100mM solutions of palmitic acid dissolved in 100% ethanol and sodium oleate dissolved in 50% ethanol were heated to 100°C to ensure full dispersion were used to supplement the complete growth media prior to experimental incubation to a final concentration of 200µM respectively. The media was supplemented with 2% fatty acid free BSA and allowed to incubate at 37°C for a minimum of one hour to allow fatty acid conjugation to BSA. Media was filtered with 0.2µM Millipore PES membrane filters. Individual experimental conditions of high glucose and fatty acids alone or combination are stated in text and figure legends.

2.5. Gene and Protein Expression Analysis

2.5.1. RNA Analysis

2.5.1.1. RNA Extraction

Total RNA was extracted from cells grown in stated conditions using RNeasy Microkit and RNAse free DNAse I kit (Qiagen, UK). Spent media was discarded and cells detached with trypsin before centrifugation at 400 x G for 5 minutes. Appropriate amount of RLT buffer was used to homogenise cell pellet before addition of equal volume of 70% ethanol. Samples were transferred to RNeasy MinElute spin column and centrifuged at 8000g for 15 seconds. Flow through was discarded and 10µl of DNAse I stock solution and 70µl buffer RDD placed in column and allowed to incubate for 15 minutes at room temperature. 350µl of RWI buffer was added and column centrifuged at 8000g for 15 seconds. 500µl of RPE buffer was added before centrifuging again at 8000g for 15 seconds. Flow through was discarded and 500µl of ethanol added to column before centrifugation at 8000g for 2 minutes. Flow through again was discarded and column spun for 5 minutes without lid to dry membrane. 20µl of DNAse free water was added to centre of membrane and sample collected by centrifugation at maximum speed for 1 minute. Samples were stored at -80°C when not in use.

2.5.1.2. RNA Quantification

Extracted total RNA was quantified and quality checked using NanoDrop^{TM} 8000 spectrophotometer (ThermoFisher, UK). The absorbance of samples was measured after blanking with H_2O at 260nm. Absorbance increased linearly with concentration of RNA allowing quantification. RNA absorbs at 260nm whilst sample impurities such

as protein, and ethanol content absorbs at 280nm. The resultant ratio of absorbance at 260nm to 280nm indicates RNA purity with a value of 2 considered pure.

2.5.1.3. cDNA Synthesis via Reverse Transcription

The reaction setup for cDNA was as follows using cDNA synthesis kit (ThermoFisher, UK):

Reagents	Volume (µl) for 1 X reaction
RT buffer	2
dNTPs	0.8
Random Primers	2
Reverse Transcription enzyme	1
RNA	1.5µg
dH_2O	Make up to 20

Table 2. 6; Reverse transcription reaction for cDNA synthesis

1.5µg of RNA was reverse transcribed with a total reaction volume made up to 20µl with deionised water for each RNA sample. The samples were placed in thermocycler set to 25°C for 10 mins, prior to two hours at 37°C then 5 minutes at 85°C. Samples were left at 4°C until collection and analysis.

2.5.1.4. Quantitative PCR

Real time qPCR allows the measurement of amplified PCR product per round of amplification through the use of a fluorescent label. During amplification, a

fluorescent tag (SYBR GREEN – BioRad, UK) binds either directly or indirectly to a labelled hybridising probe. The accumulating fluorescent double stranded DNA molecules are recorded after each cycle of amplification and quantified. The fluorescent signal is proportionate to increasing DNA concentration and therefore allows comparison between RNA samples. The threshold cycle (Ct) value is the point at which fluorescence is first detected to be statistically significant above the background and determines the amplification cycle number of detectable DNA sample. The lower the cycle number that the amplified product takes to be detected, the lower the Ct value. This is inverse to specific RNA expression. Briefly, the sooner a sample is detected, the more RNA for the specific targeted gene is expressed in the sample and vice versa.

2.5.1.4.1. Primer Design

Primers were designed using idt primer design tool and purchased from Sigma (UK). Specific qPCR primers 18-25 base pairs long were designed with a GC content between 30 and 80%, melting temperature of 61.5°C, desalted purification and a concentration of 0.05µM. Primer specificity was then determined using NCBI primer blast search and returned corresponding amplicons between 100 and 150 base pairs allowing the procurement of high level fluorescence without compromising efficiency. Primers are listed in Appendix A.

2.5.1.4.2. Primer Denaturing and Specificity Analysis

A Taq polymerase master mix was prepared containing cDNA and both forward and reverse primers. Samples were placed into the thermocycler with denaturing temperatures ranging from 58-62.5°C. Products were then ran on a 1.5% agarose gel

dissolved in TAE buffer that was heated until agarose was fully dissolved and poured to set in a gel cassette. Samples were loaded with a loading dye alongside a SYBR safe DNA gel stain ladder. The gel was run at 90volts for 50 minutes before visualisation using GeneSnap software. Primer specificity was determined by presence of product bands (figure 2.3).

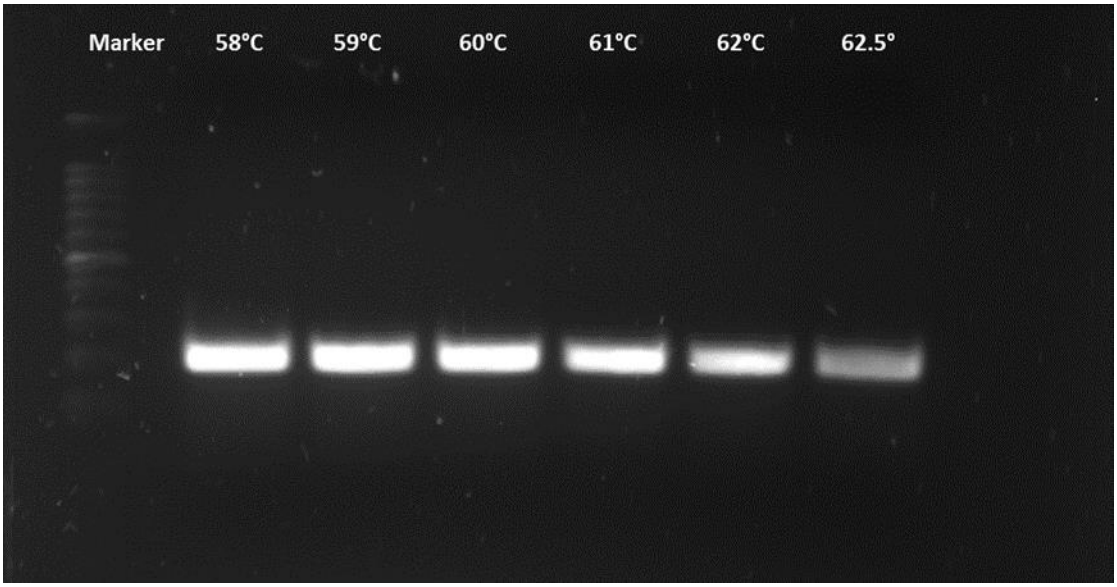

Figure 2. 3; Primer denaturing and specificity analysis.
Example of primer testing using TAAR 2 forward and reverse primer pair

2.5.1.4.3. qPCR Reaction Set up

qPCR reactions were performed using SYBR GREEN (BioRad, UK), specifically designed forward and reverse primers for target gene and cDNA reverse transcribed from extracted total RNA. The reactions were set up as follows:

Reagents	Volume (µl) for 1 X reaction
SYBR GREEN	10
Forward Primer	0.8
Reverse Primer	0.8
cDNA	0.5
dH_2O	7.9

Table 2. 7; qPCR reaction set up quantities

Reactions were performed in triplicate using Corbett Rotor Gene^{TM} 6000 (Qiagen, UK) with the following thermal profile:

Number of Cycles	Temperature (°C)	Time
1	95	5 mins
35	95	5 seconds
	61.5	10 seconds
	72	12 seconds
1	72	3 minutes
∞	10	∞

Table 2. 8; qPCR reaction programme.

2.5.1.4.4. qPCR Data Analysis

Data was analysed using comparative delta delta Ct ($\Delta\Delta_{CT}$) method. This method quantifies the ratio between the amount of the target gene and reference control gene in a sample. The advantage of this is that using an internal reference standard or 'housekeeping' gene target that does not change expression between samples with minimise potential variation by normalising for slight deviations in sample RNA

concentration. GAPDH was used throughout as housekeeping gene for gene expression normalisation.

Having obtained a Ct value for each sample, the $\Delta\Delta_{CT}$ can be used to calculate fold change in gene expression relative to control samples using equation 2^ $\Delta\Delta_{CT}$

2.5.2. RNA Sequencing

2.5.2.1. DNAse Treatment

Contaminant genomic DNA was removed from extracted total RNA samples by treating with DNA-free DNA removal kit (Life Technologies, UK). 0.1 volumes of 10X DNAse buffer was added to each RNA sample before incubating for 10 minutes at 37°C with gentle agitation. 0.1 volumes of DNAse activation agent was subsequently added to each sample and incubated for a further 2 minutes at room temperature mixing regularly. Samples were centrifuged at 1000 X g for 1.5 minutes and RNA transferred to fresh tubes.

2.5.2.2. RNA Quality Assessment

Before performing genome wide RNA sequencing analysis, it is vital to check the quality of extracted RNA. Whilst the aforementioned Nanodrop™ 8000 can determine RNA concentration and RNA purity, it cannot assess other parameters of RNA quality, primarily RNA degradation. RNA integrity was therefore determined using an Agilent Bioanalyser (Santa Clara, CA). This machine assesses the integrity of RNA through the detection of ribosomal RNA (rRNA) which accounts for ~80% of total RNA as opposed to messenger RNA (mRNA), which accounts for only 1-3% that would reduce detection and therefore overall sensitivity. Ribosomal RNA is primarily

comprised of 18S and 28S rRNA species which using a micro fabricated chip, can be separated by mass-to-charge ratio via capillary electrophoresis. An included fluorescent dye intercalates between RNA strands and is quantified where data is translated as an image with bands at different weights and presented as electropherograms. This method assumes that rRNA quality is a true reflection of the mRNA population with an approximate ratio of 2:1 of 28S and 18S respectively, set as the benchmark for intact RNA. Degraded RNA will therefore typically peak before 18S and indicate poor RNA quality. An RNA Integrity number (RIN) value is calculated using an algorithm built-in to the software and given a value from 0-10. A RIN value of 8 and above is considered adequate quality.

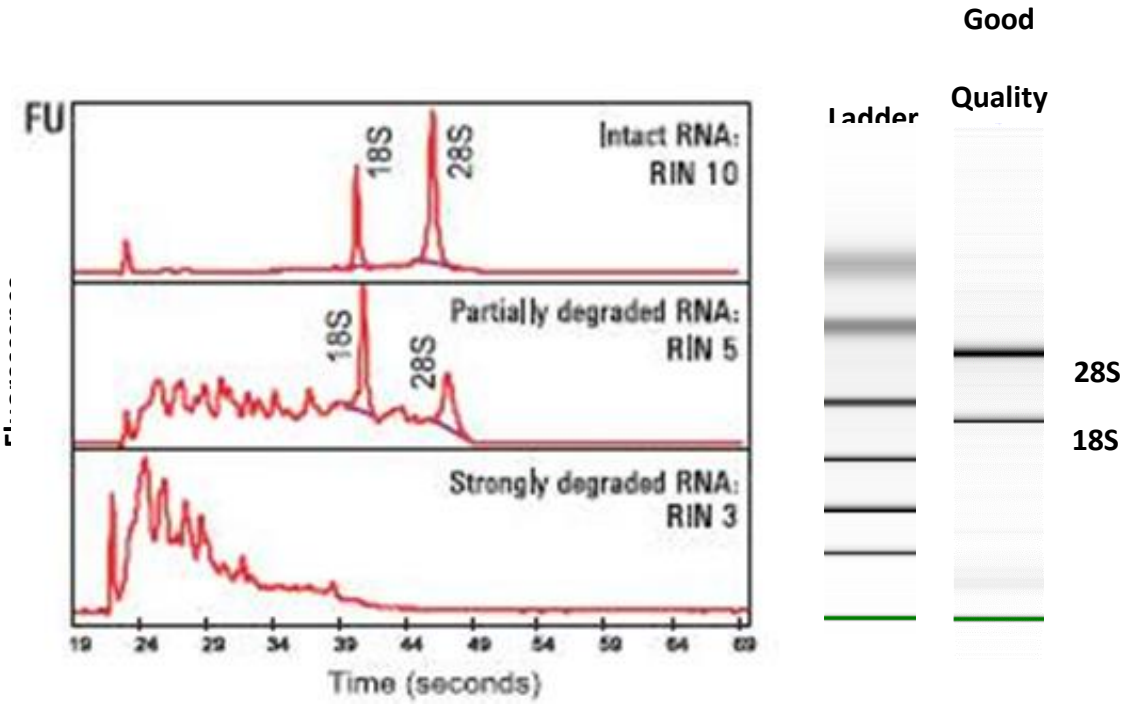

Figure 2. 4; RNA Integrity number (RIN).

RIN scores are calculated from the ratio of 18S to 28S rRNA and used as a measurement of RNA quality and integrity. Scores range from 1-10 with a score of 8 and above considered as a good quality RNA sample. (Figure adapted from Agilent technologies protocol and resultant data).

RNA samples were analysed using a RNA 6000 Nanochip (Agilent, Santa Clara, US) following manufacturers standard protocol. Nanochip wells were preloaded with included gel and fluorescent dye before setting and addition of 1µl of each RNA sample and molecular weight ladder. Nanochip was vortexed for 10 minutes and analysed on Agilent Bioanalyser software. Only samples with a RIN score of 8 and above were used for further analysis.

2.5.2.3. Library Preparation

Known high quality RNA (RIN score >8) was sent to the Sarah Lamble laboratory in Oxford for subsequent library preparation and sequencing using Illumina mRNA seq sample preparation kit (Illumina, San Diego, US).

Initially, samples were ribo-depleted, removing the majority of rRNA allowing increased sensitivity and analysis power of transcriptomes and less abundant sequences.

The library was then generated with the fragmentation of small pieces of mRNA using cations under increased temperatures, before reverse transcription with random primers and resultant cDNA strand synthesis. Double strand cDNA was synthesised by removing the RNA template and synthesising a replacement cDNA strand. The fragments were then 'end-repaired' by blunting the overhanging sequence ends using T4 DNA polymerase and Klenow DNA polymerase. The 3' to 5' exonuclease activity of the added enzymes removes the 3' end overhand, whilst the polymerase activity fills in the 5' overhang. The fragments were then prepared for ligation to

adapters that have a T base overhang at their 3’ end by adenylation at the 3’ end (A base added to 3’ end) through the Klenow antibody polymerase activity.

Adapters were subsequently ligated to the DNA fragments. Fragments were size selected (~200bp) and purified on a gel for downstream enrichment before amplification via PCR with primers that target the adapters. The resultant library was validated, and quality control assured using Agilent Bioanalyser method described previously, before sequencing.

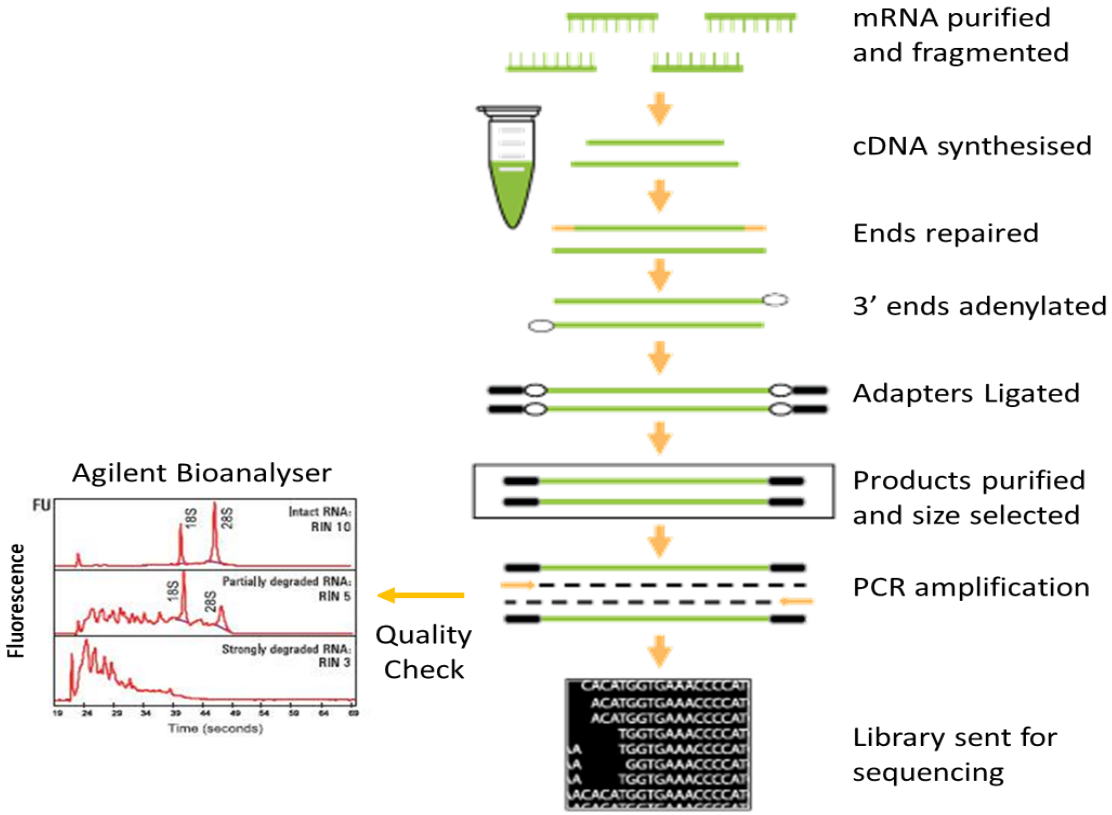

Figure 2. 5; RNAseq library preparation.

RNA is purified by removing rRNA and fragmented into small pieces. Double stranded cDNA is synthesised via reverse transcription before the ends are repaired and adenylated. Adapters are ligated, and samples are size selected and purified before quality check, amplification and resultant library sequencing (Figure adapted from EpiGentek and Agilent Websites).

2.5.2.4. Sequencing

The aforementioned library was used to perform paired end sequencing over one lane of a flow cell on Illumina-HiSeq 2000 instrument in Oxford. This technology depends on random fragmented genomic DNA attachment to an optically transparent planar surface. The attached DNA is extended and amplified to produce and ultra-high-density sequencing flow cell, containing hundreds of millions of DNA clusters, each consisting of roughly 1000 copies of each template. The templates were sequenced using a four-colour DNA sequencing by synthesis technology used reversible terminators with removable fluorescent dyes.

2.5.2.5. Data Analysis

The raw RNAseq data was analysed by Dr. Rob Lowe (Blizard Institute). The output sequencing data (compressed FASTQ files) from the Illumina machine run were aligned to an annotated reference genome using Top Hat v 2.0.9: http://tophat.cbcb.umd.edu. Reads that were aligned to exons, genes and splice junctions were counted using a reference genome 'rn4' extracted from UCSC (http://genome.ucsc.edu/goldenPath/credits.html#rat_credits).

Using the HTseq-count programme (http://www-huber.embl.de/users/anders/HTSeq/doc/count.html), data was visualised and interpreted, calculating gene and transcript expression, and then citing variations in expression between samples and conditions.

Using the programme DEseq (http://www.bioconductor.org/packages/devel/bioc/html/DESeq.html) samples were normalised to correct in-sample distributional differences. Statistical

significance of gene expression fold changes was then calculated by comparing read counts from experimental samples to that of corresponding control samples with p values adjusted using the Bonferroni formula.

2.5.2.6. Network Analysis

To identify enriched pathways and functions between differently expressed genes, data was sent to Dr. Tania Jones (Blizard Institute). Data was loaded into pathway analysis programmes: PANTHER (http://www.pantherdb.org/) and Metacore, version 6.34 from Thomson Reuters (http://thomsonreuters.com/metacore/) which identify enriched networks, pathways, molecular functions, biological processes, cellular components, protein classes and diseases associated with the resultant list of differentially expressed genes. Enrichment is calculated with statistical values for genes within a specific pathway and considered significant if more genes of a given pathway are listed than would be expected by chance, based on the complete number of genes associated with that pathway. Bespoke enriched networks were created indicating directionality and expression change of genes within that pathway.

2.5.3. Protein Analysis

2.5.3.1. Protein Extraction

Cells were cultured for stated period in control or experimental conditions before supernatant was removed and cells were washed in PBS three times. Cells were then scraped in RIPA buffer containing protease inhibitors (1ml/35cm^2 growth area) to destroy cellular integrity and collected in microcentrifuge tubes. Samples were stored on ice for at least 30mins with regular vortexing to disaggregate protein from cell debris. Samples were centrifuged at 400 x G for 10minutes to remove any cell

debris before supernatant was transferred to new microcentrifuge tubes ready for analysis. For short-term storage, protein extracts were stored at 80°C.

2.5.3.2. Protein Quantification - Bicinchoninic acid (BCA) Assay

BCA protein assay (Pierce™ BCA Protein Assay Kit – ThermoFisher Scientific, UK) allows the quantification of protein by chelating copper to protein in an alkaline environment whereby peptides of three amino acids or more form a coloured chelate complex with cupric ions. BCA then reacts with the reduced cuprous ions to produce a quantifiable purple coloured precipitate of one cuprous ion to two BCA molecules with an absorbance at 562nm. The absorbance is concentration dependent with a linear trend within the working range of 20-2000µg/ml. BSA included in the kit was diluted to concentrations ranging from 0-2000µg/ml to establish a calibration curve.

10µl of extracted protein sample or BSA calibrator standard was added to each well of a 96 well plate with 200µl working solution which was prepared following manufacturer's instructions diluting 1 part of BCA reagent B in 50 parts reagent A. Subsequently the plate was incubated for 30 minutes at 37°C before absorbance was read at 595nm (closest absorbance possible using iMark™ microplate absorbance reader – BioRad, UK). The standard curve was set plotting BSA concentration (X-axis) and absorbance (Y-axis) with unknown sample concentration values deduced from this.

2.5.3.3. Western Blotting

2.5.3.3.1. SDS Gel Preparation

Gels were handcast using BioRad Mini-Protean tetra handcast system. A 12.5% polyacrylamide running gel mix was prepared as shown in table 2.5.3.3.1. and was poured between one short and one spacer plate assembled in a casting clamp. This mixture was topped with 100% ethanol to ensure a linear set. Subsequently, once the gel had set, the ethanol was removed and replaced with prepared stacking gel (table 2.9) and a ten 30µl teeth comb and allowed to set.

Ingredients for one gel	Running Gel (µl)	Stacking Gel (µl)
Water	1875	1560
30 Acrylamide Bis-Acrylamide	2475	600
Lower buffer	1560	0
Upper Buffer	0	780
10% SDS	60	30
Temed (Tetramethylethylenediamine)	6	3
10% APS (Ammonium Persulfate)	60	30

Table 2. 9; Recipe for one 12.5% polyacrylamide gel

2.5.3.3.2 Sample preparation, loading, separation and transfer

Known concentration samples were normalised and diluted in RIPA buffer to a final protein content of 20µg and volume of 20µl. 5µl of 4X denaturing sample buffer (950µl denaturing buffer with 50µl β-mercaptoethanol) (BioRad, UK) was added to each sample before incubation at 95°C for 5 minutes. Gels were placed in an electrophoretic tank containing an adequate volume of running buffer and the comb removed. Samples were loaded in a known order alongside a molecular weight marker. Gels were run at 80V for ~20 minutes to ensure no sample overflow. Voltage was then increased to 120V and run until sample front approached the bottom of the gel.

Subsequently, protein were transferred from gel to a nitrocellulose membrane using Trans-Blot Turbo^{TM} Transfer system (BioRad, UK) with the gel placed on top of the membrane and sandwiched between filter paper soaked in transfer buffer. A roller was used to remove air bubbles and excess transfer buffer. Transfer was carried out using manufactures preprogramed protocol for mixed molecular weights (5-150 kDA) 1.3A; up to 25V for 7 minutes. An example of a transferred membrane is shown in figure 2.6.

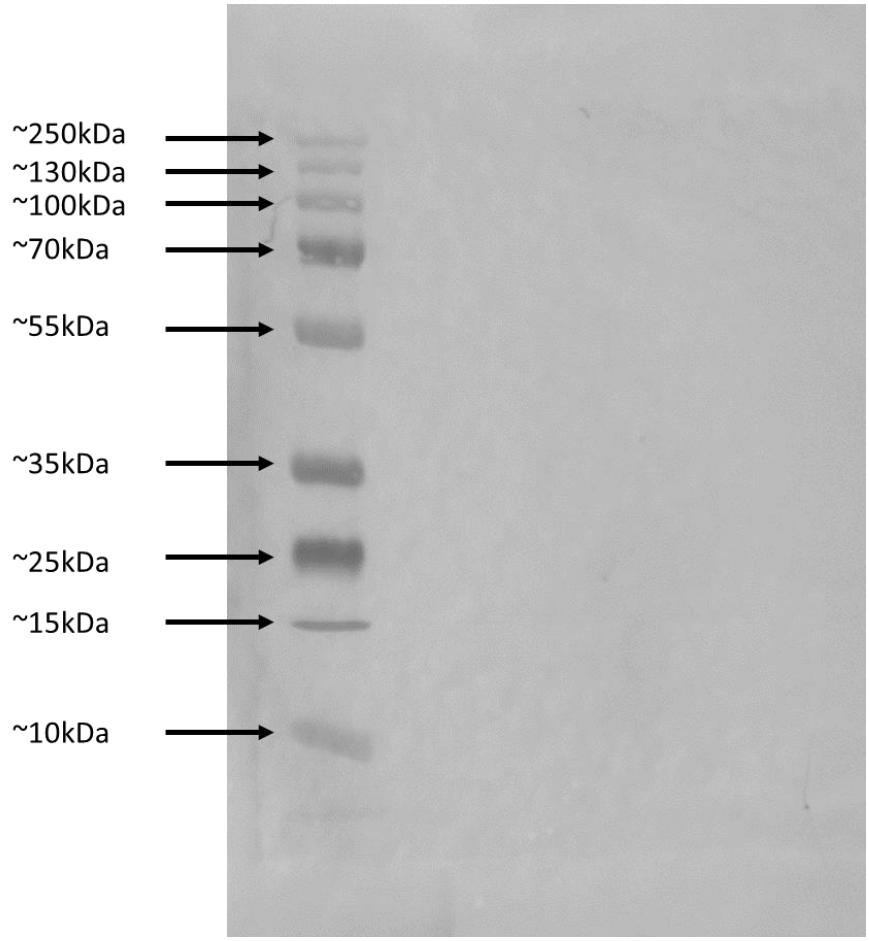

Figure 2. 6; Western Blot Transfer Example.

Separated protein samples were transferred to nitrocellulose membrane using Trans-Blot Turbo^{TM} with preprogramed setting for mixed molecular weights; 25 volts constant for 7 minutes. Tranfer was of good quality as shown by the weight markers.

2.5.3.3.3. Immunoblotting

Membrane was soaked in panceau solution (Sigma, UK) to check for adequate transfer from gel to membrane. Panceau was removed by numerous washes in TBST. Membrane was blocked in 5% (w/v) milk (marvel original dried skimmed milk powder) in TBST for 2 hours. Subsequently membrane was incubated overnight with desired primary antibody (see appendix 2) diluted in 5% (w/v) milk in TBST at 4°C. Membrane was washed three times in TBST for 10 minutes before incubation in appropriate peroxidase-conjugated (HRP) secondary antibody (anti-rabbit or mouse

IgG) diluted in 5% milk in TBST for ~1 hour at room temperature. Membrane was washed three times in TBST for 10 minutes each before being developed in ECL plus mix solution (GE Healthcare, UK) for 5 minutes in darkness and imaged by chemiluminescence sensitive Image reader LAS4000 (GE Healthcare, UK).

Protein band densitometry was performed using programme Image J where intensity of protein of interest band was divided by corresponding housekeeping protein band and data represented as fold change between conditions in comparison to control.

2.6. Cell Function Analysis

2.6.1. Cell Viability

Calcein AM cell viability dye (ThermoFisher, Loughborough) was used to assess cell viability. Calcein AM is a non-fluorescent cell permeable dye that is converted to a green-fluorescent calcein after acetoxymethyl ester hydrolysis by intracellular esterases that viable eukaryotic cells possess. Cells were cultured in standard or experimental conditioned growth media for the stated time period before cell viability assay was performed as follows: Spent media was aspirated and cells were washed 3 times in KREBS. A final concentration of 5µM Calcein AM cell viability dye resuspended in KREBS was loaded for 1 hour before washing again 3 times with KREBS. Cell viability was measured via fluorescence, with excitation and emission at 490nm and 520nm respectively with viability represented as percentage change compared to standard control conditions.

2.6.2. Radical Species Quantification

Reactive species quantification was determined using 2',7'-Dichlorofluorescin diacetate (DCFDA), a non-fluorescent cell-permeable probe that is de-esterified intracellularly and highly fluoresces upon oxidation by intracellular reactive species and conversion to 2',7'-dichlorofluorescein. Within literature, DCFDA is commonly referred to a measurement of reactive oxygen species, however, DCFDA can be oxidised by some reactive nitrogen species as well. The use of DCFDA in this body of work will therefore refer to the presence of all reactive species, not just reactive oxygen (Kalyanaraman, et al. 2012).

Cells were cultured in standard or experimental conditioned growth media for the stated period of time before radical species was quantified as follows: Spent media was aspirated and cells were washed 3 times in KREBS before a final concentration of 20µM DCFDA in KREBS was loaded for 1 hour before washing again 3 times in KREBS. Radical species measured via fluorescence, with excitation and emission at 495nm and 530nm respectively with quantification presented as percentage change compared to control conditions

2.6.3. 3-Nitrotyrosine (3-NT) Quantification

3-Nitrotyrosine (3-NT) residue formation is a product of reactive nitrogen species such as peroxynitrite caused by oxidative stress. Cells were cultured in standard or experimental conditioned growth media for the stated period before 3-NT was quantified as follows: cells were lysed in extraction buffer containing protease inhibitor at a concentration ~ 2 million cells/ml and incubated on ice for 20 minutes. Samples were centrifuged at 16,000 x g for 20mins at 4°C to remove cell debris before

the supernatant was transferred to clean tubes for testing. Samples were diluted to appropriate concentration (8-1000ng/ml) before 3-NT residue formation was determined following 3-NT ELISA kit protocols (Abcam, Cambridge). Cellular protein content was assayed using BCA protein assay (Pierce^{TM} BCA Protein Assay Kit – ThermoFisher Scientific, UK) and used to normalise 3-NT data to protein content.

2.6.4. 4-Hydroxynonenal (4-HNE) Quantification

The α,β-unsaturated hydroxyalkenal 4-Hydroxynonenal (4-HNE) is the primary product of lipid peroxidation caused by oxidative stress. Cells were cultured in standard or experimental condition growth media for the stated period before 4-HNE was quantified as follows. Cells were lysed in RIPA buffer at a concentration of ~2million cells/ml and stored on ice for one hour with regular vortexing, before centrifugation at 400 x G for 10 minutes to remove cell debris and supernatant was transferred to clean tubes for testing. Samples were diluted in RIPA to the appropriate concentration (0.63-40ng/ml) before 4-HNE formation was determined following 4-HNE ELISA kit protocol (Abbexa, UK). Cellular protein content was assayed using BCA protein assay (Pierce^{TM} BCA Protein Assay Kit – ThermoFisher Scientific, UK) and used to normalise 4-HNE data to protein content.

2.6.5. Insulin Secretion

2.6.5.1. INS-1 Insulin Secretion

Cells were grown in standard or experimental conditioned growth media for stated period of time before cells were washed in KREBS 3 times and subsequently incubated for 2 hours in KREBS with or without insulin secretagogue cocktail containing 1mM Tolbutamide, 10mM Leucine, 10mM Glutamine, 1mM 3-isobutyl-1-

methylxanthine (IBMX), 1µM phorbol 12-myristate 13-acetate (PMA) and 10mM glucose. Supernatant was collected and centrifuged at 300 x G for 2 minutes to remove any cell debris before insulin secretion was determined following standard ELISA kit protocols (Mercodia, Sweden). Cellular protein content was assayed using BCA kit protocol (ThermoFisher, Loughborough) and used to normalise insulin secretion data to protein content.

2.6.5.2. Islet Insulin Secretion

In collaboration with King's college; sized match islets were pre-incubated in buffer containing 2mM glucose, 2mM CaCl2 and 0.5mg/ml BSA (pH7.4) for 1 hour at 37°C before incubation in buffer containing 2mM or 20mM glucose for one hour at 37°C with gentle shaking. Islet insulin secretion was determined using radioimmunoassay with an in-house Bovine ^{125}I-insulin raised in guinea pig by repeated subcutaneous injection of insulin coupled to albumin. Diluted 1:60,000, antiserum allowed a detection limit of 8pg. Purified mouse insulin was used as standard.

2.6.6. Cyclic Adenosine Monophosphate (cAMP) Accumulation Quantification

cAMP is an important second messenger in many biological systems and is a known insulin secretion enhancer in β-cells. Cells were cultured in standard or experimental conditioned growth media for stated period of time before cells were washed in KREBS 3 times. Cells were stimulated with KREBS containing 0.5mM IBMX (3-isobutyl-1-methylxanthine) and various trace amine associated receptor ligands at stated concentrations for 30 minutes. Supernatant was removed, and cells were incubated in 0.1M Hydrochloric acid (1ml/35cm^2 culture area) and left at room temperature for 20 minutes. Cells were scraped, collected and centrifuged at 1000 X g for 10 minutes

to remove cell debris before supernatant was transferred to clean tubes for testing. cAMP accumulation was determined following standard Select ELISA kit protocols (Cayman Chemical, US).

2.7. High Performance Liquid Chromatography (HPLC) – Amino Acid Analysis (AAA)

HPLC is a type of column chromatography that allows the identification and quantification of different analytes depending on their polarities and interactions. Analytes in a solvent are pushed through a chromatographic packing material filled column at high pressure. The sample is then carried by a gas stream of either helium or nitrogen where its retention times of the separated sample is measured. This retention time corresponds to known samples allowing the identification of unknowns. This technology can separate and identify concentrations of analytes as low as one parts per trillion making it incredibly accurate and sensitive even at miniscule concentrations. HPLC analysis was carried out in collaboration with Dr James from the NTU sports science department as follows.

2.7.1. Sample Preparation

Cells were detached with Trypsin-EDTA (Life Technologies, UK) by incubating for 5 minutes at 37°C. Cells were pelleted by centrifuging at 300 X G for 5 minutes before washing twice with DPBS (Life Technologies, UK). 15µl of 8M Urea was added to the pellet followed by 20µl of 0.05% ProteaseMAX™ surfactant (Promega, UK) and vortexed to ensure full cell lysis. To the cell mix, 58.5µl of 50mM TEAB (Triethyl ammonium bicarbonate) was added and incubated at 4°C (on ice) for a minimum of 15 minutes. The debris was pelleted by centrifugation at 14000 X G for 10 minutes

and supernatant transferred to fresh tubes. To boost cell lysis, the supernatants were alternated three times being placed in a water bath sonicator at full power for 5 minutes and then ice for 5 minutes. Cell debris was pelleted again by centrifugation at 13000 X G for 5 minutes and supernatant transferred ready for analysis.

100µl of lysed sample was added to 100µl of sulphosalicyclic acid deproteiniser with internal standard or norleucine (500µMol/L). Samples were vortexed thoroughly to ensure complete mixing and left on ice or in 4°C fridge for 30 minutes. A white precipitate formed. Samples were then centrifuged at 10,000 X G for 5 minutes before the supernatant was collected and transferred into correspondingly labelled filter tubes. Samples were centrifuged through the filter for ~1 minute. Filters were discarded and the ultrafiltrate solute was transferred into corresponding amino acid analysis tube for analysis.

2.7.2. Standard Preparation

Firstly, the stock solution was made by mixing 100µl of the acidic and neutral amino acids, 100µl of the basic amino acids, 100µl of glutamine stock buffer and 200µl of the lithium loading buffer.

The first three standards were made as shown in table 2.10.

Standard Concentration (µMol)	Stock solution (µl)	Lithium Buffer (µl)	Sulphosalicyclic acid deproteiniser with 500µMol/L Norleucine (µl)
250	100	0	100
200	80	20	100
150	60	40	100

Table 2. 10; Recipe for higher concentration three AAA standards.

The remaining three standards require diluted stock buffer. This was made by mixing 200µl of the original stock buffer with 500µl of lithium buffer. The remaining standards were made as shown in table 2.11.

Standard Concentration (µMol)	Diluted Stock solution (µl)	Lithium Buffer (µl)	Sulphosalicyclic acid deproteiniser with 500µMol/L Norleucine (µl)
100	100	0	100
50	100	100	100
25	100	300	100

Table 2. 11; Recipe for lower concentration three AAA standards.

All standards were aspirated to mix thoroughly and labelled ready for analysis.

2.7.3. HPLC Sample Analysis

In collaboration with Dr Ruth James (NTU), 40µl of sample or standards ranging from 250-25µMol/L were injected onto analytical column for analysis. Amino acid concentrations were determined using a Biochrom 30+ high-performance liquid

chromatography ion exchange system with OPA derivatisation. Analytes were normalised to the internal standard of norleucine and presented as μM/L concentrations.

2.8. Computation Aided Carnosinase Inhibitor Drug Design

In collaboration with the NTU chemistry department (Dr Garner, Suniya Khatun and Daniel Cotton), the MayBridge library (https://www.maybridge.com) which contains over 53,000 diverse compounds was prepared in OMEGA (https://www.eyesopen.com/omega) for virtual screening in ROCS (https://www.eyesopen.com/rocs). The ROCS system uses an algorithm to identify potentially similarly active compounds to that of a known active compound (in this case carnosine), by virtual 3D shape and chemistry compound comparison, with the theory that molecules with similar shapes and chemistry may have similar function. The top 50 hits, using the Tanimoto combo scoring function in ROCS from the MayBridge library, using carnosine as the reference molecule were selected for further analysis.

The resulting top 50 hits from the library were then tested for their docking ability into the A1 active site of carnosinase-2 using the crystalline structure of this compound pocket and a programme named GOLD https://www.ccdc.cam.ac.uk/solutions/csd-discovery/components/gold/. The analysis provides a binding interaction score which was set to a threshold of 50 to identify compounds with the stronger binding interactions, whilst remaining much lower than that of carnosine to resist enzymatic hydrolysis. Bestatin, the known non-specific competitive inhibitor of human carnosinase-2 (PEPPERS and LENNEY 1988)

was run alongside all compounds as an internal control, as any changes in bestatin docking scores are indicative of internal software errors.

Of the 50 compounds initially screened, 14 scored above the threshold. Of these, 9 were purchased and screened for their capacity as carnosinase inhibitors and were coded M4, M8, M14, M21, M28, M38, M44, M48 and M49. Compounds were disaggregated and dissolved in 1ml of 100% ethanol before dilution in sterilised KREBS and used at a final concentration of 100µM.

2.10. Statistical Analysis

All data were expressed as mean ± standard error of the mean (SEM) (n = 3 or more independent experiments) and calculated as follows:

$$= \frac{Stdev(mean\ values)}{SQRT(Count(mean\ values))}$$

Parameters were compared using one-tailed student t-test assuming equal variance, with statistical significance determined using an alpha value of 5%. A *p* value below 0.05 was therefore considered statistically significant.

3. Carnosine Scavenging of Glucolipotoxic Free Radicals Enhances Insulin Secretion and Glucose Uptake

3.1. Introduction

Type 2 diabetes is a metabolic disorder characterised by pancreatic β-cell dysfunction and cell death, as well as insulin resistance in peripheral tissues. The highest risk factor and leading cause of developing type 2 diabetes is obesity (Cerf 2013). Molecular mechanisms leading to cell failure result from the associated chronic exposure to high circulating sugar and free fatty acid concentrations that are typically ingested from the diet. These conditions typically induce a compensatory increase in cell mass, insulin production and insulin secretion, in order to maintain glucose homeostasis. This is thought to occur primarily in response to the increased free fatty acid concentration rather than glucose, however many of the mechanisms of β-cell adaptation are still largely unknown (Cusi, et al. 2007; Poitout 2008).

After an unspecified period of time depending on the individual pre-dispositions to diabetes, the first specific β-cell specific loss is that of glucose stimulated insulin secretion. This is followed by a decrease is insulin mRNA, thereby resulting in loss of insulin synthesis. Consequently β-cells can no longer adapt as part of a compensatory response and begin to fail from the detrimental effects of circulating sugar and fat levels in the blood. Unless effectively treated, from this point systemic blood glucose concentrations permanently fall within the hyperglycaemic range (Poitout, et al. 2010).

Reactive species generation is a hallmark of type 2 diabetes. In the presence of toxically high glucose and fat concentrations, unwarranted reactive species are generated, including production of O_2^- by mitochondrial processes such as fatty acid

oxidation, as well as *NOS2* gene induction encoding *iNOS* and resulting in increased NO production. These elevated radical species perturb insulin synthesis and the secretory capacity of β-cells by inhibiting PDX1 and MAFA transcription factor expression and activity (Rosca, et al. 2012; Hasnain, et al. 2016). These, along with downstream products resulting from lipid peroxidation and glycation reactions, can interfere with cellular function by disrupting molecular conformation and altering activity and degradation processes (Baynes 2002). It is this, alongside the continual pressure on β-cells to synthesise and secrete more and more insulin in sub-optimal 'stress' conditions that causes a constant feedback cycle, eventual loss of cell function and therefore loss of glycaemic control.

As type 2 diabetes is characterised by multiple defects across several cell and tissue types, numerous different pharmaco-intervention strategies that work through different methods of actions are required. The two main targets for this are drugs that increase insulin secretion from failing β-cells, and medicines that increase insulin sensitivity at target tissues or decrease gluconeogenesis in the liver. Currently, there are a limited amount of options to treat the disease, with metformin and the thiazolidinedione; pioglitazone currently prescribed to increase insulin sensitivity, and sulphonylureas, GLP-1 agonist analogs and DPP-4 inhibitors prescribed to enhance impaired insulin secretion (DeFronzo 2010; Consoli and Formoso 2013). The issue with these either oral or injectable medications is that they often loose effectiveness over time. Thus, there is an urgent need to not only better characterise the underlying causes of the onset of diabetes, and particularly relating to

glucolipotoxicity, but to then identify and develop new targets and treatments that can be used either alone or in combination with existing pharmacotherapies.

Carnosine, a dipeptide synthesised from β-alanine and L-histidine has recently emerged as a promising molecule as a recent study studying the effect of a dietary supplement containing cinnamon, carnosine and chromium was shown to lower fasting plasma glucose and increase lean mass in overweight or obese patients (Liu, et al. 2015). It was also shown to increase fasting insulin and disrupt insulin resistance, resulting in a significant reduction in circulating glucose concentrations in response to a glucose tolerance test (de Courten, et al. 2016). Despite these beneficial findings, there is however a significant absence of literature detailing molecular mechanisms of carnosine action on the pancreas itself.

This project focuses on the dysregulation of insulin secretion in response to a glucolipotoxic model of type 2 diabetes. The aim of this chapter of work was to characterise the scavenging effects of carnosine supplementation in INS-1 β-cells exposed to chronic high glucose and free fatty acid concentrations utilising various ELISA and fluorescent dye techniques. Subsequent experiments were initiated to identify the resultant effect on stimulated insulin secretion in both INS-1 β-cells and primary *ex vivo* mouse islets. Following this, similar supplementation procedures were used in skeletal muscle myotubes to characterise the potential for carnosine as a treatment for both insulin augmentation and insulin sensitivity.

3.2. Results

3.2.1. β-Cell Self Recovery from Glucolipotoxic Exposure

It is well established that chronic exposure to both high sugar and high fat diminishes β-cells ability to secrete insulin secretion in response to a stimuli (Marshak, et al. 1999; Ling, et al. 1996; Marshall, et al. 2007). *In-vitro* studies in the cell line HIT-T15 suggest that diminished insulin content, secretion and gene expression in response to gluocotoxic media incubation can be fully reversed if moved to standard control media. The likelihood of full β-cell functional recovery is however decreased with increasing periods of antecedent glucotoxicity (Gleason, et al. 2000).

In order to investigate whether β-cells have the ability to self-recover from damaging combinative glucolipotoxic (GLT) exposure, INS-1 cells were incubated in the presence of GLT growth media (control growth media supplemented to 28mM glucose and 200µM palmitic acid and 200µM oleic acid) for 3 days, before being removed and replaced with control media for a further 2 days prior to analysis. Cells were then incubated in KREBS buffer or a secretagogue cocktail for 2h and insulin secretion determined. As can be seen in Figure 3.1, cells that were incubated for a full 5 days in GLT media had significantly diminished stimulated insulin secretion, reduced from 5.8 ± 0.2 ng/µg protein in control to 3.8 ± 0.3 ng/µg ($p=0.003$). By contrast, when cells were initially grown in GLT media but then changed to control growth media after 3 days, stimulated insulin secretion was significantly increased compared to GLT conditions increasing to 5.0 ± 0.1 ng/µg ($p=0.01$).

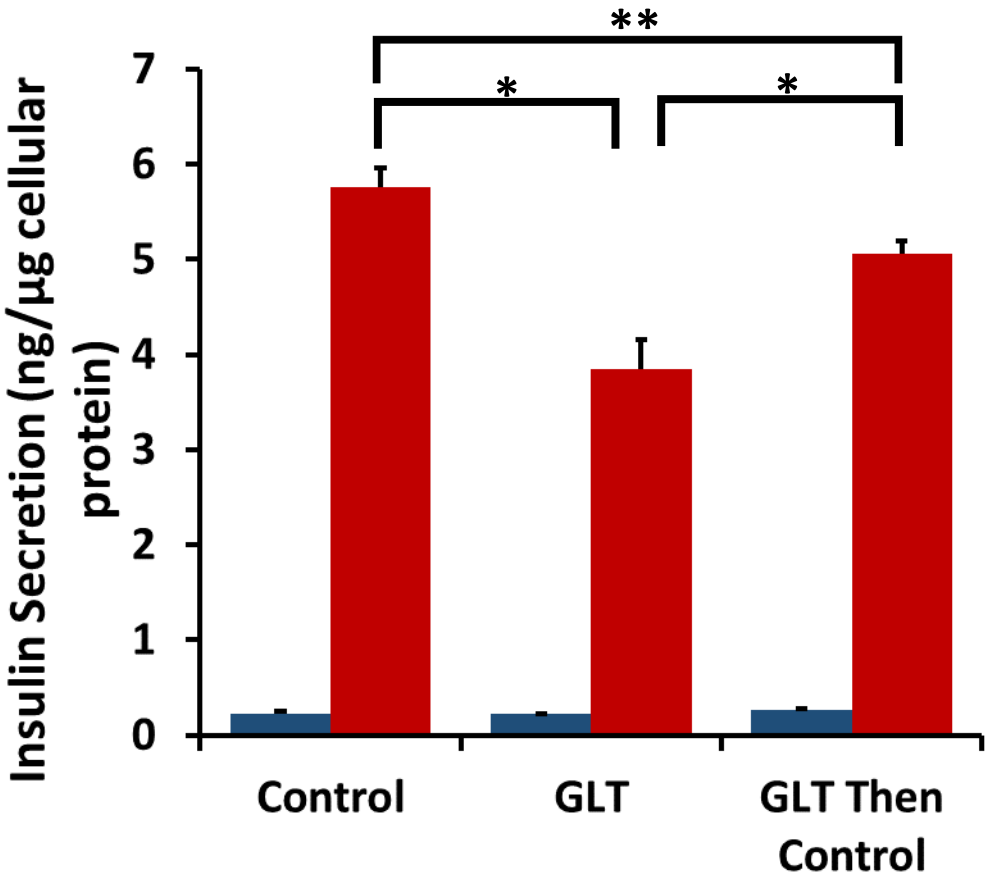

Figure 3. 1; INS-1 cells can partially recover the ability to secrete stimulated insulin secretion in response to 3 day glucolipotoxic exposure.

INS-1 cells were cultured in RPMI-1640 media, or GLT media for 5 days, or 3 days followed by 2 days in control growth media. Insulin secretion was determined by ELISA following incubation ± secretagogue cocktail for 2 hs [(-) blue, (+) red] with data normalised to cellular protein content. Data are expressed as mean ± SEM from 3 independent experiments. *p<0.05, **p<0.005

This result indicates that INS-1 β-cells have the ability to recover some of their lost functionality, if removed from the toxic growth conditions. Despite the potential for some recovery, it is not practical as a therapeutic strategy in terms of type 2 diabetic patients, as patients cannot simply remove the hyperglycaemic and hyperlipidaemid environment which causes the deleterious effect on β-cell function. However, as the

harmful effects of this toxic environment is widely attributed to oxidative stress, non-enzymatic glycation and their resultant products, pharmacotherapy interventions that counteract reactive species could offer a similar and potentially more pronounced effect at maintaining β-cell function.

3.2.2. Effect of Carnosine on β-cells

The data presented here reports the beneficial actions of carnosine upon insulin secretion and glucose uptake in β-cells and skeletal muscle myotubes respectively.

3.2.2.1. Carnosine Scavenging of Glucolipotoxicity-Associated Reactive Species and their Products

It has been shown that carnosine is an effective scavenger of reactive carbonyl species (RCS) generated by lipoxidation such as hydroxynonenal (Aldini, et al. 2002) in a rodent model of diabetic nephropathy (Albrecht, et al. 2017). Carnosine was therefore investigated as a potential scavenger of reactive oxygen and nitrogen species (RONS) the building blocks of downstream RCS generation and cause for ablated β-cell function and viability.

INS-1 cells were incubated in control or GLT media for 5 days, before a final incubation for 1h with or without 10mM carnosine supplemented to fresh experimental condition media. To determine the amount of reactive species present in each condition, 20 μM 2’7’-dichlorofluorescein diacetate (DCFDA), a cell permeant fluorogenic dye that detects and quantifies peroxyl, hydroxyl and other reactive species, was added for 1h and results shown in Figure 3.2. GLT increased reactive species significantly to 180.4 ± 8.2% ($p=0.0006$) normalised to control, whilst a 1h 10mM carnosine treatment reversed the upregulation back to within control limits

(77.5 ± 19.7%, p=0.003 v GLT). A 1h treatment of carnosine in control conditions caused a non-statistically significant yet modest reduction in reactive species compared to control, reducing detection to 69.1 ± 20.9%.

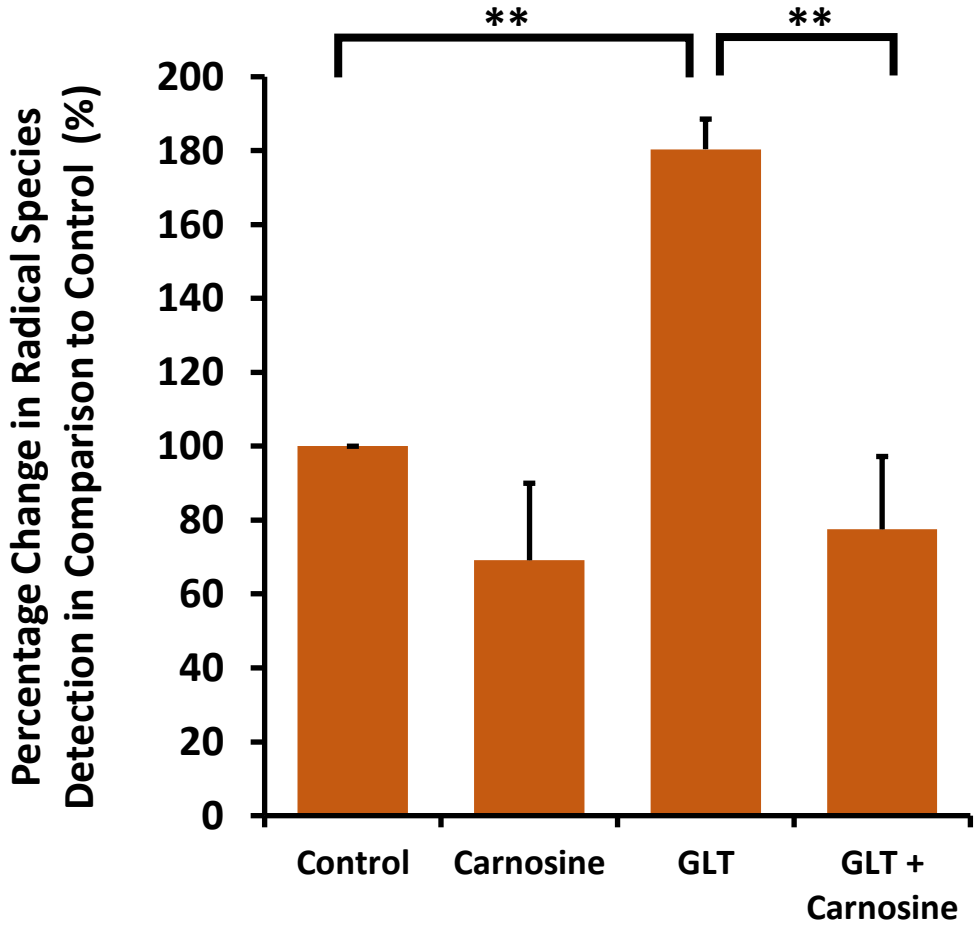

Figure 3. 2; Carnosine is an effective scavenger of glucolipotoxic reactive species in β-cells.

INS-1 cells were cultured in RPMI-1640 media or GLT media for 5 days before incubation with media supplemented ± 10mM carnosine for 1h. 20µM DCFDA was loaded in KREBS buffer for 1h and reactive species detected via fluorescence with excitation and emission of 495nm and 530nm respectively. Reactive species is expressed as percentage change in comparison to control from 4 independent experiments ± SEM. **p<0.005

As radical species detection with DCFDA was not normalised to cell number or protein content it was important to investigate the effect of GLT on cell number and viability to ensure the witnessed effect was not an artefact of glucolipotoxic driven cell death, or glucose driven cell proliferation. Using calcein AM, a cell permeable dye that fluoresces upon acetoxymethyl ester hydrolysis by eukaryotic intracellular esterases is indicative of cell viability and can be quantified. All viable eukaryotic cells will have the esterases required for the dye esterification and is therefore an accepted model of cell viability/number. The increase in reactive species in chronic GLT exposure conditions shown in Figure 3.2 were not caused by glucolipotoxic changes in β-cell viability. As shown in Figure 3.3, INS-1 cells treated for 5 days in GLT media showed only a small and non-statistically significant increase in viability to 112.2 ± 7.0% compared to control ($p>0.05$).

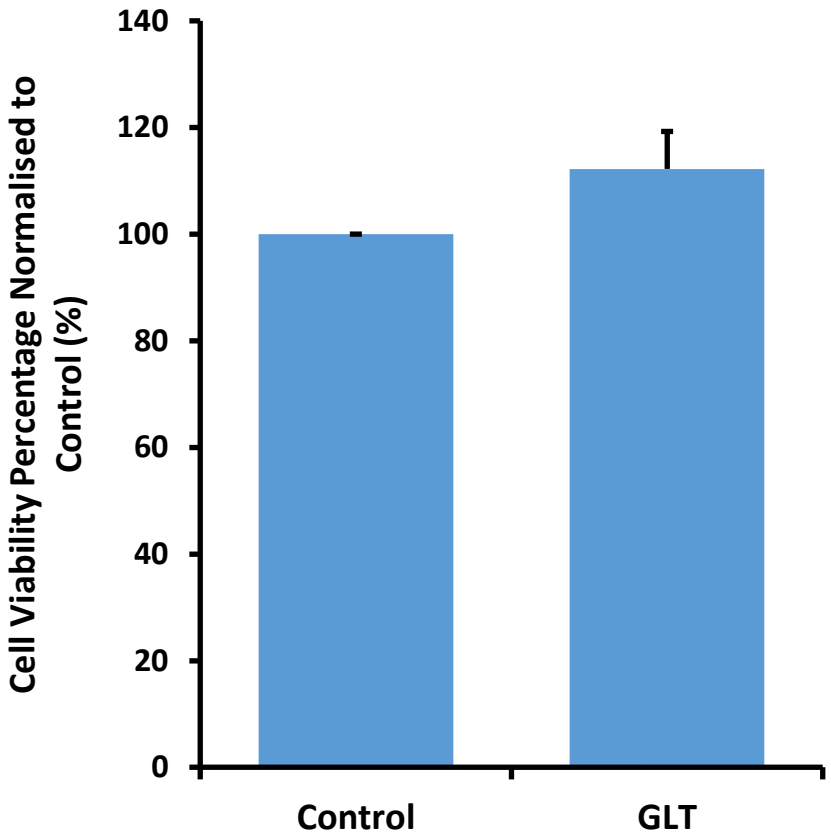

Figure 3. 3; GLT doesn't alter cell viability over 5 days.

INS-1 cells were cultured in control or GLT media for 5 days prior to addition of 5µM calcein AM for 1h before detection via fluorescence with excitation and emission of 490nm and 520nm respectively and expressed as percentage change compared to control from 3 independent experiments ± SEM.

To determine whether carnosine can influence reactive nitrogen species concentrations in response to glucolipotoxic exposure, INS-1 cells were incubated in control or GLT media ± 10mM carnosine for 5 days before cells were lysed and proteins separated by sodium dodecyl sulphate polyacrylamide gel electrophoresis (SDS-PAGE). Protein were subsequently transferred to nitrocellulose membrane and immunoblotted with an anti-inducible nitric oxide synthase (iNOS) antibody. iNOS is

the enzyme responsible for nitric oxide (NO) production from oxidisation of L-arginine using oxygen NADPH electrons (Lowenstein and Padalko 2004). Increased iNOS expression would infer that nitrogen reactive species were equally upregulated.

Figure 3.4 demonstrates an example of protein band intensity, supportive of data published (Cripps, et al. 2017), that determined a 5 day GLT incubation caused significant fold change upregulation of iNOS expression by 3.7 ± 0.6 (p=0.0075), whilst a combined treatment of GLT and 10mM carnosine repressed the GLT driven upregulation of iNOS by 79.1 ± 4.7% (p=0.017). This data demonstrates that carnosine offers another protective method of action in β-cells, as a long term exposure to it can alter protein expression of key enzymes involved in harmful species formation.

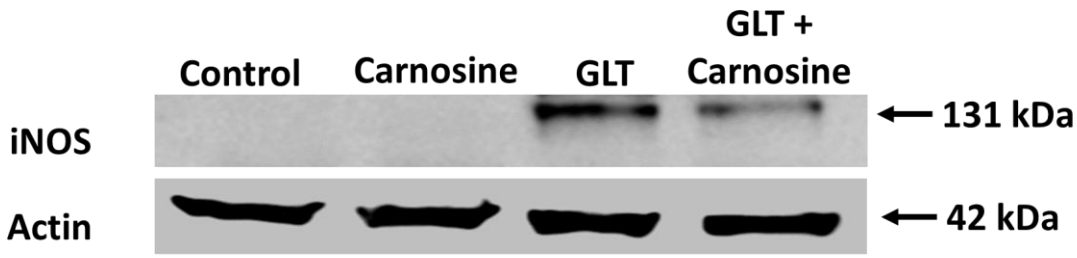

Figure 3. 4; Carnosine inhibits GLT driven upregulation of iNOS.
INS-1 cells were cultured in control or GLT media supplemented with or without 10mM carnosine for 5 days before cells were lysed, protein extracted and separated via SDS-PAGE, transferred to nitrocellulose and immunoblotted using anti-iNOS or anti-actin antibody.

As both nitrous oxide (NO) and superoxide ($O_2^{\cdot -}$) species have been revealed to be significantly elevated by glucolipotoxicity, peroxynitrite, another harmful reactive

species formed from the combination of these species is also likely to be elevated. Peroxynitrite (ONO_2^-) itself is hard to detect, but the downstream residue adduction product of peroxynitrite, 3-nitrotyrosine (3-NT) can be quantified by ELISA. 3-nitrotyrosine is an indicative biomarker for peroxynitrite and therefore reactive nitrogen species. It is produced from peroxynitrite targeting and reacting with L-tyrosine and protein bound tyrosine to produce free circulating or protein bound 3-NT respectively. The resultant alteration or adduction of key regulatory proteins is then likely to interfere with their cellular processes (Ahsan 2013).

In order to investigate the presence of peroxynitrite, INS-1 cells were again cultured in control or GLT media supplemented with or without 10mM carnosine for 5 days prior to cells being lysed in suppled extraction buffer and extracts analysed. A 5 day GLT incubation significantly increased 3-NT modification of proteins by 32.9 ± 7.4% ($p=0.005$) compared to control. A 10mM carnosine dose combined with GLT, again significantly reversed the GLT upregulation ($p=0.007$) causing 3-NT detected adductions to fall to 94.3 ± 6.0% compared to control.

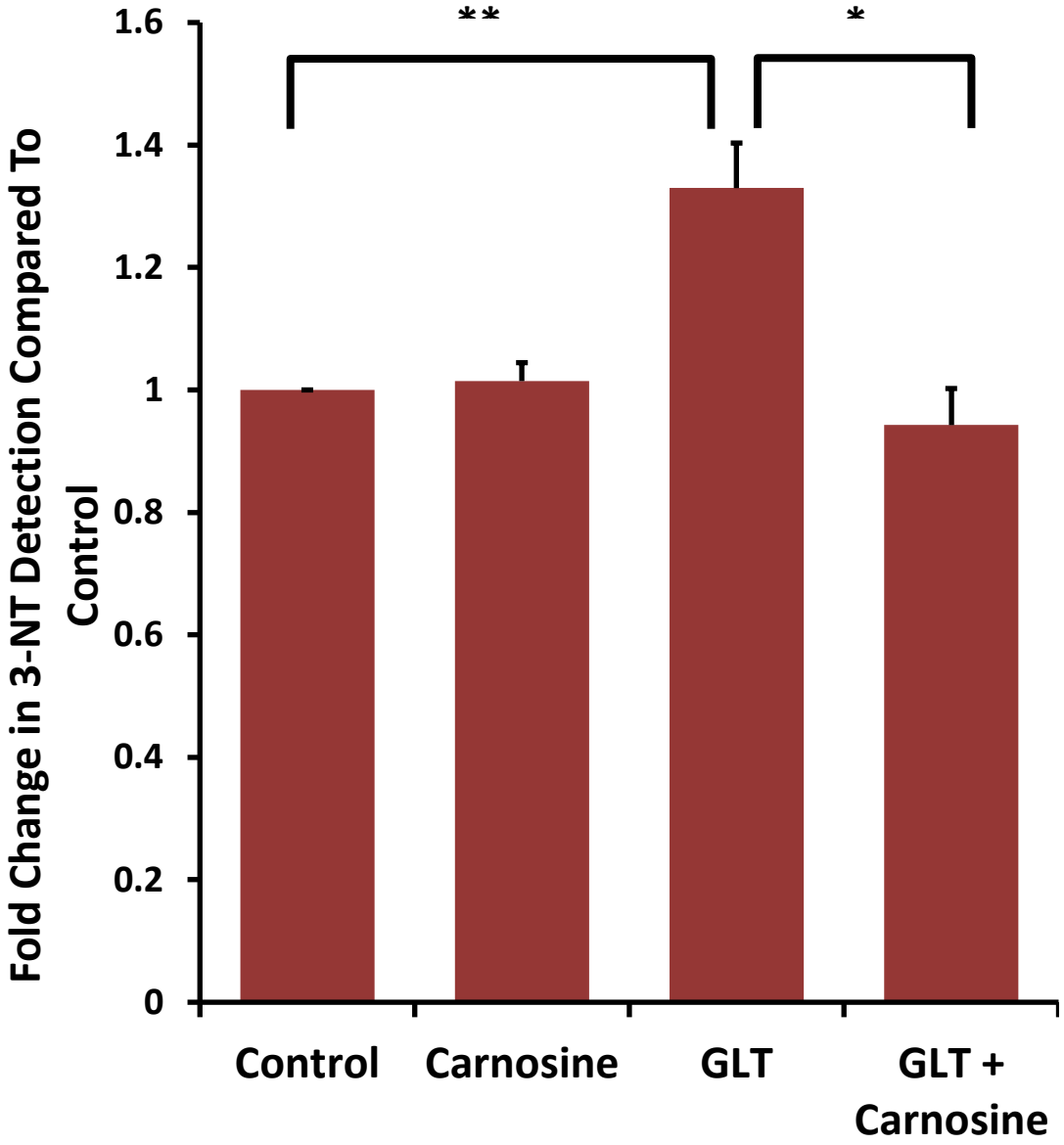

Figure 3. 5; Carnosine reverses glucolipotoxic driven 3-NitroTyrosine production. INS-1 cells were cultured in control or GLT media supplemented ± 10mM carnosine for 5 days. Cells were lysed and extracts 3-NT determined by ELISA with absorbance measured at 450nm and normalised to protein content. Results are expressed as percentage change compared to control from 3 independent experiments ± SEM. *p<0.05 **p<0.005

Next, 4-HNE an α,β-unsaturated hydroxyalkenal produced from lipid peroxidation, and hence a hallmark of oxidative stress, was similarly determined via ELISA. Again

INS-1 cells were cultured in control or GLT media with or without 10mM carnosine for 5 days before cells were lysed in RIPA buffer and samples analysed for 4-HNE formation shown in Figure 3.6. As anticipated, GLT drove up 4-HNE formation by 43.5 ± 3.4% compared to control. Importantly, a 10mM carnosine dose was able to completely prevent GLT induced 4-HNE species production (p=0.026) to a 12.6 ± 8.5% compared to control samples.

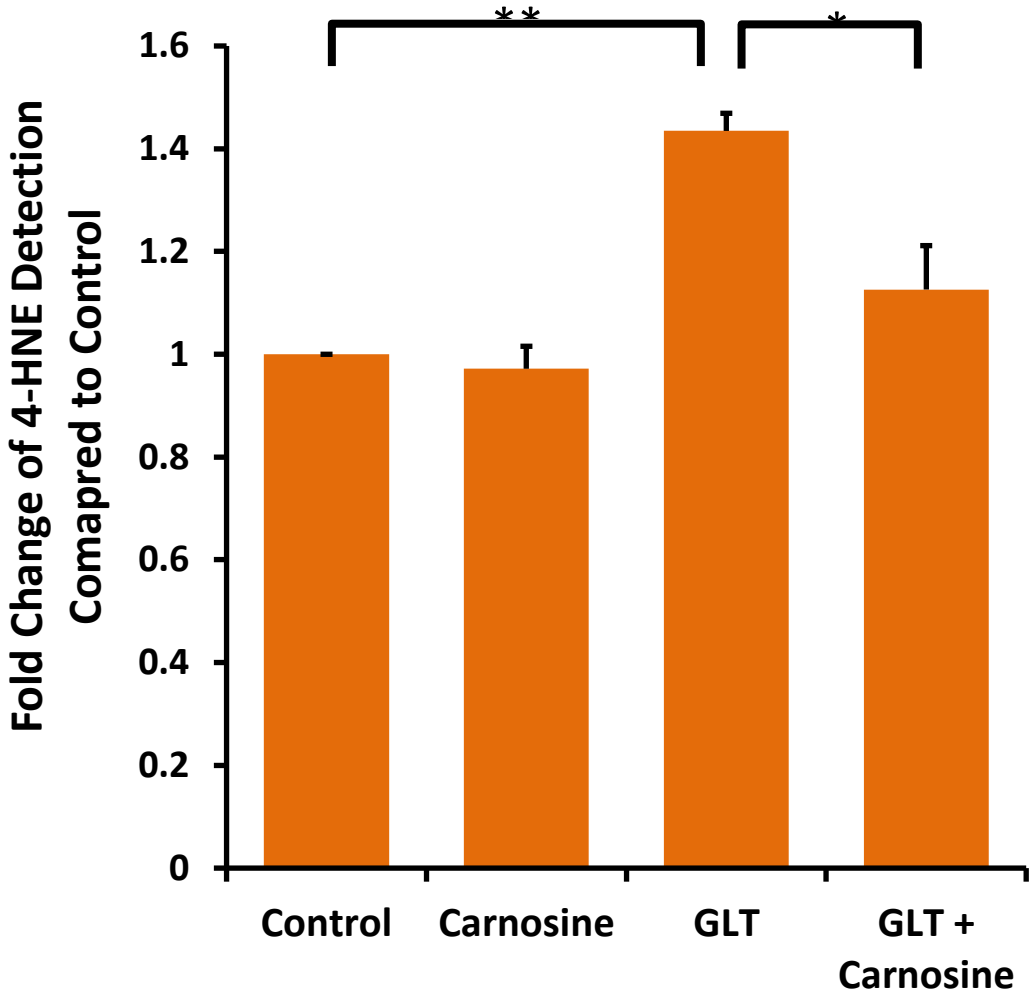

Figure 3. 6; Carnosine reverses glucolipotoxic driven 4-HNE production.

INS-1 cells were cultured in control or GLT media supplemented ± 10mM carnosine for 5 days. Cells were lysed and extracts 4-HNE determined by ELISA and normalised to protein content. Results are expressed as percentage change compared to control from 3 independent experiments ± SEM. *p<0.05 **p<0.005

3.2.2.2. Carnosine Increases Stimulated Insulin Secretion in *in vitro* and *ex vivo* β-cells

As carnosine has been shown to be effective at scavenging reactive species and inhibiting harmful residue formations, it was important to determine if chronic treatment with carnosine can improve β-cell function, and in particular its main role, insulin secretion. INS-1 cells were incubated in standard growth media in the absence or presence of 1mM and 10mM carnosine for 5 days. This is well within the physiological range that has been shown to range from 2-20mM in wet human skeletal muscle (Artioli, et al. 2010; Guiotto, et al. 2005), and more specifically 12-60mmol/kg dm in the human vastus lateralis muscle and ~2.25mmol/kg dm for the male rat soleus and rectus femoris muscles (Sale, et al. 2013; Naderi, et al. 2017). No data however exists for clonal or primary pancreatic β-cell carnosine concentrations.

After a 5 day incubation, cells were washed and incubated in either KREBS or a secretagogue cocktail for 2h. Insulin secretion was quantified between conditions using an ELISA and normalised to protein content. As shown in Figure 3.7, secretagogue stimulated insulin secretion was moderately increased by 34.6 ± 8.1% when treated with 1mM carnosine increasing from 3.11 ± 0.48 ng/µg cellular protein to 4.13 ± 0.2 ng/µg. A 10mM treatment of carnosine however, significantly increased insulin secretion per cellular protein by 77.2 ± 18.7% rising to 5.14 ± 0.46 ng/µg ($p=0.018$).

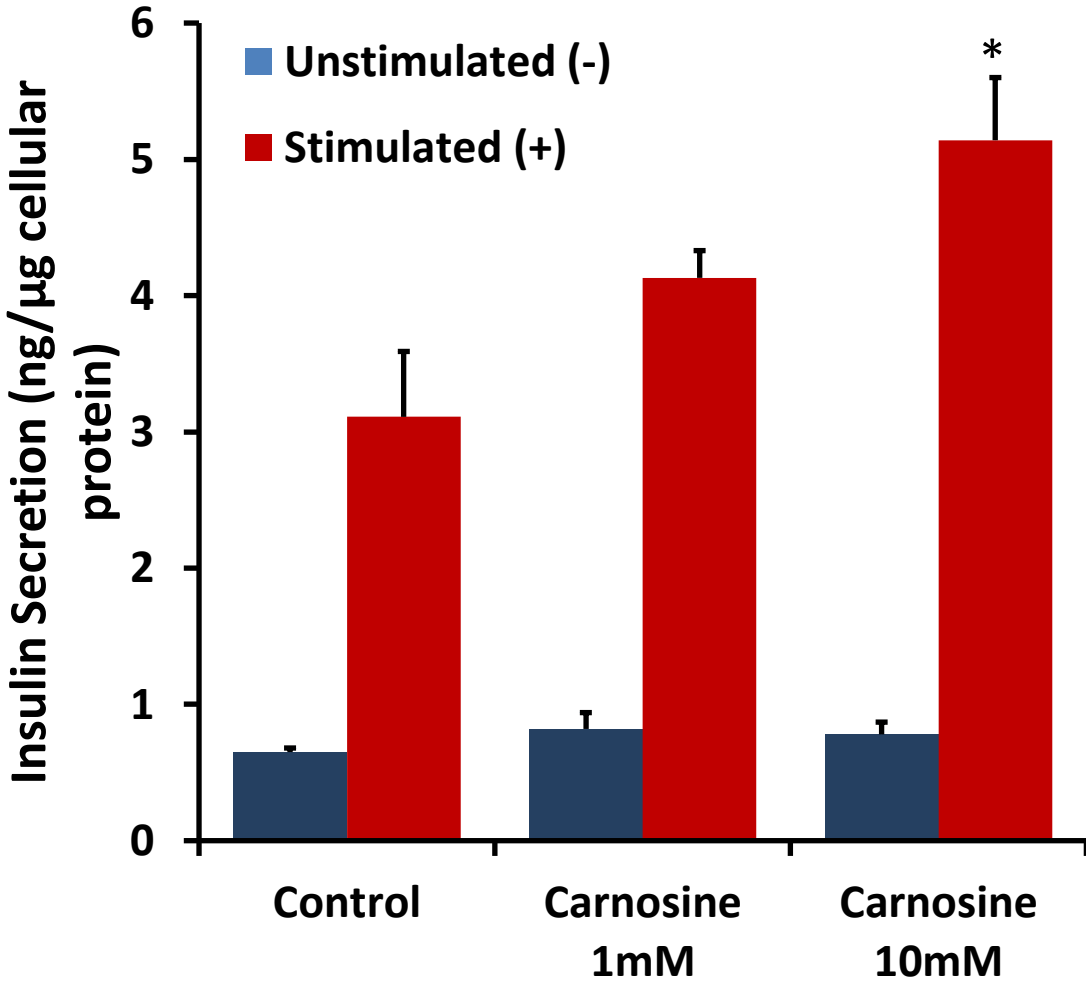

Figure 3. 7; Carnosine increases secretagogue stimulated insulin secretion dose dependently in INS-1 cells.

INS-1 cells were cultured in RPMI-1640 media in the presence of 1mM or 10mM carnosine for 5 days. Insulin secretion was determined by ELISA following incubation ± secretagogue cocktail for 2h [(-) blue, (+) red] with data normalised to cellular protein content. Data are expressed as mean ± SEM from 3 independent experiments. *$p<0.05$, compared to control stimulated samples (+).

As previously detailed, INS-1 cells are a well characterised, stable and wholly accepted β-cell clonal line that secretes insulin in response to stimuli within the physiological range. However, as transformed cell lines are not a completely true

representative of full animal physiology, it is essential to support any findings where possible with *in vitro* studies. Therefore, through collaboration with King's College London (Dr Sophie Sayers and Dr Paul Caton), islets from CD-1 male mice were isolated and cultured in standard growth media, or media supplemented again with either 1mM or 10mM carnosine for 2 days (48h). After incubation, islets were spun down and incubated in KREBS supplemented to 2mM or 20mM glucose for 1h, before insulin secretion was determined using an iodine labelled insulin tracer and quantified by radioimmunoassay. Primary mice islets glucose-stimulated insulin secretion displayed in figure 3.8, increased modestly from 1.23 ± 0.25 to 1.87 ± 0.33 an increase of 51.9 ± 26.8% when incubated in 1mM carnosine for 2 days. A significant rise to 2.37 ± 0.34 indicative of a 93.1 ± 27.5% increase in glucose-stimulated insulin secretion occurred when incubated in 10mM carnosine for 2 days compared to control conditions ($p=0.013$). At a concentration of 10mM, carnosine treatment therefore offered moderate enhancement of both an immortal tissue culture β-cell line and primary tissues innate ability to secrete insulin in response to stimuli.

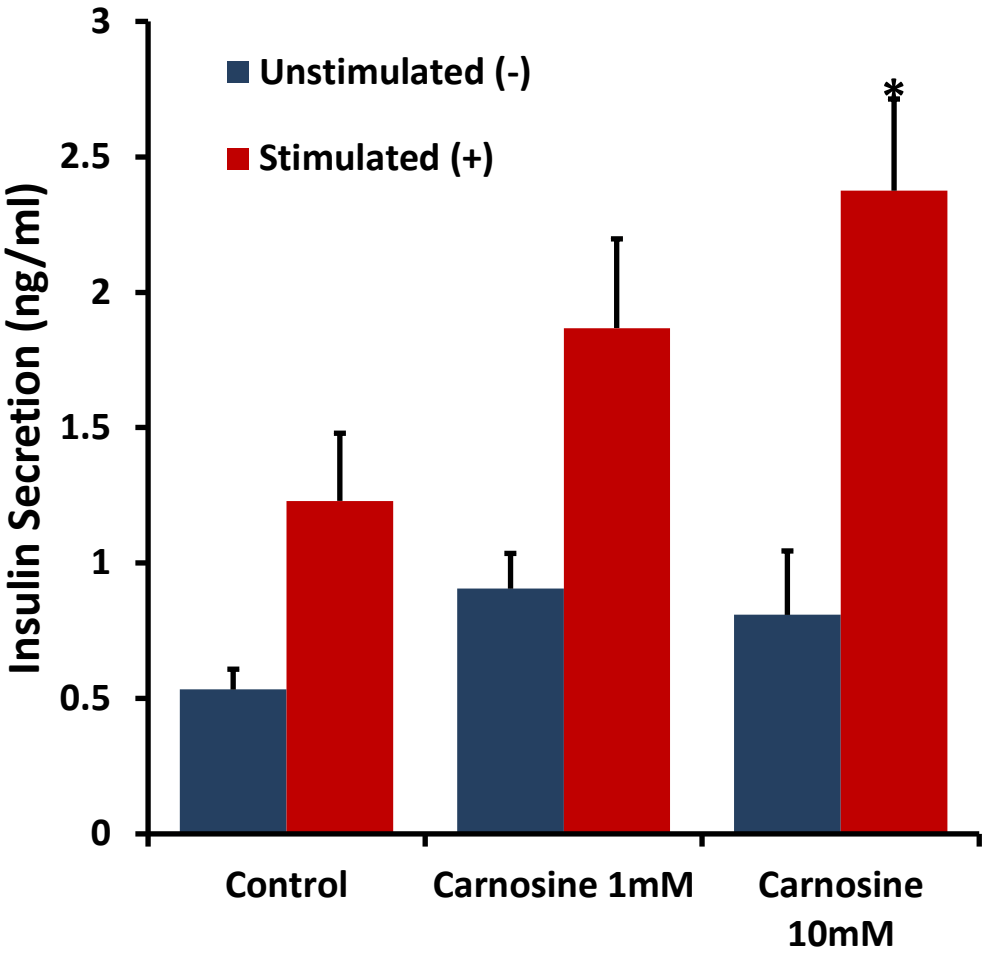

Figure 3. 8; Carnosine increases glucose-stimulated insulin secretion dose dependently in ex-vivo mouse islets.

Islets were isolated from CD-1 mice and cultured in RPMI-1640 media supplemented with 1mM or 10mM carnosine for 2 days. Islets were subsequently incubated in 2mM [(-) blue] or 20mM [(+) red] glucose for 1h and insulin secretion determined by radioimmunoassay. Data is presented as the mean ± SEM from a minimum of 6 independent experiments. *p<0.05 compared to control stimulated samples

3.2.2.3. N-Acetylcysteine Supports Carnosine's Method of Action

To support the view that carnosine can enhance stimulated insulin secretion through its ability to scavenge reactive species and inhibit harmful adduct formation, another known anti-oxidant, N-acetylcysteine (NAC), was investigated. NAC was investigated at 10mM; the same concentration previously used by Al-Nahdi, John and Raza (2018)

investigating the cytoprotective effects of NAC in the β-cell clonal line RIN-5F (Al-Nahdi, John and Raza 2018). This concentration was also consistent with the concentration of carnosine used in previous experiments. NAC is an aminothiol and synthetic precursor of intracellular glutathione and cysteine (Sun 2010) which has been shown to mimic the effects of naturally occurring antioxidants by inhibiting ROS-dependent apoptosis and inhibited hydrogen peroxide induced ROS detection (Curtin, Donovan and Cotter 2002; Halasi, et al. 2013). INS-1 cells were therefore cultured in control or GLT media for 5 days prior to supplementation with or without 10mM NAC for 1h. After 1h cells were washed and incubated in 20μM DCFDA for 1h before radical species quantification via fluorescence. GLT as shown before, increased reactive species significantly over the 5 days by 62.3 ± 20.1% compared to control ($p=0.003$). Similarly, to a 1h 10mM carnosine dose, a 10mM treatment of NAC with GLT decreased reactive species detected to 79.4 ± 2.0% compared to control. This therefore represented a significant reduction from GLT conditions ($p=0.001$).

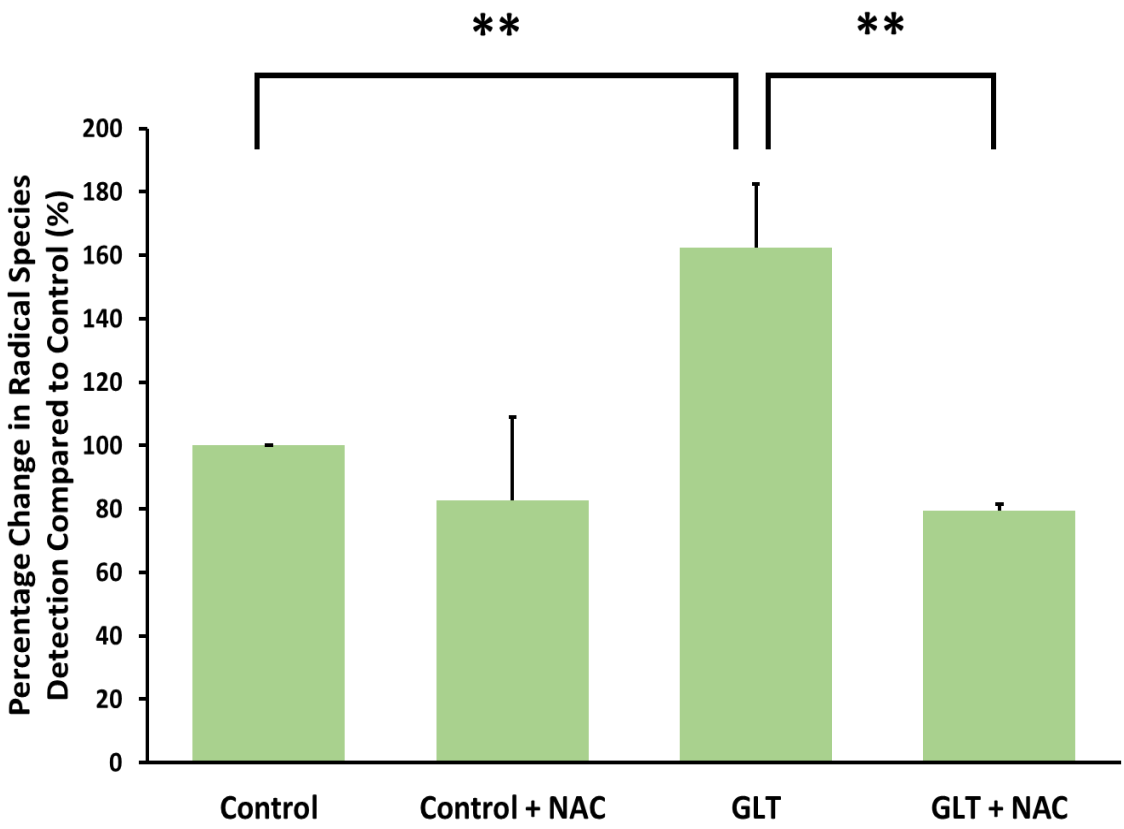

Figure 3. 9; NAC scavenges glucolipotoxic driven reactive species.

INS-1 cells were cultured in RPMI-1640 media or GLT media for 5 days before incubation with media supplemented ± 10mM NAC for 1h. 20µM DCFDA was loaded in KREBS buffer for 1h and reactive species detected via fluorescence with excitation and emission of 495nm and 530nm respectively. Reactive species is expressed as percentage change in comparison to control from 4 independent experiments ± SEM. **p<0.005

As expected, the known anti-oxidant NAC and therefore viable internal control for reactive species related function, can scavenge glucolipotoxic driven reactive species in INS-1 β-cells. However, the downstream effects of carnosine on insulin secretion which was attributed to its ability to scavenge radical species depends on a similar response when treated with NAC. If they share similar effects, it can be established

that the increase in stimulated secretion can be attributed to the reduction in free circulating radicals which are upregulated in the physiology of type 2 diabetes. Therefore INS-1 cells were cultured for 5 days in the presence or absence of 10mM carnosine or 10mM NAC in standard growth media. As shown in Figure 3.10, 2h secretagogue stimulation significantly increased by 54.8 ± 17.0% when treated with carnosine for 5 days ($p=0.013$), consistent with previously presented and published data. Similarly, a 5 day treatment of NAC increased secretagogue stimulated insulin secretion significantly by 50.5 ± 20.8% ($p=0.025$)

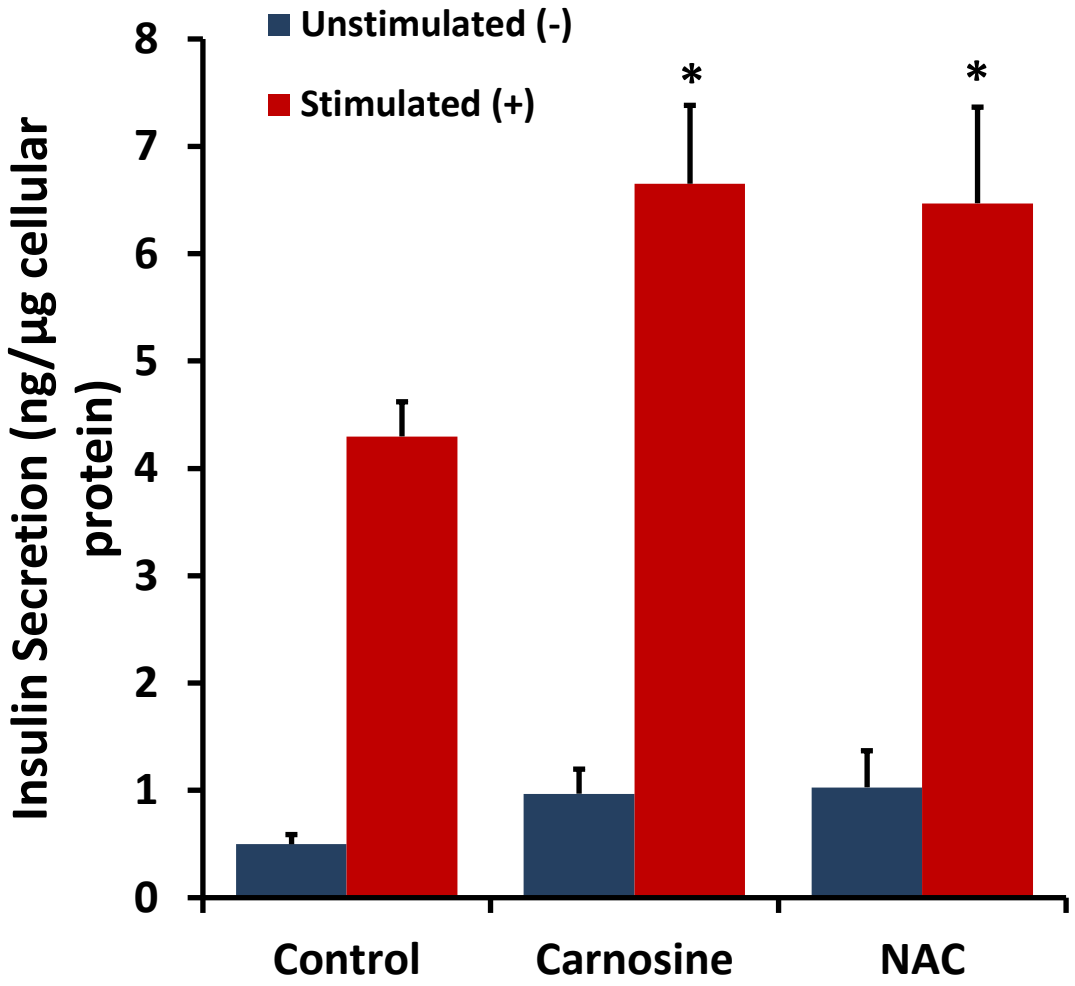

Figure 3. 10; NAC increases secretagogue stimulated insulin secretion similarly to carnosine.

INS-1 cells were cultured in RPMI-1640 media in the presence of 10mM carnosine or 10mM NAC for 5 days. Insulin secretion was determined by ELISA following incubation ± secretagogue cocktail for 2h [(-) blue, (+) red] with data normalised to cellular protein content. Data are expressed as mean ± SEM from 3 independent experiments. *$p<0.05$, compared to control stimulated samples (+).

This data is therefore supportively indicative that carnosine's ability to enhance stimulated insulin secretion is dependent upon its capacity as a scavenger of harmful reactive species.

3.2.2.4. Carnosine Reversal of Glucolipotoxic Inhibited Insulin Secretion

As mentioned, it has previously been published by this research group that a 72h incubation of INS-1 cells in glucolipotoxicity inhibits stimulated insulin secretion (Marshall, et al. 2007). To determine whether carnosine could reverse this GLT associated inhibition, these experiments were repeated but with an extended incubation time of 5 days to maximise not only harmful effects of GLT without triggering apoptosis (identified in previous research carried out by Turner Research team), but to maximise any potential beneficial protective actions that carnosine could have.

INS-1 cells were initially cultured in control or GLT media for 5 days before the addition of 10mM carnosine 2h prior to secretagogue stimulation (Figure 3.11). Consistent with previous data, GLT significantly diminished secretagogue stimulated insulin secretion from 4.7 ± 0.2 ng/μg cellular protein in control to 2.4 ± 0.08 ng/μg representing a decrease of 48.1 ± 1.9% ($p=1.5 \times 10^{-6}$). A 2h acute dose of 10mM carnosine partially reversed this diminished insulin release to 3.3 ± 0.04 ng/μg. This still represents a significant decrease from control conditions by 28.0 ± 0.9% ($p=4.5 \times 10^{-5}$), yet also a statistically significant increase from GLT treatment alone ($p=3.1 \times 10^{-6}$). Interestingly, 2h carnosine treatment in control conditions had no apparent effect on stimulated insulin secretion. This data therefore indicates that carnosine, even over a short period can start to reverse the damage caused by GLT. This is likely due to its rapid quenching of free radicals which cause an adverse effect on the insulin secretory pathway.

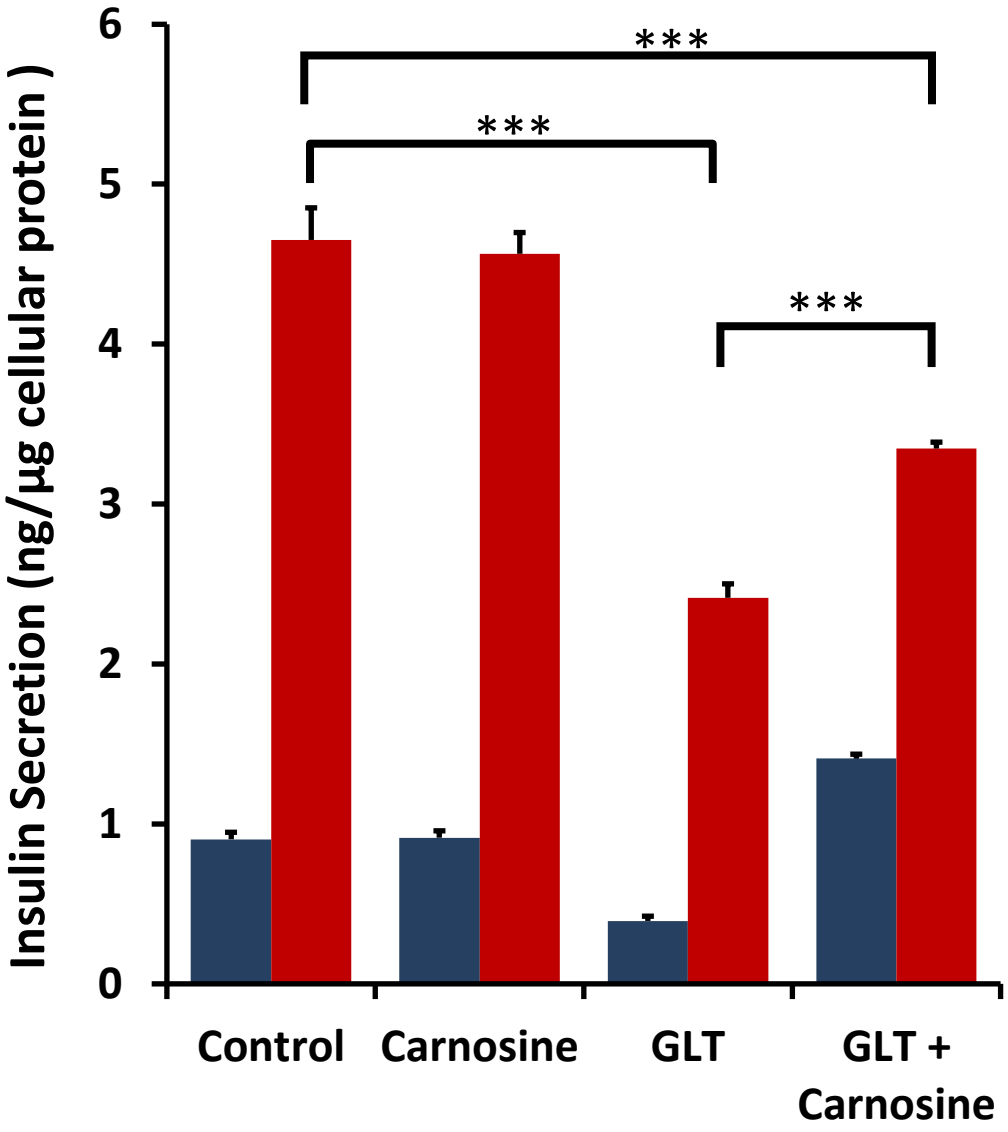

Figure 3. 11; An Acute 2h treatment of carnosine starts to reverse GLT inhibited insulin secretion.

INS-1 cells were cultured in RPMI-1640 media in control or GLT RPMI-1640 media for 5 days. 2h prior to stimulation, cells were incubated with or without experimental condition media supplemented with 10mM carnosine. Subsequently Insulin secretion was determined by ELISA following incubation ± secretagogue cocktail for 2h [(-) blue, (+) red] with data normalised to cellular protein content. Data is expressed as mean ± SEM from 5 independent experiments. ***p<0.0005

If an acute 2h dose of carnosine could cause a significant change to insulin secretion it was warranted to investigate if a longer exposure of carnosine would be able to reverse the damage entirely. For this reason, INS-1 cells were similarly incubated in control or GLT media for 5 days, but carnosine was supplemented 2 days as opposed to 2h prior to stimulation and insulin secretion quantification (Figure 3.12). Consistently GLT reduced stimulated insulin secretion significantly by 63.1 ± 0.4% as expected ($p=7.5 \times 10^{-11}$). In agreement with previously offered data, 48h treatment of 10mM carnosine in control conditions increased secretagogue stimulated insulin secretion by 29.9 ± 2.0% ($p=1.1 \times 10^{-6}$). This increase is consistent with earlier data as it is a smaller increase than witnessed in Figure 3.8 with a 5 day carnosine incubation period, yet higher than when acutely incubated for 2h. One possible explanation for these findings could be that in β-cells already exposed to chronic GLT carnosine may require a longer period of time to exert full benefit, suggesting that GLT-adducted proteins may first need to turn over in order for non-adducted fully functional proteins to replace them.

Importantly, 2 day treatment of carnosine was able to fully reverse GLT-associated loss of insulin secretion. In fact, it enhanced secretion above control by 42.4 ± 0.4%. This is a statistically significant change from both control and GLT conditions with p values of 1.7×10^{-9} and 2.5×10^{-16} respectively. This data therefore indicates that carnosine is not only able to enhance insulin secretion, but it can reverse and inhibit the damaging effects that would have already accrued from the initial 3 days and succeeding 2 days co-exposure to a high sugar and high fatty acid environment.

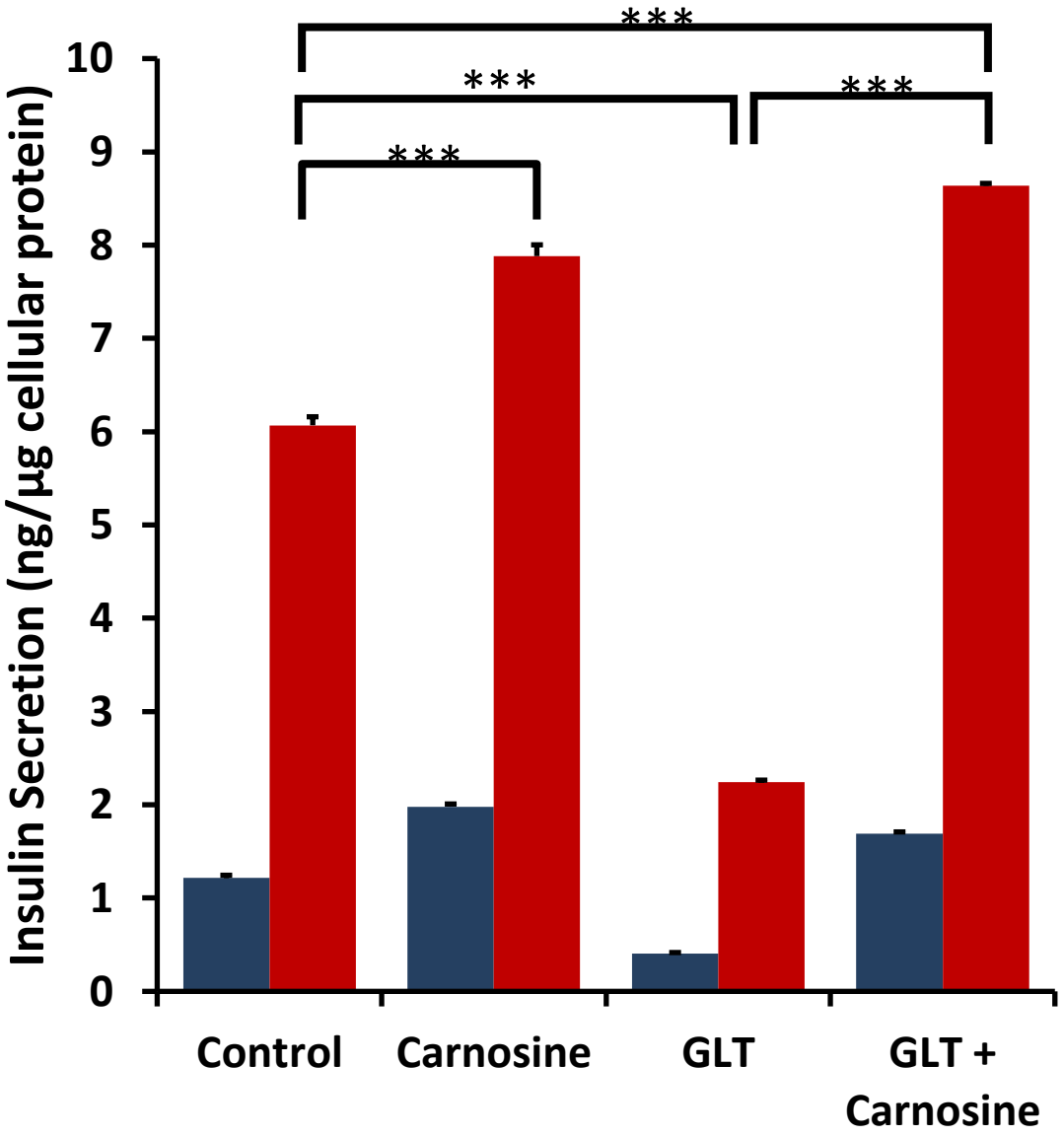

Figure 3. 12; A 5 day carnosine treatment fully reverses GLT inhibited insulin secretion.

INS-1 cells were cultured in control or GLT media for 5 days. 2 days prior to stimulation, cells were incubated with or without experimental conditioned media supplemented with 10mM carnosine. Insulin secretion was determined by ELISA following incubation ± secretagogue cocktail for 2h [(-) blue, (+) red] with data normalised to protein content. Data is expressed as mean ± SEM from 5 independent experiments. ***p<0.0005

3.2.3. Effect of Carnosine on Skeletal Muscle Myotubes

As carnosine was shown to have protective qualities in clonal β-cells through reactive species scavenging, it was sought to determine whether the same scavenging effect could be elicited in C2C12 skeletal muscle myotube cells and resultantly increase diminished glucose uptake. Therefore, working in collaboration with a colleague (Charlie Lavilla) myocytic differentiation was induced in C2C12 cells, before cells were cultured in DMEM media or DMEM supplemented to 28mM glucose and 200μM oleic acid and 200μM palmitic acid for 5 days. Cells were then cultured in the presence or absence of 10mM carnosine for 1h, before further incubation in 20μM DCFDA for 1h. Total reactive species were then measured and quantified via fluorescence and presented in Figure 3.13.

A 5 day incubation of skeletal muscle cells in GLT media caused a significant increase in reactive species by 169.6 ± 23.9% compared to control ($p=0.001$). A 1h dose of 10mM carnosine significantly reduced reactive species in control conditions ($p=0.03$) but importantly significantly reduced the GLT driven upregulation of reactive species back to within control conditions (122.1 ± 37.1% compared to control $p=0.014$). This data again suggests that carnosine can directly scavenge reactive species in numerous tissue types, due to the nature of the acutely timed treatment.

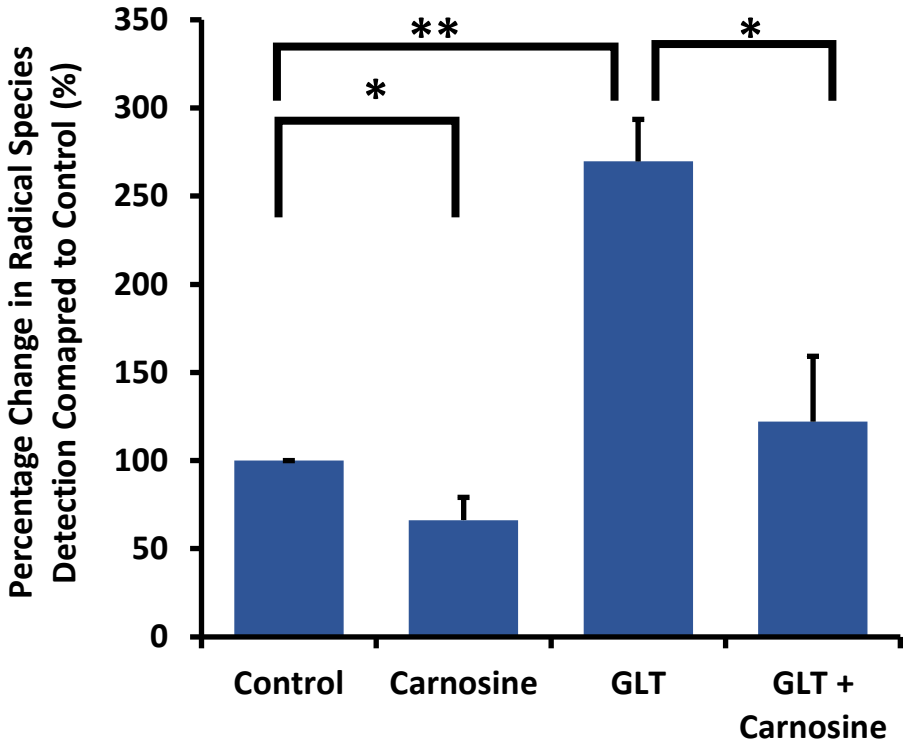

Figure 3. 13; Carnosine is an effective scavenger of glucolipotoxic reactive species in skeletal muscle.

C2C12 cells were differentiated and cultured in DMEM media or GLT media for 5 days before incubation with media supplemented ± 10mM carnosine for 1h. 20µM DCFDA was loaded in KREBS buffer for 1h and reactive species detected via fluorescence with excitation and emission of 495nm and 530nm respectively. Reactive species is expressed as percentage change in comparison to control from 3 independent experiments ± SEM. *p<0.05 **p<0.005

C2C12 cells were subsequently incubated in media ± GLT, ± 10mM carnosine for 5 days to investigate insulin stimulated glucose uptake via 2DG6P detection. Carnosine addition resulted in a statistically significant increase in glucose uptake in comparison to the diminished amount of glucose uptake observed in GLT treated cells (p=0.04). This was not the result of altered cell viability (p>0.05) (data not shown) (Cripps, et al. 2017). This body of work therefore demonstrates that carnosine has the ability to

exert dual beneficial actions on glucose homeostasis through the enhancement of both clonal INS-1 and primary mouse β-cell insulin secretion and also target tissue skeletal muscle glucose uptake.

3.3. Discussion

The damaging effects of glucolipotoxicity have been attributed to many molecular mechanisms, including but not limited to oxidative stress, activation of protein kinase C, increased production of mitochondrial superoxide and the generation reactive carbonyl species (Ahmad, He and King 2005; Brownlee 2001). Reactive carbonyls can be produced both via lipid-peroxidation and glycoxidation resulting in ALE and AGE respectively. The former is derived through a series of intracellular oxidation and cleavage reactions on membrane-derived polyunsaturated fatty acids (Esterbauer, et al. 1982) to produce most commonly aldehydes. Malondialdehyde (MDA) is the most common lipid peroxidation product produced, accounting for roughly 70% of the total products, hexanal roughly 15% and hydroxynonenal (HNE) 5% (Benedetti, Comporti and Esterbauer 1980; Esterbauer, et al. 1991). 4-HNE is the most extensively researched lipid-peroxidation end-product as it is incredibly more reactive and therefore more damaging in comparison to more abundant products (Ayala, Munoz and Arguelles 2014).

AGEs (advanced glycation end products) are heterogenous compounds formed from carbonyls produced via glycoxidation through covalent bonding of either aldehyde or ketone groups of reducing sugars to free amino groups on proteins. This is known as the Maillard reaction. This creates a Schiff's base, which can spontaneously rearrange to form a more stable reactive carbonyl intermediate keto-amine. These species can

then complete a series of structural and reactive reconfirmations yielding an irreversible and damaging AGE structure (Basta, Schmidt and De Caterina 2004; Sato, et al. 2006; Ellis 2007). Increased AGE production as seen in diabetes, gradually accumulates both in sera and tissues and contributes to retinopathy, cataract, neuropathy, nephropathy and many other downstream complications associated with diabetes (Ahmed 2005; Goh and Cooper 2008).

Many of the resultant carbonyl species produced from these two methods are extremely reactive. Alkenals containing a C=C α,β-unsaturated double bond are the most reactive of the subset of species. HNE's are extremely reactive because of this and is one of the most cytotoxic aldehydes that can cause significant damage at micromolar concentrations (Brambilla, et al. 1986). Reactive carbonyl species can interact and interfere directly with proteins responsible for cellular function, trigger apoptosis as well as damage, delete or mutate DNA (Ellis 2007). Reactive aldehydes can also disrupt and significantly lower intracellular glutathione levels (White and Rees 1984). Glutathione enzymes are specifically suited to HNE detoxification as they have low Km values for HNE catalysis making them very efficient controllers intracellularly (Tiedge, et al. 1997). This observed reactive aldehyde driven downregulation of glutathione is particularly important in pancreatic islets, as they are already regarded as one of the least protected in terms of an anti-oxidant defence system and hence particularly susceptible to oxidative stress related damage (Robertson and Harmon 2007).

Taken together, these modifications exert a negative impact on cellular function, and in the case of β-cells can perturb insulin secretion. This may also shed some light on

why β-cells, if removed from toxic stress, have the ability to partially recover functional capacity lost from glucolipotoxicity. However, perhaps it is because the defence system needed to mop up the remaining reactive compounds simply isn't strong enough to exhibit a full recovery over a short period of time that explains why we only see a partial recovery. Nevertheless, administration of an anti-oxidant compound such as carnosine to patients with T2D as a daily therapy might prove more effective. Moreover, even if only partially effective this is still likely to enhance insulin secretion and reduce the loss of β-cell mass seen in patients with longstanding T2D, thereby delaying the onset of diabetic complications and improving patient prognosis.

Consistent with our aim and hypothesis, the data presented here shows that glucolipotoxic media generates reactive oxygen and nitrogen species, which in turn generated 3-NT protein adduct formation. The presence of 3-NT indicates that peroxynitrite is just one of the reactive species present, formed from the combination of superoxide with nitric oxide which were also shown to be significantly upregulated by GLT. Similarly, the harmful reactive carbonyl species of α,β-unsaturated hydroxyalkenal, 4-HNE was also upregulated in GLT, most likely produced from the aforementioned peroxidation of membrane derived lipids.

In order to offset the damaging effects of reactive oxygen, nitrogen and carbonyl species that result in AGE and ALE production that are known to have a devastating effect on β-cells, and the self-defence anti-oxidant system being weak and potentially reduced even further by reactive stress, other molecules are also likely required to protect cell function and viability. As significantly diminished reactive species were

detected after a 1h acute treatment of carnosine, it indicates that carnosine is a potent scavenger of reactive species in INS-1 β-cells. This can be deduced as reactive species scavenging reaction happens very quickly, whereas protein turnover or gene perturbation that could alter reactive species generation would take a longer exposure of at least 48-72h to witness any changes. This work demonstrated that the dipeptide carnosine is not only an effective scavenger of reactive metabolites but can also inhibit harmful adduct formation on potentially key protein targets resulting in an increase in insulin secretion demonstrated both in vitro and vivo.

4-HNE as mentioned is one of the most abundant and most reactive carbonyl species. Carnosine's wide biological functions are still largely unknown, but it is accepted that it can sequester 4-HNE and other reactive carbonyl species alike, through a reaction called Michael's addition (figure 3.14).

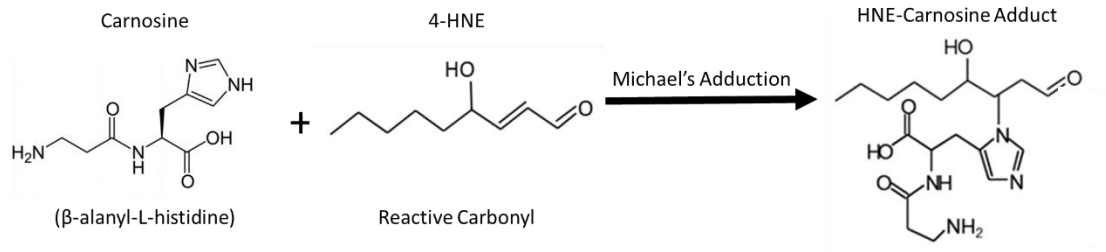

Figure 3. 14; Carnosine sequestering of 4-HNE reaction.
Carnosine reacts with 4-HNE on the imidazole ring of the histidine amino acid. Adapted from (Song, et al. 2014)

It is the histidine component (particularly the imidazole ring) of the carnosine compound that reacts with nucleophilic residue within the HNE protein, forming a stable and 'sacrificial' non-reactive adduct (Aldini, et al. 2003; Aldini, et al. 2002). This inhibits any future potential damage that molecule of HNE can cause to other intracellular proteins.

Histidine containing dipeptides such as carnosine are therefore thought to act at two key points within oxidative stress biology; by scavenging reactive oxygen species directly before any of their toxic downstream products (reactive carbonyls) are produced, and by directly reacting and forfeiting itself by forming non-reversible adducts with any carbonyl species that are produced from prolonged stress exposure (Song, et al. 2014). This is most likely why this work also presented carnosine's ability to be able to reverse the damage caused by 5 day glucolipotoxic exposure from just a 2 day carnosine incubation. This demonstrated carnosine's potential use as not only a preventative medication for patients in a pre-diabetic state, but also for fully diagnosed diabetic patients that still have some β-cell function remaining that could be enhanced. Furthermore, in addition to having a protective role in clonal β-cells in terms of preserving insulin secretion in the face of glucolipotoxicity, carnosine also demonstrated a positive effect on glucose uptake in skeletal muscle through what we believe the same scavenging and adduction preventative action. Further characterisation of this in vivo is required.

In conclusion, the data presented here demonstrates that β-cells may have some capacity for self-recovery if removed from toxic conditions. This illustrates the need for tight glycaemic control in patients with existing T2D, and the need for strict dietary control and aggressive therapy with existing therapeutic agents such as sulphonylureas to help manage and control blood sugar levels. Alongside this, the data presented indicates that taking the nutritional supplement of carnosine might further improve patient prognosis, as carnosine is a potent scavenger of reactive species in β-cells, inhibiting the harmful adduction of proteins by reactive carbonyls

and reactive nitrogen species resulting in an increase in insulin secretion. Importantly, it was also shown that carnosine can inhibit and reverse the damaging effects of GLT on both insulin secretion and glucose uptake, implicating a potential use for carnosine as a treatment for type 2 diabetes to stabilise glucose homeostasis on two fronts.

3.4. Future Directions

Controversial findings have reported diminished endogenous carnosine concentration in type 2 diabetic mouse and human tissues (Gualano, et al. 2012; Peters, et al. 2015; Liu, et al. 2016). Future studies could address this through the generation of carnosine synthase (CARNS1-/-), carnosinase-1 (CNDP1-/-), and carnosinase-2 (CND2-/-) knockout animals - which would provide depleted tissue carnosine, full plasma carnosine, and full tissue carnosine models respectively. The resultant tissues from these animals would then provide fresh insight to the debate of carnosine metabolism and altered carnosine contents in various pathologies, whilst also providing a plethora of full physiological samples for further analysis.

There are also a number of additional avenues for investigation surrounding carnosine's role in influencing glucose homeostasis in type 2 diabetes. The body of work presented in this thesis and elsewhere has already indicated the ability of carnosine to inhibit protein adduction by advanced lipidation and glycation end products. Whilst the beneficial action upon glucose homeostasis in both β-cell and skeletal muscles has now been shown, it is currently unreported in the literature which specific proteins are adducted by these glucolipotoxic driven species, and equally importantly, which proteins carnosine protects.

Utilising immunoprecipitation techniques in conjunction with mass spectrometry, ongoing work within the Turner research group aims to identify key regulators that are adducted by either 4-HNE and 3-NT in both β-cells and skeletal muscle in response to chronic glucolipotoxic exposure. Subsequently, samples will also identify proteins protected by carnosine to develop a deeper understanding of carnosine's potential therapeutic use in this disease. Preliminary data has been generated in tissue culture cells and has identified specific functional classes of target proteins prone to adduction by these separate reactive species. Future studies will replicate this work using both animal models of diabetes and human patient samples in order to both validate existing data and indicate likely patient benefit.

Also if β-cells express the protein carnosine synthase, supplementation through the dietary intake of β-alanine should also allow β-cells to synthesise their own carnosine to increase the intracellular pool. This endogenously synthesised carnosine would potentially have the same capacity to influence glucose metabolism as demonstrated in this chapter. However, one issue with either carnosine or β-alanine strategies are that carnosine is rapidly hydrolysed by carnosinase enzymes, both in serum and tissue, so the development of non-hydrolysable carnosinase inhibitors and carnosine mimetics may represent a more effective treatment strategy that provides greater sustained efficacy. This strategy forms the basis for work presented in Chapter 4.

4. β-alanine and Carnosine Analogs as an Alternative Therapeutic Treatment for Glucolipotoxic Stress

4.1. Introduction

Previous work from the Turner group (Cripps et al, 2017) showed that carnosine regulates glucose homeostasis by increasing glucose uptake and insulin secretion. This occurs as a consequence of scavenging glucolipotoxicity-mediated reactive species. Nevertheless, one problem arising from using carnosine supplementation as a treatment for any pathophysiology is the rapid hydrolysis by serum and tissue carnosinases (Teufel, et al. 2003). Dietary carnosine, once ingested, can cross the intestinal enterocyte cellular membrane through PEPT1 transporters, whereupon it is either broken down by carnosinase-2, or else further transported out into the blood stream. There carnosinase-1 can also hydrolyses the dipeptide before it reaches any peripheral tissues, where its potential for beneficial action is highest (Boldyrev, et al. 2013). One solution to this could be regular administration of high doses of carnosine that would offset rapid hydrolysis, thereby potentially increasing the circulating pool of carnosine to high enough levels to elicit a biological effect. However constant oral dosing isn't very practical in terms of medicating or monitoring purposes, and other more suitable options working around the same strategy may exist.

In addition to being present in food such as red meat, carnosine is also synthesised endogenously by carnosine synthase from the amino acids β-alanine and L-histidine. β-alanine is a non-proteogenic amino acid that is synthesised from the breakdown of uracil in the liver, yet has a very slow production rate resulting in an almost untraceable concentration in the serum, and as low as 40μmol/l in skeletal muscle where it is primarily stored and utilised (Bakardjiev and Bauer 1994; Harris, et al.

2006). This is much lower than the reported 3.24mol/l concentration of the standard α-alanine amino acid in skeletal muscle and ~350-450μmol/l in plasma and whole blood samples of normal individuals (Lewis, Waterhouse and Jacobs 1980; Roth, et al. 1985). For this reason, the rate limiting step of carnosine synthesis is thought to be β-alanine concentration, as whilst endogenous concentrations may be low, the affinity for carnosine synthase is high with a Km of roughly 1.0-2.3mM, meaning any possible synthesis is rapid (Ng and Marshall 1978; Skaper, Das and Marshall 1973b).

It has previously been reported that β-alanine supplementation could increase intramuscular carnosine content in humans where it was shown to have a positive effect on cellular performance (Harris, et al. 2006; Hill, et al. 2007). If carnosine synthase is present in our INS-1 β-cells (currently unreported), it is therefore possible that supplementation with β-alanine might increase the intracellular pool of carnosine, thereby resulting in similar downstream positive effects on insulin secretion as discussed previously.

The other constituent part of carnosine, L-histidine is also a topic of current research for its potential use as an amino acid supplementation, as it is the imidazole ring that is thought to be functional element of carnosine (Boldyrev, et al. 2013). Lower than typical L-histidine concentrations have been shown to occur in patients with chronic kidney disease (Watanabe, et al. 2008), obese women compared to non-obese women (Niu, et al. 2012), and young obese patients and patients with type 2 diabetes (Mihalik, et al. 2012). Decreased L-histidine concentrations therefore correlate with reactive species related diseases. L-histidine will therefore also be investigated as a potential tool to decrease reactive species and improve insulin secretion from β-cells.

As previously mentioned, whilst carnosine synthesis may be possible, the other half to the carnosine challenge is rapid high affinity hydrolysis of carnosine to its constituent amino acids by carnosinases both in the blood and in tissue. This could simply negate any synthesis that may be possible through amino acid supplementation. Therefore a second treatment strategy, working alongside colleagues with expertise in medicinal chemistry at NTU, is to screen chemical libraries for potential compounds that can serve as carnosinase inhibitors. A recent study reported that reduced serum carnosinase activity as a result of treating with cysteine compounds, protected type 2 diabetic patients from diabetic nephropathy (Peters, et al. 2017). Using the crystalline structure of carnosinase-2 (CN2), chemical library databases have been screened *in-silico* for compounds that closely fit the catalytic cleft of CN2, whilst not being hydrolysed themselves, thereby potentially acting as carnosinase inhibitors.

The aim of this chapter is to identify if β-alanine or l-histidine supplementation can have a similar scavenging effect to that of carnosine in a type 2 diabetic model of glucolipotoxicity, and like carnosine, augment but importantly reverse glucolipotoxic driven loss of insulin secretion in β-cells. Secondly the aim was to identify carnosinase inhibitors using *in silico* docking techniques and screen the compounds for their ability to influence endogenous carnosine action, resulting in reversal of glucolipotoxic driven reactive species and loss of stimulated insulin secretion capacity in INS-1 β-cells.

4.2. Results

4.2.1. Carnosine Synthase is Expressed in β-cells

To determine if INS-1 β-cells express the protein capable of synthesising carnosine intracellularly, INS-1 cells were cultured in control media until confluent. Cells were lysed using RIPA buffer, and the resulting protein samples separated via SDS-PAGE. Protein was then transferred to nitrocellulose membrane and immunoblotted using anti-ATPGD1 (carnosine synthase) (Santa Cruz, USA) goat polyclonal antibody that reacts with rat species antigens.

Figure 4.1 shows that carnosine synthase is expressed in clonal INS-1 β-cells but is at the very edge of detection even when loading high levels of protein (30µg). This is likely either a result of low carnosine synthase expression in β-cells, or due to ageing, or low efficacy of the antibody. Either way, its presence in β-cells, which has never been previously reported, is suggestive that carnosine synthesis occurs in these cells. Furthermore, if β-alanine can enter these cells, then carnosine synthesis, and therefore the readily active pool of carnosine, should increase. As such, this therefore warranted investigation into the supplementation of β-alanine in INS-1 β-cells.

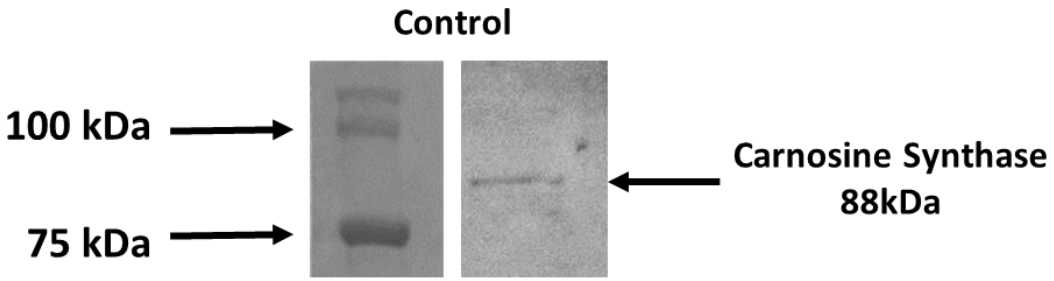

Figure 4. 1; Carnosine synthase is expressed in INS-1 β-cells.

INS-1 cells were cultured in control RPMI-1640 media, then lysed and protein separated by SDS-PAGE. Samples were transferred to a nitrocellulose membrane and immunoblotted using anti-ATPGD1 antibody (Santa Cruz) n=1.

4.2.2. Effect of β-alanine Supplementation on Glucolipotoxicity-Mediated Reactive Species

As carnosine was shown to scavenge reactive species generated by incubation of INS-1 β-cells in a glucolipotoxic environment, it was first sought to determine whether β-alanine supplementation could offer similar protection. INS-1 were therefore cultured in control or GLT media for 5 days. 1h prior to reactive species detection cells were then incubated in experimental media conditions ± 10mM β-alanine for 1h. Reactive species were detected using DCFDA dye and fluorescence quantified.

Consistent with previously presented data, 5 day incubation of INS-1 cells in GLT media (Figure 4.2) increased reactive species by 68.8 ± 27.7% compared to control ($p=0.024$). However, 1h incubation with β-alanine in control conditions had no significant effect upon reactive species level. Similarly, a 1h dose of β-alanine in cells incubated in GLT for 5 days also had no effect on reversing GLT driven reactive species, with reactive species increased 67.1 ± 25.5% compared to control ($p=0.019$). As shown in chapter 3, carnosine was able to reverse GLT driven reactive species back to within control level in the space of 1h, as the reaction for free radical quenching is

rapid upon addition of a scavenger. This data therefore implies that β-alanine has no scavenging potential *per se* in itself, yet may still provide a protective action if dosed for long enough to allow carnosine synthesis to occur.

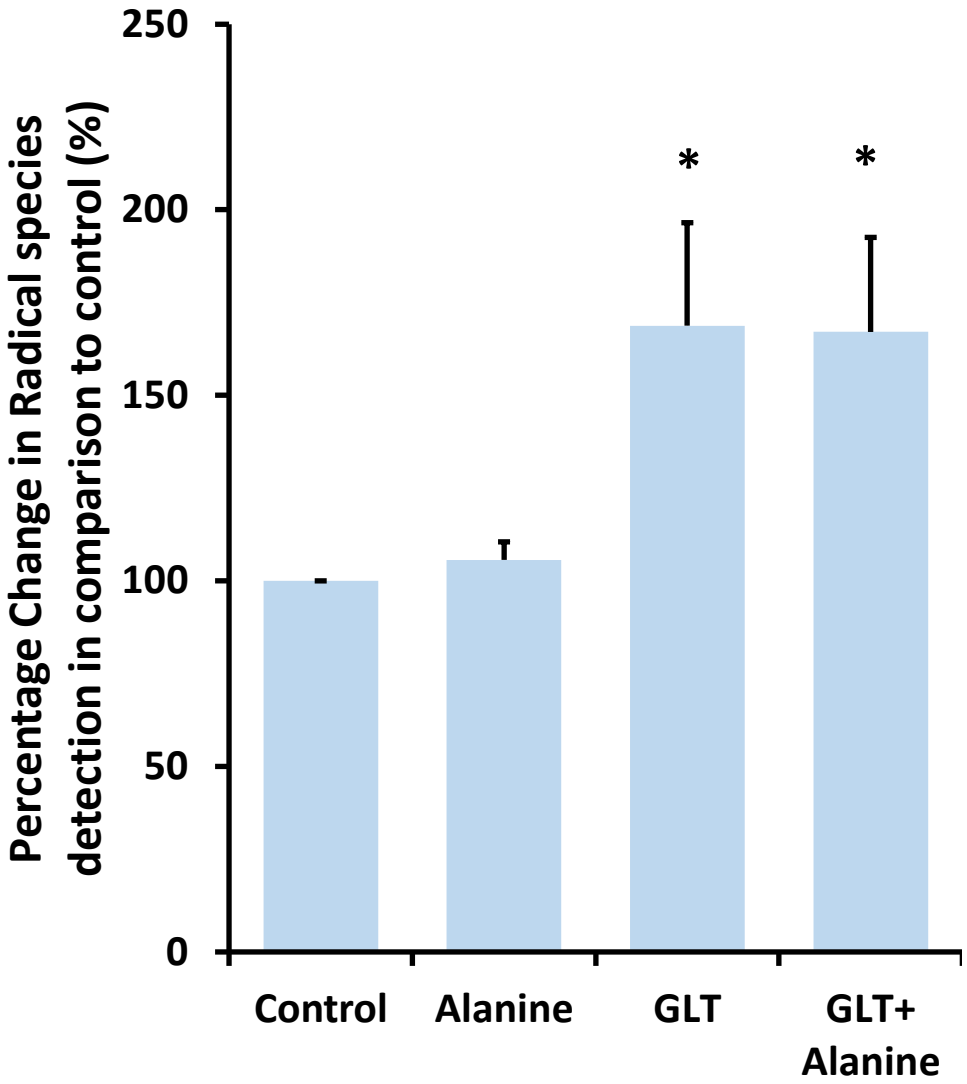

Figure 4. 2; 1h treatment of β-alanine has no effect on glucolipotoxicity-mediated reactive species.

INS-1 cells were cultured in control or GLT media for 5 days before the addition of 10mM β-alanine for 1h. Cells were washed and incubated in 20μM DCFDA for 1h prior to measurement, with reactive species measured via fluorescence at excitation 495nm and emission 530nm. Reactive species is expressed as percentage change in comparison to control from 4 independent experiments. *$p<0.05$ compared to control.

INS-1 cells were next cultured in control or GLT media ± 10mM β-alanine for 5 days prior to reactive species detection via DCFDA (Figure 4.3). This resulted in a statistically significant increase in GLT condition by 57.4 ± 15.6 compared to control ($p=0.006$). Importantly, whereas a 1h treatment of β-alanine had no effect on reactive species, 5 day treatment caused a significant reduction compared to that of GLT, reducing reactive species level to 118.6 ± 12.1% ($p=0.039$) relative to control. This indicates that long-term treatment with β-alanine can potentially reverse glucolipotoxic driven reactive species generation.

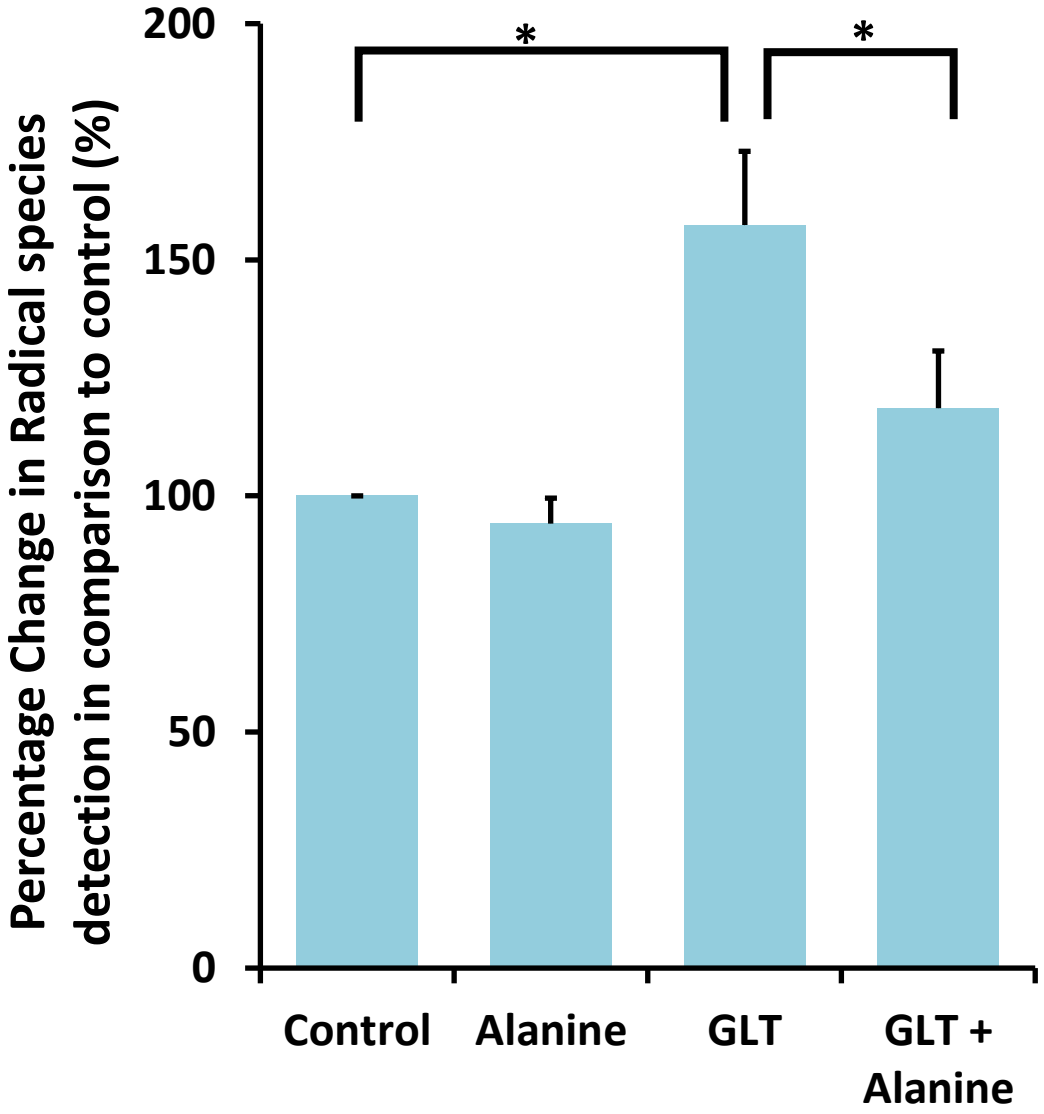

Figure 4. 3; 5 day treatment of β-alanine reverses glucolipotoxic driven reactive species.

INS-1 cells were cultured in control or GLT media ± 10mM β-alanine for 5 days prior to the addition of 20µM DCFDA for 1h. Reactive species were measured via fluorescence with an excitation and emission of 495nm and 530nm respectively. Reactive species is expressed as percentage change in comparison to control from 6 independent experiments. *p<0.05

4.2.3. β-Alanine Supplementation Increases Stimulated Insulin Secretion

As damaging glucolipotoxic driven reactive species were substantially reduced following 5 day treatment of β-alanine, the logical next step was to determine whether this resulted in increased insulin secretion. INS-1 cells were cultured in the presence of ± 10mM β-alanine for 5 days prior to secretagogue stimulation, and insulin secretion determined by ELISA (Mercodia, Sweden). Incubation of INS-1 cells with 10mM β-alanine for 5 days increased secretagogue-stimulated insulin secretion from 4.5 ± 0.4 ng/μg cellular protein to 6.0 ± 0.6 ng/μg cellular protein. This corresponds to a significant increase of 31 ± 14.0% ($p=0.045$) (Figure 4.4). Whilst not as big an increase as dosing with carnosine directly (chapter 3), this nevertheless offers a promising alternative for use as a dietary supplement.

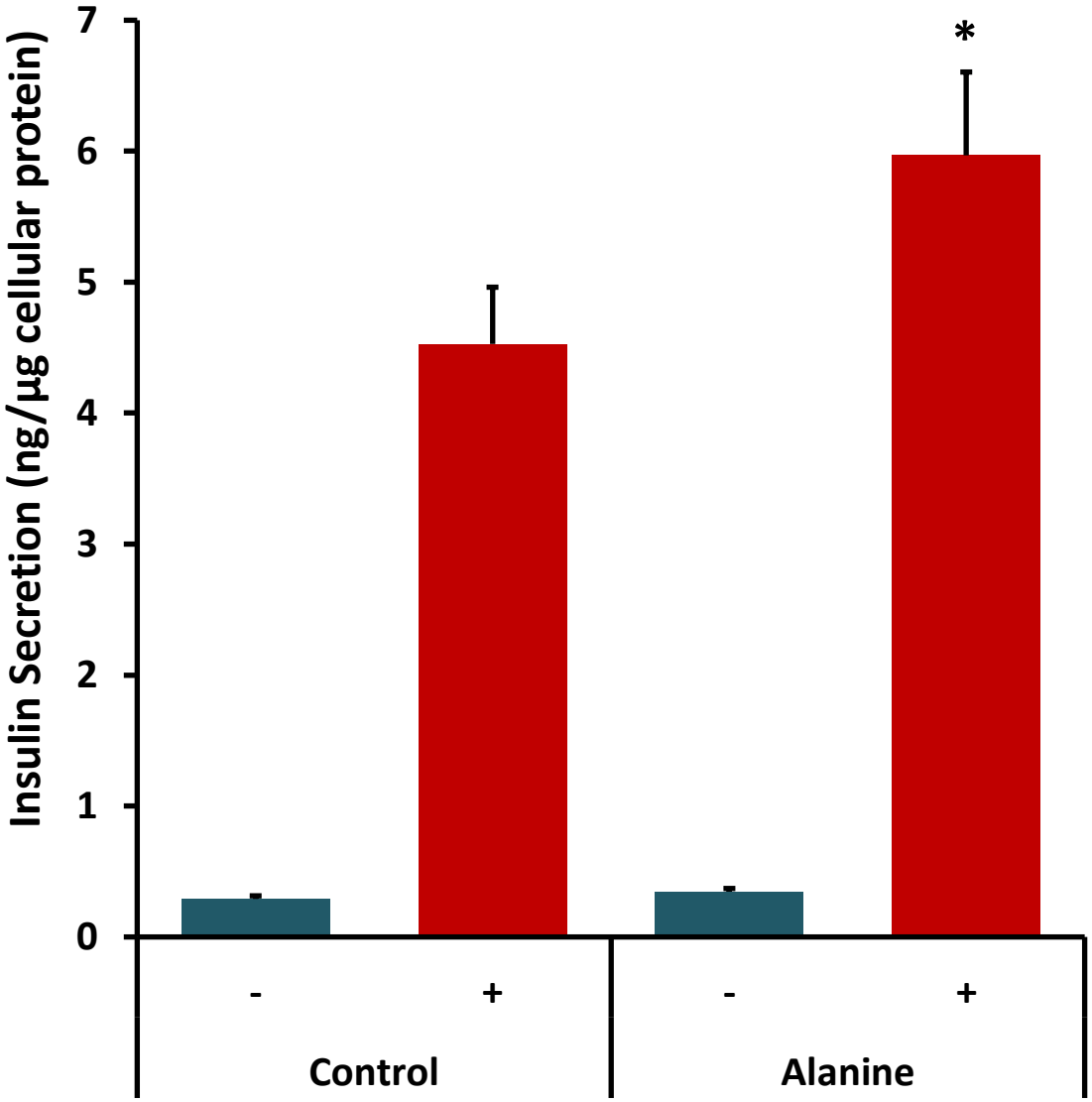

Figure 4. 4; β-alanine increases stimulated insulin secretion.

INS-1 cells were cultured in RPMI-1640 media in the presence of 10mM β-alanine for 5 days. Insulin secretion was determined by ELISA following incubation ± secretagogue cocktail for 2h [(-) blue, (+) red] with data normalised to cellular protein content. Data are expressed as mean ± SEM from 6 independent experiments. *p<0.05 compared to control stimulated samples (+).

4.2.4. β-alanine Reversal of Glucolipotoxic Inhibition of Insulin Secretion

As β-alanine was shown to increase the secretory output from β-cells as a consequence of reducing glucolipotoxic driven reactive species, it was important to investigate whether, like carnosine, it could also reverse the associated inhibition of

insulin secretion that results from chronic exposure to a glucotoxic environment. INS-1 cells were resultantly cultured in control or GLT media ± 10mM carnosine for 5 days and stimulated with a secretagogue cocktail and insulin secreted determined (Figure 4.5). Consistent with previously reported data, both in this thesis and the literature, incubation in GLT media for 5 days resulted in a significant reduction in secretagogue-stimulated insulin secretion. Specifically, secretion was reduced from 5.3 ± 0.5 ng/μg cellular protein in control stimulated conditions to 3.8 ± 0.2 ng/μg cellular protein in GLT ($p=0.016$). Similar to the data presented in Figure 4.4, a 5 day 10mM dose of β-alanine again increased stimulated insulin secretion to 7.0 ± 0.6 ng/μg cellular protein, representative of significant increase by 31.3 ± 12.0% compared to control ($p=0.04$). Importantly, when β-alanine was added to GLT media insulin secretion rose, to 4.7 ± 0.5 ng/μg cellular protein ($p=0.22$ v control), indicating a significant reversal of glucolipotoxic inhibition ($p=0.049$).

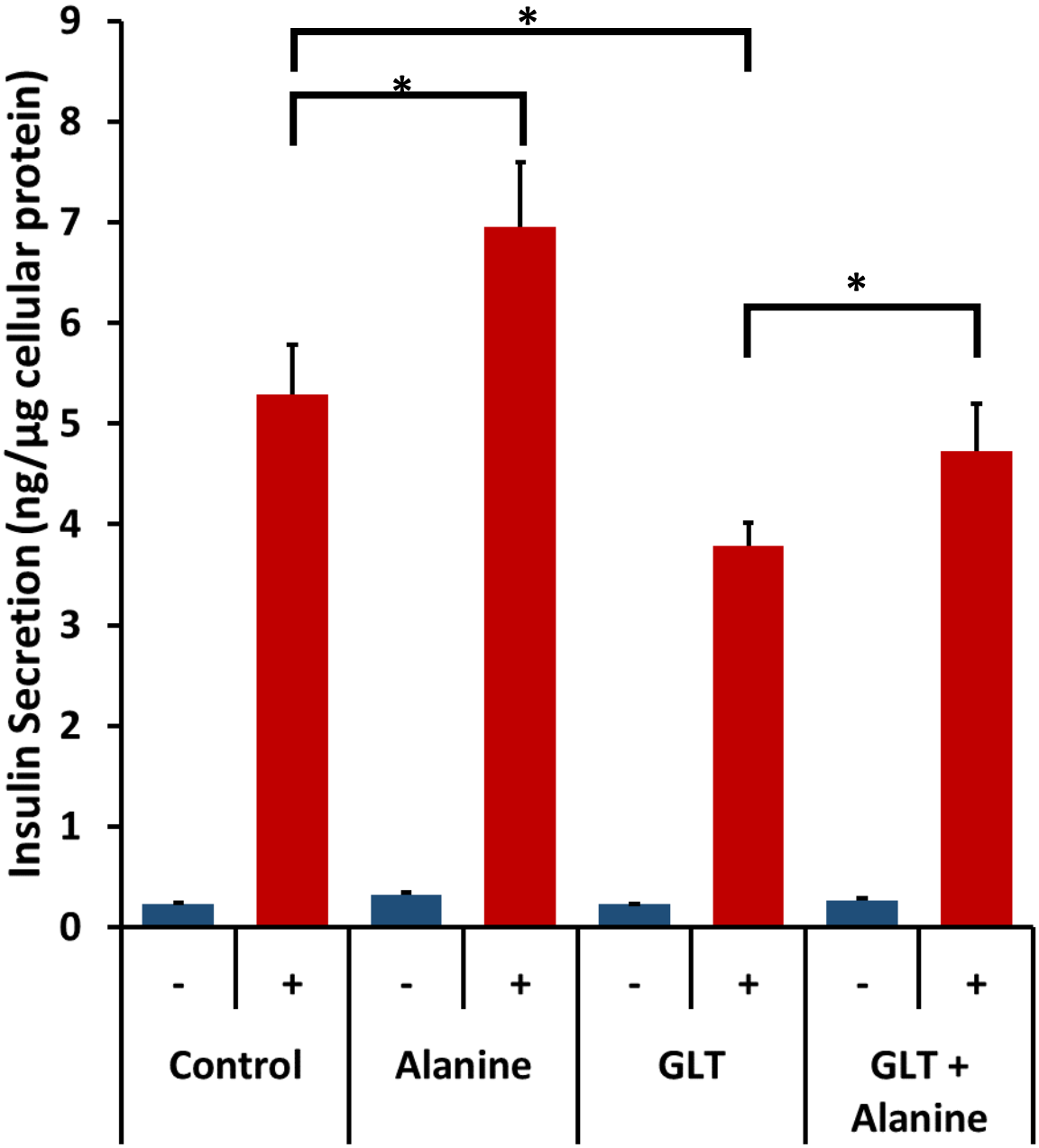

Figure 4. 5; β-alanine reverses GLT inhibited insulin secretion.

INS-1 cells were cultured in control or GLT media ± 10mM β-alanine for 5 days. Insulin secretion was determined by ELISA following incubation ± secretagogue cocktail for 2h [(-) blue, (+) red] with data normalised to protein content. Data is expressed as mean ± SEM from 4 independent experiments. *p<0.05

4.2.4. β-alanine Supplementation Increases Intracellular β-alanine, But Not Carnosine

Whilst this work theorises that β-alanine's positive effect scavenging reactive species and decreasing GLT driven inhibition of insulin secretion is the result of increased carnosine synthesis by carnosine synthase (which was shown earlier to be expressed in INS-1 β-cells), it is important to support this with quantifiable data. Therefore, in collaboration with Dr Ruth James and Dr Katie Hanna at NTU, INS-1 cells were prepared for high performance liquid chromatography (HPLC) analysis. HPLC is a column chromatography technique that pumps analytes through a high-pressured column. The sample is carried by a moving gas stream which separates and resultantly identifies compounds in a sample by measuring its retention time in the column.

INS-1 cells were therefore cultured in standard media and supplemented with 10mM β-alanine for 5 days prior to sample lysis. The samples were then added to an equal volume of sulphosalicyclic acid deproteiniser with an internal standard of norleucine at a concentration of 500μM. Samples alongside known standards were injected onto the analytical HPLC column and amino acid concentrations determined using a Biochrom 30+ HPLC ion exchange system with OPA derivatisation. Amino acid concentrations were normalised using the internal norleucine control allowing direct comparison between different samples.

Preliminary HPLC data (n=2) indicates that INS-1 cells supplemented with 10mM β-alanine for 5 days had an increased intracellular β-alanine concentration rising from 7.6 ± 3.2 μM to 527.8 ± 12.2μM. Unfortunately, there was an issue with quality

control on the third repeat of β-alanine supplementation, so this particular data point must for the moment be considered as preliminary data only. The data is however consistent with the idea that INS-1 β-cells express transporters responsible for amino acid transport across the cell membrane, and that β-alanine can utilise these to increase intracellular β-alanine concentration. However intracellular concentrations are still much lower than the dose of 10mM, suggesting that either transport across the membrane is slow, or else that transported β-alanine is rapidly utilised for cellular processes.

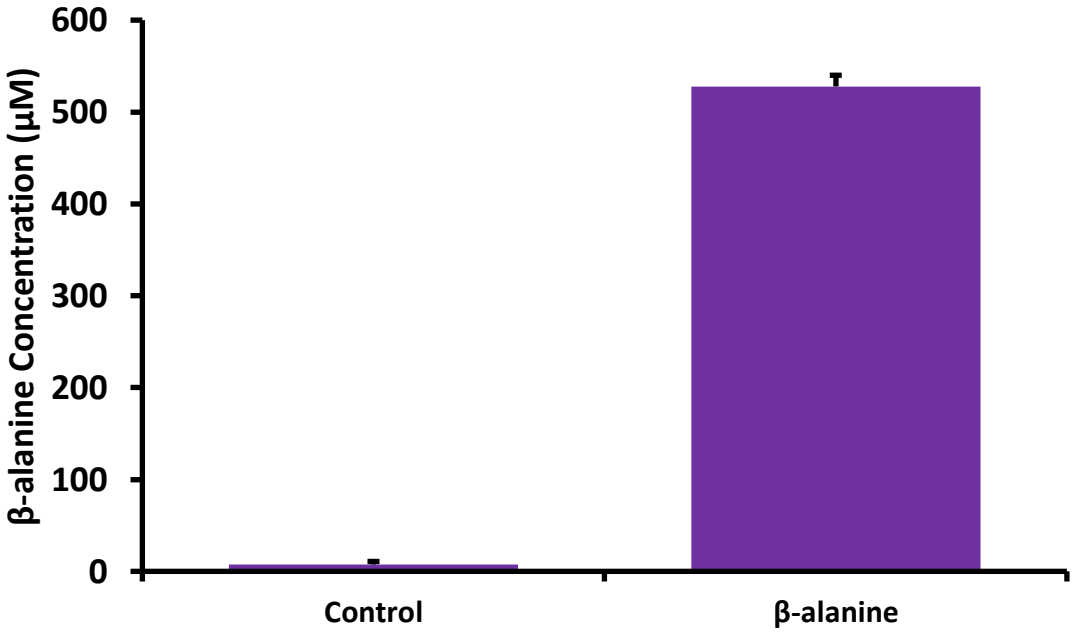

Figure 4. 6; Supplemented β-alanine is transported into INS-1 β-cells.

INS-1 cells were cultured for 5 days in standard growth media ± 10mM β-alanine before protein extraction. Samples were mixed with sulphosalicyclic acid deproteiniser with internal standard or norleucine (500µM) before ultrafiltrate sample was collected and analysed using Biochrom 30+ high-performance liquid chromatography ion exchange system with OPA derivatisation. Analytes were normalised to the internal standard of norleucine and presented as β-alanine µM concentrations. Control n=3, β-alanine n=2.

Surprisingly, when the same samples were used to determine intracellular carnosine concentrations following β-alanine supplementation, the carnosine concentration did not significantly change (Figure 4.7). The working hypothesis had been that it was β-alanine driven carnosine synthesis that caused the downstream effect on both reactive species scavenging and insulin secretion, yet in the current experiment carnosine concentrations remain effectively unchanged. However, the hypothesis may still be valid. If endogenous carnosine produced by carnosine synthase is rapidly utilised to quench high levels of circulating reactive species in the face of low anti-oxidant defence systems in β-cells then consequently, the intracellular carnosine pool would show little change in the HPLC analysis shown here. Unfortunately, the answer to this question lies outside the scope of current experiments, but more in-depth enzymatic analysis in future studies will hopefully answer this dilemma.

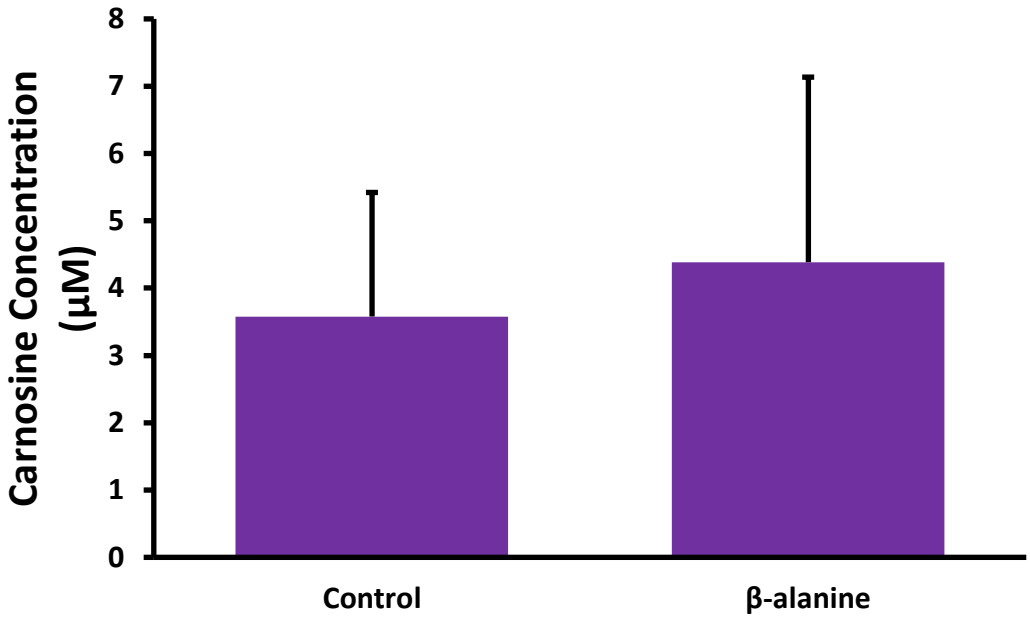

Figure 4. 7; β-alanine supplementation does not significantly increase carnosine concentration in INS-1 cells.

INS-1 cells were cultured for 5 days in standard growth media ± 10mM β-alanine before protein extraction. Samples were mixed with sulphosalicyclic acid deproteiniser with internal standard or norleucine (500µM) before ultrafiltrate sample was collected and analysed using Biochrom 30+ high-performance liquid chromatography ion exchange system with OPA derivatisation. Analytes were normalised to the internal standard of norleucine and presented as carnosine µM/L concentrations. Control n=3, β-alanine n=2.

4.2.5. L-histidine Supplementation is Toxic to β-cells

Whilst β-alanine is defined as the rate limiting step in carnosine synthesis, it is actually the imidazole ring of the L-histidine amino acid that is credited for its protective action in reactive species biology (Fontana, et al. 2002b). It was therefore investigated whether L-histidine supplementation would cause a decrease in reactive species, and thereby consequently result in enhanced insulin secretion from β-cells. INS-1 were cultured in control or GLT media ± 10mM l-histidine for 5 days prior to radical species detection using DCFDA (Figure 4.8). In line with previous experiments,

GLT resulted in a rise of reactive species by 46.0 ± 7.0% relative to control (p=0.001). Unexpectedly however, incubation with L-histidine in either control or GLT conditions caused a rise in reactive species by 53.6 ± 8.3% (p=0.001) and 79.5 ± 21.4% (p=0.01) respectively. This effect was mirrored by a decrease in secretagogue-stimulated insulin secretion of 20.0 ± 10.3% (p=0.11) relative to control (Figure 4.9).

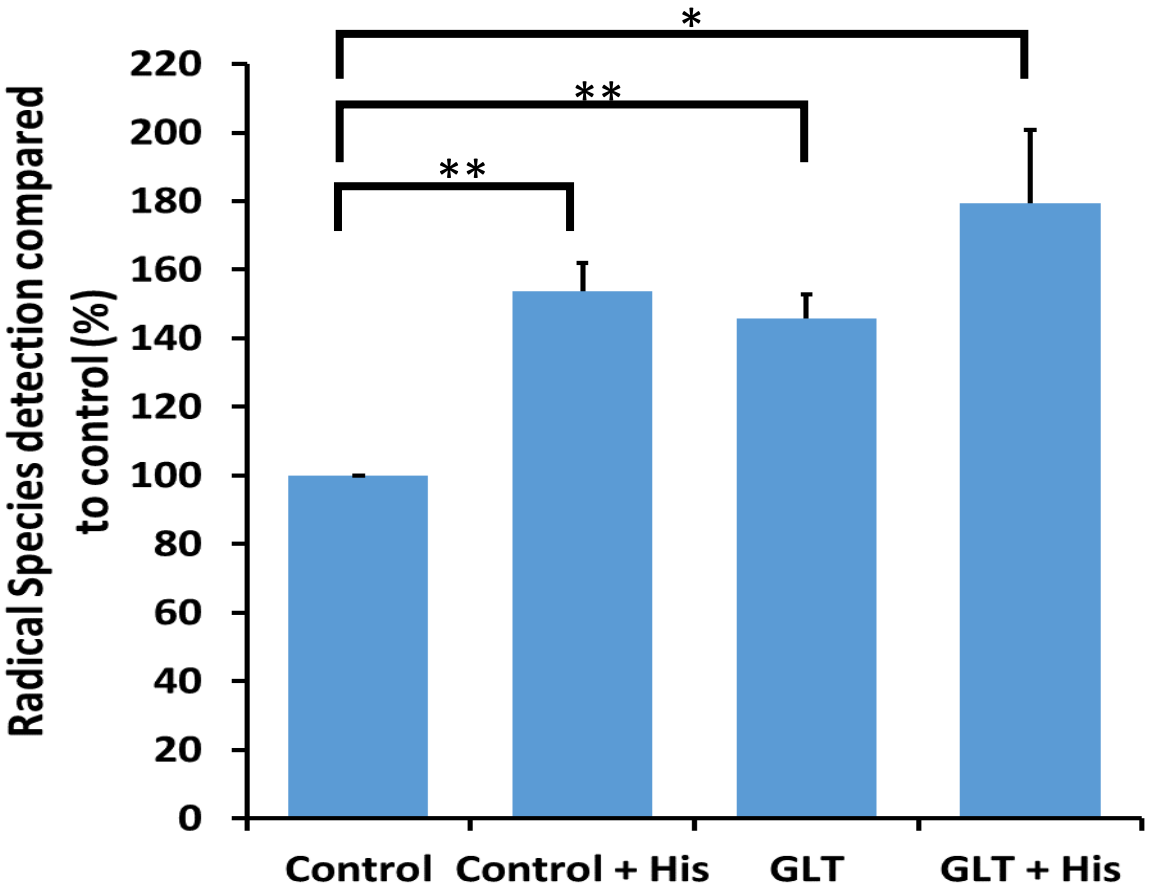

Figure 4. 8; L-histidine increase in reactive species.

INS-1 cells were cultured in control or GLT media for 5 days ± 10mM L-histidine prior to the addition of 20μM DCFDA for 1h. Reactive species were measured via fluorescence with an excitation and emission of 495nm and 530nm respectively. Reactive species is expressed as percentage change in comparison to control from 3 independent experiments. *p<0.05 **p<0.005

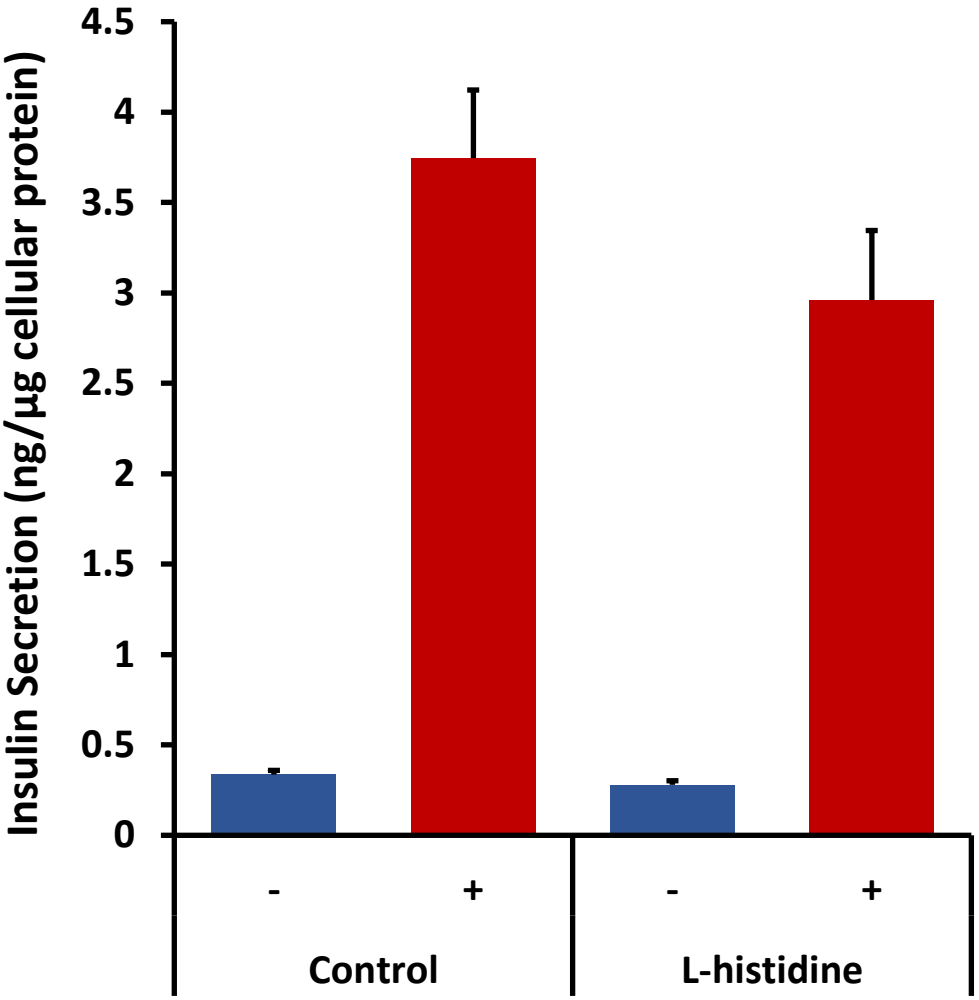

Figure 4. 9; L-histidine decreases secretagogue stimulated insulin secretion.

INS-1 cells were cultured in control or GLT media ± 10mM l-histidine for 5 days. Insulin secretion was determined by ELISA following incubation ± secretagogue cocktail for 2h [(-) blue, (+) red] with data normalised to protein content. Data is expressed as mean ± SEM from 3 independent experiments.

4.2.6. Carnosinase-2 is Expressed in β-cells

Carnosinase-2 is the physiological intracellular tissue carnosinase. As it degrades carnosine back down to its constituent parts once carnosine either enters into cells, or upon endogenous synthesis, carnosinase-2 is a potential major barrier to supplementation strategies. It is therefore important to determine whether carnosinease-2 is expressed in β-cells. INS-1 cells were cultured in control media, then cells lysed and protein separated by SDS-PAGE. Resultant proteins were transferred to nitrocellulose and immunoblotted using an anti-CNDP2 antibody (Abcam, UK). Membranes were developed and demonstrated that carnosinase 2 is indeed expressed in INS-1 β-cells (figure 4.10).

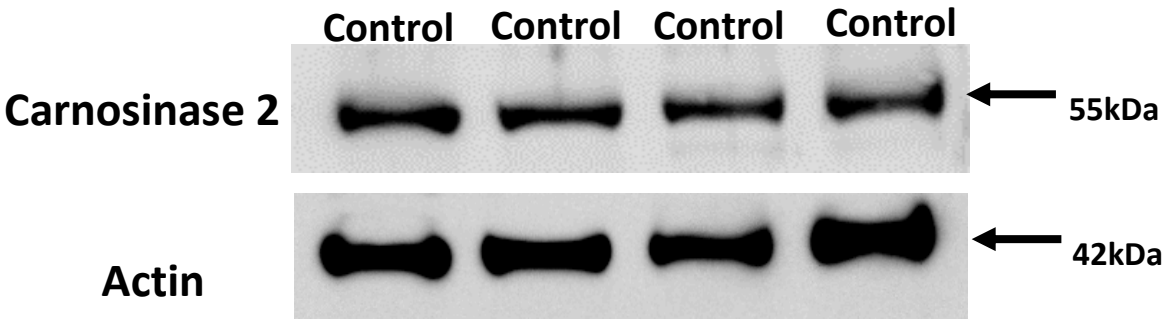

Figure 4. 10; INS-1 β-cells express carnosinase-2.

INS-1 cells were cultured in RPMI-1640 media until 70% confluent, cells lysed, and proteins separated by SDS-PAGE. Samples were transferred to a nitrocellulose membrane and immunoblotted using anti-CNDP2 or anti-actin antibody (Abcam, UK).

4.2.7. Compounds Designed as Carnosine-2 Inhibitors have Varied Effect on β-cell Viability

Given the challenge of carnosine supplementation as a practical solution to enhance insulin secretion in the face of β-cell carnosinase-2, alternative solutions could be to either enhance endogenous carnosine action through delivery of carnosine inhibitors

into the β-cell, or else adopt a supplementation strategy that instead utilises weakly hydrolysable carnosine mimetic molecules.

In order to develop the first of these strategies, computational docking analysis was undertaken. As detailed in chapter 2.8, the top 50 MayBridge compounds identified from ROCS virtual screenings as having similar chemistry and structural shape to carnosine and measured using the Tanimoto combo scoring were docked in the A1 active site of CN2 using carnosinase-2's crystalline structure, in the programme GOLD, alongside bestatin. Bestatin is a competitive inhibitor of human tissue carnosinase-2 and acted as an internal control with any variation in docking best fit percentage scores indicative of errors or malfunction in the software that would need retesting. A binding interaction score of 50 (which is lower than that of carnosine binding) was chosen as the benchmark score. As the aim of the *in-silico* screening process was to find carnosine-shaped molecules stable against carnosinase hydrolysis, a score of 50 is a high enough score to theoretically fit the active site yet low enough to have only a relatively weak interaction with the enzyme. As such this should result in an insufficient interaction for carnosine 2 to adopt the active conformation around the compound required for hydrolysis.

Of the 50 compounds screened, 14 had a score above 50. M28 had the highest score and M47 having the lowest (with 70 and 20 respectively). All structures with a score of 50 and over were relatively small in size and had an either a 6 or 5 membered aromatic ring joined by an alkyl chain bridge to the rest of the molecule. The 6 membered rings were mainly benzene or pyridine, whilst the compounds with a five membered ring consisted of either furan, azol or imidazole. Imidazole is the same

aromatic character as carnosine (the L-histidine component). Unfortunately however, due to IP / patent considerations, the remaining structure of the chosen compounds must remain confidential at this time.

The top 9 highest scoring compounds (M4, M8, M14, M21, M28, M38, M44, M48 and M49) were purchased from MayBridge and screened for their potential. Upon arrival, the newly purchased compounds were disaggregated in 1ml of 100% sterile ethanol and diluted in sterile KREBS to a final concentration of 10mM. These were then diluted 1:100 into experimental media to give a final concentration of 100μM. This final concentration was chosen as pharmaceutical compounds would be expected to have significantly greater efficacy than carnosine (Peters, et al. 2017). As carnosine is optimally effective at a concentration of 10mM, 100μM was selected as a starting concentration for throughput screening purposes. However, once an effective compound is identified, more comprehensive dose-response experiments will be carried out to determine the most suitable concentration for physiological application moving forward.

In control and GLT control conditions, a vehicle of ethanol was added to act as a vehicle control. This vehicle control did not affect cell viability, as shown in Figure 4.11. The effect of the 9 screened compounds upon cell viability is detailed in Table 4.1. Of the 9 compounds, only M4, M8, M14, and M28 did not decrease cell viability - as determined through observation down a light-microscope over the 5 day incubation period. M21, M38, M44, M48 and M49 by contrast were toxic, decreasing cell proliferation and killing cells. Example images of a number of the treated

compounds are displayed in Figure 4.11. Based on this data, only compounds that had no visible effect on cell phenotype and viability was taken forward for trials.

Compound Code Name	Cells Viable after 5 day exposure
M4	✔
M8	✔
M14	✔
M21	✘
M28	✔
M38	✘
M44	✘
M48	✘
M49	✘

Table 4. 1; Effect of Maybridge compounds on β-cell viability.

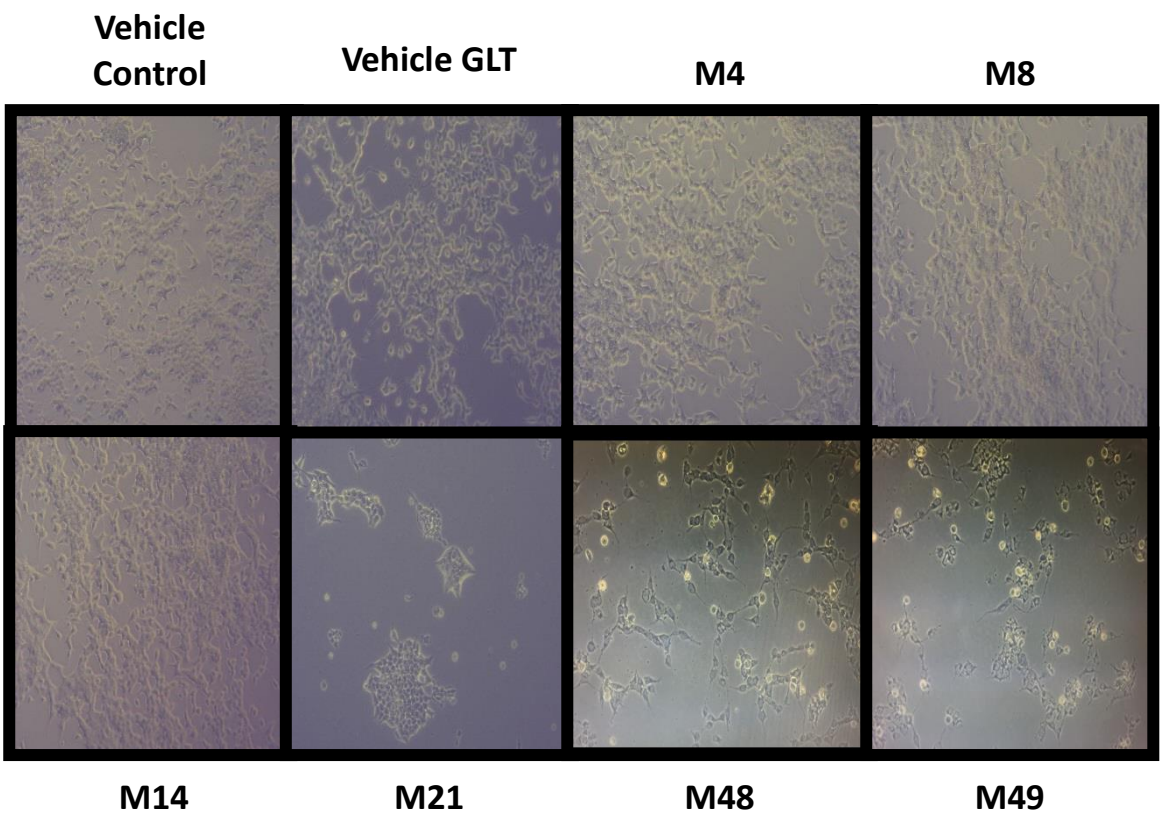

Figure 4. 11; Effect of selected compounds on cell viability.

INS-1 cells were grown in RPMI-1640 media supplemented with labelled compound (vehicle, M4, M8, M14, M21, M48 and M49) for five days prior to imaging at 10X magnification using Zeiss Primovert microscope with AxioCam ERc5s camera.

4.2.8. Compounds Designed as Carnosine-2 Inhibitors are Ineffective at Reversing Glucolipotoxic Reactive Species in β-cells

Compounds that were not toxic were next taken forward to functional analysis screening. Reactive species quantification was chosen as an initial screening experiment for these compounds based on cost and the relatively high throughput generation of data that had previously been observed when INS-1 cells were incubated in GLT media incubated +/- carnosine. INS-1 cells were therefore cultured in vehicle control or GLT media, or control or GLT media supplemented with the compound of interest to a final concentration of 100μM. As the compounds were chosen on the ability to fit the active site of carnosinase-2, the theory is that

carnosinase-2 activity should be diminished, and endogenous carnosine then able to scavenge radical species without being turned over. Consequently, should this in fact be the case, then this should potentially increase insulin secretion, as observed previously. As such, after 5 days incubation in control or GLT media supplemented with the compounds, cells were washed and then treated with DCFDA before their intracellular reactive species were quantified by fluorescence and normalised to control (Figure 4.12).

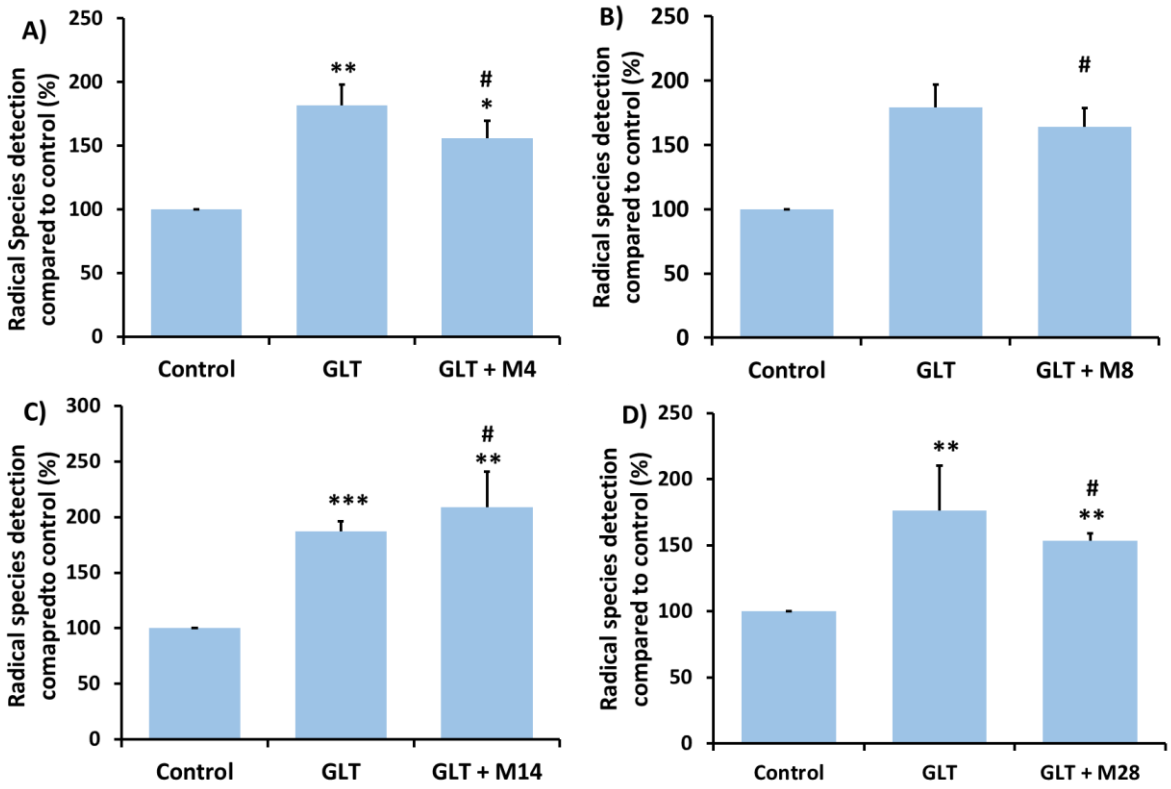

Figure 4. 12; Compounds designed as carnosinase inhibitors have no significant effect upon glucolipotoxic driven reactive species.

INS-1 cells were cultured in control or GLT media supplemented with a) M4, b) M8, c) M14 and d) M28 for 5 days. Cells were washed and incubated in 20µM DCFDA for 1h prior to measurement, with reactive species measured via fluorescence at excitation 495nm and emission 530nm. Reactive species is expressed as percentage change in comparison to control from a minimum of 3 independent experiments. *p<0.05, **p<0.005, ***p<0.0005 compared to control, #p>0.05 compared to GLT.

Unfortunately, the compounds that were chosen for their ability to fit the active site of carnosinase-2 and were non-toxic (i.e. had no clear effect on cell viability) to β-cells over a 5 day period had no significant effect on reactive species. GLT as expected resulted in significant increase in reactive species compared to control in all instances. Reactive species were still increased by 55.7 ± 13.8%, 63.9 ± 14.8%, 53.5 ± 3.3% respectively compared to control for a co-treatment of GLT and either M4, M8 and M28. These were all statistically significant increases compared to control ($p<0.05$). Compound M4, M8 and M28 did however slightly reduce GLT driven reactive species modestly, however the change was small and statistically non-significant with p values of 0.15, 0.21 and 0.16 respectively compared to GLT treatment alone.

Conversely, GLT and M14 compound treatment increased reactive species above GLT conditions alone to 209.2 ± 31.8% ($p=0.004$ compared to control, $p=0.26$ compared to GLT), suggesting this compound is causing additional yet non-significant stress when INS-1 cells were cultured in GLT co-treatment and was therefore deemed toxic.

4.2.9. Compounds Designed as Carnosine-2 Inhibitors had No Effect on Reversing Glucolipotoxic Inhibition of Insulin Secretion

As a modest decrease in average reactive species for 3 of the screened compounds was observed, insulin secretion was therefore determined. Compounds were screened just once to determine the likelihood of them having any beneficial effect on insulin secretion (as the insulin secretion kits are very expensive) and if so, more insulin secretion experiments would be carried out for positive compound hits.

INS-1 cells were therefore incubated in control media, GLT media or GLT media supplemented with a final concentration of 100μM of M4, M8 or M28 for 5 days. On

the fifth day, cells were stimulated with a secretagogue cocktail or incubated in KREBS for 2h and secreted insulin determined by ELISA (figure 4.13).

Consistent with both previously presented data here and in literature, a 5 day GLT incubation caused a reduction in secretagogue stimulated insulin secretion compared to control. Co-incubation with the chemical compounds that had a limited and insignificant effect on reactive species, had no effect on reversing the loss of insulin secretion from GLT. In fact, some lowered secretion below that of GLT alone. For this reason, it was decided to discontinue insulin secretion analysis with these compounds. As no compounds were seen to illicit a direct positive effect upon insulin secretion from β-cells, further experimentation in other tissue types, and the generation of more compounds is needed.

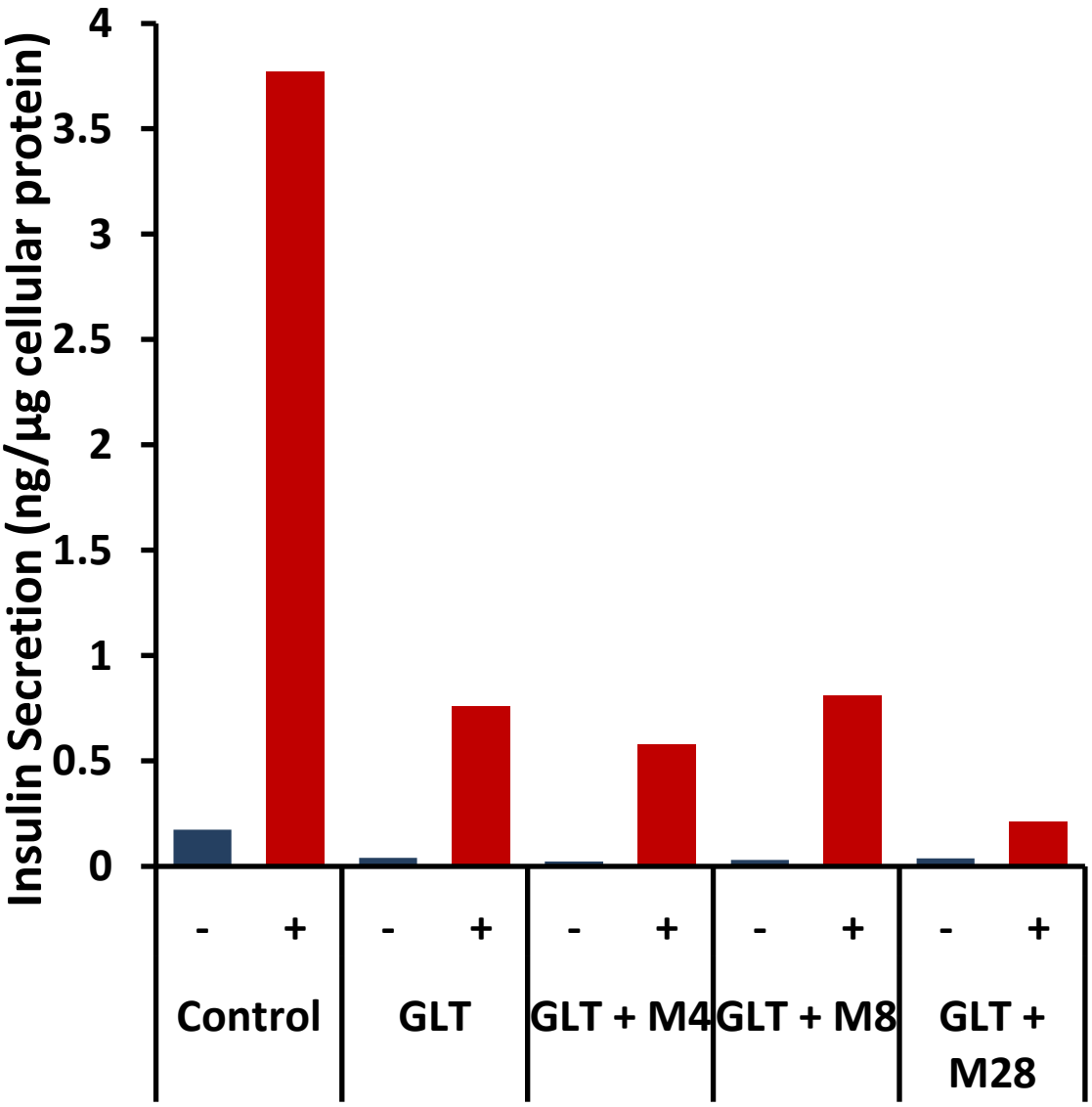

Figure 4. 13; Compounds designed as carnosinase inhibitors have no significant effect on reversing glucolipotoxic diminished insulin secretion.

INS-1 cells were cultured in control and GLT media or GLT media ± 100µM of compound M4, M8 or M28 for 5 days. Insulin secretion was determined by ELISA following incubation ± secretagogue cocktail for 2h [(-) blue, (+) red] with data normalised to cellular protein content. Data are expressed as mean from one initial screening experiments.

4.3. Discussion

Data presented here shows for the first time that carnosine synthase is expressed in clonal INS-1 β-cells. Whilst the concentration of carnosine synthase is yet to be determined, this is at least proof of principle that carnosine can be synthesised intracellularly within β-cells. This suggests that β-alanine supplementation could therefore potentially increase endogenous carnosine concentration, and thus elicit the same protective effect as administration of extracellular carnosine (Cripps, et al. 2017).

In terms of a full physiological model this would also have several benefits over carnosine supplementation. Carnosine and β-alanine from oral dosing would have to be transported through intestinal cells and then again into the blood for circulation to the pancreas. This opens carnosine up to rapid hydrolysis to its constituent parts, both by carnosinase-2 in the intestinal tissue cells and carnosinase-1 in the blood. Supplementation of the same concentration of β-alanine would therefore in theory result in similar circulating β-alanine concentrations as when carnosine was hydrolysed to its component parts.

The data presented indicates that β-alanine supplementation whilst having no scavenging potential of its own, can elicit a protective effect over glucolipotoxic driven reactive species if chronically dosed over 5 days. This would suggest that the protective action is coming from β-alanine's utilisation to form carnosine. This is in keeping with previously reported data, as 5 day β-alanine supplementation resulted in both an increase in stimulated insulin secretion in control conditions, but

importantly was able to reverse the glucolipotoxic inhibition of insulin secretion seen in β-cells.

Interestingly, the HPLC data presented in this chapter indicates that β-alanine can be transported into these cells, yet surprisingly there was little increase observed in intracellular carnosine concentration. One potential explanation for this might be that carnosine is difficult to quantify with high sensitivity using HPLC, as due to its highly hydrophilic nature it is poorly retained in the reverse phase C18 HPLC columns as well as lacking sufficient absorbance in the UV-visible spectra (Xie, et al. 2013). This would however seem unlikely to account for the scale of the discrepancy observed. Instead there may be a biological explanation for the findings.

As mentioned previously, carnosine synthase has a very high affinity for β-alanine (Skaper, et al. 1973b; Ng and Marshall 1978), suggesting that upon entry into cells, synthesis to carnosine is likely to be rapid. However, given the high levels of reactive species found within β-cells and low intracellular anti-oxidant defence systems (Robertson and Harmon 2007) this newly synthesised carnosine might therefore be utilised immediately, thereby resulting in the decrease of reactive species and increase in secretagogue stimulated insulin secretion presented here. This would explain why, despite the observed functional effects, no change was observed in intracellular carnosine concentration following cellular exposure to β-alanine. Future experiments should therefore aim to determine the rate of carnosine synthesis within β-cells, as well as investigate the potential functional role of β-alanine as a therapeutic tool to regulate glucose homeostasis in type 2 diabetes.

In contrast to β-alanine, L-histidine supplementation had adverse effects both on cellular reactive stress and function. The reason for this is unknown, as L-histidine is regarded as the protective component of carnosine. However, there is a noticeable difference between the histidine component of carnosine and that of free histidine. The imidazole ring of carnosine has a pKa of 6.83 and is the undisputed effecter of carnosine's role as a pH buffer. However, in free histidine, the pKa of the imidazole ring is lower at 5.83 (Smith 1938; Hill, et al. 2007). pKa is a measure of acid strength, therefore the lower the value the more acidic the compound. As free histidine's pKa is lower, dosing with concentrations as high as 10mM may have elicited an acidic toxic effect resulting in an increase in reactive stress, accompanied by a decrease in insulin secretion capabilities. For this reason, as well as β-alanine concentration reportedly being the more likely rate limiting component of the carnosine synthesis pathway, L-histidine supplementation alone was not considered for further research as a therapeutic agent to combat type 2 diabetes.

Carnosinase-2 was shown to be expressed in INS-1 β-cells, and could potentially therefore counteract either carnosine supplementation or enhanced carnosine synthesis as a strategy through rapid hydrolysis by this enzyme. However, compounds that were derived from *in-silico* screening for their ability to fit the active site of carnosinase-2, whilst not binding with high enough precision to be hydrolysed, were screened as potential non-hydrolysable carnosinase inhibitors. Surprisingly, they were shown to be ineffective in INS-1 β-cells at reversing the damage caused by glucolipotoxicity. This was witnessed through a non-ability to reduce reactive species

that are significantly upregulated in the presence of GLT, thereby resulting in no change to glucolipotoxicity-associated loss of insulin secretion.

We should not be too hasty to disregard the potential of this strategy however, as data from a colleague in the Turner group working with skeletal muscle myotubes and the very same compounds, shows them to be effective at reducing glucolipotoxicity-associated reactive species in these cells, thereby resulting in enhanced glucose uptake. What might be the reason for such differing cellular outcomes?

These compounds were chosen for their ability to fit the active site of carnosinase-2 and therefore function as carnosinase inhibitors. As such, this strategy is dependent upon there being a high enough existing concentration of carnosine within the cell to elicit an effect. In skeletal muscle, carnosine concentrations are reportedly as high as 5-8mmol/L in wet weight (Derave, et al. 2010), yet in β-cells this concentration is unknown and unpublished. Therefore, if the β-cell carnosine concentration were substantially lower than that of skeletal muscle, this might account for their effectiveness in skeletal muscle, but lack of efficacy in β-cells. Therefore, it is imperative to identify the endogenous carnosine concentration in β-cells. Preliminary data presented in this chapter indicates that this in fact the case, with intracellular carnosine concentration in INS-1 β-cells in the low μM range. This might therefore explain why the carnosinase inhibitors were ineffective in β-cells. This data is therefore also consistent with islets being reported as one of the least protected tissues in terms of intrinsic antioxidant activity. This renders these cells particularly susceptible to damage from oxidative stress resulting from prolonged exposure to

glucolipotoxicity (Robertson and Harmon 2007). Other therapeutic strategies based on carnosine mimetics, rather than carnosinase inhibition, may however prove effective at enhancing insulin secretion.

4.4. Future Directions

β-alanine continues to be a promising amino acid supplement that could offer a protective action against glucolipotoxicity driven diabetes. However, similar to carnosine, its method of action is still not fully understood. Future work will therefore aim to identify both its mechanism of action and the rate of carnosine synthesis in β-cells. By so doing we should be able to determine whether β-alanine supplementation offers real promise as a therapeutic strategy.

Whilst the drug discovery compounds investigated in this chapter were designed as carnosinase inhibitors, it may be more beneficial to select and screen non-hydrolysable carnosine mimetics. These mimetics would be based more on biological function as opposed to structural shape and should elicit the same advantageous actions of carnosine but without rapid hydrolysis by carnosinase enzymes (both in tissue and sera). This would allow for a much lower dosing concentration, thereby decreasing the probability of the compounds having idiopathic toxic effects whilst also offering a longer lasting action on reducing reactive stress and increasing insulin secretion. This will be the basis for future collaborative work at Nottingham Trent University.

5. Downregulation of Heterotrimeric G-Protein Coupled Receptor Signalling Contributes to Glucolipotoxic Inhibition of Insulin Secretion

5.1. Introduction

The transcriptome is a complete set of transcripts contained within a cell. The number of transcripts per gene varies specifically, dependent upon the physiological condition or developmental stage of that particular cell. Developing an understanding of the transcriptome will allow the interpretation of the whole genome, in turn identifying novel functional molecular elements within both cell and tissue. This depth of understanding will also make it possible to recognise clear changes within the transcriptome in response to disease. Novel key regulators of disease onset will be elucidated to allow further characterisation of their functional role within certain diseases, with the aim to generate new treatment strategy targets.

There are various technologies developed to quantify the transcriptome, these include but are not limited to hybridisation with custom made microarray approaches or sequence-based approaches. The Turner research team recently published a transcriptomic study into the effect of glucolipotoxicity upon pro-inflammatory β-cell gene expression utilising microarray technology (Bagnati, et al. 2016). This identified that hyperglycaemia and hyperlipidaemia upregulation of tumour necrosis factor (TNF)-5 activates the transcription factors NF-κB and signal transducer and activator of transcription (STAT-1), and that this in turn ultimately triggers the onset of islet cell death.

Whilst microarray technology has proven useful and successful for the identification of novel gene regulators, the development of next generation sequencing (RNAseq), offers numerous different advantages over microarray technology. Hybridisation techniques depend on pre-existing knowledge of the genome sequence to design the

custom microarray and can sometimes have limited detection powers owing to high background level readings as a result of cross-hybridisation (Okoniewski and Miller 2006; Royce, Rozowsky and Gerstein 2007).

RNAseq technology converts a whole population of purified RNA to cDNA fragments before the overhanging ends are blunted and adenylated. Amplification adapters are added to one or both ends of the fragments and amplified accordingly. The resulting sample is then sequenced in a high-throughput manner obtaining short sequence reads from one end of the fragments to the other, typically 30-400 base pairs long. The presence, but more importantly the quantity of each RNA can be calculated and directly compared between different biological samples. The advantage of RNAseq over technologies such as microarray is that RNAseq doesn't have an upper limit for detection. This allows highly sensitive and highly reproducible detection of expression ranges of each transcriptome increasing the likelihood of accurate results (Wang, Gerstein and Snyder 2009).

Building from the previous microarray dataset from the Turner research group, the aim of this chapter of work was to utilise Illumina-HiSeq gene expression analysis data to more accurately examine transcriptome changes in INS-1 β-cells that are driven or exacerbated by glucolipotoxicity. Upon the identification of TAARs as a family of receptors whose gene expression was particularly altered by glucolipotoxicity, the aim was to characterise the mechanistic action of TAAR stimulation to investigate these receptors as a potential therapeutic strategy to treat type 2 diabetes.

5.2. Results

5.2.1. Identification of Protein Families Differentially Expressed in Glucolipotoxicity

To characterise and better understand mechanisms in which chronic exposure to high glucose and/or high fatty acid concentrations affects cellular function across the genome, INS-1 β-cells were incubated in standard RPMI growth media, or media supplemented to 28mM glucose and or 200µM oleic acid and 200µM palmitic acid for 72h. After 3 days, total RNA was isolated and purified before quality assessment using an Agilent Bioanalyser (Santa Clara, CA). High quality samples (RIN score above 8 – see section 2.5.2.2.) were then sent to the Sarah Lamble laboratory in Oxford for sequencing and library preparation using an Illumin HiSeq^{TM} 2000 instrument (Illumina, San Diego, USA). The resultant raw RNAseq data was analysed by Dr Rob Lowe (Blizard Institute, Barts and The Royal London School of Medicine) who aligned the raw data to an annotated reference genome (rn4 extracted from UCSC http://genome.ucsc.edu/goldenPath/credits.html#rat_credits) using Top Hat v 2.0.9 (http://tophat.cbcb.umd.edu.) with reads that aligned to exons, genes and splice junctions counted. The data was visualised using the programme HTseq-count (http://www-huber.embl.de/users/anders/HTSeq/doc/count.html), the data was visualised and interpreted citing gene and transcript expression as read counts. DEseq (http://www.bioconductor.org/packages/devel/bioc/html/DESeq.html) was then used to normalise the expression data to in-sample distributional changes.

Genes significantly differentially expressed in a combinative treatment of both high sugar and high fatty acids (GLT) relative to control ($p<0.05$), were analysed by Dr Tania Jones, using PANTHER gene ontology software (http://www.pantherdb.org/).

This software determined genes that had the greatest differential expression when cultured in glucolipotoxic media for 72h and calculates the number of genes that are significantly enriched within a specific biochemical pathway. Enrichment was only considered significant when there were more differentially expressed genes listed for a specific pathway than would be expected randomly, determined by the total number of genes associated with that given pathway.

As shown in Table 5.1, G-protein coupled receptors (GPCRs) were the highest of any specific protein class in terms of significance of differentially expressed genes (p=1.67 X $10E^{-24}$). This chapter of work will therefore focus on GPCR families that are differentially expressed when exposed to glucolipotoxicity within the RNAseq dataset, to determine whether their dysregulation contributes to glucolipotoxic β-cell dysfunction.

Protein Class	*P* Value
Receptor	1.88 E-38
G-protein coupled receptor	1.67 E-24
RNA binding protein	3.54 E-20
Ribosomal protein	1.54 E-18
Signalling molecule	1.28 E-17
Nucleic acid binding	2.91 E-17
Transporter	8.91 E-16
Immunoglobulin	1.13 E-13
Ion Channel	2.72 E-13
Cell adhesion molecule	4.58 E-11

Table 5. 1; Differential expression of protein family classes when exposed to glucolipotoxicity.

Comparative analysis using PANTHER of protein family gene expression when INS-1 cells were cultured in control or GLT media for 72h compared to control. Data is ordered in significance and compiled from 3 independent RNAseq analyses per condition.

5.2.2. Glucolipotoxic Down Regulation of Trace Amine Associated Receptor (TAAR) Expression in INS-1 β-cells

G-protein coupled receptors are essential mediators of communication between intracellular and extracellular environments. They are characterised typically by having seven membrane spanning α-helical structures, divided by alternating internal and external loop regions. Whilst GPCR's have a multifaceted functionality, the classical role is to couple the binding of its agonist, to the activation of an associated

heterotrimeric G-protein which modulates downstream effectors (Rosenbaum, Rasmussen and Kobilka 2009a).

One GPCR family of note that were differentially expressed within the Illumina HiSeq data set when INS-1 cells were exposed to glucolipotoxicity for 72h was the family of trace amine associated receptors (TAAR). TAARs were first identified in 2001 as receptors for trace amines such as *p*-tyramine, *2*-phenyethylamine and others. Stimulation of receptors with these ligands resulted in an increase in cAMP production, implicating its potential use as a novel pharmacological intervention tool (Borowsky, et al. 2001; Bunzow, et al. 2001).

The Illumina HiSeq data (Figure 5.1) indicated that TAAR3, 4, 5, 6, 7a, 7b, 7c, 7d, 7e, 7g, 7h, 8b, 8c and 9 were all infinitely downregulated when exposed to GLT for 72h. This meant that there were no read counts for these genes in GLT, where there previously was in control conditions, and all of which corresponded to a statistically significant reduction ($p<0.05$). TAAR1, 2 and 8a, also had a significant reduction in read counts for GLT conditions compared to control, with p values of 0.02, 0.0001 and 0.001 respectively. All TAAR family member RNA expression was also significantly driven down ($p<0.05$) in solo treatments of high sugar or high fatty acid concentrations, bar TAAR1 in high fat ($p=0.12$). Importantly for this work, a combination treatment had the largest downregulation effect across all TAAR members and therefore this combinative treatment was used for all subsequent experiments.

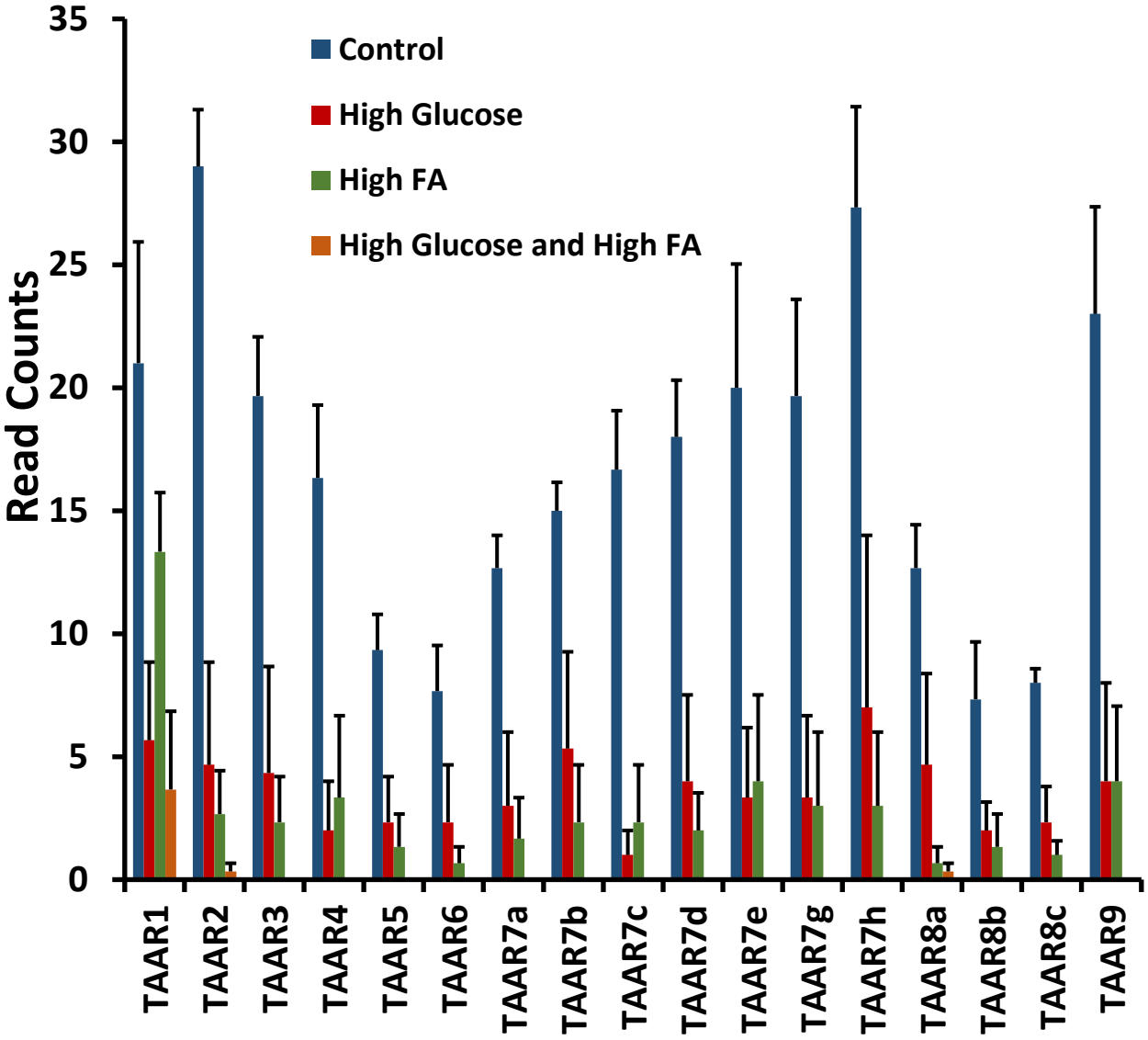

Figure 5. 1; Illumina HiSeq expression data of TAAR family members.

INS-1 cells were cultured for 72h in standard growth media or media supplemented to 28mM glucose and or 200µM oleic acid and 200µM palmitic acid. RNA was extracted, and quality assessed before Illumina HiSeq sequencing and analysis was undertaken. Data is expressed as mean RNA read counts per condition ±SEM, from 3 independent RNAseq analyses per condition

In order to validate these RNAseq findings, independent qRT-PCR analysis was performed on TAAR family members TAAR1, 2, 3, 4, 5, 6, 7b and 9. INS-1 cells were cultured in control or GLT media for 72h before RNA isolation, cDNA synthesis was

carried out and qRT-PCR analysis performed (Figure 5.2). 72h incubation in GLT caused all TAAR family member RNA expression to significantly decrease (p<0.05). RNA expression decreased by 34.8 ± 8.7%, 53.0 ± 12.1%, 50.3 ± 12.1%, 30.1 ± 12.0%, 43.8 ± 6.3%, 51.2 ± 5.5%, 60.8 ± 10.2% and 54.3 ± 8.4% for TAAR1, 2, 3, 4, 5, 6, 7b and 9 family members respectively.

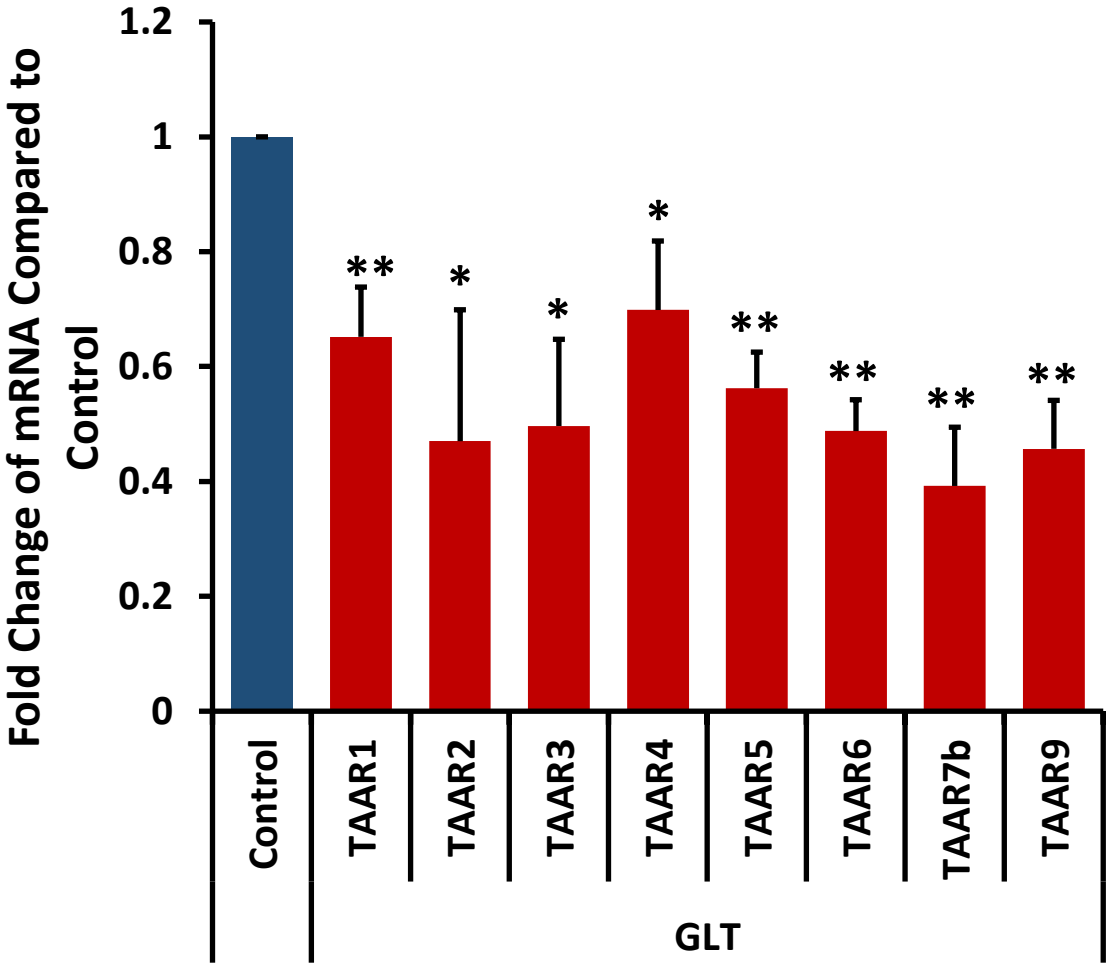

Figure 5. 2; qRT-PCR expression data for TAAR family members in GLT.

INS-1 cells were cultured in control or GLT media for 72h before RNA extraction and qRT-PCR analysis performed using primers and cycle conditions detailed in materials and methodology section. Data is expressed as fold change in RNA expression ± SEM compared to control using comparative delta delta Ct ($\Delta\Delta_{CT}$) method from 3 independent experiments. *p<0.05, **p<0.005 v control

Whilst the PCR data validated the RNAseq data, RNA expression changes do not always correspond to protein expression. It was therefore important to quantify protein expression changes of TAAR's in GLT compared to control. Therefore INS-1 β-cells were cultured in control or GLT media for 72h prior to protein extraction using RIPA buffer. Protein was quantified, normalised and separated by SDS-PAGE. The subsequent gel was transferred to nitrocellulose membrane and immunoblotted using an anti-TAAR1 antibody (Figure 5.3). An anti-TAAR1 primary antibody was the only TAAR family member antibody that was commercially available (Abcam, UK). Densitometry analysis of 4 independent experiments demonstrated that a 72h GLT incubation decreased TAAR1 protein expression by 42.6 ± 9.1% compared to control (p=0.0017).

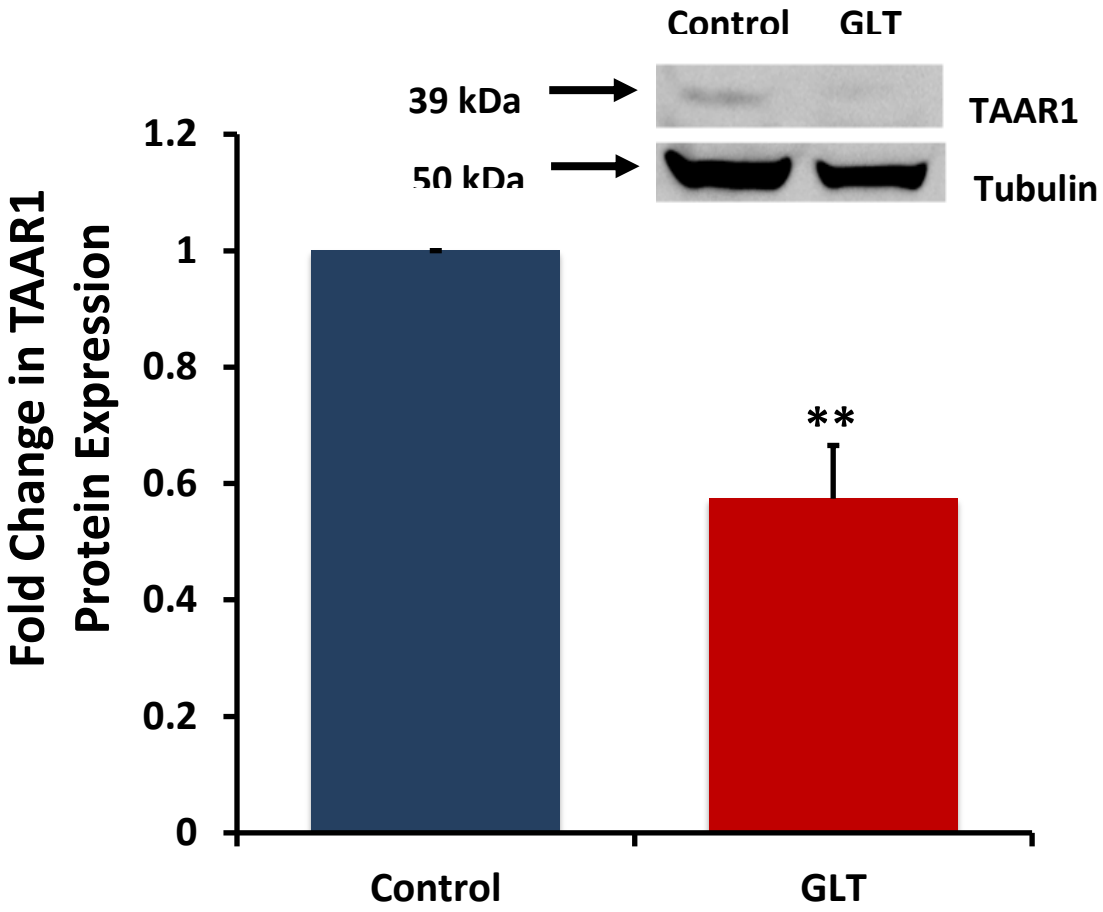

Figure 5. 3; TAAR1 Protein Expression in GLT.

INS-1 cells were cultured in control or GLT media for 72h prior to protein extraction, separation via SDS-PAGE, transferred to nitrocellulose and immunoblotted using anti-TAAR1 primary antibody (Abcam, UK). Data was normalised to β-tubulin and is expressed as mean fold change ± SEM using densitometry analysis from 4 independent experiments. ***p*<0.005 v control.

5.2.3. TAAR-Associated Adenylyl Cyclase Signalling is Downregulated by Glucolipotoxicity

To more fully understand the role of glucolipotoxic driven TAAR downregulation and how this impacts the functional capacity of β-cells, network analysis was performed using MetaCore, an integrated knowledge database of pathways from Thomson Reuters (https://portal.genego.com). This programme uses pre-existing literature to build interactome maps that can be enriched with transcriptomic data indicating

directionality and expression changes of genes within that pathway. Utilising the RNAseq expression data as an input list, the analyse network algorithm (with default settings – reactome version 29, http://www.reactome.org) (Matthews, et al. 2008) generated a bespoke network of molecules predicted to interact with TAAR1, the most extensively characterised member of the TAAR family. As can be seen in Figure 5.4, a network of TAAR1 interaction was produced, with genes with a red adjacent circle indicating GLT-associated upregulation, and genes with a blue adjacent circle indicating GLT -associated down-regulation. This interactome indicates that TAAR1 (shown as TAR1 within the interactome) is downregulated by 72h glucolipotoxic exposure. It also shows that TAAR1 has both a positive and negative downstream effector pathway on GPCR signalling through G_{α} proteins. Specifically, the inhibitory pathway through $G_{\alpha i}$ is upregulated by GLT exposure, whereas the stimulatory pathway through $G_{\alpha s}$ is downregulated. The consequence of these complimentary effects is a concerted downstream negative action upon adenylyl cyclase's. Adenylyl cyclase expression was also downregulated within the interactome. Adenylyl cyclase's are the enzyme responsible for cAMP formation from ATP, which once released intracellularly acts to regulate a vast array of cellular processes (Steer 1975). Of importance to this body of work, cAMP is a molecule known to augment insulin secretion in β-cells (Phang, et al. 1984).

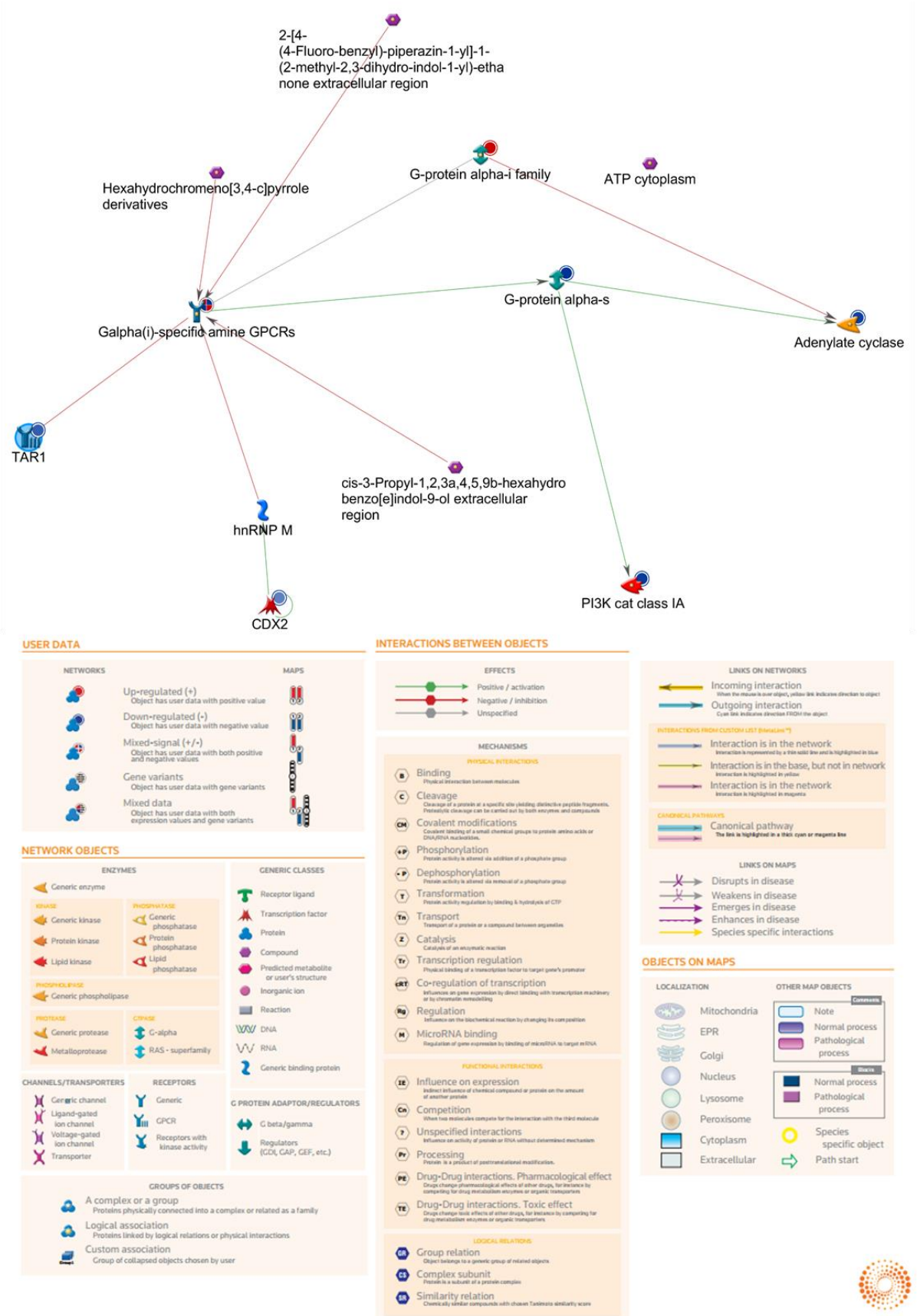

Figure 5. 4; Glucolipotoxic MetaCore pathway and network analysis of TAAR.

The Illumina HiSeq data was utilised to enrich a bespoke TAAR interactome using MetaCore network analysis programme (Thomson Reuters - http://genego.com). Blue circles indicate a significant glucolipotoxic driven downregulation, whilst the red circles indicate a significant upregulation using Bonferroni corrected *p* value smaller than 0.05. Green arrows indicate the direction of a positive interaction, and ted a negative interaction.

To further validate the bespoke network analysis and Illumina HiSeq data used to enrich it, protein expression of adenylyl cyclase's were carried out to confirm their downregulation by glucolipotoxicity. INS-1 cells were therefore cultured in control or GLT media for 72h prior to protein extraction. Proteins were separated via SDS-PAGE, then transferred to nitrocellulose and immunoblotted using anti-ADCY5/6 and anti-ADCY9 primary antibodies (Abcam, UK). ADCY5/6 protein expression was reduced by 11.3 ± 1.9% (p=0.0003) when cells were exposed to glucolipotoxicity for 72h. Likewise, ADCY9 protein expression was significantly reduced by glucolipotoxic exposure by 40.0 ± 17.2% (p=0.04) compared to control.

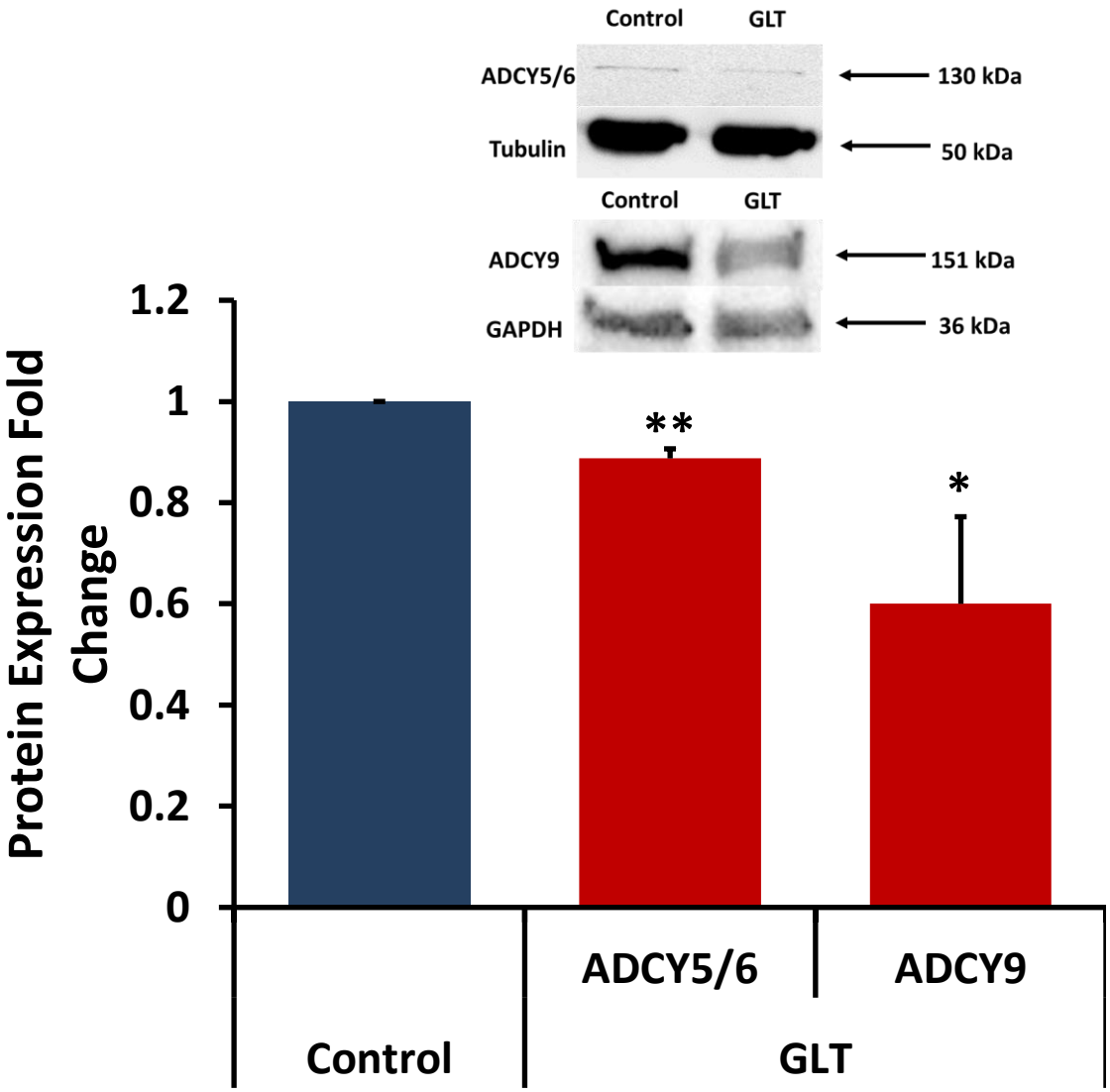

Figure 5. 5; Adenylyl cyclase 5/6 and 9 are downregulated by GLT.

INS-1 cells were cultured in control or GLT media for 72h prior to protein extraction and separation via SDS-PAGE before transfer to nitrocellulose membrane. Proteins were immunoblotted using anti-ADCY5/6 and anti-ADCY9 primary antibody (Abcam, UK). Data is expressed as the mean fold change ± SEM in densitometry from a minimum of three experiments between bands of control and GLT conditions and normalised to housekeeping protein density immunoblotting using anti-GAPDH or anti-β-tubulin antibodies (Abcam, UK). *p<0.05, **p<0.005 v control

5.2.4. Effect of TAAR Signalling on INS-1 β-cell Function

5.2.4.1 Effect of TAAR Stimulation with Amine Ligands on Intracellular cAMP

The TAAR1 bespoke interactome (Figure 5.4) is consistent with previous literature demonstrating adenylyl cyclase activation via $G_{\alpha s}$ proteins associated with TAAR1 signalling (Bunzow, et al. 2001). It was therefore investigated to see whether TAAR stimulation with known amine ligands could enhance cAMP production via adenylyl cyclase in INS-1 β-cells resulting in augmented insulin secretion. INS-1 cells were therefore cultured in control growth media until ~70% confluent before being washed and incubated in KREBS and 0.5mM 3-Isobutyl-1-methylxanthine (IBMX) or KREBS, 0.5mM IBMX ± trace amine ligands isopentylamine (Iso) (TAAR3), *p*-tyramine (Tyr) (TAAR1 and TAAR4), *2*-phenylethylamine (Phe) (TAAR1 and TAAR4), agmatine (Agm) (putative TAAR6 and TAAR8 ligand), *N,N*-dimethylcyclohexylamine (Cyclo) (TAAR7, TAAR8 and TAAR9 isoforms), and *N,N*- dimethyloctylamine (Ctyl) (TAAR7 isoforms) at a final concentration of 10μM, or the TAAR1 inverse agonist EPPTB at a concentration of 10nM, for 30min. Cells were then lysed in 0.1M hydrochloric acid and cAMP determined via select cAMP ELISA (Cayman Chemical, USA) (figure 5.6). The presence of the adenosine (A1) receptor antagonist IBMX in both conditions inhibits cAMP hydrolysis via phosphodiesterase (Cherry and Pho 2002). This allows the quantification of differences in cAMP accumulation over the 30min incubation time with or without the individual amine ligands.

Isopentylamine significantly increased cAMP accumulation fold change by 3.5 ± 0.6 (p=0.019). The same was true for *p*-tyramine, *2*-phenylethylamine and agmatine that likewise increased cAMP accumulation fold change by 3.7 ± 0.5 (p=0.01), 4.1 ± 0.74

(*p*=0.021) and 2.7 ± 0.27 (p=0.005) respectively. By contrast to this, amine ligands *N,N*-dimethyloctylamine and *N,N*-dimethylcyclohexylamine resulted in a very modest, yet significant decrease in cAMP accumulation decreasing to 0.83 ± 0.05 (*p*=0.01) and 0.90 ± 0.01 (*p*=0.003). The inverse agonist of TAAR1, EPPTB similarly resulted in a decrease in cAMP accumulation to 0.78 ± 0.04 (*p*=0.004).

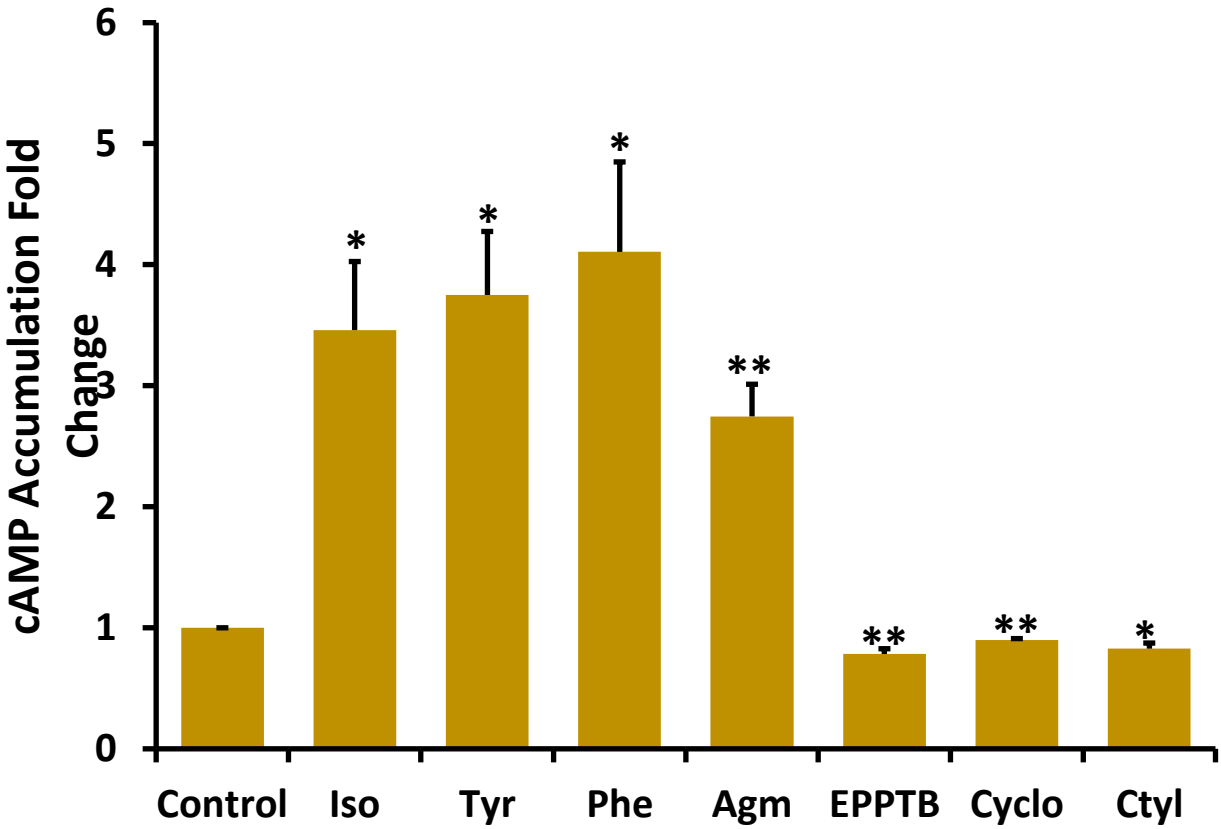

Figure 5. 6; Trace amine supplementation increases cAMP accumulation.

INS-1 cells were cultured in standard RPMI growth media until confluent before being washed and incubated in KREBS and 0.5mM IBMX, or KREBS, 0.5mM IBMX and either Isopentylamine (Iso), *p*-tyramine (Tyr), *2*-phenylethylamine (Phe), Agmatine (Agm), *N,N*-dimethycyclohexylamine (Cyclo) or *N,N*-dimethylocytlamine (Ctyl) to a final concentration of 10µM or the TAAR1 inverse agonist EPPTB to a final concentration of 10nM for 30 minutes. After 30 minutes cells were lysed in 0.1M hydrochloric acid and cAMP accumulation determined via cAMP select ELISA. Data is expressed as the mean fold change compared to control ± SEM from 3 independent experiments. *$p<0.05$, **$p<0.005$ v control

5.2.4.2. Effect of TAAR Stimulation with Amine Ligands on Insulin Secretion *in vitro* and *vivo*

As stimulation with a number of the trace amines resulted in a significant increase in cAMP accumulation over a 30min period, it was sought to determine if this increase augmented secretagogue stimulated insulin secretion as cAMP is a known enhancer. INS-1 cells were therefore cultured in standard RPMI growth media to 70 % confluency, before being incubated in KREBS or secretagogue cocktail (KREBS supplemented with 13.5mM glucose, 1µM phorbol 12-myristate 13-acetate, 1mM isobutyl methylxanthine, 1mM tolbutamide, 10mM leucine, 10mM glutamine) with or without the addition of Isopentylamine (Iso), *p*-tyramine (Tyr), *2*-phenylethylamine (Phe), Agmatine (Agm), *N,N*-dimethycyclohexylamine (Cyclo) or *N,N*-dimethylocytlamine (Ctyl) to a final concentration of 10µM or the TAAR1 inverse agonist EPPTB to a final concentration of 10nM for 2h. After 2h insulin secretion was determined via ELISA (Mercodia, Sweden) and normalised to cellular protein content via BCA assay (figure 5.7). In accordance with the cAMP accumulation data, the trace amines that increased cAMP also increased stimulated insulin secretion. Isopentylamine, p-tyramine and 2-phenylethylamine all significantly increased secretagogue stimulated insulin secretion to 1.14 ± 0.03 (p=0.007), 1.23 ± 0.09 (p=0.046), 1.26 ± 0.07 (p=0.016) fold change respectively, compared to control. Agmatine which also increased cAMP showed a modest increase in secretagogue stimulation that was just outside statistical significance (p=0.056) increasing by 16.0 ± 6.9% compared to control. Of the amine ligands that increased cAMP, agmatine had the lowest effect on cAMP accumulation, and was mirrored by the non-significant modest effect on insulin secretion. Also in keeping with the cAMP

accumulation data, *N,N*-dimethycyclohexylamine had no significant change upon secretagogue stimulated insulin secretion demonstrating a modest decrease by 7.8 ± 5.7% (p=0.12), whereas *N,N*-dimethylocytlamine and EPPTB decreased stimulated insulin secretion by 13.2 ± 5.0% (p=0.029) and 18.2 ± 4.0% (p=0.005) compared to stimulated control. This data therefore supports the role of TAAR stimulation with cAMP accumulation and resultant cAMP mediated increases in stimulated insulin secretion.

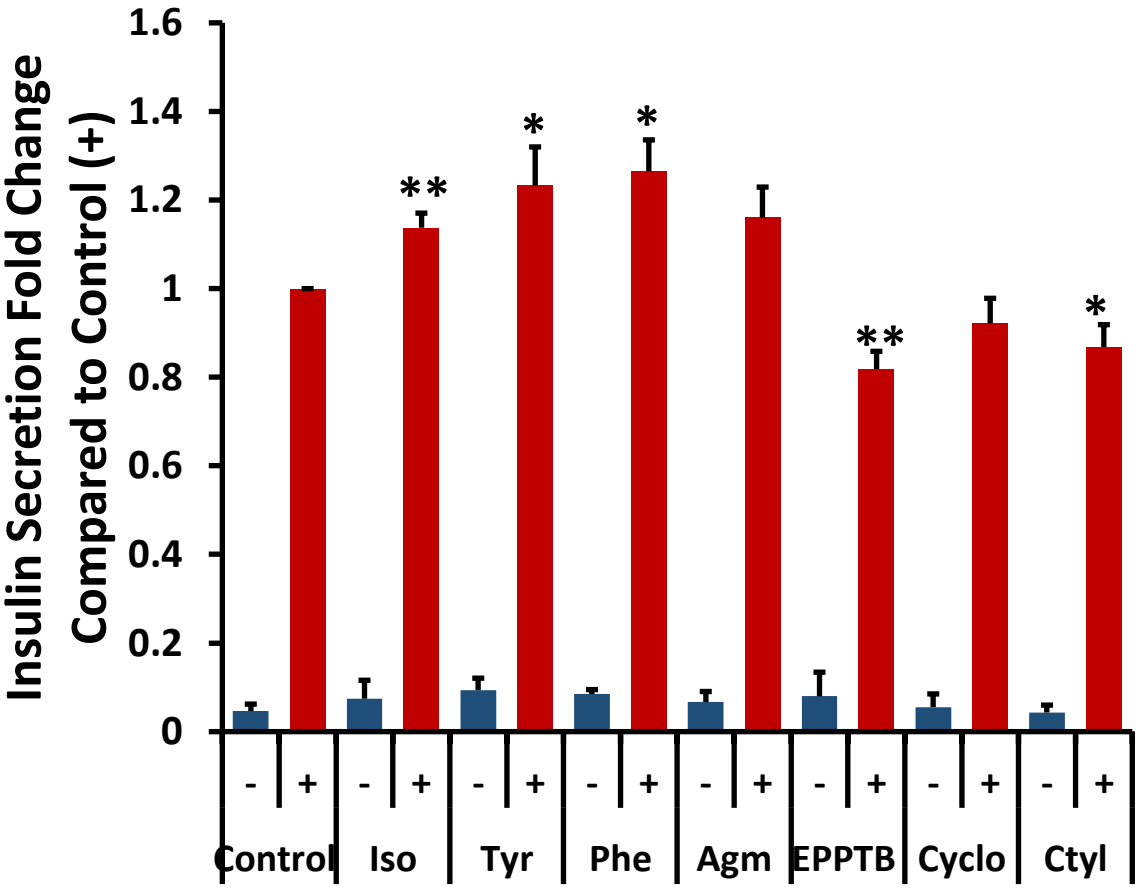

Figure 5. 7; Trace amine supplementation increases Insulin secretion.

INS-1 cells were cultured in control growth media until 80% confluent. Subsequently Insulin secretion was determined by ELISA following incubation ± secretagogue cocktail for 2h [(-) blue, (+) red] with or without the addition of Isopentylamine (Iso), *p*-tyramine (Tyr), *2*-phenylethylamine (Phe), Agmatine (Agm), *N,N*-dimethycyclohexylamine (Cyclo) or *N,N*-dimethylocytlamine (Ctyl) to a final concentration of 10µM or the TAAR1 inverse agonist EPPTB to a final concentration

of 10nM for 2h. Data was normalised to cellular protein content and expressed as the mean fold change compared to control ± SEM from a minimum of 3 independent experiments. *p<0.05, **P<0.005 v control stimulated (+)

Whilst INS-1 cells are an accepted well characterised and stable immortal β-cell line, it is imperative, where possible to carry out *vivo* studies to further validate key findings in primary cells. Therefore, in collaboration again with Dr Sophie Sayers and Dr Paul Caton of Kings College London, islets from CD1 male mice were isolated and cultured in standard growth media. The islets were size matched and pre-incubated in a buffer containing 2 mM glucose, 2 mM $CaCl_2$ and 0.5 mg/ml BSA, pH 7.4 for 1h at 37°C. Islets were then incubated in this buffer containing 2mM or 20mM glucose ± *p*-tyramine or *2*-phenylethylamine at ranging concentrations from 0.1-100µM (alongside the monoamine oxidase inhibitor paragyline or deprenyl respectively) for 1h with gentle shaking at 37°C, before insulin secretion was determined via radioimmunoassay with an in house ^{125}I-labelleled insulin tracer. In keeping with the clonal cell line secretion data*, p*-tyramine increased glucose stimulated insulin secretion by 33.2% ± 20.3% (p=0.199), 83.2% ± 11.8% (p=0.004), 41.2% ± 23.4% (p=0.156) and 47.8% ± 26.8% (p=0.067) at concentrations of 0.1, 1, 10 and 100µM respectively (figure 5.8a). Incubation with *2*-phenylethylamine likewise increased insulin secretion at the lower concentration of 0.1 and 1µM by 49.1 ± 23.7% (p=0.08) and 14.8 ± 12.2% (p=0.30) respectively (Figure 5.8b). Whilst in this latter case this is not a statistically significant change, it follows a similar pattern to *p*-tyramine and is

likely an issue of needing further repeats to combat the nature of inter-experimental variability when using primary tissues.

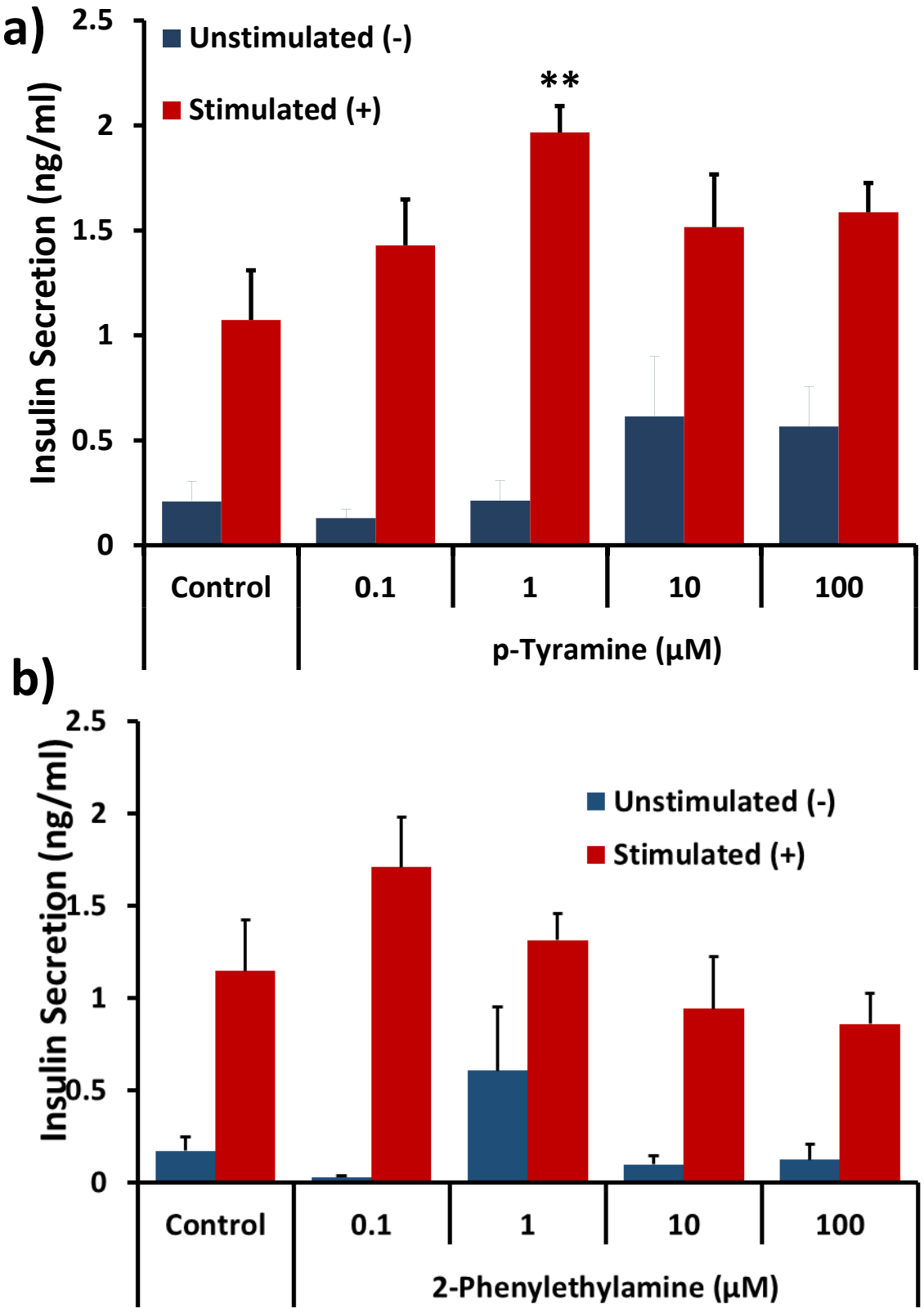

Figure 5. 8; Trace amines increase insulin secretion in CD1 mouse islets.

Islets were isolated from male CD-1 mice and cultured in RPMI-1640 media for 2 days prior to analysis. Islets were subsequently incubated in 2mM [(-) blue] or 20mM [(+) red] ± stated concentration of (a) *p*-tyramine with the monoamine oxidase inhibitor

paragyline or (b) 2-phenylethylamine with the monoamine oxidase inhibitor deprenyl for 1h and insulin secretion determined by radioimmunoassay. Data is presented as the mean ± SEM from a minimum of 5 independent experiments. $**p<0.005$ compared to control stimulated samples (+)

5.2.4.3. Potential Ancestral Origin of Adenylyl Cyclase modulation

From the experiments investigating both cAMP and insulin secretion, it was clear there was a split in cellular response to the different trace amines in standard conditions. As these ligands are known to stimulate different members of the TAAR family, it was sought to determine whether there may be an evolutionary explanation for this disagreement in functional capacity between receptors. The resulting phylogenetic tree alongside ligand responsiveness (Figure 5.9) demonstrates a clear divergence within the TAAR family separating TAAR members 1-4 from 5-9. This along with the previously shown data indicate that there is a possible conserved ancestral ability for receptors 1-4 to modulate cAMP production via adenylyl cyclase regulation and activation as ligands that had a positive effect (*p*-tyramine, *2*-phenylethylamine and Isopentylamine) all bind with receptors on this branch. Whereas the *N,N*-dimethylalkyamines that had no cellular response fall on the TAAR arm of receptors 5-9.

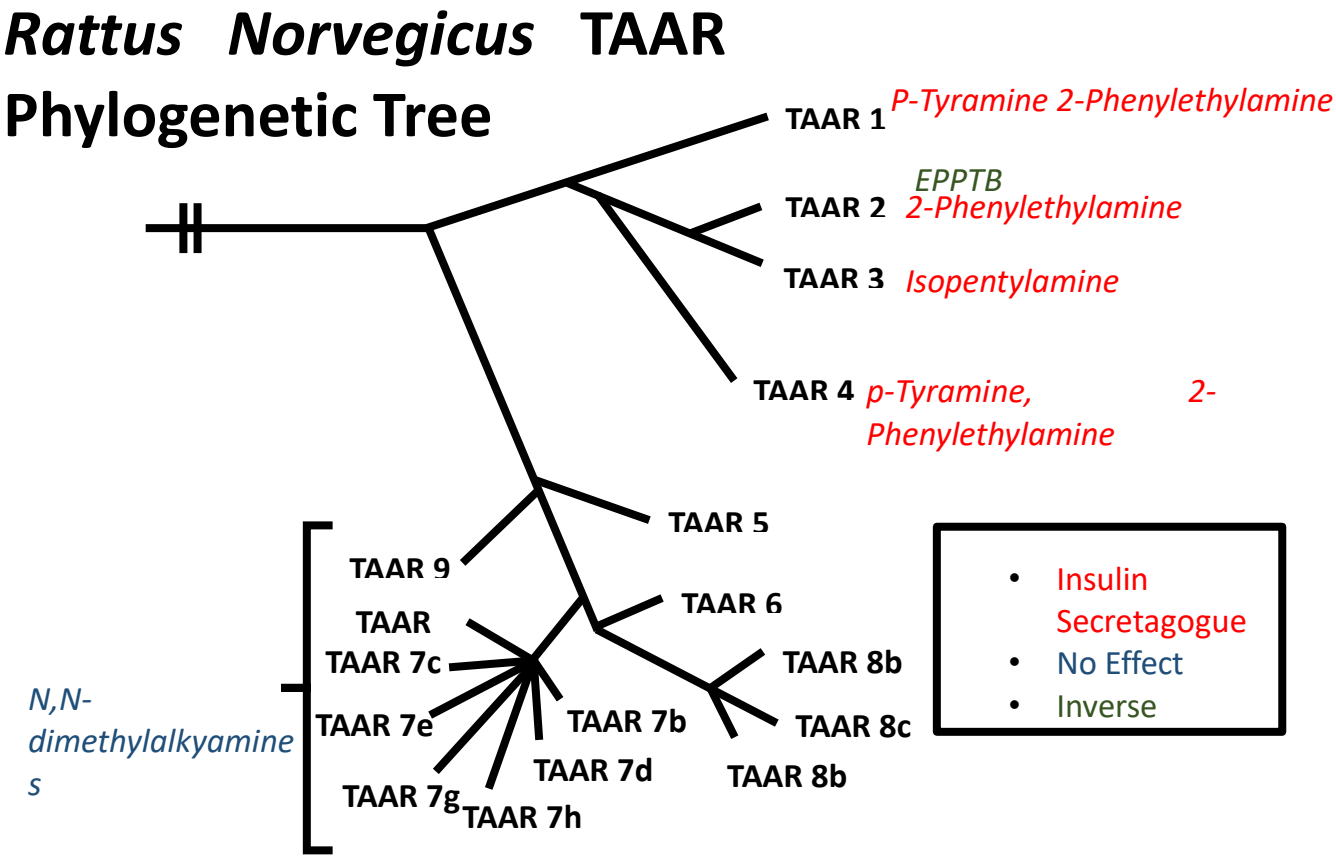

Figure 5. 9; Phylogenetic tree of TAAR with trace amine ligand responsiveness.

5.2.4.4. TAAR Stimulation Cannot Reverse Glucolipotoxic Inhibition of Insulin Secretion

Whilst these trace amines were shown to increase cAMP and insulin secretion in control conditions, to assess their potential use as suitable drug candidates to treat type 2 diabetes, it was important to repeat the insulin secretion experiments when β-cells are exposed to glucolipotoxicity to see if they elicit the same response. INS-1 cells were cultured in control or GLT media for 3 days prior to a 2h incubation in KREBS or secretagogue cocktail ± 10µM of the amine ligands that previously had a positive effect on insulin secretion; Isopentylamine, *p*-tyramine, *2*-phenylethylamine and agmatine (figure 5.10). In the absence of any trace amines, GLT decreased insulin

secretion by 73.3 ± 9.6% as expected, and in line with previously reported data here. Crucially however, all trace amines that previously had a positive effect on augmenting insulin secretion in control conditions no longer had any effect. Secretagogue stimulation was still reduced drastically from control and was not significantly different to GLT treatment alone (p>0.05). GLT with the addition of Isopentylamine, *p*-tyramine, *2*-phenylethylamine and agmatine still saw reduction in secretion to 33.6 ± 13.9%, 25.5 ± 10.6%, 32.1 ± 13.3% and 28.2 ± 11.5% respectively compared to control. The ability for the trace amines to affect insulin secretion which was lost when INS-1 cells were exposed to glucolipotoxic conditions most likely stems from the glucolipotoxic driven diminished receptor expression also previously reported within this chapter.

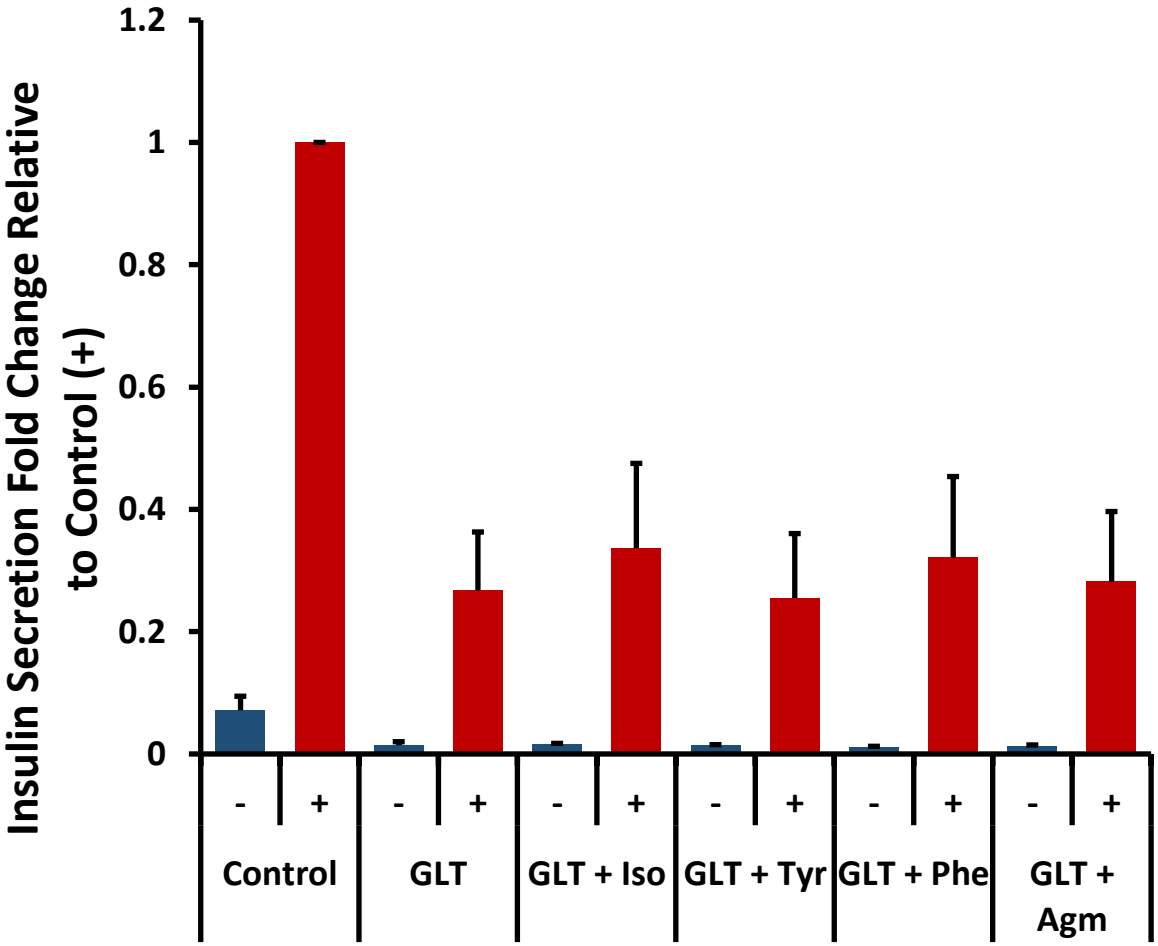

Figure 5. 10; Trace amine have no effect on reversing glucolipotoxic diminished insulin secretion.

INS-1 cells were cultured in control or GLT media for 72h prior to incubation ± secretagogue cocktail for 2h [(-) blue, (+) red] with or without the addition of Isopentylamine (Iso), *p*-tyramine (Tyr), *2*-phenylethylamine (Phe), Agmatine (Agm), to a final concentration of 10µM. Insulin secretion was determined via ELISA and normalised to cellular content and expressed as the mean fold change compared to control ± SEM from a minimum of 3 independent experiments.

5.2.5. Olfactory Receptor Signalling Contributes to Glucolipotoxicity

All family members of the TAAR family, except TAAR1, have previously been shown to also function as olfactory receptors (Liberles and Buck 2006; Horowitz, et al. 2014; Maguire, et al. 2009). Unlike TAAR1 that signals via $G_{\alpha s}$ to activate adenylyl cyclase and therefore increase intracellular cAMP concentration (Bunzow, et al. 2001), in the

olfactory epithelium all other TAAR members are thought to couple to $G_{olf.}$ Howver, G_{olf} is also associated with adenylyl cyclase activation that in turn increase cAMP (Liberles and Buck 2006; Ferrero, et al. 2012a; J. Zhang, et al. 2013). It was therefore important to identify whether other olfactory receptors that have the potential to augment insulin secretion via cAMP production are also sensitive to glucolipotoxicity. Utilising the Illumina HiSeq data, all olfactory receptor RNA read counts were measured in control and 72h glucolipotoxic exposure. Of the 1199 olfactory receptors identified in the RNAseq data, 734 receptors were significantly downregulated by GLT ($p<0.05$). From those receptors 619 had a higher read count than the threshold for control conditions. These receptors, like TAARs, are on the very cusp of detection, nonetheless, read count threshold was set at 10. Figure 5.11 demonstrated the quantity of receptors significantly downregulated by GLT and above the threshold, ordered by the read counts for control, highest to lowest.

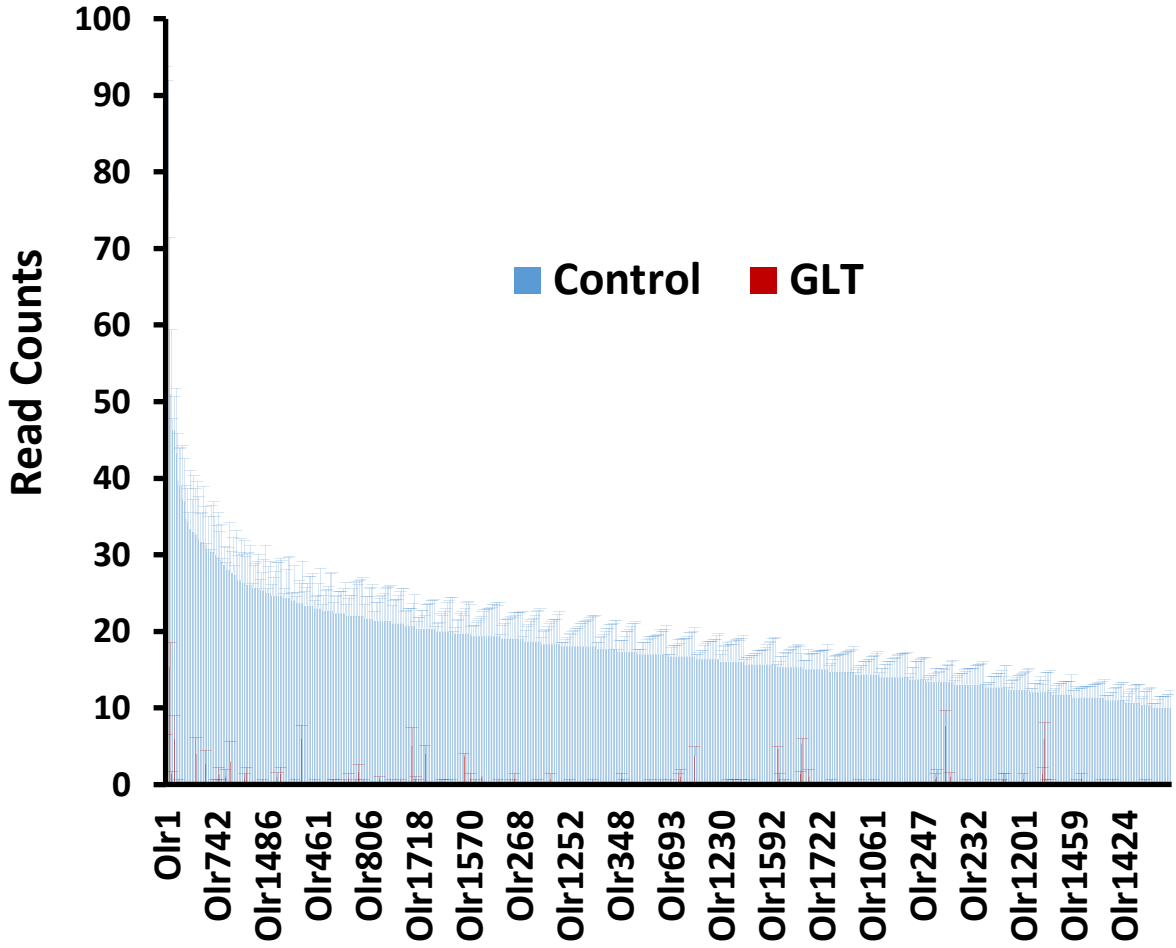

Figure 5. 11; Glucolipotoxicity downregulates olfactory receptor RNA expression. INS-1 cells were cultured for 72h in standard growth media or GLT media. RNA was extracted, and quality assessed before Illumina HiSeq sequencing and analysis was undertaken. 734 Olfactory receptors (with read counts above ten) presented were all significantly downregulated in GLT conditions ($p<0.05$) and ordered from most read counts in control conditions to least. Data is expressed as mean RNA read counts per condition ±SEM, from 3 independent RNAseq analyses per condition

The top 20 of these receptors ordered by significance in expression change between control and GLT are shown in Figure 5.12 and had *p* values smaller than 0.001 in all instances. All of the top 20 olfactory receptors RNA expression when ordered by

significance were infinitely downregulated when INS-1 cells were cultured in GLT for 72h, except for Olr693 and Olr1735.

As olfactory receptors expressed in β-cells have the ability to modulate cAMP production via adenylyl cyclase G-protein coupled receptor signalling, and therefore the potential ability to augment insulin secretion, this data therefore indicates that olfactory receptor signalling could also contribute to glucolipotoxic inhibitory effect on insulin secretion in INS-1 β-cells.

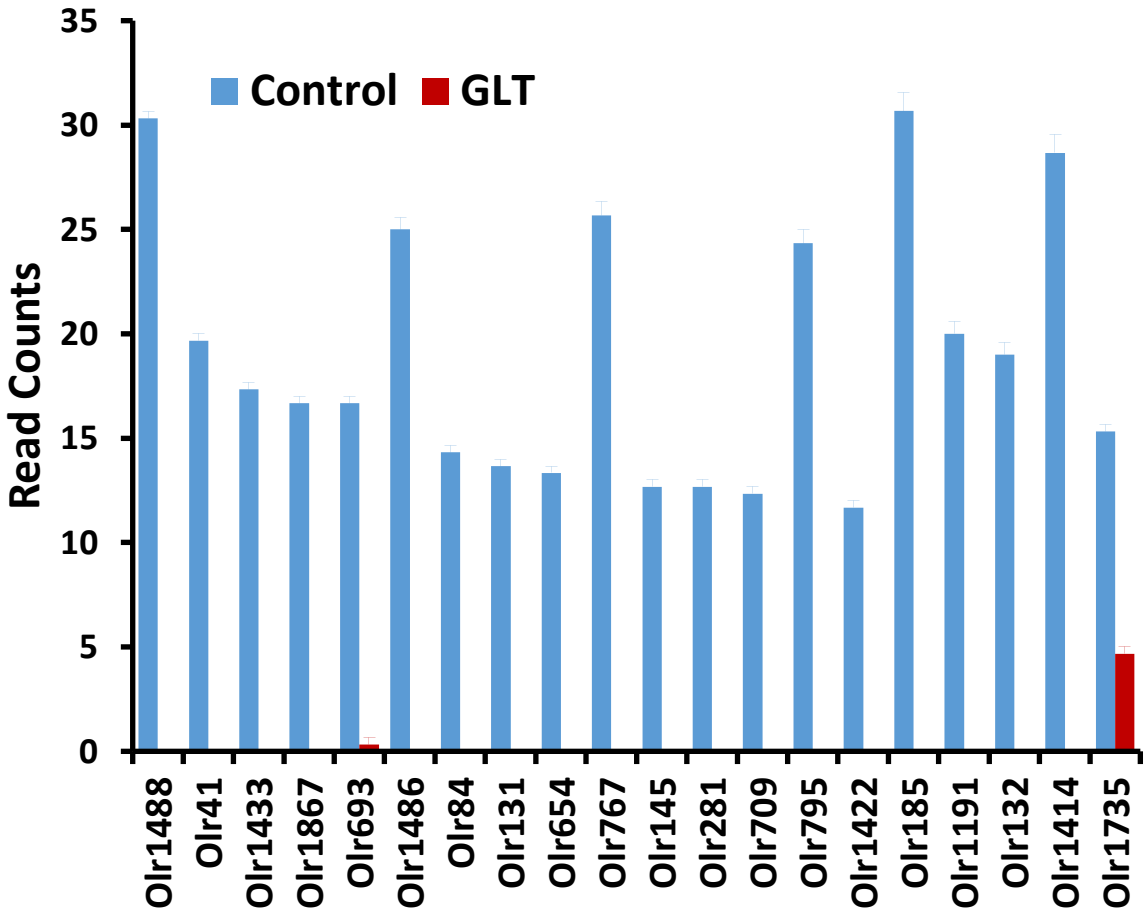

Figure 5. 12; Top 20 olfactory receptor RNA expression by statistical significance. INS-1 cells were cultured for 72h in standard growth media or GLT media. RNA was extracted, and quality assessed before Illumina HiSeq sequencing and analysis was undertaken. The top 20 olfactory receptors were ordered by statistically significant change between control and GLT conditions are presented. Data is expressed as

mean RNA read counts per condition ±SEM, from 3 independent RNAseq analyses per condition.

5.3. Discussion

Utilising Illumina HiSeq RNA sequencing analysis technology, RNA that was isolated from INS-1 β-cells in both control conditions, and diabetic glucolipotoxic conditions was sequenced and counted, allowing the identification of genes dysregulated following chronic exposure to high concentrations of free fatty acids and glucose. Of the genes dysregulated by chronic glucolipotoxic exposure, receptors in general had the highest statistical change compared to control conditions. In conjunction with previous findings from the Turner group utilising microarray technology (Bagnati et al, 2016) this is indicative that glucolipotoxicity, in INS-1 β-cells at least, primarily affects molecules involved in cell signalling pathways, protein trafficking, and transcription factor binding regulation. The current RNAseq data however did identify GPCR signalling as the highest statistically significant differentially expressed, specific protein class.

GPCRs comprise the largest family of proteins within the mammalian genome (Venter, et al. 2001; International Human Genome Sequencing Consortium 2001). They have two specific requirements; that their structure spans the membrane with seven α-helices (roughly 25-35 residues long each) to form the agonist recognition site, and that the receptor interacts with a G-protein enabling activation to transduce a signal through a downstream pathway. GPCRs have enormous variability in both ligand stimulation (ligands vary from ions, peptides, protein lipids, odorants and many more) and the signalling pathways the function within (ranging from vision to

olfaction and taste). GPCRs in vertebrates are commonly classified into five subfamilies depending on sequence, structure and activation. The largest and most diverse of these is the rhodopsin family that contains a further 13 sub-classes, with the other families being secretin, glutamate, adhesion and frizzles/taste2 (Fredriksson, et al. 2003). The typical role of GPCRs is to activate specific heterotrimeric G-protein protein signalling upon agonist binding to the recognition site, leading to downstream modulation (either activation or inactivation) of effector proteins (Rosenbaum, et al. 2009a). This can be annulled directly by inverse agonist binding or other intracellular processes such as receptor phosphorylation or desensitisation by GPCR activated β-arrestin translocation and resultant promotion of GPCR internalisation (Ma and Pei 2007).

One such family of the rhodopsin class of GPCRs, are trace amine associated receptors (TAAR), all of which were significantly down regulated when cells were exposed to glucolipotoxicity for 72h, many of them infinitely. Whilst solo treatments of either high sugar or high fat, also had significant effects in reducing TAAR members gene expression, a combined treatment of both high sugar and fat had the largest effect across all TAAR family members. This therefore identified TAARs as potential prime contenders to play a role in glucolipotoxicity driven β-cell dysfunction, and particularly diminished insulin secretory capability, which is a main hallmark of type 2 diabetes.

TAARs were first identified in 2001 (Borowsky, et al. 2001; Bunzow, et al. 2001), as receptors for trace amine compounds tryptamine, *2*-phenylethylamine and *p*-tyramine. However, the term trace amine was fashioned much earlier in the year

1974 as a way to distinguish between endogenous monoamine compounds that had low tissue concentrations (as low as ~100nM) from the more abundant (100-fold higher) structurally similar neurotransmitters (Berry 2004; Boulton 1974). The novel GPCR identified in the cDNA of a rat pancreatic tumour cell clonal line in 2001 (Bunzow, et al. 2001) was termed trace amine associated receptor 1 (TAAR1). This receptor has low expression levels in many tissue types, however its expression is uniquely abundant in β-cells (Regard, et al. 2007; Raab, et al. 2016). This was somewhat overlooked when TAAR1 was first identified yet has now alerted many to its potential role in glucose homeostasis.

In humans, the TAAR genes are located on chromosome 6q23.2 (Borowsky, et al. 2001; Bunzow, et al. 2001) of which there are six functional genes (TAAR1, 2, 5, 6, 8 and 9) and three pseudogenes (TAAR3, 4 and 7). Mice have fifteen TAAR genes and one pseudogenes, whilst rats have seventeen TAAR genes and two pseudogenes (Lindemann, et al. 2005; Lindemann and Hoener 2005). Work carried out in 2006 demonstrated that essentially all TAAR family members, bar TAAR1, were localised to the olfactory epithelium and functioned as olfactory receptors with minute (usually undetectable) protein expression in other tissues, and is therefore why as a result, there is limited literature on other TAAR family members to that of TAAR1 (Liberles and Buck 2006; Maguire, et al. 2009; Horowitz, et al. 2014).

Similarly, to the well characterised type 2 β-adrenergic receptor, TAAR1 couples to the stimulatory and inhibitory G α-proteins; $G_{\alpha s}$ and $G_{\alpha i}$. These proteins differentially regulate adenylyl cyclase's which in turn converts ATP to cAMP (Rosenbaum, et al. 2009a; Sotnikova, Caron and Gainetdinov 2009). It has therefore been shown that

TAAR1 stimulation with known ligands increases intracellular cAMP (Wainscott, et al. 2007; Barak, et al. 2008). Unlike TAAR1, all other TAAR family members in the olfactory epithelium have been shown to signal via G_{olf} proteins, however, likewise these proteins also associate with adenylyl cyclases and can therefore also regulate cAMP production (Ferrero, et al. 2012a; Zhang, et al. 2013). As cAMP is a known enhancer of stimulated insulin secretion through both PKA dependent and independent mechanisms (Seino and Shibasaki 2005; Malaisse and Malaisse-Lagae 1984), GPCR regulation of adenylyl cyclases have huge potential as a therapeutic strategy for type 2 diabetes where β-cells have started to fail and insulin secretion is diminished. Moreover, MIN-6 β-cell administration with the TAAR1 ligand 3-iodothyronamine markedly enhanced insulin secretion (Regard, et al. 2007). TAAR 1 activation with a selective agonist (RO5166017), increased glucose stimulated insulin secretion in both clonal β-cells (INS-1E) and human islets as well as elevating mice plasma PYY and GLP-1 levels. The same selective agonist also improved glucose tolerance in diabetic *db/db* mice and reduced body weight and food consumption in diet-induced obese mice (Raab, et al. 2016). These studies therefore suggested that TAAR1 has potential as a therapeutic target to treat type 2 diabetes, however, other members of the TAAR family have scarcely been studied for their potential use.

Archetypal trace amines such as p-tyramine and 2-phenylethylamine are synthesised endogenously as the by-product of monoamine neurotransmitter production after decarboxylation of precursor amino acids via L-amino acid decarboxylase (Gainetdinov, Hoener and Berry 2018). Synthesis is not limited as previously thought to neuronal cells, and L-amino acid carboxylase has been reported in many tissue

types, including importantly, the pancreas (Lindstrom and Shelin 1983; Rorsman, et al. 1995). These class of amines are promiscuous in their receptor affinity with the majority of the whole family of TAARs having a known amine ligand.

In order to investigate the potential of these receptors as novel drug development targets, amines that bind to the wider range of TAAR family members were studied for their affect upon cAMP production, and importantly, insulin secretion in INS-1 β-cells and primary *ex-vivo* mouse islets. Pharmacological studies in both mice and humans demonstrate that that p-tyramine and 2-phenylethylamine activate both TAAR1 and TAAR4 (Borowsky, et al. 2001; Berry, et al. 2017; Pei, Asif-Malik and Canales 2016). Isopentylamine is described as a ligand for TAAR3 (Liberles and Buck 2006), whilst agmatine is only reported as an agonist for TAAR13c which is only reported to be expressed in zebrafish (Li, et al. 2015). All of these compounds increased cAMP and this was reflected by an increase in insulin secretion from INS-1 β-cells. This was further validated, as the modest non-significant increase in insulin secretion exhibited from agmatine administration, was mirrored by also having the smallest effect on cAMP accumulation.

The commercially available antagonist EPPTB (previously called RO5212773) is selective against TAAR1 and showed a negative, albeit very minor effect on cAMP accumulation and insulin secretion. Due to the lack of other antagonists, characterising EPPTB is difficult. It is still unclear whether EPPTB is an antagonist or more likely an inverse agonist to TAAR1 (Bradaia, et al. 2009; Stalder, Hoener and Norcross 2011). N,N-dimethylcyclohexylamine activates TAAR7, including the mouse and rat paralogs of TAAR7b, 7f, 7b and 7d (Ferrero, et al. 2012a) and TAAR16e in

zebrafish (Li, et al. 2015). *N,N*-dimethylocytlamine was reported to similarly activate TAAR7 including the paralogs TAAR7e, 7f and 7h (Ferrero, et al. 2012a). Both of these *N,N*-dimethylalkyamines had no, or adverse effects on cAMP accumulation and therefore had no effect on stimulated insulin secretion.

As shown from the phylogenetic tree of TAAR evolution (figure 5.9), TAAR1-4 form one of the two major clades and appear to be tuned to primary amines such as *p*-tyramine and *2*-pheylethylamine. The TAARs 5-9 that fall on the other main arm of the tree are more tuned to tertiary amines. This would therefore suggest that there is a genetic ancestry of functional ability within this family via primary amine binding to regulate cAMP production from ATP by adenylyl cyclase activation (Ferrero, et al. 2012a). As presented here, only amines that are known ligands to receptors one to four had a positive effect on both cAMP and insulin secretion, whilst the tertiary amines, *N,N*-dimethylalkyamines, that bind to TAAR7 had no positive effect whatsoever.

Within this body of work, agmatine is the only exception to the rule of increasing cAMP and insulin secretion whilst not hitting the receptors on the primary branch of the tree. As mentioned previously, agmatine is only thought to bind to TAAR13c which is reported to currently be expressed solely in zebrafish (Li, et al. 2015). TAAR13c does however share a conserved binding site with TAAR6 and TAAR8, which were shown to fall on the branch of the tree that had no effect on insulin secretion. However, TAAR13c itself despite this, does fall on the same branch of the phylogenetic tree as receptors 1-4 (Hussain, et al. 2013). Whilst agmatine is known to have no effect on TAAR1 signalling (Hu, et al. 2009), it is conceivable that agmatine

could bind to one of the other receptors on the conserved mammalian branch of the phylogenetic tree capable of adenylyl cyclase activation and is just yet to be fully characterised.

The work reported here is consistent with TAAR signalling reported in the literature, however it is not without its complications as a novel therapeutic strategy. Adenylyl cyclases (ADCY) have 10 different isoforms, of which 9 are regulated by GPCRs coupled to $G_{\alpha s}$ or $G_{\alpha i}$ (Tengholm and Gylfe 2017). Consistent with previous literature that suggests that a 48-72h β-cell exposure to glucotoxic hyperglycaemia can alter ADCY8 expression in both rat and human islets (Roger, et al. 2011), and 48h exposure to 0.5mM palmitate can reduce ADCY9 and ADCY5 in human and mice isolated islets respectively (Tian, et al. 2015) resulting in a reduction in cAMP accumulation and glucose stimulated insulin secretion, data here presents that both ADCY5/6 and ADCY9 were significantly downregulated in INS-1 β-cells exposed to glucolipotoxicity for 72h. This reduced adenylyl cyclase protein expression combined with reduced expression of TAARs mentioned previously would culminate in a reduction in the positive $G_{\alpha s}$ pathway signalling and an increase in $G_{\alpha i}$ signalling as shown in the MetaCore network analysis map. This would therefore result in reduced cAMP production and loss of cAMP augmented insulin secretion within the condition. This is in agreement with our data, whereby the positive effect of our ligands on stimulated insulin secretion was lost when INS-1 cells were cultured in glucolipotoxicity for 72h in response to decreased expression. Whilst this may therefore appear as the potential protective action of TAARs are lost when exposed to glucolipotoxicity, and therefore impractical for diabetic patients in a state of

hyperglycaemia and hyperlipidaemia, it is important to note that a positive feedback loop of TAAR agonist induced increase in TAAR expression has been reported in other cell types. A 6h exposure to the placental cell culture line BeWo with 0.1-0.01nM of the endogenous trace amines 3-iodothyromine and triiodothyronine increased TAAR1 expression. The selective agonist RO5203548 at the higher concentration of 0.1nM also has a significant effect on increasing TAAR1 expression via Western blot analysis (Stavrou, et al. 2018). Likewise, in T-cells, incubation with the 100 μM of the non-selective agonist methamphetamine for 6h drastically increased TAAR1 mRNA ~200-fold compared to the untreated control human peripheral blood mononuclear cells. This work also demonstrated that a longer-term treatment (24h) of either 100μM *2*-phenylethylamine, 100μM *p*-tyramine or 100μM methamphetamine all significantly increased TAAR1 protein expression in human T-cells measured via fluorescence (Sriram, et al. 2016). If a similar response can occur in β-cells with a longer timed exposure to endogenous trace amines than the 2h shown here, TAAR agonists administration may represent a viable treatment to overcome glucolipotoxic driven diminished TAAR expression, and then have a positive effect on augmenting insulin secretion. This is an incredibly exciting and promising area for future systematic research and characterisation.

There are already numerous treatment strategies to treat the failure of insulin secretion in overt diabetes. Sulphonylurea compounds were first introduced as a prescribed medication in the 1950s with the sole purpose of augmenting insulin secretion, and these remain key pharmacotherapy compounds 70 years on for the regulation of glucose homeostasis within the condition. However, recent safety

concerns about sulphonylurea side effects have arisen in recent years resulting in patient weight gain and hypoglycaemia, all of which are detrimental to the longevity of treatment (Sola, et al. 2015). Additionally, like most pharmacotherapy intervention tools, they become less effective over time and therefore it is imperative to constantly discover novel targets that action via different mechanisms to increase stimulated insulin secretion, not exhausted by pre-existing treatments. Unlike sulphonylureas, administration of TAAR agonists offer significant additional benefits in comparison to previous treatments as they not only promote weight loss but have also shown to reduce binge eating phenotypes (Raab, et al. 2016; Revel, et al. 2013; Ferragud, et al. 2017). TAARs also function through a completely separate mechanism. Sulphonylureas increase the exocytosis of insulin-containing secretory granules by the binding and closing of β-cell K_{ATP} channels. This channel closure causes the cell membrane to depolarise resulting in L_c-type Ca^{2+} channels opening and calcium influx and insulin secretion (Proks, et al. 2002). TAARs however, effect insulin secretion via the same mechanism as the increasingly popular pharmacotherapy treatment; incretin mimetics.

Incretin mimetics stimulate cell membrane incretin receptors (glucagon-like peptide-1 receptor), which are GPCRs linked to adenylyl cyclases. This, similar to the data reported here, increases cAMP, reflected by an increase in stimulated insulin secretion (Drucker 2006; Holst 2007). DPP4 inhibitors or gliptins as they are sometimes referred as, similarly increase stimulatory GPCR signalling, amplifying cAMP and therefore insulin secretion. However, they do this by inhibiting enzymatic hydrolysis of endogenous incretins, increasing their intracellular concentrations

causing a more pronounced stimulatory effect (McIntosh, et al. 2005). Incretin mimetics are also not without their problems however. Not only does hyperglycaemia significantly reduce incretin receptor expression, they also need to be administered by injection which can often be unpopular with patients (Xu, et al. 2007). The fact that incretin receptors are downregulated by hyperglycaemia and still has a marked effect on amplifying insulin secretion when treated with incretin mimetics or DPP4 inhibitors, offers more validity to TAAR as a potential strategy as their expression is also downregulated by glucolipotoxicity but may therefore still exhibit positive functionality with what receptors are expressed.

As current therapies utilise adenylyl cyclase activation to increase insulin secretion, olfactory receptors may too provide a fresh therapeutic strategy to treat diabetes induced failed insulin secretion, as they too have the ability to couple G-proteins associated to adenylyl cyclases. Recently olfactory receptors shown to be expressed in MIN6 β-cells promoted glucose stimulated insulin secretion when stimulated with odorants, suggesting a chemo-sensory function in β-cells to regulate glucose homeostasis that could be targeted for therapeutic intervention. This work did however suggest a mechanism independent of G_{olf}-cAMP-PKA, but this work only investigated two receptors out of hundreds of possible candidates (Munakata, et al. 2018). Therefore, further research is required to truly understand olfactory receptors and their mechanism(s) of action. Olfactory and TAAR ligands can also be administered orally, instead of via subcutaneous injection, thereby offering another benefit over some other treatment options.

In conclusion, whilst exposure to glucolipotoxicity decreases expression of TAARs, adenylyl cyclases, and olfactory receptors alike, stimulation of TAAR 1-4 in control conditions lead to a significant increase in cAMP accumulation and enhancement of insulin secretion. This ability was lost by a 72h GLT incubation, insinuating TAARs likely contribute to the pathophysiology of type 2 diabetes. Regardless of this, current, and more importantly, new treatment therapies that regulate cAMP production via adenylyl cyclase activation through stimulation of heterotrimeric G-protein coupled receptors have the potential to be effective treatments to offset the insulin secretion deficiency of the type 2 diabetic pathophysiology.

5.4. Future Work

As mentioned previously, future work will investigate if a more chronic exposure (longer than 2h) to endogenous trace amines that had a positive effect in the body of work presented here (*p*-tyramine, *2*-phenylethylamine, isopentylamine and agmatine) can have a positive feedback loop on TAAR expression in β-cells that is diminished in response to glucolipotoxicity. If TAAR expression can be reversed by longer periods of amine administration, the positive effect presented here on both cAMP production and therefore insulin secretion in control conditions could be retained even in the face of toxic high sugar and high fat conditions. If this is the case, *in-vivo* studies with long term oral administration of trace amines on high fed spontaneously diabetic mice may be carried out to investigate TAAR expression changes and effect on glucose homeostasis in a full animal model of diabetes could be observed. If a positive effect is seen on both TAAR expression, glucose tolerance, food consumption, fasting plasma glucose and glycated haemoglobin levels, this then

makes TAAR a worthy and viable candidate for a treatment strategy in type 2 diabetic human patient trials.

In parallel to this future work will also aim to validate the illumina HiSeq olfactory receptors expression findings via qRT-PCR and Western blotting, as well as researching the mechanism(s) of olfactory signalling. If, as thought, olfactory receptors also couple to G_{olf} signalling pathways with the ability to augment cAMP production via adenylyl cyclases, then this may too represent another potential treatment strategy to augment insulin secretion in response to glucolipotoxicity.

6. General Discussion and Conclusions

6.1. General Discussion

Diabetes mellitus is a polygenic metabolic disorder that is characterised by the synergistic failing of insulin secretion from pancreatic β-cells and decreased insulin sensitivity at target tissues such as skeletal muscle, thereby resulting in a state of hyperglycaemia. Type 2 diabetes is the most common classification accounting for ~90% of all incidences and is typically developed over many years in response to numerous contributing risk factors ranging from genetics, to smoking, to the main risk contributor; obesity and high sugar and fat diets (Wu, et al. 2014). Global diabetes prevalence is on the rise and is currently thought to affect over 425 million people worldwide, costing 1.8% of the world's total GDP (Bommer, et al. 2017). Insulin resistance in response to chronic exposure to toxic concentrations of sugar and fat is normally the first sign on type 2 diabetes onset (Petersen, et al. 2007), followed by β-cell adaptation resulting in increased insulin production and secretion to compensate and maintain healthy blood sugar levels. However, prolonged exposure to high glucose and fat concentrations results in amplified oxidative and ER stress, and increased circulating toxic FFA's culminating in β-cell failure, death and resultant loss of glycaemic control. Downstream complications of this can be fatal ranging from nephropathy and retinopathy to cardiovascular disease (Papatheodorou, et al. 2016). Numerous anti-diabetic medications exist and are prescribed to tailor the individual patient's condition. However, like most, these treatments lose effectiveness over time, and it is therefore incredibly important to continually identify and develop new targets and strategies separate to mechanisms of those already defined to combat the condition.

The aim of this thesis was to identify novel targets and treatments for type 2 diabetes, investigating changes in stimulated insulin secretion using a model of glucolipotoxicity in INS-1 β-cells. Clonal INS-1 β-cells were cultured in RPMI-1640 standard growth media supplemented to 28mM glucose and 200µM oleic and 200µM palmitic acid for 3 or 5 days to mimic a glucolipotoxic state. Both palmitic acid and oleic acid were used to more wholly represent the human diet, with palmitic being the most abundant saturated FA and oleic monounsaturated FA, allowing a truer representation of β-cell pathophysiology in response to type 2 diabetes onset (Ricchi, et al. 2009). Previous published and unpublished research from the Turner research group has demonstrated that this model of glucolipotoxicity dosed for 3 or 5 days in INS-1 cells was sufficient to inhibit stimulated insulin secretion (a hallmark of type 2 diabetes) whilst not effecting cell viability (Marshall, et al. 2007), therefore confirming it as a valid model to assess glucolipotoxic mechanisms in INS-1 β-cells with the aim to identify new treatments that can inhibit or reverse the damaging consequences.

Data shown in Chapter 3 demonstrated the damaging effect of glucolipotoxicity, and carnosine's potential as a treatment for type 2 diabetes. Consistent with the literature, 5 day glucolipotoxic exposure was shown to increase reactive oxygen, nitrogen, and carbonyl species, which in turn increased 4-HNE and 3-NT protein adduct formation. The reactive carbonyls can form adducts on key cellular proteins which can result in cellular function perturbation (Ellis 2007). Glutathione is one of the most suited enzymes to detoxify one such reactive carbonyl; HNE (Tiedge, et al. 1997). However, β-cells have much lower glutathione expression levels compared to

other tissues making them much more susceptible to oxidative stress related damage by reactive carbonyls (Robertson and Harmon 2007). Therefore 5 day exposure to glucolipotoxicity and ensuing oxidative stress coupled with β-cells low anti-oxidant defence system culminated in significantly diminished stimulated insulin secretion. Some recovery of cellular function is observed when cells were removed from the toxic environment, however it is likely the low capacity of the anti-oxidant defence system limits this to only the partial recovery exhibited. Therefore, to offset the damaging effects of glucolipotoxicity-driven reactive species other protective compounds are required.

Carnosine is an endogenous dipeptide of β-alanine and L-histidine ingested primarily from red meat, but this is also available as a dietary supplement. Carnosine has already been shown to increase fasting insulin and lower insulin resistance, thereby increasing glucose tolerance (de Courten, et al. 2016). It has also been demonstrated to lower fasting glucose in obese individuals when ingested as a component of a dietary supplement alongside cinnamon and chromium (Liu, et al. 2015). It was more recently shown to be an effective scavenger of reactive carbonyls in a rodent model of retinopathy (Albrecht, et al. 2017), although there was no direct investigation of carnosine function on β-cells in the literature. Data presented here shows that carnosine is an effective scavenger of reactive species, as a 1h acute treatment was able to significantly reduce reactive species detection. A longer exposure of carnosine over 5 days was also able to reverse glucolipotoxic driven increases in iNOS expression, as well as reversing glucolipotoxic 3-NT and 4-HNE protein adduction. This reactive metabolite inhibition resulted in significant increases in insulin secretion

both *in vitro* and *in vivo.* Importantly a 2 day carnosine treatment after 3 days of glucolipotoxic exposure was shown to reverse the damage on the insulin secretory pathway, suggesting carnosine can act through two different methods of action: 1) scavenge reactive species directly before they can have downstream toxic effects and 2) sacrificially react with downstream carbonyls forming non-reversible less reactive adducts (Song, et al. 2014). Carnosine also exhibited a similar function in C2C12 skeletal muscle where a 1h and 5 day treatment period decreased reactive species and increased insulin sensitivity respectively. Carnosine can act via a multitude of functionalities in numerous tissue types and therefore represents a promising agent to combat type 2 diabetes alongside pre-existing treatments that aim to augment insulin secretion in β-cells and increase insulin sensitivity and resultant glucose uptake in skeletal muscle.

This work was also able to demonstrate that INS-1 β-cells express the enzyme responsible for carnosine synthesis, thereby making β-alanine supplementation and increased endogenous carnosine synthesis a potentially viable treatment option. β-alanine is already extensively researched for its positive role in enhanced skeletal muscle cellular performance in response to physical activity (Hill, et al. 2007) and work here reports that β-alanine supplementation can elicit a protective action against glucolipotoxic driven stress. However this function is not directly instigated by β-alanine, as a 1h dose had no effect on reactive species, yet a 5 day exposure period significantly reduced their detection. This would suggest β-alanine's 'scavenging' action is a result of its utilisation to form carnosine, which can then elicit a protective outcome. HPLC experimentation in collaboration with Dr James (NTU)

alone was unable to confirm this theory as carnosine concentrations remained consistent in control and with β-alanine supplementation, which may have been a result of immediate carnosine synthesis and consumption via reactive species sequestering. Further research is therefore required to support this hypothesis. Nevertheless, a 5 day β-alanine supplementation resulted in significant increases in stimulated insulin secretion and a significant reversal of glucolipotoxicity-mediated inhibition of insulin secretion, and may therefore represent a valid agent to combat the onset of type 2 diabetes.

Carnosinase-2; the enzyme responsible for carnosine hydrolysis within tissues was also shown to be expressed in INS-1 β-cells. To combat rapid carnosine hydrolysis by this enzyme, in collaboration with Dr Garner and team in the Department of Chemistry, NTU, carnosine-like compounds were identified in the MayBridge compound library using *in silico* analysis, initially based on structural shape and chemistry (ROCS), before threshold analysis for percentage fit into the active site of carnosine hydrolysis on the enzyme carnosinase-2 in GOLD. Compounds that had a similar structure and chemical makeup as carnosine, with a high enough percentage fit to bind with the carnosinase-2 active site, yet low enough to avoid hydrolysis thereby acting as inhibitors, were purchased. Disappointingly, of the 9 compounds that were purchased, 5 were toxic to INS-1 cells, whilst the other 4 exhibited no abilities to reduce reactive species in β-cells or influence insulin secretion. In contrast, these same compounds exhibit a pronounced effect in skeletal muscle in terms of reducing glucolipotoxic driven reactive species and increasing insulin sensitivity. This is not so surprising when one considers the endogenous concentrations of carnosine

in the different tissue types. These compounds were selected to act as carnosine-2 inhibitors thereby allowing endogenous carnosine to have a larger effect that normal in reducing glucolipotoxic stress. As endogenous carnosine is as high as 5-8mmol/L in skeletal muscle (Derave, et al. 2010), yet as low as preliminary data in this chapter would suggest (within the μM range) then these compounds potentially still offer protective actions in a full physiological context.

As the aim of the thesis was to identify novel targets for the treatment of type 2 diabetes, a transcriptomic approach was also used to identify genes and proteins that contribute to glucolipotoxic inhibition of insulin secretion. Building from previous microarray datasets obtained in the Turner research group, Illumina-HiSeq gene expression analysis was utilised to characterise changes in the INS-1 β-cells transcriptome exposed to glucolipotoxicity. RNA isolated from INS-1 cells cultured in glucolipotoxic media for 3 days identified G-protein coupled receptors (GPCR) as the specific protein class with the highest statistically significant gene perturbation compared to control. One such family of GPCRs with particularly high gene expression alterations were trace amine associated receptors (TAARs), of which all 15 that are expressed in the rat transcriptome were downregulated by glucolipotoxicity. TAAR gene and protein downregulation was confirmed via qRT-PCR and Western blot, establishing the whole family as prime contenders to contribute to glucolipotoxic damaging downstream consequences.

TAAR1 couples to the stimulatory and inhibitory G α-proteins; $G_{\alpha s}$ and $G_{\alpha i}$ which regulate adenylyl cyclases, the protein responsible for ATP conversion to cAMP (Rosenbaum, Rasmussen and Kobilka 2009b; Sotnikova, et al. 2009). As cAMP is

known to potentiate secretagogue-stimulated insulin secretion through both PKA dependent and independent mechanisms (Seino and Shibasaki 2005; Malaisse and Malaisse-Lagae 1984), modulation of GPCR-mediated cAMP pathways is an active area of emerging type 2 diabetic therapeutic investigation. Work in chapter 5 demonstrated that stimulation of TAARs with endogenous primary amine ligands increase cAMP accumulation, thereby resulting in enhanced stimulated insulin secretion in both cell culture and primary *ex vivo* mouse islets. Interestingly, stimulation with tertiary amines had no effect, which may suggest a conserved genetic ancestry for TAAR regulation of adenylyl cyclase, as primary amines stimulate receptors 1-4, whilst tertiary amines stimulate receptors 5-9 (figure 5.9) (Ferrero, et al. 2012b). Further data presented in this chapter however, also indicated that reduced TAAR and adenylyl cyclase protein expression in response to glucolipotoxicity expectantly diminishes their ability to influence glucose metabolism by losing the ability to enhance insulin secretion. TAARs should not be discredited though, as recent literature suggests that longer term exposure of TAARs to their ligands reverses loss of protein expression in human T-cells (Sriram, et al. 2016), which if true for pancreatic β-cells may represent a viable treatment option to overcome glucolipotoxic driven diminished protein expression and resultantly enable the amplification of cAMP augmented stimulated insulin secretion.

6.2. Conclusions

This thesis identified that the dipeptide carnosine has the ability to inhibit and reverse the damaging effects of glucolipotoxic driven cellular stress in β-cells

associated with type 2 diabetes, thereby resulting in enhanced insulin secretion. Carnosine treatment was also shown to increase insulin sensitivity and therefore glucose uptake in a skeletal cell model through what we believe is the same scavenging mechanism. This dietary supplement is therefore a potential agent that could improve patient prognosis via increased blood sugar level management.

β-alanine, one amino acid constituent of carnosine was also shown to increase insulin secretion and reduce glucolipotoxic driven reactive species in INS-1 β-cells when dosed for longer periods of time suggesting a potential protective action derived from its utilisation to form carnosine intracellularly. Carnosine derived compounds were also screened for their potential to act as carnosinase-2 inhibitors and thereby improve control of glucose homeostasis via this mechanism. However, these were unsuccessful in terms of β-cell physiology, but potential still exists for these compounds in tissues where endogenous carnosine concentrations are higher. Further investigation is required though.

This body of work through a transcriptomic approach also identified that glucolipotoxic exposure decreases expression of the GPCR family TAARs, as well as olfactory receptors and adenylyl cyclases alike, yet stimulation of TAARs 1-4 in control conditions augmented cAMP production and insulin secretion, which was lost when INS-1 β-cells were exposed to glucolipotoxicity. Therefore, downregulation of GPCR signalling through these families likely contributes to glucolipotoxic inhibition of insulin secretion, and therefore marks these proteins as future potential treatment targets for type 2 diabetes.

7. Future Directions

7.1. Results

As detailed in chapter 5, utilising the RNAseq dataset, GPCRs (TAARs and olfactory receptors) were identified as being differentially expressed in INS-1 β-cells when exposed to glucolipotoxicity for 72h. This alteration in gene expression was validated via qRT-PCR and Western blot and was shown to have a significant functional impact on the insulin secretory pathway.

Carrying on from this work, non-biased enrichment analysis of the full RNAseq data sets between control and glucolipotoxic conditions identified cell adhesion and extracellular matrix remodelling as key pathways of dysregulated gene expression following exposure of INS-1 β-cells to high glucose and fatty acids for 72h (Table 7.1). As shown in Table 7.1, cell adhesion and ECM enrichment pathway maps ranked second, third and eighth for statistically significant changes in gene expression, with p values of $2.365E^{-09}$, $2.815E^{-09}$ and $7.989E^{-06}$ and similarly small false detection rates when comparing control gene expression to 3-day glucolipotoxic exposure.

Enrichment by pathway maps

#	Maps	Total gene number	p Value	Min FDR
1	Immune response - T cell co-signalling receptors, schema	55	9.980E-12	8.184E-09
2	Cell adhesion_ECM remodelling	53	2.365E-09	7.695E-07
3	Cell adhesion_Cell-matrix glycoconjugates	38	2.815E-09	7.695E-07
4	Protein folding and maturation_Bradykinin / Kallidin maturation	32	1.478E-07	3.030E-05
5	Rheumatoid arthritis (general schema)	50	1.620E-06	2.657E-04
6	Blood coagulation_Blood coagulation	39	2.137E-06	2.920E-04
7	Role of cell adhesion in vaso-occlusion in Sickle cell disease	43	7.313E-06	8.188E-04
8	Cell adhesion_Integrin inside-out signalling in neutrophils	77	7.989E-06	8.188E-04
9	Development_Neural stem cell lineage commitment (schema)	38	9.976E-06	9.089E-04
10	Development_BMP7 in brown adipocyte differentiation	39	7.563E-05	6.202E-03

Table 7. 1; Pathway map enrichment analysis report of RNAseq Data.
Using non-biased enrichment analysis, the top 10 statistically significant pathway maps when comparing control to 3 day glucolipotoxic exposure RNAseq data were ordered along their false detection limits.

In response to this, to further investigate the role of extracellular matrix changes in glucolipotoxic conditions, MetaCore, an integrated knowledge database, was again

utilised to generate a ranked pathway interactome linked to table 7.1 based on the extent of dysregulation. The pathway map linked to ECM remodelling (Figure 7.1) identified 5 cellular membrane proteins as being significantly downregulated when INS-1 β-cells were exposed to glucolipotoxicity for 72h. These particular proteins have been singled out initially due to their cell membrane residency, which makes them more amenable for further study (in comparison to extracellular matrix proteins) when using tissue culture clonal cell lines. These proteins are the matrix metalloproteins (MMP) 14, MMP15 and MMP16, the adhesion receptor CD44 and the tyrosine kinase ErbB4.

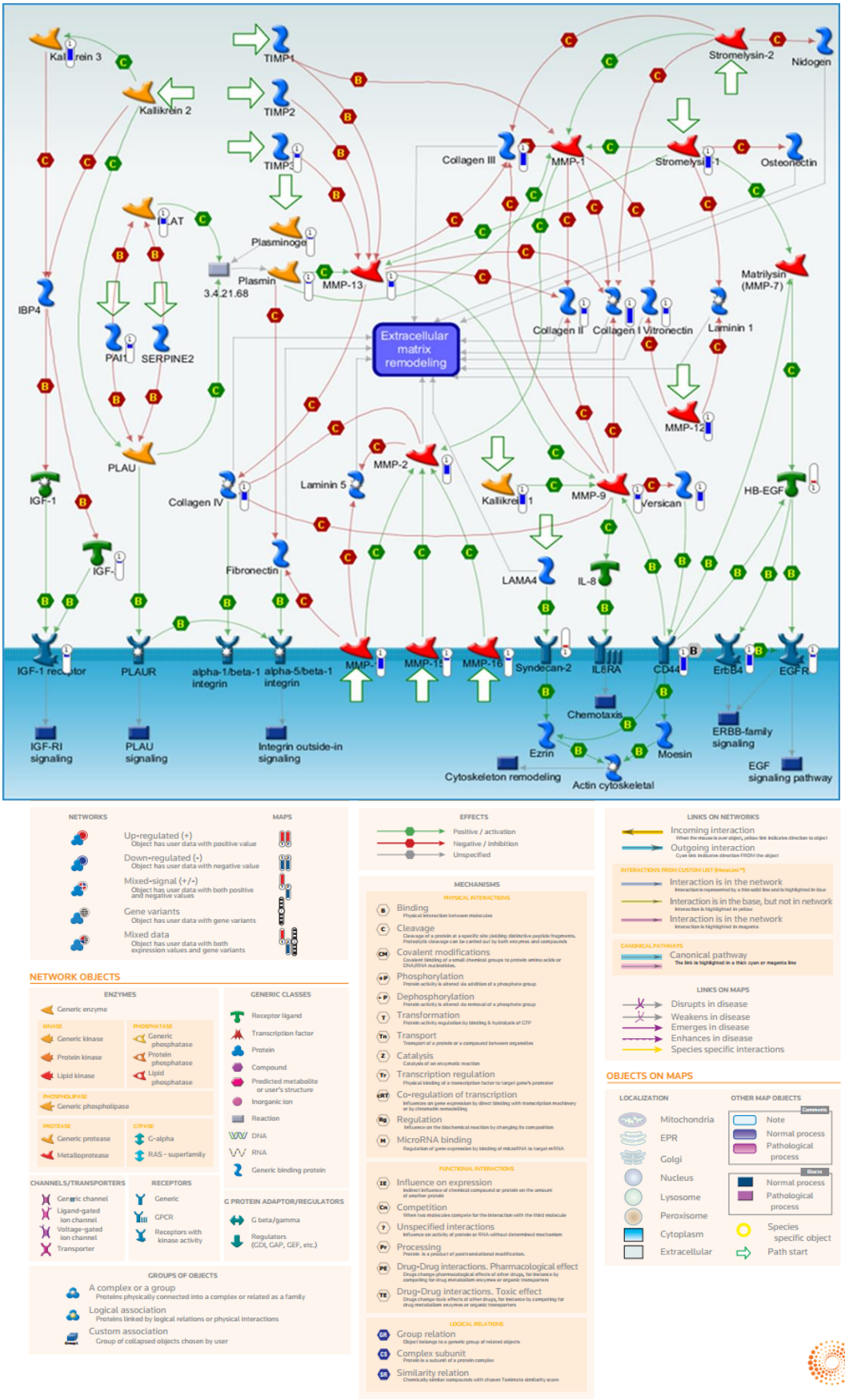

Figure 7. 1; Glucolipotoxic driven changes in extracellular matrix remodelling interactome.

Illumina HiSeq data was incorporated into the MetaCore network analysis programme (Thomson Reuters - http://genego.com). The blue thermometers represent the level of significant downregulation of gene expression ($P<0.05$), whilst the red thermometers indicate the level of significant upregulation of gene expression between INS-1 β-cells cultured in control or glucolipotoxic media for 72h.

Figure 7.2 indicates the RNA read counts in control and GLT conditions of the 5 implicated membrane proteins. Read counts were significantly reduced in 72h glucolipotoxicity by 37.2 ± 1.3% ($p=0.001$), 38.3 ± 13.2% ($p=4.67e^{-6}$), 98.1 ± 1.9% ($p=9.55e^{-9}$), 99.1 ± 0.9% ($p= 7.89e^{-13}$) and 98.1 ± 0.9% ($p=8.68e^{-10}$) for MMP15, MMP16, MMP14, CD44 and ErbB4 respectively.

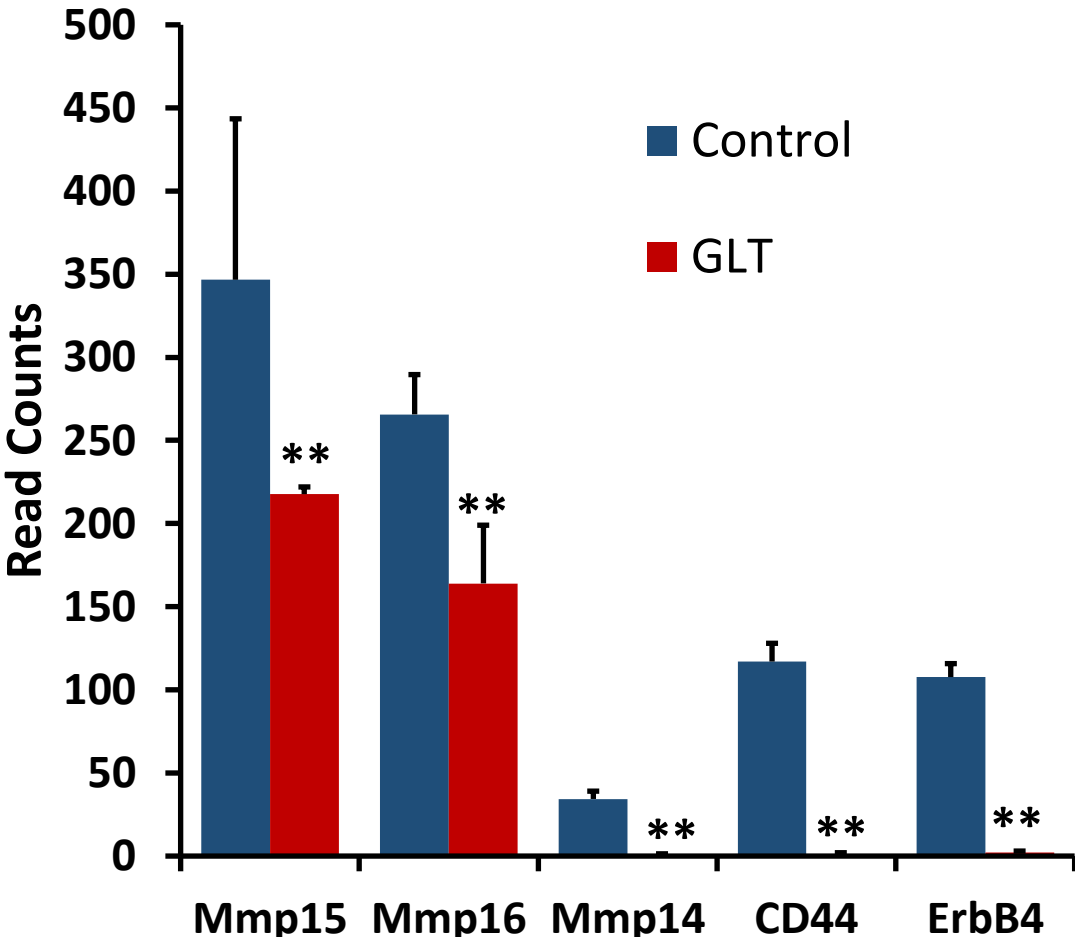

Figure 7. 2; Illumina HiSeq RNA expression data for ECM membrane proteins dysregulated by GLT.

INS-1 cells were cultured for 72h in standard growth media or media supplemented to 28mM glucose and 200µM oleic acid and 200µM palmitic acid. RNA was extracted, and quality assessed before Illumina HiSeq sequencing and analysis was undertaken. Data is expressed as mean RNA read counts per condition of MMP15, MMP16, MMP14, CD44 and ErbB4 ± SEM, from 3 independent RNAseq analyses per condition. $p<0.005$ v control

In order to validate these RNAseq findings and therefore the interactome, independent qRT-PCR analysis was performed for the genes MMP15, MMP16, MMP14, CD44 and ErbB4. INS-1 cells were therefore cultured in control or GLT media for 72h prior to RNA extraction, cDNA synthesis via reverse transcription and qRT-

PCR analysis (Figure 7.3). A 3 day incubation in GLT caused MMP15 gene expression to significantly decrease by 81.2 ± 2.0% ($p=1.14e^{-6}$), MMP14 gene expression to significantly decrease by 48.1 ± 13.5% (p=0.012) and ErbB4 gene expression to significantly decrease by 60.2 ± 20.0% (p=0.02). Unfortunately, due to time constraints and availability of reagents, only one result was obtained for CD44 and MMP16. However, these preliminary findings for these two gene targets suggests a similar pattern of glucolipotoxic driven downregulation of gene expression consistent with the RNAseq dataset.

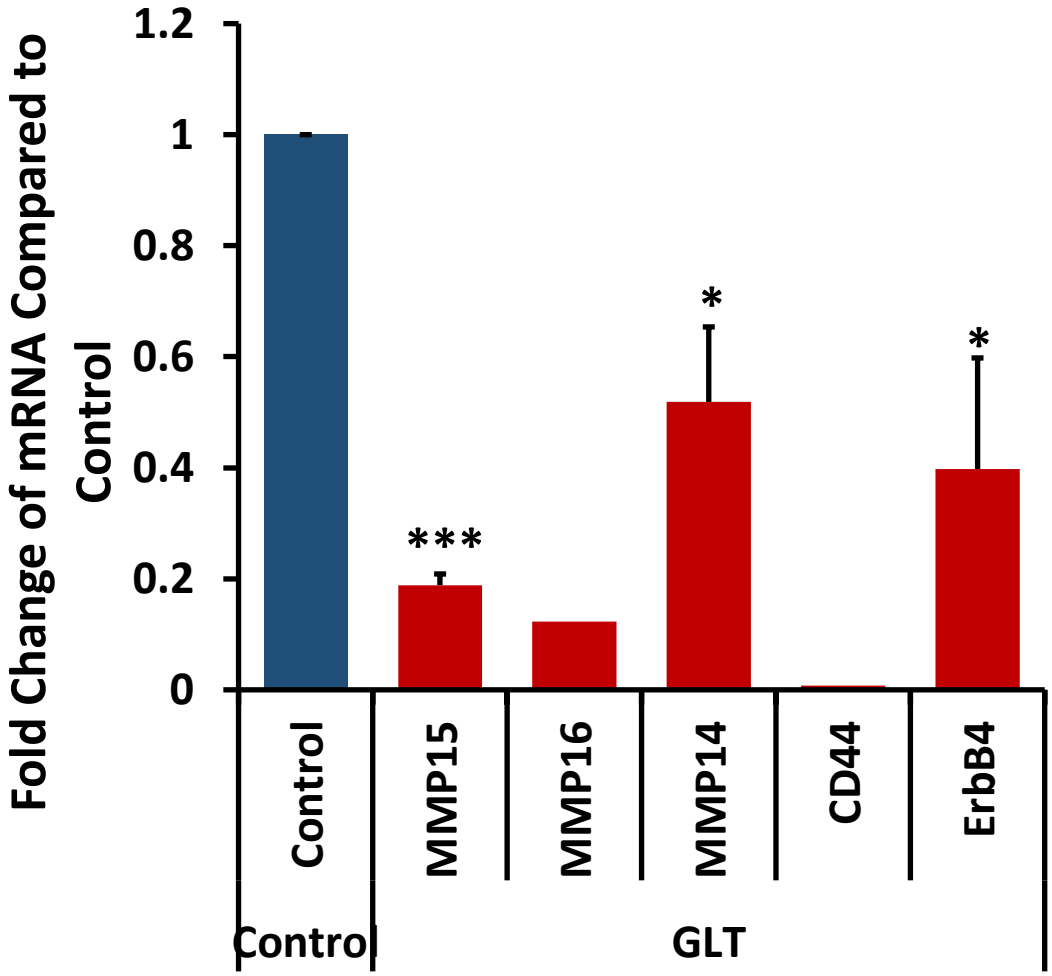

Figure 7. 3; Glucolipotoxic changes of qRT-PCR expression data of ECM implicated proteins.

INS-1 cells were cultured in control or GLT media for 72h before RNA extraction and qRT-PCR analysis performed using primers and cycle conditions detailed in materials and methodology section. Data is expressed as fold change in RNA expression of MMP15, MMP16, MMP14, CD44 and ErbB4 ± SEM compared to control using comparative delta delta Ct ($\Delta\Delta_{CT}$) method from 3 independent experiments (MMP15, MMP15 and ErbB4). One repeat for MMP16 and CD44. *p<0.05 ***p<0.005

7.2. Discussion and Future Work

Utilising the Illumina HiSeq RNA sequencing data, the identification of extracellular matrix remodelling was identified as one of the most significantly dysregulated cellular events when INS-1 β-cells are exposed to high concentrations of glucose and

fatty acids for 72h. This was partially validated via qRT-PCR expression data, confirming downregulation of gene expression of the membrane proteins MMPs, CD44 and ErbB4 that featured in the network map.

The extracellular matrix (ECM) is a non-cellular network of structural proteins that provide a flexible three-dimensional scaffold for the tissue structure and connective junctions, as well as providing chemical and physical cues for migration, differentiation and growth. The ECM is constantly undergoing controlled remodelling to regulate tissue homeostasis and the dysregulation of ECM composition, protein abundance, structure and loss of elasticity has been implicated in numerous pathological conditions such as fibrosis and various cancer types (Bonnans, Chou and Werb 2014). The ability for β-cells to communicate via the extracellular matrix and connexin channels is also vital to synchronised insulin secretion. β-cells not coupled with connexin junctions show poor insulin gene expression and secretion in response to glucose compared to coupled β-cells (Meda, et al. 1990). If the ECM, and therefore tissue communication, is dysregulated in response to glucolipotoxicity as preliminary data would suggest, this is likely to contribute to the failure of β-cell insulin secretion witnessed in type 2 diabetes.

MMPs are the main enzymes involved in ECM degradation, an initial key component of the remodelling process. MMPs are activated via proteolytic cleavage from other MMPs or oxidation by reactive species and are then able to degrade all known ECM proteins (Lu, et al. 2011). As reactive species are a hallmark of obesity and type 2 diabetes onset, MMP expression and activity is expected to increase. MMP2 and MMP9 which have been researched in type 2 diabetes particularly attack laminin,

fibronectin, and collagen IV in blood vessels in cerebrovascular disease (Mun-Bryce and Rosenberg 1998). However, the relationship between MMP and hyperglycaemia and hyperlipidaemia are much more complex. Blood concentrations of MMP2 and MMP9 have been reported to be increased in type 2 diabetic patients (Signorelli, et al. 2005), however, conflicting data suggest the opposite of decreased MMP concentrations in type 2 diabetic patients (Sampson, et al. 2004; Lewandowski, et al. 2011). Whilst these studies investigate blood concentration as opposed to solely β-cell concentrations, the latter studies would agree with our findings that chronic exposure to high glucose and high fat decrease MMP expression. There is currently no published link between MMP derived ECM dysregulation and β-cell failure, however any disruption to ECM remodelling or loss of coordinated function via connexin channels in response to high glucose and fat may contribute to glucolipotoxic driven loss of insulin secretion, but further investigation into this would be required.

Similarly, our enriched interactome suggests that the majority of members of the collagen family are highly downregulated in response to glucolipotoxic exposure. Various studies have already demonstrated the beneficial function of culturing β-cells on ECM gel environments containing collagen I and IV. Both β-cell survival and insulin secretion was promoted with specific extracellular protein concentrations suggesting a role of ECM interaction and signalling between cells in the insulin secretory pathway (Nagata, et al. 2001; Weber, Hayda and Anseth 2008). If collagen is downregulated in response to glucolipotoxic exposure as preliminary data suggests,

this may contribute to the loss of ECM remodelling and consequentially insulin secretion.

The membrane protein CD44 was also shown to be downregulated and linked to actin cytoskeletal remodelling via moesin. Actin is a key regulator of insulin secretion as it transiently depolymerises in response to glucose allowing nearby insulin granule access to the membrane (Thurmond 2007). It also facilitates transport of intracellular granules to replenish the readily releasable pool where they can dock with SNARE proteins. As CD44 was downregulated when exposed to GLT for 72h, future work that was beyond the scope of this PhD will aim to knock down CD44 and look at the functional consequences on the insulin secretory pathway. The aim is to determine if CD44 is a regulator of glucose stimulated actin reorganisation and whether its loss contributes to glucolipotoxic inhibition of insulin secretion.

In conclusion, this preliminary data suggests that glucolipotoxicity alters both extracellular matrix remodelling and cytoskeletal remodelling which may play a key role in the dysregulation of insulin secretion in type 2 diabetes and this, alongside other future research avenues discussed at the end of chapters 3, 4 and 5 will be the basis for future work.

Bibliography

- Ackermann, A.M., and Gannon, M., 2007. Molecular regulation of pancreatic beta-cell mass development, maintenance, and expansion. *Journal of Molecular Endocrinology,* 38 (1-2), 193-206.
- Aganna, E., Burrin, J.M., Hitman, G.A. and Turner, M.D., 2006. Involvement of calpain and synaptotagmin Ca2 sensors in hormone secretion from excitable endocrine cells. *Journal of Endocrinology,* 190 (3), R1-R7.
- Ahmad, F.K., He, Z. and King, G.L., 2005. Molecular targets of diabetic cardiovascular complications. *Current Drug Targets,* 6 (4), 487-494.
- Ahmed, N., 2005. Advanced glycation endproducts—role in pathology of diabetic complications. *Diabetes Research and Clinical Practice,* 67 (1), 3-21.
- Ahsan, H., 2013. 3-Nitrotyrosine: a biomarker of nitrogen free radical species modified proteins in systemic autoimmunogenic conditions. *Human Immunology,* 74 (10), 1392-1399.
- Albrecht, T., Schilperoort, M., Zhang, S., Braun, J.D., Qiu, J., Rodriguez, A., Pastene, D.O., Krämer, B.K., Köppel, H. and Baelde, H., 2017. Carnosine attenuates the development of both type 2 diabetes and diabetic nephropathy in BTBR ob/ob mice. *Scientific Reports,* 7, 44492.
- Aldini, G., Carini, M., Beretta, G., Bradamante, S. and Facino, R.M., 2002. Carnosine is a quencher of 4-hydroxy-nonenal: through what mechanism of reaction? *Biochemical and Biophysical Research Communications,* 298 (5), 699-706.
- Aldini, G., Granata, P., Orioli, M., Santaniello, E. and Carini, M., 2003. Detoxification of 4-hydroxynonenal (HNE) in keratinocytes: characterization of conjugated metabolites by liquid chromatography/electrospray ionization tandem mass spectrometry. *Journal of Mass Spectrometry,* 38 (11), 1160-1168.
- Al-Nahdi, A.M., John, A. and Raza, H., 2018. Cytoprotective Effects of N-Acetylcysteine on Streptozotocin-Induced Oxidative Stress and Apoptosis in RIN-5F Pancreatic β-Cells. *Cellular Physiology and Biochemistry,* 51 (1), 201-216.
- American Diabetes Association, 2014. Diagnosis and classification of diabetes mellitus. *Diabetes Care,* 37 Suppl 1, S81-90.
- Andrali, S.S., Sampley, M.L., Vanderford, N.L. and Özcan, S., 2008. Glucose regulation of insulin gene expression in pancreatic β-cells. *Biochemical Journal,* 415 (1), 1-10.
- Artioli, G.G., Gualano, B., Smith, A., Stout, J. and Lancha Jr, A.H., 2010. Role of beta-alanine supplementation on muscle carnosine and exercise performance. *Med Sci Sports Exerc,* 42 (6), 1162-1173.
- Artioli, G.G., Sale, C. and Jones, R.L., 2018. Carnosine in health and disease. *European Journal of Sport Science,* , 1-10.
- Asfari, M., Janjic, D., Meda, P., Li, G., Halban, P.A. and Wollheim, C.B., 1992. Establishment of 2-mercaptoethanol-dependent differentiated insulin-secreting cell lines. *Endocrinology,* 130 (1), 167-178.
- Ayala, A., Munoz, M.F. and Arguelles, S., 2014. Lipid peroxidation: production, metabolism, and signaling mechanisms of malondialdehyde and 4-hydroxy-2-nonenal. *Oxidative Medicine and Cellular Longevity,* 2014, 360438.
- Backer, J.M., Kahn, C.R., Cahill, D.A., Ullrich, A. and White, M.F., 1990. Receptor-mediated internalization of insulin requires a 12-amino acid sequence in the juxtamembrane region of the insulin receptor beta-subunit. *The Journal of Biological Chemistry,* 265 (27), 16450-16454.
- Bagnati, M., Ogunkolade, B.W., Marshall, C., Tucci, C., Hanna, K., Jones, T.A., Bugliani, M., Nedjai, B., Caton, P.W. and Kieswich, J., 2016. Glucolipotoxicity initiates

pancreatic β-cell death through TNFR5/CD40-mediated STAT1 and NF-κB activation. *Cell Death & Disease,* 7 (8), e2329.
- Bailey, C.J., 2017. Metformin: historical overview. *Diabetologia,* 60 (9), 1566-1576.
- Bakardjiev, A., and Bauer, K., 1994. Transport of β-alanine and biosynthesis of carnosine by skeletal muscle cells in primary culture. *European Journal of Biochemistry,* 225 (2), 617-623.
- Bansal, V., Kalita, J. and Misra, U.K., 2006. Diabetic neuropathy. *Postgraduate Medical Journal,* 82 (964), 95-100.
- Barak, L.S., Salahpour, A., Zhang, X., Masri, B., Sotnikova, T.D., Ramsey, A.J., Violin, J.D., Lefkowitz, R.J., Caron, M.G. and Gainetdinov, R.R., 2008. Pharmacological characterization of membrane-expressed human trace amine-associated receptor 1 (TAAR1) by a bioluminescence resonance energy transfer cAMP biosensor. *Molecular Pharmacology,* 74 (3), 585-594.
- Baran, E., 2000. Metal complexes of carnosine. *Biochemistry C/C of Biokhimiia,* 65 (7), 789-797.
- Barg, S., Eliasson, L., Renstrom, E. and Rorsman, P., 2002. A subset of 50 secretory granules in close contact with L-type Ca2+ channels accounts for first-phase insulin secretion in mouse beta-cells. *Diabetes,* 51 Suppl 1, S74-82.
- Basta, G., Schmidt, A.M. and De Caterina, R., 2004. Advanced glycation end products and vascular inflammation: implications for accelerated atherosclerosis in diabetes. *Cardiovascular Research,* 63 (4), 582-592.
- Baumann, C.A., Ribon, V., Kanzaki, M., Thurmond, D.C., Mora, S., Shigematsu, S., Bickel, P.E., Pessin, J.E. and Saltiel, A.R., 2000. CAP defines a second signalling pathway required for insulin-stimulated glucose transport. *Nature,* 407 (6801), 202.
- Baynes, J.W., 2002. The Maillard hypothesis on aging: time to focus on DNA. *Annals of the New York Academy of Sciences,* 959 (1), 360-367.
- Benedetti, A., Comporti, M. and Esterbauer, H., 1980. Identification of 4-hydroxynonenal as a cytotoxic product originating from the peroxidation of liver microsomal lipids. *Biochimica Et Biophysica Acta (BBA)-Lipids and Lipid Metabolism,* 620 (2), 281-296.
- Berne, C., 1975. The metabolism of lipids in mouse pancreatic islets. The biosynthesis of triacylglycerols and phospholipids. *The Biochemical Journal,* 152 (3), 667-673.
- Berry, M.D., 2004. Mammalian central nervous system trace amines. Pharmacologic amphetamines, physiologic neuromodulators. *Journal of Neurochemistry,* 90 (2), 257-271.
- Berry, M.D., Gainetdinov, R.R., Hoener, M.C. and Shahid, M., 2017. Pharmacology of human trace amine-associated receptors: therapeutic opportunities and challenges. *Pharmacology & Therapeutics,* .
- Bevan, P., 2001. Insulin signalling. *Journal of Cell Science,* 114 (Pt 8), 1429-1430.
- Biden, T.J., Boslem, E., Chu, K.Y. and Sue, N., 2014. Lipotoxic endoplasmic reticulum stress, β cell failure, and type 2 diabetes mellitus. *Trends in Endocrinology & Metabolism,* 25 (8), 389-398.
- Bloom, G.S., 2014. Amyloid-β and tau: the trigger and bullet in Alzheimer disease pathogenesis. *JAMA Neurology,* 71 (4), 505-508.
- Boldyrev, A., 2012. Carnosine: new concept for the function of an old molecule. *Biochemistry (Moscow),* 77 (4), 313-326.
- Boldyrev, A.A., Aldini, G. and Derave, W., 2013. Physiology and pathophysiology of carnosine. *Physiological Reviews,* 93 (4), 1803-1845.
- Boldyrev, A., Fedorova, T., Stepanova, M., Dobrotvorskaya, I., Kozlova, E., Boldanova, N., Bagyeva, G., Ivanova-Smolenskaya, I. and Illarioshkin, S., 2008. Carnisone

increases efficiency of DOPA therapy of Parkinson's disease: a pilot study. *Rejuvenation Research,* 11 (4), 821-827.

- Bommer, C., Heesemann, E., Sagalova, V., Manne-Goehler, J., Atun, R., Bärnighausen, T. and Vollmer, S., 2017. The global economic burden of diabetes in adults aged 20–79 years: a cost-of-illness study. *The Lancet Diabetes & Endocrinology,* 5 (6), 423-430.
- Bonnans, C., Chou, J. and Werb, Z., 2014. Remodelling the extracellular matrix in development and disease. *Nature Reviews Molecular Cell Biology,* 15 (12), 786.
- Borowsky, B., Adham, N., Jones, K.A., Raddatz, R., Artymyshyn, R., Ogozalek, K.L., Durkin, M.M., Lakhlani, P.P., Bonini, J.A., Pathirana, S., Boyle, N., Pu, X., Kouranova, E., Lichtblau, H., Ochoa, F.Y., Branchek, T.A. and Gerald, C., 2001. Trace amines: identification of a family of mammalian G protein-coupled receptors. *Proceedings of the National Academy of Sciences of the United States of America,* 98 (16), 8966-8971.
- Borradaile, N.M., Han, X., Harp, J.D., Gale, S.E., Ory, D.S. and Schaffer, J.E., 2006. Disruption of endoplasmic reticulum structure and integrity in lipotoxic cell death. *Journal of Lipid Research,* 47 (12), 2726-2737.
- Bosco, D., Armanet, M., Morel, P., Niclauss, N., Sgroi, A., Muller, Y.D., Giovannoni, L., Parnaud, G. and Berney, T., 2010. Unique arrangement of alpha- and beta-cells in human islets of Langerhans. *Diabetes,* 59 (5), 1202-1210.
- Botka, C.W., Wittig, T.W., Graul, R.C., Nielsen, C.U., Sadée, W., Higaki, K. and Amidon, G.L., 2000. Human proton/oligopeptide transporter (POT) genes: identification of putative human genes using bioinformatics. *AAPS PharmSci,* 2 (2), 76.
- Boulton, A., 1974. Amines and theories in psychiatry. *The Lancet,* 304 (7871), 52-53.
- Bradaia, A., Trube, G., Stalder, H., Norcross, R.D., Ozmen, L., Wettstein, J.G., Pinard, A., Buchy, D., Gassmann, M. and Hoener, M.C., 2009. The selective antagonist EPPTB reveals TAAR1-mediated regulatory mechanisms in dopaminergic neurons of the mesolimbic system. *Proceedings of the National Academy of Sciences,* , pnas. 0906522106.
- Brambilla, G., Sciaba, L., Faggin, P., Maura, A., Marinari, U., Ferro, M. and Esterbauer, H., 1986. Cytotoxicity, DNA fragmentation and sister-chromatid exchange in Chinese hamster ovary cells exposed to the lipid peroxidation product 4-hydroxynonenal and homologous aldehydes. *Mutation Research/Genetic Toxicology,* 171 (2-3), 169-176.
- Brownlee, M., 2001. Biochemistry and molecular cell biology of diabetic complications. *Nature,* 414 (6865), 813.
- Bulygina, E., and Kramarenko, G., 1995. Isolation of carnosine synthetase from animal and human muscles. *Voprosy Meditsinskoi Khimii,* 41 (6), 27-30.
- Bunzow, J.R., Sonders, M.S., Arttamangkul, S., Harrison, L.M., Zhang, G., Quigley, D.I., Darland, T., Suchland, K.L., Pasumamula, S., Kennedy, J.L., Olson, S.B., Magenis, R.E., Amara, S.G. and Grandy, D.K., 2001. Amphetamine, 3,4-methylenedioxymethamphetamine, lysergic acid diethylamide, and metabolites of the catecholamine neurotransmitters are agonists of a rat trace amine receptor. *Molecular Pharmacology,* 60 (6), 1181-1188.
- Butler, A.E., Janson, J., Bonner-Weir, S., Ritzel, R., Rizza, R.A. and Butler, P.C., 2003. Beta-cell deficit and increased beta-cell apoptosis in humans with type 2 diabetes. *Diabetes,* 52 (1), 102-110.
- Camastra, S., Manco, M., Mari, A., Baldi, S., Gastaldelli, A., Greco, A.V., Mingrone, G. and Ferrannini, E., 2005. Beta-Cell Function in Morbidly Obese Subjects during Free Living: Long-Term Effects of Weight Loss. *Diabetes,* 54 (8), 2382-2389.

- Cerf, M.E., 2013. Beta cell dysfunction and insulin resistance. *Frontiers in Endocrinology,* 4, 37.
- Chamberlain, J.J., Rhinehart, A.S., Shaefer, C.F. and Neuman, A., 2016. Diagnosis and management of diabetes: synopsis of the 2016 American Diabetes Association standards of medical care in diabetes. *Annals of Internal Medicine,* 164 (8), 542-552.
- Chang-Chen, K., Mullur, R. and Bernal-Mizrachi, E., 2008. β-cell failure as a complication of diabetes. *Reviews in Endocrine and Metabolic Disorders,* 9 (4), 329.
- Chaturvedi, N., 2007. The burden of diabetes and its complications: trends and implications for intervention. *Diabetes Research and Clinical Practice,* 76 (3), S3-S12.
- Chaudhury, A., Duvoor, C., Dendi, R., Sena, V., Kraleti, S., Chada, A., Ravilla, R., Marco, A., Shekhawat, N.S. and Montales, M.T., 2017. Clinical review of antidiabetic drugs: Implications for type 2 diabetes mellitus management. *Frontiers in Endocrinology,* 8, 6.
- Cheatham, B., and Kahn, C.R., 1995. Insulin action and the insulin signaling network. *Endocrine Reviews,* 16 (2), 117-142.
- Cherry, J.A., and Pho, V., 2002. Characterization of cAMP degradation by phosphodiesterases in the accessory olfactory system. *Chemical Senses,* 27 (7), 643-652.
- Chiang, S., Baumann, C.A., Kanzaki, M., Thurmond, D.C., Watson, R.T., Neudauer, C.L., Macara, I.G., Pessin, J.E. and Saltiel, A.R., 2001. Insulin-stimulated GLUT4 translocation requires the CAP-dependent activation of TC10. *Nature,* 410 (6831), 944.
- Cnop, M., Ladrière, L., Igoillo-Esteve, M., Moura, R.F. and Cunha, D., 2010. Causes and cures for endoplasmic reticulum stress in lipotoxic β-cell dysfunction. *Diabetes, Obesity and Metabolism,* 12, 76-82.
- Consoli, A., and Formoso, G., 2013. Do thiazolidinediones still have a role in treatment of type 2 diabetes mellitus? *Diabetes, Obesity and Metabolism,* 15 (11), 967-977.
- Corona, C., Frazzini, V., Silvestri, E., Lattanzio, R., La Sorda, R., Piantelli, M., Canzoniero, L.M., Ciavardelli, D., Rizzarelli, E. and Sensi, S.L., 2011. Effects of dietary supplementation of carnosine on mitochondrial dysfunction, amyloid pathology, and cognitive deficits in 3xTg-AD mice. *PloS One,* 6 (3), e17971.
- Cripps, M.J., Hanna, K., Lavilla, C., Sayers, S.R., Caton, P.W., Sims, C., Girolamo, L., Sale, C. and Turner, M.D., 2017. Carnosine scavenging of glucolipotoxic free radicals enhances insulin secretion and glucose uptake. *Scientific Reports,* 7 (1), 13313.
- Cunha, D.A., Hekerman, P., Ladrière, L., Bazarra-Castro, A., Ortis, F., Wakeham, M.C., Moore, F., Rasschaert, J., Cardozo, A.K. and Bellomo, E., 2008. Initiation and execution of lipotoxic ER stress in pancreatic β-cells. *Journal of Cell Science,* 121 (14), 2308-2318.
- Curtin, J.F., Donovan, M. and Cotter, T.G., 2002. Regulation and measurement of oxidative stress in apoptosis. *Journal of Immunological Methods,* 265 (1-2), 49-72.
- Cusi, K., Kashyap, S., Gastaldelli, A., Bajaj, M. and Cersosimo, E., 2007. Effects on insulin secretion and insulin action of a 48-h reduction of plasma free fatty acids with acipimox in nondiabetic subjects genetically predisposed to type 2 diabetes. *American Journal of Physiology.Endocrinology and Metabolism,* 292 (6), E1775-81.
- Da Silva Xavier, G., 2018. The cells of the islets of langerhans. *Journal of Clinical Medicine,* 7 (3), 54.
- Danaei, G., Finucane, M.M., Lu, Y., Singh, G.M., Cowan, M.J., Paciorek, C.J., Lin, J.K., Farzadfar, F., Khang, Y. and Stevens, G.A., 2011. National, regional, and global trends in fasting plasma glucose and diabetes prevalence since 1980: systematic analysis of

health examination surveys and epidemiological studies with 370 country-years and 2· 7 million participants. *The Lancet,* 378 (9785), 31-40.

- Daniel, S., Noda, M., Straub, S.G. and Sharp, G.W., 1999. Identification of the docked granule pool responsible for the first phase of glucose-stimulated insulin secretion. *Diabetes,* 48 (9), 1686-1690.
- Davidson, H.W., Rhodes, C.J. and Hutton, J.C., 1988. Intraorganellar calcium and pH control proinsulin cleavage in the pancreatic β cell via two distinct site-specific endopeptidases. *Nature,* 333 (6168), 93.
- de Courten, B., Jakubova, M., de Courten, M.P., Kukurova, I.J., Vallova, S., Krumpolec, P., Valkovic, L., Kurdiova, T., Garzon, D. and Barbaresi, S., 2016. Effects of carnosine supplementation on glucose metabolism: Pilot clinical trial. *Obesity,* 24 (5), 1027-1034.
- De Meyts, P., 2004. Insulin and its receptor: structure, function and evolution. *Bioessays,* 26 (12), 1351-1362.
- Dean, P., 1973. Ultrastructural morphometry of the pancreatic β-cell. *Diabetologia,* 9 (2), 115-119.
- Decker, E., Livisay, S. and Zhou, S., 2000. A re-evaluation of the antioxidant activity of purified carnosine. *Biochemistry C/C of Biokhimiia,* 65 (7), 766-770.
- Decker, E.A., Crum, A.D. and Calvert, J.T., 1992. Differences in the antioxidant mechanism of carnosine in the presence of copper and iron. *Journal of Agricultural and Food Chemistry,* 40 (5), 756-759.
- DeFronzo, R.A., 2010. Overview of newer agents: where treatment is going. *The American Journal of Medicine,* 123 (3), S38-S48.
- Derave, W., Everaert, I., Beeckman, S. and Baguet, A., 2010. Muscle carnosine metabolism and β-alanine supplementation in relation to exercise and training. *Sports Medicine,* 40 (3), 247-263.
- Derosa, G., and Maffioli, P., 2012. alpha-Glucosidase inhibitors and their use in clinical practice. *Archives of Medical Science : AMS,* 8 (5), 899-906.
- Diabetes Prevention Program Research Group, 2012. Long-term safety, tolerability, and weight loss associated with metformin in the Diabetes Prevention Program Outcomes Study. *Diabetes Care,* 35 (4), 731-737.
- Diabetes UK, 2014. *Diabetes: Facts and Stats.* 3rd ed.
- Dixon, G., Nolan, J., McClenahan, N., Flatt, P. and Newsholme, P., 2003. A comparative study of amino acid consumption by rat islet cells and the clonal beta-cell line BRIN-BD11 - the functional significance of L-alanine. *Journal of Endocrinology,* 179 (3), 447-454.
- Dong, Y., Wan, Q., Yang, X., Bai, L. and Xu, P., 2007. Interaction of Munc18 and Syntaxin in the regulation of insulin secretion. *Biochemical and Biophysical Research Communications,* 360 (3), 609-614.
- Drozak, J., Veiga-da-Cunha, M., Vertommen, D., Stroobant, V. and Van Schaftingen, E., 2010. Molecular identification of carnosine synthase as ATP-grasp domain-containing protein 1 (ATPGD1). *The Journal of Biological Chemistry,* 285 (13), 9346-9356.
- Drucker, D.J., 2006. The biology of incretin hormones. *Cell Metabolism,* 3 (3), 153-165.
- Du, X.L., Edelstein, D., Rossetti, L., Fantus, I.G., Goldberg, H., Ziyadeh, F., Wu, J. and Brownlee, M., 2000. Hyperglycemia-induced mitochondrial superoxide overproduction activates the hexosamine pathway and induces plasminogen activator inhibitor-1 expression by increasing Sp1 glycosylation. *Proceedings of the National Academy of Sciences of the United States of America,* 97 (22), 12222-12226.

- Duckworth, W.C., Bennett, R.G. and Hamel, F.G., 1998. Insulin degradation: progress and potential. *Endocrine Reviews,* 19 (5), 608-624.
- Egea, P.F., Stroud, R.M. and Walter, P., 2005. Targeting proteins to membranes: structure of the signal recognition particle. *Current Opinion in Structural Biology,* 15 (2), 213-220.
- Elayat, A.A., el-Naggar, M.M. and Tahir, M., 1995. An immunocytochemical and morphometric study of the rat pancreatic islets. *Journal of Anatomy,* 186 (Pt 3) (Pt 3), 629-637.
- Ellis, E.M., 2007. Reactive carbonyls and oxidative stress: potential for therapeutic intervention. *Pharmacology & Therapeutics,* 115 (1), 13-24.
- Esterbauer, H., Schaur, R.J. and Zollner, H., 1991. Chemistry and biochemistry of 4-hydroxynonenal, malonaldehyde and related aldehydes. *Free Radical Biology and Medicine,* 11 (1), 81-128.
- Esterbauer, H., Cheeseman, K.H., Dianzani, M.U., Poli, G. and Slater, T.F., 1982. Separation and characterization of the aldehydic products of lipid peroxidation stimulated by ADP-Fe2+ in rat liver microsomes. *The Biochemical Journal,* 208 (1), 129-140.
- Fava, E., Dehghany, J., Ouwendijk, J., Müller, A., Niederlein, A., Verkade, P., Meyer-Hermann, M. and Solimena, M., 2012. Novel standards in the measurement of rat insulin granules combining electron microscopy, high-content image analysis and in silico modelling. *Diabetologia,* 55 (4), 1013-1023.
- Ferragud, A., Howell, A.D., Moore, C.F., Ta, T.L., Hoener, M.C., Sabino, V. and Cottone, P., 2017. The trace amine-associated receptor 1 agonist RO5256390 blocks compulsive, binge-like eating in rats. *Neuropsychopharmacology,* 42 (7), 1458.
- Ferrero, D.M., Wacker, D., Roque, M.A., Baldwin, M.W., Stevens, R.C. and Liberles, S.D., 2012a. Agonists for 13 trace amine-associated receptors provide insight into the molecular basis of odor selectivity. *ACS Chemical Biology,* 7 (7), 1184-1189.
- Ferrero, D.M., Wacker, D., Roque, M.A., Baldwin, M.W., Stevens, R.C. and Liberles, S.D., 2012b. Agonists for 13 trace amine-associated receptors provide insight into the molecular basis of odor selectivity. *ACS Chemical Biology,* 7 (7), 1184-1189.
- Fisher-Wellman, K.H., and Neufer, P.D., 2012. Linking mitochondrial bioenergetics to insulin resistance via redox biology. *Trends in Endocrinology & Metabolism,* 23 (3), 142-153.
- Fitzgerald, E., Mathieu, S. and Ball, A., 2009. Lesson of the week: Metformin associated lactic acidosis. *BMJ: British Medical Journal,* 339 (7732), 1254-1256.
- Fong, D.S., Aiello, L., Gardner, T.W., King, G.L., Blankenship, G., Cavallerano, J.D., Ferris, F.L.,3rd, Klein, R. and American Diabetes Association, 2004. Retinopathy in diabetes. *Diabetes Care,* 27 Suppl 1, S84-7.
- Fontana, M., Pinnen, F., Lucente, G. and Pecci, L., 2002a. Prevention of peroxynitrite-dependent damage by carnosine and related sulphonamido pseudodipeptides. *Cellular and Molecular Life Sciences CMLS,* 59 (3), 546-551.
- Fontana, M., Pinnen, F., Lucente, G. and Pecci, L., 2002b. Prevention of peroxynitrite-dependent damage by carnosine and related sulphonamido pseudodipeptides. *Cellular and Molecular Life Sciences CMLS,* 59 (3), 546-551.
- Fredriksson, R., Lagerstrom, M.C., Lundin, L.G. and Schioth, H.B., 2003. The G-protein-coupled receptors in the human genome form five main families. Phylogenetic analysis, paralogon groups, and fingerprints. *Molecular Pharmacology,* 63 (6), 1256-1272.

- Fuhlendorff, J., Rorsman, P., Kofod, H., Brand, C.L., Rolin, B., MacKay, P., Shymko, R. and Carr, R.D., 1998. Stimulation of insulin release by repaglinide and glibenclamide involves both common and distinct processes. *Diabetes,* 47 (3), 345-351.
- Fujii, T., Takaoka, M., Muraoka, T., Kurata, H., Tsuruoka, N., Ono, H., Kiso, Y., Tanaka, T. and Matsumura, Y., 2003. Preventive effect of L-carnosine on ischemia/reperfusion-induced acute renal failure in rats. *European Journal of Pharmacology,* 474 (2-3), 261-267.
- Gainetdinov, R.R., Hoener, M.C. and Berry, M.D., 2018. Trace Amines and Their Receptors. *Pharmacological Reviews,* 70 (3), 549-620.
- Gao, Z., Reavey-Cantwell, J., Young, R.A., Jegier, P. and Wolf, B.A., 2000. Synaptotagmin III/VII isoforms mediate Ca2+-induced insulin secretion in pancreatic islet beta -cells. *The Journal of Biological Chemistry,* 275 (46), 36079-36085.
- Gehring, W.J., Affolter, M. and Burglin, T., 1994. Homeodomain proteins. *Annual Review of Biochemistry,* 63 (1), 487-526.
- Gerber, P.A., and Rutter, G.A., 2017. The role of oxidative stress and hypoxia in pancreatic beta-cell dysfunction in diabetes mellitus. *Antioxidants & Redox Signaling,* 26 (10), 501-518.
- German, M., Ashcroft, S., Docherty, K., Edlund, H., Edlund, T., Goodison, S., Imura, H., Kennedy, G., Madsen, O. and Melloul, D., 1995. The insulin gene promoter. A simplified nomenclature. *Diabetes,* 44 (8), 1002-1004.
- German, M.S., Wang, J., Chadwick, R.B. and Rutter, W.J., 1992. Synergistic activation of the insulin gene by a LIM-homeo domain protein and a basic helix-loop-helix protein: building a functional insulin minienhancer complex. *Genes & Development,* 6 (11), 2165-2176.
- Gleason, C.E., Gonzalez, M., Harmon, J.S. and Robertson, R.P., 2000. Determinants of glucose toxicity and its reversibility in the pancreatic islet β-cell line, HIT-T15. *American Journal of Physiology-Endocrinology and Metabolism,* 279 (5), E997-E1002.
- Goh, S., and Cooper, M.E., 2008. The role of advanced glycation end products in progression and complications of diabetes. *The Journal of Clinical Endocrinology & Metabolism,* 93 (4), 1143-1152.
- Gualano, B., Everaert, I., Stegen, S., Artioli, G.G., Taes, Y., Roschel, H., Achten, E., Otaduy, M.C., Junior, A.H.L. and Harris, R., 2012. Reduced muscle carnosine content in type 2, but not in type 1 diabetic patients. *Amino Acids,* 43 (1), 21-24.
- Guiotto, A., Calderan, A., Ruzza, P. and Borin, G., 2005. Carnosine and carnosine-related antioxidants: a review. *Current Medicinal Chemistry,* 12 (20), 2293-2315.
- Gulewitsch, W., and Amiradžibi, S., 1900. Ueber das carnosin, eine neue organische base des fleischextractes. *Berichte Der Deutschen Chemischen Gesellschaft,* 33 (2), 1902-1903.
- Gustavsson, N., Wang, X., Wang, Y., Seah, T., Xu, J., Radda, G.K., Südhof, T.C. and Han, W., 2010. Neuronal calcium sensor synaptotagmin-9 is not involved in the regulation of glucose homeostasis or insulin secretion. *PLoS One,* 5 (11), e15414.
- Gustavsson, N., Lao, Y., Maximov, A., Chuang, J.C., Kostromina, E., Repa, J.J., Li, C., Radda, G.K., Sudhof, T.C. and Han, W., 2008. Impaired insulin secretion and glucose intolerance in synaptotagmin-7 null mutant mice. *Proceedings of the National Academy of Sciences of the United States of America,* 105 (10), 3992-3997.
- Hagman, D.K., Hays, L.B., Parazzoli, S.D. and Poitout, V., 2005. Palmitate inhibits insulin gene expression by altering PDX-1 nuclear localization and reducing MafA expression in isolated rat islets of Langerhans. *The Journal of Biological Chemistry,* 280 (37), 32413-32418.

- Halasi, M., Wang, M., Chavan, T.S., Gaponenko, V., Hay, N. and Gartel, A.L., 2013. ROS inhibitor N-acetyl-L-cysteine antagonizes the activity of proteasome inhibitors. *The Biochemical Journal,* 454 (2), 201-208.
- Hamilton, J.A., and Kamp, F., 1999. How are free fatty acids transported in membranes? Is it by proteins or by free diffusion through the lipids? *Diabetes,* 48 (12), 2255-2269.
- Harris, R.C., Tallon, M., Dunnett, M., Boobis, L., Coakley, J., Kim, H.J., Fallowfield, J.L., Hill, C., Sale, C. and Wise, J.A., 2006. The absorption of orally supplied β-alanine and its effect on muscle carnosine synthesis in human vastus lateralis. *Amino Acids,* 30 (3), 279-289.
- Hasnain, S.Z., Prins, J.B. and McGuckin, M.A., 2016. Oxidative and endoplasmic reticulum stress in β-cell dysfunction in diabetes. *Journal of Molecular Endocrinology,* 56 (2), R33-R54.
- Hauck, A.K., and Bernlohr, D.A., 2016. Oxidative stress and lipotoxicity. *Journal of Lipid Research,* 57 (11), 1976-1986.
- Hauner, H., 2002. The mode of action of thiazolidinediones. *Diabetes/Metabolism Research and Reviews,* 18 (S2), S10-S15.
- Hay, C.W., and Docherty, K., 2006. Comparative analysis of insulin gene promoters: implications for diabetes research. *Diabetes,* 55 (12), 3201-3213.
- Henquin, J., and Nenquin, M., 2014. Activators of PKA and Epac distinctly influence insulin secretion and cytosolic Ca2 in female mouse islets stimulated by glucose and tolbutamide. *Endocrinology,* 155 (9), 3274-3287.
- Herculano, B., Tamura, M., Ohba, A., Shimatani, M., Kutsuna, N. and Hisatsune, T., 2013. β-alanyl-L-histidine rescues cognitive deficits caused by feeding a high fat diet in a transgenic mouse model of Alzheimer's disease. *Journal of Alzheimer's Disease,* 33 (4), 983-997.
- Hex, N., Bartlett, C., Wright, D., Taylor, M. and Varley, D., 2012. Estimating the current and future costs of Type 1 and Type 2 diabetes in the UK, including direct health costs and indirect societal and productivity costs. *Diabetic Medicine,* 29 (7), 855-862.
- Hill, C., Harris, R.C., Kim, H., Harris, B., Sale, C., Boobis, L., Kim, C. and Wise, J.A., 2007. Influence of β-alanine supplementation on skeletal muscle carnosine concentrations and high intensity cycling capacity. *Amino Acids,* 32 (2), 225-233.
- Holst, J.J., 2007. The physiology of glucagon-like peptide 1. *Physiological Reviews,* 87 (4), 1409-1439.
- Holz, G.G., 2004. Epac: A new cAMP-binding protein in support of glucagon-like peptide-1 receptor-mediated signal transduction in the pancreatic beta-cell. *Diabetes,* 53 (1), 5-13.
- Horinishi, H., Grillo, M. and Margolis, F.L., 1978. Purification and characterization of carnosine synthetase from mouse olfactory bulbs. *Journal of Neurochemistry,* 31 (4), 909-919.
- Horowitz, L.F., Saraiva, L.R., Kuang, D., Yoon, K.H. and Buck, L.B., 2014. Olfactory receptor patterning in a higher primate. *The Journal of Neuroscience : The Official Journal of the Society for Neuroscience,* 34 (37), 12241-12252.
- Hou, J.C., Min, L. and Pessin, J.E., 2009. Insulin granule biogenesis, trafficking and exocytosis. *Vitamins & Hormones,* 80, 473-506.
- Hovorka, R., Powrie, J., Smith, G., Sonksen, P., Carson, E. and Jones, R., 1993. Five-compartment model of insulin kinetics and its use to investigate action of chloroquine in NIDDM. *American Journal of Physiology-Endocrinology and Metabolism,* 265 (1), E162-E175.

- Howell, S., 1984. The mechanism of insulin secretion. *Diabetologia,* 26 (5), 319-327.
- Hu, L.A., Zhou, T., Ahn, J., Wang, S., Zhou, J., Hu, Y. and Liu, Q., 2009. Human and mouse trace amine-associated receptor 1 have distinct pharmacology towards endogenous monoamines and imidazoline receptor ligands. *The Biochemical Journal,* 424 (1), 39-45.
- Huang, X.F., and Arvan, P., 1995. Intracellular transport of proinsulin in pancreatic beta-cells. Structural maturation probed by disulfide accessibility. *The Journal of Biological Chemistry,* 270 (35), 20417-20423.
- Hulse, R.E., Ralat, L.A. and Wei-Jen, T., 2009. Structure, Function, and Regulation of Insulin-Degrading Enzyme. *Vitamins & Hormones,* 80, 635-648.
- Hussain, A., Saraiva, L.R., Ferrero, D.M., Ahuja, G., Krishna, V.S., Liberles, S.D. and Korsching, S.I., 2013. High-affinity olfactory receptor for the death-associated odor cadaverine. *Proceedings of the National Academy of Sciences of the United States of America,* 110 (48), 19579-19584.
- Iezzi, M., Eliasson, L., Fukuda, M. and Wollheim, C.B., 2005. Adenovirus-mediated silencing of Synaptotagmin 9 inhibits Ca2 -dependent insulin secretion in islets. *FEBS Letters,* 579 (23), 5241-5246.
- Inagaki, N., Maekawa, T., Sudo, T., Ishii, S., Seino, Y. and Imura, H., 1992. c-Jun represses the human insulin promoter activity that depends on multiple cAMP response elements. *Proceedings of the National Academy of Sciences of the United States of America,* 89 (3), 1045-1049.
- International Diabetes Federation, 2017. *IDF Diabetes Atlas.* 8th ed. http://www.diabetesatlas.org: International Diabetes Federation, Brussels, Belgium.
- International Human Genome Sequencing Consortium, 2001. Initial sequencing and analysis of the human genome. *Nature,* 409 (6822), 860.
- Iovine, B., Oliviero, G., Garofalo, M., Orefice, M., Nocella, F., Borbone, N., Piccialli, V., Centore, R., Mazzone, M. and Piccialli, G., 2014. The anti-proliferative effect of L-carnosine correlates with a decreased expression of hypoxia inducible factor 1 alpha in human colon cancer cells. *PLoS One,* 9 (5), e96755.
- Isaiah Pittman, Louis H Philipson, Donal F Steiner, 2010. ***INSULIN BIOSYNTHESIS, SECRETION, STRUCTURE, AND STRUCTURE-ACTIVITY RELATIONSHIPS*** [online]. . Available at: http://diabetesmanager.pbworks.com/w/page/17680216/Insulin%20Biosynthesis,%20Secretion,%20Structure,%20and%20Structure-Activity%20Relationships [Accessed 08.22 2018].
- Izquierdo, J.M., Majós, N., Bonnal, S., Martínez, C., Castelo, R., Guigó, R., Bilbao, D. and Valcárcel, J., 2005. Regulation of Fas alternative splicing by antagonistic effects of TIA-1 and PTB on exon definition. *Molecular Cell,* 19 (4), 475-484.
- Jacobs, S., and Cuatrecasas, P., 1981. Insulin receptor: structure and function. *Endocrine Reviews,* 2 (3), 251-263.
- Jaishy, B., and Abel, E.D., 2016. Lipids, lysosomes, and autophagy. *Journal of Lipid Research,* 57 (9), 1619-1635.
- Janssen, B., Hohenadel, D., Brinkkoetter, P., Peters, V., Rind, N., Fischer, C., Rychlik, I., Cerna, M., Romzova, M., de Heer, E., Baelde, H., Bakker, S.J., Zirie, M., Rondeau, E., Mathieson, P., Saleem, M.A., Meyer, J., Koppel, H., Sauerhoefer, S., Bartram, C.R., Nawroth, P., Hammes, H.P., Yard, B.A., Zschocke, J. and van der Woude, F.J., 2005. Carnosine as a protective factor in diabetic nephropathy: association with a leucine repeat of the carnosinase gene CNDP1. *Diabetes,* 54 (8), 2320-2327.
- Kalyanaraman, B., Darley-Usmar, V., Davies, K.J., Dennery, P.A., Forman, H.J., Grisham, M.B., Mann, G.E., Moore, K., Roberts II, L.J. and Ischiropoulos, H., 2012.

Measuring reactive oxygen and nitrogen species with fluorescent probes: challenges and limitations. *Free Radical Biology and Medicine,* 52 (1), 1-6.

- Kalyankar, G.D., and Meister, A., 1959. Enzymatic synthesis of carnosine and related beta-alanyl and gamma-aminobutyryl peptides. *The Journal of Biological Chemistry,* 234, 3210-3218.
- Kampmann, U., Madsen, L.R., Skajaa, G.O., Iversen, D.S., Moeller, N. and Ovesen, P., 2015. Gestational diabetes: A clinical update. *World Journal of Diabetes,* 6 (8), 1065-1072.
- Kaneto, H., Xu, G., Song, K., Suzuma, K., Bonner-Weir, S., Sharma, A. and Weir, G.C., 2001. Activation of the hexosamine pathway leads to deterioration of pancreatic β-cell function through the induction of oxidative stress. *Journal of Biological Chemistry,* 276 (33), 31099-31104.
- Karlsson, O., Thor, S., Norberg, T., Ohlsson, H. and Edlund, T., 1990. Insulin gene enhancer binding protein Isl-1 is a member of a novel class of proteins containing both a homeo-and a Cys–His domain. *Nature,* 344 (6269), 879.
- Kebede, M., Alquier, T., Latour, M.G., Semache, M., Tremblay, C. and Poitout, V., 2008. The fatty acid receptor GPR40 plays a role in insulin secretion in vivo after high-fat feeding. *Diabetes,* 57 (9), 2432-2437.
- Kimura, A., Baumann, C.A., Chiang, S.H. and Saltiel, A.R., 2001. The sorbin homology domain: a motif for the targeting of proteins to lipid rafts. *Proceedings of the National Academy of Sciences of the United States of America,* 98 (16), 9098-9103.
- Klebanov, G., Teselkin, Y.O., Babenkova, I., Popov, I., Levin, G., Tyulina, O., Boldyrev, A. and Vladimirov, Y.A., 1997. Evidence for a direct interaction of superoxide anion radical with carnosine. *IUBMB Life,* 43 (1), 99-106.
- Klip, A., and Leiter, L.A., 1990. Cellular mechanism of action of metformin. *Diabetes Care,* 13 (6), 696-704.
- Knepel, W., Vallejo, M., Chafitz, J.A. and Habener, J.F., 1991. The pancreatic islet-specific glucagon G3 transcription factors recognize control elements in the rat somatostatin and insulin-I genes. *Molecular Endocrinology,* 5 (10), 1457-1466.
- Komatsu, M., Takei, M., Ishii, H. and Sato, Y., 2013. Glucose-stimulated insulin secretion: A newer perspective. *Journal of Diabetes Investigation,* 4 (6), 511-516.
- Kulkarni, R.N., 2004. The islet β-cell. *The International Journal of Biochemistry & Cell Biology,* 36 (3), 365-371.
- Lai, Y., Diao, J., Cipriano, D.J., Zhang, Y., Pfuetzner, R.A., Padolina, M.S. and Brunger, A.T., 2014. Complexin inhibits spontaneous release and synchronizes Ca2 -triggered synaptic vesicle fusion by distinct mechanisms. *Elife,* 3, e03756.
- Langlais, P.R., Mandarino, L.J. and Garvey, W.T., 2015. Mechanisms of insulin signal transduction. *International Textbook of Diabetes Mellitus, 2 Volume Set,* 1, 163.
- Lee, H.B., Yu, M.R., Yang, Y., Jiang, Z. and Ha, H., 2003. Reactive oxygen species-regulated signaling pathways in diabetic nephropathy. *Journal of the American Society of Nephrology : JASN,* 14 (8 Suppl 3), S241-5.
- Lei, X.G., and Vatamaniuk, M.Z., 2011. Two tales of antioxidant enzymes on β cells and diabetes. *Antioxidants & Redox Signaling,* 14 (3), 489-503.
- Lenney, J.F., George, R.P., Weiss, A.M., Kucera, C.M., Chan, P.W. and Rinzler, G.S., 1982. Human serum carnosinase: characterization, distinction from cellular carnosinase, and activation by cadmium. *Clinica Chimica Acta,* 123 (3), 221-231.
- Leon, B.M., and Maddox, T.M., 2015. Diabetes and cardiovascular disease: Epidemiology, biological mechanisms, treatment recommendations and future research. *World Journal of Diabetes,* 6 (13), 1246-1258.

- Lewandowski, K.C., Banach, E., Bienkiewicz, M. and Lewinski, A., 2011. Matrix metalloproteinases in type 2 diabetes and non-diabetic controls: effects of short-term and chronic hyperglycaemia. *Archives of Medical Science : AMS,* 7 (2), 294-303.
- Lewis, A.M., Waterhouse, C. and Jacobs, L.S., 1980. Whole-blood and plasma amino acid analysis: gas-liquid and cation-exchange chromatography compared. *Clinical Chemistry,* 26 (2), 271-276.
- Li, Q., Tachie-Baffour, Y., Liu, Z., Baldwin, M.W., Kruse, A.C. and Liberles, S.D., 2015. Non-classical amine recognition evolved in a large clade of olfactory receptors. *Elife,* 4, e10441.
- Li, N., Brun, T., Cnop, M., Cunha, D.A., Eizirik, D.L. and Maechler, P., 2009. Transient oxidative stress damages mitochondrial machinery inducing persistent beta-cell dysfunction. *The Journal of Biological Chemistry,* 284 (35), 23602-23612.
- Liberles, S.D., and Buck, L.B., 2006. A second class of chemosensory receptors in the olfactory epithelium. *Nature,* 442 (7103), 645.
- Lim, G.E., and Brubaker, P.L., 2006. Glucagon-like peptide 1 secretion by the L-cell: the view from within. *Diabetes,* 55 (Supplement 2), S70-S77.
- Lindemann, L., Ebeling, M., Kratochwil, N.A., Bunzow, J.R., Grandy, D.K. and Hoener, M.C., 2005. Trace amine-associated receptors form structurally and functionally distinct subfamilies of novel G protein-coupled receptors. *Genomics,* 85 (3), 372-385.
- Lindemann, L., and Hoener, M.C., 2005. A renaissance in trace amines inspired by a novel GPCR family. *Trends in Pharmacological Sciences,* 26 (5), 274-281.
- Lindstrom, P., and Shelin, J., 1983. Mechanisms underlying the effects of 5-hydroxytryptamine and 5-hydroxytryptophan in pancreatic islets. A proposed role for L-aromatic amino acid decarboxylase. *Endocrinology,* 112 (4), 1524-1529.
- Ling, Z., Kiekens, R., Mahler, T., Schuit, F.C., Pipeleers-Marichal, M., Sener, A., Kloppel, G., Malaisse, W.J. and Pipeleers, D.G., 1996. Effects of chronically elevated glucose levels on the functional properties of rat pancreatic beta-cells. *Diabetes,* 45 (12), 1774-1782.
- Lipson, K.L., Fonseca, S.G., Ishigaki, S., Nguyen, L.X., Foss, E., Bortell, R., Rossini, A.A. and Urano, F., 2006. Regulation of insulin biosynthesis in pancreatic beta cells by an endoplasmic reticulum-resident protein kinase IRE1. *Cell Metabolism,* 4 (3), 245-254.
- Liu, Y., Su, D., Zhang, L., Wei, S., Liu, K., Peng, M., Li, H. and Song, Y., 2016. Endogenous L-carnosine level in diabetes rat cardiac muscle. *Evidence-Based Complementary and Alternative Medicine,* 2016.
- Liu, Y., Cotillard, A., Vatier, C., Bastard, J., Fellahi, S., Stévant, M., Allatif, O., Langlois, C., Bieuvelet, S. and Brochot, A., 2015. Correction: A Dietary Supplement Containing Cinnamon, Chromium and Carnosine Decreases Fasting Plasma Glucose and Increases Lean Mass in Overweight or Obese Pre-Diabetic Subjects: A Randomized, Placebo-Controlled Trial. *PloS One,* 10 (12), e0145315.
- Lowenstein, C.J., and Padalko, E., 2004. iNOS (NOS2) at a glance. *Journal of Cell Science,* 117 (Pt 14), 2865-2867.
- Lu, P., Takai, K., Weaver, V.M. and Werb, Z., 2011. Extracellular matrix degradation and remodeling in development and disease. *Cold Spring Harbor Perspectives in Biology,* 3 (12), 10.1101/cshperspect.a005058.
- Ma, L., and Pei, G., 2007. Beta-arrestin signaling and regulation of transcription. *Journal of Cell Science,* 120 (Pt 2), 213-218.
- Maguire, J.J., Parker, W.A., Foord, S.M., Bonner, T.I., Neubig, R.R. and Davenport, A.P., 2009. International Union of Pharmacology. LXXII. Recommendations for trace amine receptor nomenclature. *Pharmacological Reviews,* 61 (1), 1-8.

- Makris, K., and Spanou, L., 2016. Acute Kidney Injury: Definition, Pathophysiology and Clinical Phenotypes. *The Clinical Biochemist.Reviews,* 37 (2), 85-98.
- Malaisse, W., and Malaisse-Lagae, F., 1984. The role of cyclic AMP in insulin release. *Experientia,* 40 (10), 1068-1075.
- Marshak, S., Leibowitz, G., Bertuzzi, F., Socci, C., Kaiser, N., Gross, D.J., Cerasi, E. and Melloul, D., 1999. Impaired beta-cell functions induced by chronic exposure of cultured human pancreatic islets to high glucose. *Diabetes,* 48 (6), 1230-1236.
- Marshall, C., Hitman, G.A., Cassell, P.G. and Turner, M.D., 2007. Effect of glucolipotoxicity and rosiglitazone upon insulin secretion. *Biochemical and Biophysical Research Communications,* 356 (3), 756-762.
- Marshall, C., Hitman, G.A., Partridge, C.J., Clark, A., Ma, H., Shearer, T.R. and Turner, M.D., 2005. Evidence that an isoform of calpain-10 is a regulator of exocytosis in pancreatic β-cells. *Molecular Endocrinology,* 19 (1), 213-224.
- Matthews, L., Gopinath, G., Gillespie, M., Caudy, M., Croft, D., de Bono, B., Garapati, P., Hemish, J., Hermjakob, H. and Jassal, B., 2008. Reactome knowledgebase of human biological pathways and processes. *Nucleic Acids Research,* 37 (suppl_1), D619-D622.
- Mayo, K.E., Miller, L.J., Bataille, D., Dalle, S., Goke, B., Thorens, B. and Drucker, D.J., 2003. International Union of Pharmacology. XXXV. The glucagon receptor family. *Pharmacological Reviews,* 55 (1), 167-194.
- McGarry, J., Sen, A., Esser, V., Woeltje, K., Weis, B. and Foster, D., 1991. New insights into the mitochondrial carnitine palmitoyltransferase enzyme system. *Biochimie,* 73 (1), 77-84.
- McIntosh, C.H., Demuth, H., Pospisilik, J.A. and Pederson, R., 2005. Dipeptidyl peptidase IV inhibitors: how do they work as new antidiabetic agents? *Regulatory Peptides,* 128 (2), 159-165.
- Meda, P., Bosco, D., Chanson, M., Giordano, E., Vallar, L., Wollheim, C. and Orci, L., 1990. Rapid and reversible secretion changes during uncoupling of rat insulin-producing cells. *The Journal of Clinical Investigation,* 86 (3), 759-768.
- Meier, J., Breuer, T., Bonadonna, R., Tannapfel, A., Uhl, W., Schmidt, W., Schrader, H. and Menge, B., 2012. Pancreatic diabetes manifests when beta cell area declines by approximately 65% in humans. *Diabetologia,* 55 (5), 1346-1354.
- Melia Jr, T.J., 2007. Putting the clamps on membrane fusion: how complexin sets the stage for calcium-mediated exocytosis. *FEBS Letters,* 581 (11), 2131-2139.
- Metallo, S.J., Paolella, D.N. and Schepartz, A., 1997. The role of a basic amino acid cluster in target site selection and non-specific binding of bZIP peptides to DNA. *Nucleic Acids Research,* 25 (15), 2967-2972.
- Mihalik, S.J., Michaliszyn, S.F., de las Heras, J., Bacha, F., Lee, S., Chace, D.H., DeJesus, V.R., Vockley, J. and Arslanian, S.A., 2012. Metabolomic profiling of fatty acid and amino acid metabolism in youth with obesity and type 2 diabetes: evidence for enhanced mitochondrial oxidation. *Diabetes Care,* 35 (3), 605-611.
- Moore, D.J., West, A.B., Dawson, V.L. and Dawson, T.M., 2005. Molecular pathophysiology of Parkinson's disease. *Annu.Rev.Neurosci.,* 28, 57-87.
- Moran, B.M., Abdel-Wahab, Y.H., Flatt, P.R. and McKillop, A.M., 2014. Activation of GPR119 by fatty acid agonists augments insulin release from clonal β-cells and isolated pancreatic islets and improves glucose tolerance in mice. *Biological Chemistry,* 395 (4), 453-464.
- Munakata, Y., Yamada, T., Imai, J., Takahashi, K., Tsukita, S., Shirai, Y., Kodama, S., Asai, Y., Sugisawa, T. and Chiba, Y., 2018. Olfactory receptors are expressed in

pancreatic β-cells and promote glucose-stimulated insulin secretion. *Scientific Reports,* 8 (1), 1499.

- Mun-Bryce, S., and Rosenberg, G.A., 1998. Matrix metalloproteinases in cerebrovascular disease. *Journal of Cerebral Blood Flow & Metabolism,* 18 (11), 1163-1172.
- Murray, R.K., Granner, D.K., Mayes, P.A. and Rodwell, V.W., 2003. a LANGE medical book. *Harper's Illustrated Biochemistry.26th Ed.New York: McGraw-Hill Companies, Inc,* .
- Naderi, A., Sadeghi, M., Sarshin, A., Imanipour, V., Nazeri, S.A., Farkhayi, F. and Willems, M.E., 2017. Muscle carnosine concentration with the co-ingestion of carbohydrate with β-alanine in male rats. *Journal of Dietary Supplements,* 14 (4), 373-379.
- Nagai, K., and Suda, T., 1986. Antineoplastic effects of carnosine and beta-alanine--physiological considerations of its antineoplastic effects. *Nihon Seirigaku Zasshi.Journal of the Physiological Society of Japan,* 48 (11), 741-747.
- Nagata, N., Gu, Y., Hori, H., Balamurugan, A., Touma, M., Kawakami, Y., Wang, W., Baba, T.T., Satake, A. and Nozawa, M., 2001. Evaluation of insulin secretion of isolated rat islets cultured in extracellular matrix. *Cell Transplantation,* 10 (4-5), 447-451.
- National Institute for Health and Care Excellence, 2012. Preventing type 2 diabetes: risk identification and interventions for individuals at high risk. *NICE Public Health Guidance 38,* .
- Nauck, M., Bartels, E., Orskov, C., Ebert, R. and Creutzfeldt, W., 1993. Additive insulinotropic effects of exogenous synthetic human gastric inhibitory polypeptide and glucagon-like peptide-1-(7-36) amide infused at near-physiological insulinotropic hormone and glucose concentrations. *The Journal of Clinical Endocrinology & Metabolism,* 76 (4), 912-917.
- Nedachi, T., and Kanzaki, M., 2006. Regulation of glucose transporters by insulin and extracellular glucose in C2C12 myotubes. *American Journal of Physiology-Endocrinology and Metabolism,* 291 (4), E817-E828.
- Negre-Salvayre, A., Coatrieux, C., Ingueneau, C. and Salvayre, R., 2008. Advanced lipid peroxidation end products in oxidative damage to proteins. Potential role in diseases and therapeutic prospects for the inhibitors. *British Journal of Pharmacology,* 153 (1), 6-20.
- Newsholme, P., and Krause, M., 2012. Nutritional regulation of insulin secretion: implications for diabetes. *The Clinical Biochemist.Reviews,* 33 (2), 35-47.
- Ng, R., and Marshall, F., 1978. REGIONAL AND SUBCELLULAR DISTRIBUTION OF HOMOCARNOSINE–CARNOSINE SYNTHETASE IN THE CENTRAL NERVOUS SYSTEM OF RATS. *Journal of Neurochemistry,* 30 (1), 187-190.
- NHS, 2017. *Diabetes - Symptoms* [online]. . Available at: https://www.nhs.uk/conditions/type-2-diabetes/symptoms/ [Accessed 08/14 2018].
- Nicoletti, V.G., Santoro, A.M., Grasso, G., Vagliasindi, L.I., Giuffrida, M.L., Cuppari, C., Purrello, V.S., Stella, A.M.G. and Rizzarelli, E., 2007. Carnosine interaction with nitric oxide and astroglial cell protection. *Journal of Neuroscience Research,* 85 (10), 2239-2245.
- Niu, Y., Feng, R., Hou, Y., Li, K., Kang, Z., Wang, J., Sun, C. and Li, Y., 2012. Histidine and arginine are associated with inflammation and oxidative stress in obese women. *British Journal of Nutrition,* 108 (1), 57-61.

- Nolan, C.J., Madiraju, M.S., Delghingaro-Augusto, V., Peyot, M.L. and Prentki, M., 2006. Fatty acid signaling in the beta-cell and insulin secretion. *Diabetes,* 55 Suppl 2, S16-23.
- Ogurtsova, K., da Rocha Fernandes, J., Huang, Y., Linnenkamp, U., Guariguata, L., Cho, N., Cavan, D., Shaw, J. and Makaroff, L., 2017. IDF Diabetes Atlas: Global estimates for the prevalence of diabetes for 2015 and 2040. *Diabetes Research and Clinical Practice,* 128, 40-50.
- Oh, E., Kalwat, M.A., Kim, M.J., Verhage, M. and Thurmond, D.C., 2012. Munc18-1 regulates first-phase insulin release by promoting granule docking to multiple syntaxin isoforms. *The Journal of Biological Chemistry,* 287 (31), 25821-25833.
- Ohlsson, H., Karlsson, K. and Edlund, T., 1993. IPF1, a homeodomain-containing transactivator of the insulin gene. *The EMBO Journal,* 12 (11), 4251-4259.
- Okoniewski, M.J., and Miller, C.J., 2006. Hybridization interactions between probesets in short oligo microarrays lead to spurious correlations. *BMC Bioinformatics,* 7 (1), 276.
- Olbrot, M., Rud, J., Moss, L.G. and Sharma, A., 2002. Identification of beta-cell-specific insulin gene transcription factor RIPE3b1 as mammalian MafA. *Proceedings of the National Academy of Sciences of the United States of America,* 99 (10), 6737-6742.
- Olson, L.K., Redmon, J.B., Towle, H.C. and Robertson, R.P., 1993. Chronic exposure of HIT cells to high glucose concentrations paradoxically decreases insulin gene transcription and alters binding of insulin gene regulatory protein. *The Journal of Clinical Investigation,* 92 (1), 514-519.
- Orci, L., Ravazzola, M., Amherdt, M., Madsen, O., Perrelet, A., Vassalli, J.D. and Anderson, R.G., 1986. Conversion of proinsulin to insulin occurs coordinately with acidification of maturing secretory vesicles. *The Journal of Cell Biology,* 103 (6 Pt 1), 2273-2281.
- Pandya, V., Ekka, M.K., Dutta, R.K. and Kumaran, S., 2011. Mass spectrometry assay for studying kinetic properties of dipeptidases: Characterization of human and yeast dipeptidases. *Analytical Biochemistry,* 418 (1), 134-142.
- Papatheodorou, K., Papanas, N., Banach, M., Papazoglou, D. and Edmonds, M., 2016. Complications of diabetes 2016. *Journal of Diabetes Research,* 2016.
- Paschou, S.A., Papadopoulou-Marketou, N., Chrousos, G.P. and Kanaka-Gantenbein, C., 2018. On type 1 diabetes mellitus pathogenesis. *Endocrine Connections,* 7 (1), R38-R46.
- Patzelt, C., Labrecque, A.D., Duguid, J.R., Carroll, R.J., Keim, P.S., Heinrikson, R.L. and Steiner, D.F., 1978. Detection and kinetic behavior of preproinsulin in pancreatic islets. *Proceedings of the National Academy of Sciences of the United States of America,* 75 (3), 1260-1264.
- Pei, Y., Asif-Malik, A. and Canales, J.J., 2016. Trace amines and the trace amine-associated receptor 1: pharmacology, neurochemistry, and clinical implications. *Frontiers in Neuroscience,* 10, 148.
- PEPPERS, S.C., and LENNEY, J.F., 1988. Bestatin inhibition of human tissue carnosinase, a non-specific cytosolic dipeptidase. *Biological Chemistry Hoppe-Seyler,* 369 (2), 1281-1286.
- Pessin, J.E., Thurmond, D.C., Elmendorf, J.S., Coker, K.J. and Okada, S., 1999. Molecular basis of insulin-stimulated GLUT4 vesicle trafficking. Location! Location! Location! *The Journal of Biological Chemistry,* 274 (5), 2593-2596.

- Peters, V., Lanthaler, B., Amberger, A., Fleming, T., Forsberg, E., Hecker, M., Wagner, A.H., Yue, W.W., Hoffmann, G.F. and Nawroth, P., 2015. Carnosine metabolism in diabetes is altered by reactive metabolites. *Amino Acids,* 47 (11), 2367-2376.
- Peters, V., Schmitt, C.P., Weigand, T., Klingbeil, K., Thiel, C., van den Berg, A., Calabrese, V., Nawroth, P., Fleming, T. and Forsberg, E., 2017. Allosteric inhibition of carnosinase (CN1) by inducing a conformational shift. *Journal of Enzyme Inhibition and Medicinal Chemistry,* 32 (1), 1102-1110.
- Petersen, K.F., Dufour, S., Savage, D.B., Bilz, S., Solomon, G., Yonemitsu, S., Cline, G.W., Befroy, D., Zemany, L., Kahn, B.B., Papademetris, X., Rothman, D.L. and Shulman, G.I., 2007. The role of skeletal muscle insulin resistance in the pathogenesis of the metabolic syndrome. *Proceedings of the National Academy of Sciences of the United States of America,* 104 (31), 12587-12594.
- Phang, W., Domboski, L., Krausz, Y. and Sharp, G.W., 1984. Mechanisms of synergism between glucose and cAMP on stimulation of insulin release. *The American Journal of Physiology,* 247 (6 Pt 1), E701-8.
- Pino, M.F., Ye, D.Z., Linning, K.D., Green, C.D., Wicksteed, B., Poitout, V. and Olson, L.K., 2005. Elevated glucose attenuates human insulin gene promoter activity in INS-1 pancreatic β-cells via reduced nuclear factor binding to the A5/core and Z element. *Molecular Endocrinology,* 19 (5), 1343-1360.
- Poitoit, V., Hagman, D., Stein, R., Artner, I., Robertson, R. and Harmon, J., 2006. Regulation of the insulin gene by glucose and fatty acids. *The Journal of Nutrition,* 136 (4), 873-876.
- Poitout, V., 2008. Glucolipotoxicity of the pancreatic β-cell: myth or reality? *Biochem Soc Trans,* 36 (5), 901.
- Poitout, V., Amyot, J., Semache, M., Zarrouki, B., Hagman, D. and Fontés, G., 2010. Glucolipotoxicity of the pancreatic beta cell. *Biochimica Et Biophysica Acta (BBA)-Molecular and Cell Biology of Lipids,* 1801 (3), 289-298.
- Prentki, M., Joly, E., El-Assaad, W. and Roduit, R., 2002. Malonyl-CoA signaling, lipid partitioning, and glucolipotoxicity: role in beta-cell adaptation and failure in the etiology of diabetes. *Diabetes,* 51 Suppl 3, S405-13.
- Prentki, M., and Nolan, C.J., 2006. Islet beta cell failure in type 2 diabetes. *The Journal of Clinical Investigation,* 116 (7), 1802-1812.
- Proks, P., Reimann, F., Green, N., Gribble, F. and Ashcroft, F., 2002. Sulfonylurea stimulation of insulin secretion. *Diabetes,* 51 Suppl 3, S368-76.
- Raab, S., Wang, H., Uhles, S., Cole, N., Alvarez-Sanchez, R., Künnecke, B., Ullmer, C., Matile, H., Bedoucha, M. and Norcross, R.D., 2016. Incretin-like effects of small molecule trace amine-associated receptor 1 agonists. *Molecular Metabolism,* 5 (1), 47-56.
- Rabi, D.M., Edwards, A.L., Southern, D.A., Svenson, L.W., Sargious, P.M., Norton, P., Larsen, E.T. and Ghali, W.A., 2006. Association of socio-economic status with diabetes prevalence and utilization of diabetes care services. *BMC Health Services Research,* 6 (1), 124.
- Rabkin, R., and Kitaji, J., 1983. Renal metabolism of peptide hormones. *Mineral and Electrolyte Metabolism,* 9 (4-6), 212-226.
- Ramasamy, R., Vannucci, S.J., Yan, S.S.D., Herold, K., Yan, S.F. and Schmidt, A.M., 2005. Advanced glycation end products and RAGE: a common thread in aging, diabetes, neurodegeneration, and inflammation. *Glycobiology,* 15 (7), 16R-28R.
- Regard, J.B., Kataoka, H., Cano, D.A., Camerer, E., Yin, L., Zheng, Y.W., Scanlan, T.S., Hebrok, M. and Coughlin, S.R., 2007. Probing cell type-specific functions of Gi in vivo

identifies GPCR regulators of insulin secretion. *The Journal of Clinical Investigation,* 117 (12), 4034-4043.

- Rena, G., Hardie, D.G. and Pearson, E.R., 2017. The mechanisms of action of metformin. *Diabetologia,* 60 (9), 1577-1585.
- Renner, C., Zemitzsch, N., Fuchs, B., Geiger, K.D., Hermes, M., Hengstler, J., Gebhardt, R., Meixensberger, J. and Gaunitz, F., 2010. Carnosine retards tumor growth in vivo in an NIH3T3-HER2/neu mouse model. *Molecular Cancer,* 9 (1), 2.
- Revel, F., Moreau, J., Pouzet, B., Mory, R., Bradaia, A., Buchy, D., Metzler, V., Chaboz, S., Zbinden, K.G. and Galley, G., 2013. A new perspective for schizophrenia: TAAR1 agonists reveal antipsychotic-and antidepressant-like activity, improve cognition and control body weight. *Molecular Psychiatry,* 18 (5), 543.
- Rial, E., Rodríguez-Sánchez, L., Gallardo-Vara, E., Zaragoza, P., Moyano, E. and González-Barroso, M.M., 2010. Lipotoxicity, fatty acid uncoupling and mitochondrial carrier function. *Biochimica Et Biophysica Acta (BBA)-Bioenergetics,* 1797 (6-7), 800-806.
- Ribon, V., Herrera, R., Kay, B.K. and Saltiel, A.R., 1998. A role for CAP, a novel, multifunctional Src homology 3 domain-containing protein in formation of actin stress fibers and focal adhesions. *The Journal of Biological Chemistry,* 273 (7), 4073-4080.
- Ribon, V., and Saltiel, A.R., 1997. Insulin stimulates tyrosine phosphorylation of the proto-oncogene product of c-Cbl in 3T3-L1 adipocytes. *The Biochemical Journal,* 324 (Pt 3) (Pt 3), 839-845.
- Ricchi, M., Odoardi, M.R., Carulli, L., Anzivino, C., Ballestri, S., Pinetti, A., Fantoni, L.I., Marra, F., Bertolotti, M. and Banni, S., 2009. Differential effect of oleic and palmitic acid on lipid accumulation and apoptosis in cultured hepatocytes. *Journal of Gastroenterology and Hepatology,* 24 (5), 830-840.
- Rickman, C., Craxton, M., Osborne, S. and Davletov, B., 2004. Comparative analysis of tandem C2 domains from the mammalian synaptotagmin family. *The Biochemical Journal,* 378 (Pt 2), 681-686.
- Riser Taylor, S., and Harris, K.B., 2013. The clinical efficacy and safety of sodium glucose cotransporter-2 inhibitors in adults with type 2 diabetes mellitus. *Pharmacotherapy: The Journal of Human Pharmacology and Drug Therapy,* 33 (9), 984-999.
- Rizos, C., Elisaf, M., Mikhailidis, D. and Liberopoulos, E., 2009. How safe is the use of thiazolidinediones in clinical practice? *Expert Opinion on Drug Safety,* 8 (1), 15-32.
- Robertson, R.P., and Harmon, J.S., 2007. Pancreatic islet β-cell and oxidative stress: The importance of glutathione peroxidase. *FEBS Letters,* 581 (19), 3743-3748.
- Roger, B., Papin, J., Vacher, P., Raoux, M., Mulot, A., Dubois, M., Kerr-Conte, J., Voy, B., Pattou, F. and Charpentier, G., 2011. Adenylyl cyclase 8 is central to glucagon-like peptide 1 signalling and effects of chronically elevated glucose in rat and human pancreatic beta cells. *Diabetologia,* 54 (2), 390-402.
- Rorsman, F., Husebye, E.S., Winqvist, O., Bjork, E., Karlsson, F.A. and Kampe, O., 1995. Aromatic-L-amino-acid decarboxylase, a pyridoxal phosphate-dependent enzyme, is a beta-cell autoantigen. *Proceedings of the National Academy of Sciences of the United States of America,* 92 (19), 8626-8629.
- Rosca, M.G., Vazquez, E.J., Chen, Q., Kerner, J., Kern, T.S. and Hoppel, C.L., 2012. Oxidation of fatty acids is the source of increased mitochondrial reactive oxygen species production in kidney cortical tubules in early diabetes. *Diabetes,* 61 (8), 2074-2083.

- Rosenbaum, D.M., Rasmussen, S.G. and Kobilka, B.K., 2009a. The structure and function of G-protein-coupled receptors. *Nature,* 459 (7245), 356.
- Rosenbaum, D.M., Rasmussen, S.G. and Kobilka, B.K., 2009b. The structure and function of G-protein-coupled receptors. *Nature,* 459 (7245), 356.
- Roth, E., Zoch, G., Schulz, F., Karner, J., Muhlbacher, F., Hamilton, G., Mauritz, W., Sporn, P. and Funovics, J., 1985. Amino acid concentrations in plasma and skeletal muscle of patients with acute hemorrhagic necrotizing pancreatitis. *Clinical Chemistry,* 31 (8), 1305-1309.
- Royce, T.E., Rozowsky, J.S. and Gerstein, M.B., 2007. Toward a universal microarray: prediction of gene expression through nearest-neighbor probe sequence identification. *Nucleic Acids Research,* 35 (15), e99.
- Rui, L., 2014. *Energy Metabolism in the Liver.Compr Physiol 4 (1): 177–197,* .
- Sahin, S., and Burukoglu Donmez, D., 2018. Effects of Carnosine (Beta-Alanyl-L-Histidine) in an Experimental Rat Model of Acute Kidney Injury Due to Septic Shock. *Medical Science Monitor : International Medical Journal of Experimental and Clinical Research,* 24, 305-316.
- Sale, C., Artioli, G.G., Gualano, B., Saunders, B., Hobson, R.M. and Harris, R.C., 2013. Carnosine: from exercise performance to health. *Amino Acids,* 44 (6), 1477-1491.
- Sale, C., Saunders, B. and Harris, R.C., 2010. Effect of beta-alanine supplementation on muscle carnosine concentrations and exercise performance. *Amino Acids,* 39 (2), 321-333.
- Salt, I.P., Johnson, G., Ashcroft, S.J. and Hardie, D.G., 1998. AMP-activated protein kinase is activated by low glucose in cell lines derived from pancreatic beta cells, and may regulate insulin release. *The Biochemical Journal,* 335 (Pt 3) (Pt 3), 533-539.
- Saltiel, A.R., and Kahn, C.R., 2001. Insulin signalling and the regulation of glucose and lipid metabolism. *Nature,* 414 (6865), 799.
- Sampson, M., Davies, I., Gavrilovic, J., Sussams, B., Brown, J., Astley, S. and Hughes, D.A., 2004. Plasma matrix metalloproteinases, low density lipoprotein oxidisability and soluble adhesion molecules after a glucose load in Type 2 diabetes. *Cardiovascular Diabetology,* 3 (1), 7.
- Sander, M., Griffen, S.C., Huang, J. and German, M.S., 1998. A novel glucose-responsive element in the human insulin gene functions uniquely in primary cultured islets. *Proceedings of the National Academy of Sciences,* 95 (20), 11572-11577.
- Sander, M., Neubuser, A., Kalamaras, J., Ee, H.C., Martin, G.R. and German, M.S., 1997. Genetic analysis reveals that PAX6 is required for normal transcription of pancreatic hormone genes and islet development. *Genes & Development,* 11 (13), 1662-1673.
- Sato, T., Iwaki, M., Shimogaito, N., Wu, X., Yamagishi, S. and Takeuchi, M., 2006. TAGE (toxic AGEs) theory in diabetic complications. *Current Molecular Medicine,* 6 (3), 351-358.
- Sauerhofer, S., Yuan, G., Braun, G.S., Deinzer, M., Neumaier, M., Gretz, N., Floege, J., Kriz, W., van der Woude, F. and Moeller, M.J., 2007. L-carnosine, a substrate of carnosinase-1, influences glucose metabolism. *Diabetes,* 56 (10), 2425-2432.
- Schönfeld, P., and Wojtczak, L., 2008. Fatty acids as modulators of the cellular production of reactive oxygen species. *Free Radical Biology and Medicine,* 45 (3), 231-241.
- Schröder, L., Schmitz, C.H. and Bachert, P., 2008. Carnosine as molecular probe for sensitive detection of Cu (II) ions using localized 1H NMR spectroscopy. *Journal of Inorganic Biochemistry,* 102 (2), 174-183.

- Seabright, P.J., and Smith, G.D., 1996. The characterization of endosomal insulin degradation intermediates and their sequence of production. *The Biochemical Journal,* 320 (Pt 3) (Pt 3), 947-956.
- Seidler, N.W., Yeargans, G.S. and Morgan, T.G., 2004. Carnosine disaggregates glycated α-crystallin: an in vitro study. *Archives of Biochemistry and Biophysics,* 427 (1), 110-115.
- Seino, S., and Shibasaki, T., 2005. PKA-dependent and PKA-independent pathways for cAMP-regulated exocytosis. *Physiological Reviews,* 85 (4), 1303-1342.
- Sener, A., and Malaisse, J., 1980. L-leucine and a nonmetabolized analogue activate pancreatic islet glutamate dehydrogenase. *Nature,* 288 (5787), 187.
- Severina, I., Bussygina, O. and Pyatakova, N., 2000. Carnosine as a regulator of soluble guanylate cyclase. *Biochemistry C/C of Biokhimiia,* 65 (7), 783-788.
- Shapiro, H., Shachar, S., Sekler, I., Hershfinkel, M. and Walker, M.D., 2005. Role of GPR40 in fatty acid action on the β cell line INS-1E. *Biochemical and Biophysical Research Communications,* 335 (1), 97-104.
- Shen, Y., Yang, J., Li, J., Shi, X., Ouyang, L., Tian, Y. and Lu, J., 2014. Carnosine inhibits the proliferation of human gastric cancer SGC-7901 cells through both of the mitochondrial respiration and glycolysis pathways. *PloS One,* 9 (8), e104632.
- Shi, Y., Vattem, K.M., Sood, R., An, J., Liang, J., Stramm, L. and Wek, R.C., 1998. Identification and characterization of pancreatic eukaryotic initiation factor 2 alpha-subunit kinase, PEK, involved in translational control. *Molecular and Cellular Biology,* 18 (12), 7499-7509.
- Shieh, S.Y., and Tsai, M.J., 1991. Cell-specific and ubiquitous factors are responsible for the enhancer activity of the rat insulin II gene. *The Journal of Biological Chemistry,* 266 (25), 16708-16714.
- Shu, Y., Sheardown, S.A., Brown, C., Owen, R.P., Zhang, S., Castro, R.A., Ianculescu, A.G., Yue, L., Lo, J.C. and Burchard, E.G., 2007. Effect of genetic variation in the organic cation transporter 1 (OCT1) on metformin action. *The Journal of Clinical Investigation,* 117 (5), 1422-1431.
- Signorelli, S.S., Malaponte, G., Libra, M., Pino, L.D., Celotta, G., Bevelacqua, V., Petrina, M., Nicotra, G.S., Indelicato, M. and Navolanic, P.M., 2005. Plasma levels and zymographic activities of matrix metalloproteinases 2 and 9 in type II diabetics with peripheral arterial disease. *Vascular Medicine,* 10 (1), 1-6.
- Singh, R., Barden, A., Mori, T. and Beilin, L., 2001. Advanced glycation end-products: a review. *Diabetologia,* 44 (2), 129-146.
- Skaper, S., Das, S. and Marshall, F., 1973a. SOME PROPERTIES OF A HOMOCARNOSINE-CARNOSINE SYNTHETASE ISOLATED FROM RAT BRAIN 1. *Journal of Neurochemistry,* 21 (6), 1429-1445.
- Skaper, S., Das, S. and Marshall, F., 1973b. SOME PROPERTIES OF A HOMOCARNOSINE-CARNOSINE SYNTHETASE ISOLATED FROM RAT BRAIN 1. *Journal of Neurochemistry,* 21 (6), 1429-1445.
- Smith, E.B., 1938. The buffering of muscle in rigor; protein, phosphate and carnosine. *The Journal of Physiology,* 92 (3), 336-343.
- Smith, E.L., 1951. The specificity of certain peptidases. *Advances Enzymol,* 12, 191-257.
- Sola, D., Rossi, L., Schianca, G.P., Maffioli, P., Bigliocca, M., Mella, R., Corliano, F., Fra, G.P., Bartoli, E. and Derosa, G., 2015. Sulfonylureas and their use in clinical practice. *Archives of Medical Science : AMS,* 11 (4), 840-848.
- Song, B.C., Joo, N., Aldini, G. and Yeum, K., 2014. Biological functions of histidine-dipeptides and metabolic syndrome. *Nutrition Research and Practice,* 8 (1), 3-10.

- Sotnikova, T.D., Caron, M.G. and Gainetdinov, R.R., 2009. Trace amine-associated receptors as emerging therapeutic targets. *Molecular Pharmacology,* 76 (2), 229-235.
- Spellman, R., and Smith, C.W., 2006. Novel modes of splicing repression by PTB. *Trends in Biochemical Sciences,* 31 (2), 73-76.
- Sriram, U., Cenna, J.M., Haldar, B., Fernandes, N.C., Razmpour, R., Fan, S., Ramirez, S.H. and Potula, R., 2016. Methamphetamine induces trace amine-associated receptor 1 (TAAR1) expression in human T lymphocytes: role in immunomodulation. *Journal of Leukocyte Biology,* 99 (1), 213-223.
- Stalder, H., Hoener, M.C. and Norcross, R.D., 2011. Selective antagonists of mouse trace amine-associated receptor 1 (mTAAR1): discovery of EPPTB (RO5212773). *Bioorganic & Medicinal Chemistry Letters,* 21 (4), 1227-1231.
- Stavrou, S., Gratz, M., Tremmel, E., Kuhn, C., Hofmann, S., Heidegger, H., Peryanova, M., Hermelink, K., Hutter, S., Toth, B., Mayr, D., Mahner, S., Jeschke, U. and Vattai, A., 2018. TAAR1 induces a disturbed GSK3beta phosphorylation in recurrent miscarriages through the ODC. *Endocrine Connections,* 7 (2), 372-384.
- Steer, M.L., 1975. Adenyl cyclase. *Annals of Surgery,* 182 (5), 603-609.
- Stein, D.T., Esser, V., Stevenson, B.E., Lane, K.E., Whiteside, J.H., Daniels, M.B., Chen, S. and McGarry, J.D., 1996. Essentiality of circulating fatty acids for glucose-stimulated insulin secretion in the fasted rat. *The Journal of Clinical Investigation,* 97 (12), 2728-2735.
- Steiner, D., Chan, S., Welsh, J. and Kwok, S., 1985. Structure and evolution of the insulin gene. *Annual Review of Genetics,* 19 (1), 463-484.
- Stenesh, J.J., and Winnick, T., 1960. Carnosine-anserine synthetase of muscle. 4. Partial purification of the enzyme and further studies of beta-alanyl peptide synthesis. *The Biochemical Journal,* 77 (3), 575-581.
- Suckale, J., and Solimena, M., 2008. Pancreas islets in metabolic signaling-focus on the beta-cell. *Front Biosci,* 13, 7156-7171.
- Sudhof, T.C., and Rothman, J.E., 2009. Membrane fusion: grappling with SNARE and SM proteins. *Science (New York, N.Y.),* 323 (5913), 474-477.
- Sugita, S., Shin, O.H., Han, W., Lao, Y. and Sudhof, T.C., 2002. Synaptotagmins form a hierarchy of exocytotic Ca(2+) sensors with distinct Ca(2+) affinities. *The EMBO Journal,* 21 (3), 270-280.
- Sun, J., Cui, J., He, Q., Chen, Z., Arvan, P. and Liu, M., 2015. Proinsulin misfolding and endoplasmic reticulum stress during the development and progression of diabetes☆. *Molecular Aspects of Medicine,* 42, 105-118.
- Sun, S., 2010. N-acetylcysteine, reactive oxygen species and beyond. *Cancer Biology & Therapy,* 9 (2), 109-110.
- Suzuki, Y., Ito, O., Takahashi, H. and Takamatsu, K., 2004. The effect of sprint training on skeletal muscle carnosine in humans. *International Journal of Sport and Health Science,* 2, 105-110.
- Szwergold, B.S., 2005. Carnosine and anserine act as effective transglycating agents in decomposition of aldose-derived Schiff bases. *Biochemical and Biophysical Research Communications,* 336 (1), 36-41.
- Tang, J., Maximov, A., Shin, O., Dai, H., Rizo, J. and Südhof, T.C., 2006. A complexin/synaptotagmin 1 switch controls fast synaptic vesicle exocytosis. *Cell,* 126 (6), 1175-1187.
- Tengholm, A., 2012. Cyclic AMP dynamics in the pancreatic β-cell. *Upsala Journal of Medical Sciences,* 117 (4), 355-369.

- Tengholm, A., and Gylfe, E., 2017. cAMP signalling in insulin and glucagon secretion. *Diabetes, Obesity and Metabolism,* 19, 42-53.
- Teufel, M., Saudek, V., Ledig, J.P., Bernhardt, A., Boularand, S., Carreau, A., Cairns, N.J., Carter, C., Cowley, D.J., Duverger, D., Ganzhorn, A.J., Guenet, C., Heintzelmann, B., Laucher, V., Sauvage, C. and Smirnova, T., 2003. Sequence identification and characterization of human carnosinase and a closely related non-specific dipeptidase. *The Journal of Biological Chemistry,* 278 (8), 6521-6531.
- Thornberry, N.A., and Gallwitz, B., 2009. Mechanism of action of inhibitors of dipeptidyl-peptidase-4 (DPP-4). *Best Practice & Research Clinical Endocrinology & Metabolism,* 23 (4), 479-486.
- Thurmond, D.C., 2007. Regulation of insulin action and insulin secretion by SNARE-mediated vesicle exocytosis. *In:* Regulation of insulin action and insulin secretion by SNARE-mediated vesicle exocytosis. *Mechanisms of Insulin Action.* Springer, 2007, pp. 52-70.
- Tian, G., Sol, E.M., Xu, Y., Shuai, H. and Tengholm, A., 2015. Impaired cAMP generation contributes to defective glucose-stimulated insulin secretion after long-term exposure to palmitate. *Diabetes,* 64 (3), 904-915.
- Tiedge, M., Lortz, S., Drinkgern, J. and Lenzen, S., 1997. Relation between antioxidant enzyme gene expression and antioxidative defense status of insulin-producing cells. *Diabetes,* 46 (11), 1733-1742.
- Torreggiani, A., Bonora, S. and Fini, G., 2000. Raman and IR spectroscopic investigation of zinc (II)–carnosine complexes. *Biopolymers: Original Research on Biomolecules,* 57 (6), 352-364.
- Torreggiani, M.T.A., 1998. A pulse radiolysis study of carnosine in aqueous solution. *International Journal of Radiation Biology,* 74 (3), 333-340.
- Unno, H., Yamashita, T., Ujita, S., Okumura, N., Otani, H., Okumura, A., Nagai, K. and Kusunoki, M., 2008. Structural basis for substrate recognition and hydrolysis by mouse carnosinase CN2. *Journal of Biological Chemistry,* .
- Vander Mierde, D., Scheuner, D., Quintens, R., Patel, R., Song, B., Tsukamoto, K., Beullens, M., Kaufman, R.J., Bollen, M. and Schuit, F.C., 2007. Glucose activates a protein phosphatase-1-mediated signaling pathway to enhance overall translation in pancreatic β-cells. *Endocrinology,* 148 (2), 609-617.
- Venter, J.C., Adams, M.D., Myers, E.W., Li, P.W., Mural, R.J., Sutton, G.G., Smith, H.O., Yandell, M., Evans, C.A., Holt, R.A., Gocayne, J.D., Amanatides, P., Ballew, R.M., Huson, D.H., Wortman, J.R., Zhang, Q., Kodira, C.D., Zheng, X.H., Chen, L., Skupski, M., Subramanian, G., Thomas, P.D., Zhang, J., Gabor Miklos, G.L., Nelson, C., Broder, S., Clark, A.G., Nadeau, J., McKusick, V.A., Zinder, N., Levine, A.J., Roberts, R.J., Simon, M., Slayman, C., Hunkapiller, M., Bolanos, R., Delcher, A., Dew, I., Fasulo, D., Flanigan, M., Florea, L., Halpern, A., Hannenhalli, S., Kravitz, S., Levy, S., Mobarry, C., Reinert, K., Remington, K., Abu-Threideh, J., Beasley, E., Biddick, K., Bonazzi, V., Brandon, R., Cargill, M., Chandramouliswaran, I., Charlab, R., Chaturvedi, K., Deng, Z., Di Francesco, V., Dunn, P., Eilbeck, K., Evangelista, C., Gabrielian, A.E., Gan, W., Ge, W., Gong, F., Gu, Z., Guan, P., Heiman, T.J., Higgins, M.E., Ji, R.R., Ke, Z., Ketchum, K.A., Lai, Z., Lei, Y., Li, Z., Li, J., Liang, Y., Lin, X., Lu, F., Merkulov, G.V., Milshina, N., Moore, H.M., Naik, A.K., Narayan, V.A., Neelam, B., Nusskern, D., Rusch, D.B., Salzberg, S., Shao, W., Shue, B., Sun, J., Wang, Z., Wang, A., Wang, X., Wang, J., Wei, M., Wides, R., Xiao, C., Yan, C., Yao, A., Ye, J., Zhan, M., Zhang, W., Zhang, H., Zhao, Q., Zheng, L., Zhong, F., Zhong, W., Zhu, S., Zhao, S., Gilbert, D., Baumhueter, S., Spier, G., Carter, C., Cravchik, A., Woodage, T., Ali, F., An, H., Awe, A., Baldwin, D., Baden, H., Barnstead, M., Barrow, I., Beeson, K., Busam, D., Carver, A., Center, A., Cheng, M.L., Curry, L., Danaher, S., Davenport, L., Desilets, R., Dietz, S., Dodson, K., Doup, L.,

Ferriera, S., Garg, N., Gluecksmann, A., Hart, B., Haynes, J., Haynes, C., Heiner, C., Hladun, S., Hostin, D., Houck, J., Howland, T., Ibegwam, C., Johnson, J., Kalush, F., Kline, L., Koduru, S., Love, A., Mann, F., May, D., McCawley, S., McIntosh, T., McMullen, I., Moy, M., Moy, L., Murphy, B., Nelson, K., Pfannkoch, C., Pratts, E., Puri, V., Qureshi, H., Reardon, M., Rodriguez, R., Rogers, Y.H., Romblad, D., Ruhfel, B., Scott, R., Sitter, C., Smallwood, M., Stewart, E., Strong, R., Suh, E., Thomas, R., Tint, N.N., Tse, S., Vech, C., Wang, G., Wetter, J., Williams, S., Williams, M., Windsor, S., Winn-Deen, E., Wolfe, K., Zaveri, J., Zaveri, K., Abril, J.F., Guigo, R., Campbell, M.J., Sjolander, K.V., Karlak, B., Kejariwal, A., Mi, H., Lazareva, B., Hatton, T., Narechania, A., Diemer, K., Muruganujan, A., Guo, N., Sato, S., Bafna, V., Istrail, S., Lippert, R., Schwartz, R., Walenz, B., Yooseph, S., Allen, D., Basu, A., Baxendale, J., Blick, L., Caminha, M., Carnes-Stine, J., Caulk, P., Chiang, Y.H., Coyne, M., Dahlke, C., Mays, A., Dombroski, M., Donnelly, M., Ely, D., Esparham, S., Fosler, C., Gire, H., Glanowski, S., Glasser, K., Glodek, A., Gorokhov, M., Graham, K., Gropman, B., Harris, M., Heil, J., Henderson, S., Hoover, J., Jennings, D., Jordan, C., Jordan, J., Kasha, J., Kagan, L., Kraft, C., Levitsky, A., Lewis, M., Liu, X., Lopez, J., Ma, D., Majoros, W., McDaniel, J., Murphy, S., Newman, M., Nguyen, T., Nguyen, N., Nodell, M., Pan, S., Peck, J., Peterson, M., Rowe, W., Sanders, R., Scott, J., Simpson, M., Smith, T., Sprague, A., Stockwell, T., Turner, R., Venter, E., Wang, M., Wen, M., Wu, D., Wu, M., Xia, A., Zandieh, A. and Zhu, X., 2001. The sequence of the human genome. *Science (New York, N.Y.),* 291 (5507), 1304-1351.

- Viollet, B., Guigas, B., Sanz Garcia, N., Leclerc, J., Foretz, M. and Andreelli, F., 2012. Cellular and molecular mechanisms of metformin: an overview. *Clinical Science (London, England : 1979),* 122 (6), 253-270.
- Vistoli, G., Straniero, V., Pedretti, A., Fumagalli, L., Bolchi, C., Pallavicini, M., Valoti, E. and Testa, B., 2012. Predicting the physicochemical profile of diastereoisomeric histidine-containing dipeptides by property space analysis. *Chirality,* 24 (7), 566-576.
- Wainscott, D.B., Little, S.P., Yin, T., Tu, Y., Rocco, V.P., He, J.X. and Nelson, D.L., 2007. Pharmacologic characterization of the cloned human trace amine-associated receptor1 (TAAR1) and evidence for species differences with the rat TAAR1. *The Journal of Pharmacology and Experimental Therapeutics,* 320 (1), 475-485.
- Walter, P., and Ron, D., 2011. The unfolded protein response: from stress pathway to homeostatic regulation. *Science (New York, N.Y.),* 334 (6059), 1081-1086.
- Wang, X., Misawa, R., Zielinski, M.C., Cowen, P., Jo, J., Periwal, V., Ricordi, C., Khan, A., Szust, J. and Shen, J., 2013. Regional differences in islet distribution in the human pancreas-preferential beta-cell loss in the head region in patients with type 2 diabetes. *PloS One,* 8 (6), e67454.
- Wang, Z., Gerstein, M. and Snyder, M., 2009. RNA-Seq: a revolutionary tool for transcriptomics. *Nature Reviews Genetics,* 10 (1), 57.
- Wang, Z., and Thurmond, D.C., 2009. Mechanisms of biphasic insulin-granule exocytosis - roles of the cytoskeleton, small GTPases and SNARE proteins. *Journal of Cell Science,* 122 (Pt 7), 893-903.
- Watanabe, M., Suliman, M.E., Qureshi, A.R., Garcia-Lopez, E., Bárány, P., Heimbürger, O., Stenvinkel, P. and Lindholm, B., 2008. Consequences of low plasma histidine in chronic kidney disease patients: associations with inflammation, oxidative stress, and mortality–. *The American Journal of Clinical Nutrition,* 87 (6), 1860-1866.
- Weber, L.M., Hayda, K.N. and Anseth, K.S., 2008. Cell–matrix interactions improve β-cell survival and insulin secretion in three-dimensional culture. *Tissue Engineering Part A,* 14 (12), 1959-1968.

- Weiss, M., Steiner, D.F. and Philipson, L.H., 2000. Insulin Biosynthesis, Secretion, Structure, and Structure-Activity Relationships. *In:* L.J. De Groot, G. Chrousos, K. Dungan, K.R. Feingold, A. Grossman, J.M. Hershman, C. Koch, M. Korbonits, R. McLachlan, M. New, J. Purnell, R. Rebar, F. Singer and A. Vinik, eds., *Endotext.* South Dartmouth (MA): MDText.com, Inc, 2000, .
- White, J., and Rees, K., 1984. The mechanism of action of 4-hydroxynonenal in cell injury. *Chemico-Biological Interactions,* 52 (2), 233-241.
- Winzell, M.S., and Ahrén, B., 2007. G-protein-coupled receptors and islet function—implications for treatment of type 2 diabetes. *Pharmacology & Therapeutics,* 116 (3), 437-448.
- Wittingen, J., and Frey, C.F., 1974. Islet concentration in the head, body, tail and uncinate process of the pancreas. *Annals of Surgery,* 179 (4), 412-414.
- Wolff, S.P., and Dean, R.T., 1987. Glucose autoxidation and protein modification. The potential role of 'autoxidative glycosylation' in diabetes. *The Biochemical Journal,* 245 (1), 243-250.
- Wollerton, M.C., Gooding, C., Wagner, E.J., Garcia-Blanco, M.A. and Smith, C.W., 2004. Autoregulation of polypyrimidine tract binding protein by alternative splicing leading to nonsense-mediated decay. *Molecular Cell,* 13 (1), 91-100.
- World Health Organisation, 2016. *Global Report on Diabetes.* Geneva: World Health Organisation.
- World Health Organization, 2011. Use of glycated haemoglobin (HbA1c) in the diagnosis of diabetes mellitus. 2011. *Geneva (Switzerland): The Organization Google Scholar,* .
- Wu, Y., Ding, Y., Tanaka, Y. and Zhang, W., 2014. Risk factors contributing to type 2 diabetes and recent advances in the treatment and prevention. *International Journal of Medical Sciences,* 11 (11), 1185.
- Xie, Z., Baba, S.P., Sweeney, B.R. and Barski, O.A., 2013. Detoxification of aldehydes by histidine-containing dipeptides: from chemistry to clinical implications. *Chemico-Biological Interactions,* 202 (1-3), 288-297.
- Xu, G., Kaneto, H., Laybutt, D.R., Duvivier-Kali, V.F., Trivedi, N., Suzuma, K., King, G.L., Weir, G.C. and Bonner-Weir, S., 2007. Downregulation of GLP-1 and GIP receptor expression by hyperglycemia: possible contribution to impaired incretin effects in diabetes. *Diabetes,* 56 (6), 1551-1558.
- Yaffe, D., and Saxel, O., 1977. Serial passaging and differentiation of myogenic cells isolated from dystrophic mouse muscle. *Nature,* 270 (5639), 725.
- Yamashita, T., Shimada, S., Guo, W., Sato, K., Kohmura, E., Hayakawa, T., Takagi, T. and Tohyama, M., 1997. Cloning and functional expression of a brain peptide/histidine transporter. *The Journal of Biological Chemistry,* 272 (15), 10205-10211.
- Yapislar, H., and Taskin, E., 2014. L-carnosine alters some hemorheologic and lipid peroxidation parameters in nephrectomized rats. *Medical Science Monitor : International Medical Journal of Experimental and Clinical Research,* 20, 399-405.
- You, J., Wang, Z., Xu, S., Zhang, W., Fang, Q., Liu, H., Peng, L., Deng, T. and Lou, J., 2016. Advanced Glycation End Products Impair Glucose-Stimulated Insulin Secretion of a Pancreatic β-Cell Line INS-1-3 by Disturbance of Microtubule Cytoskeleton via p38/MAPK Activation. *Journal of Diabetes Research,* 2016.
- Zhang, B., and Roth, R.A., 1991. Binding properties of chimeric insulin receptors containing the cysteine-rich domain of either the insulin-like growth factor I receptor or the insulin receptor related receptor. *Biochemistry,* 30 (21), 5113-5117.

- Zhang, K., and Kaufman, R.J., 2008. From endoplasmic-reticulum stress to the inflammatory response. *Nature,* 454 (7203), 455.
- Zhang, Q., Xiao, X., Li, M., Li, W., Yu, M., Zhang, H., Wang, Z. and Xiang, H., 2013. Acarbose reduces blood glucose by activating miR-10a-5p and miR-664 in diabetic rats. *PloS One,* 8 (11), e79697.
- Zhang, J., Pacifico, R., Cawley, D., Feinstein, P. and Bozza, T., 2013. Ultrasensitive detection of amines by a trace amine-associated receptor. *The Journal of Neuroscience : The Official Journal of the Society for Neuroscience,* 33 (7), 3228-3239.
- Zhao, J., Shi, L. and Zhang, L., 2017. Neuroprotective effect of carnosine against salsolinol-induced Parkinson's disease. *Experimental and Therapeutic Medicine,* 14 (1), 664-670.
- Zhao, L., Cissell, M.A., Henderson, E., Colbran, R. and Stein, R., 2000. The RIPE3b1 activator of the insulin gene is composed of a protein(s) of approximately 43 kDa, whose DNA binding activity is inhibited by protein phosphatase treatment. *The Journal of Biological Chemistry,* 275 (14), 10532-10537.

Appendices

Appendix 1

Target	Species	Forward Primer	Reverse Primer
TAAR1	Rat	GAAGGAGTTGAGGAG CAGTATC	AAGACGTCATGAATG CCAGTA
TAAR2	Rat	AATGACTATTCCGGTC GTCAAG	CCATCAGCATAAGCCT CTGAA
TAAR3	Rat	GGTATGCAGAGCTAC GAGATTC	CATGATGGAGCCAGG AGTAAA
TAAR4	Rat	CATGATCGGAGCGAT AGTGATG	GTGGTAGCCATGGAG AGAATAAG
TAAR5	Rat	CTCCAAGTTCACAGTC AGGATAG	GTAGAGAAAGAAGGC AGTGTAGG
TAAR6	Rat	CAGGAATTTGCATCAG CATCTC	CTCCAGGCCATCAGCA TAAA
TAAR7b	Rat	TCTGCTCTCAGCCTCA TCTA	CCAAAGCCAAAGACT GCATAAA
TAAR9	Rat	CCAAGTTCACCATTTC GGTTTC	CTCGTTGGCTCCTGTG TAAA
ErbB4	Rat	AGTGGTCTGTCATTGC TTATCC	TGCTGTTGTCCGTGAT GTAG
MMP14	Rat	GGTGTGTGTCCAACCC TATTT	GGATGGAAGAGAAGC AGATGAC
MMP15	Rat	CTAGACTGCCCATGTT CTCTTT	GACCTCTGGTACCCTA GTATGT
MMP16	Rat	GGACCAACAGACCGA GATAAAG	ACCAATACAAGGAGG CCATAAG
CD44	Rat	GCCTGGTACGGAGTC AAATAC	TCATCAATGCCTGATC CAGAAA
GAPDH	Rat	CATCTCCCTCACAATT CCATCC	GAGGGTGCAGCGAAC TTTAT

Appendix Table 1